UiT The Arctic University of Norway

Faculty of Biosciences, Fisheries and Economics
The Norwegian College of Fishery Science

Bioprospecting of marine microorganisms for the discovery of antibacterial compounds

Isolation, structure elucidation and bioactivity assessment of marine microbial natural products

Marte Jenssen

A dissertation for the degree of Philosophiae Doctor February 2022

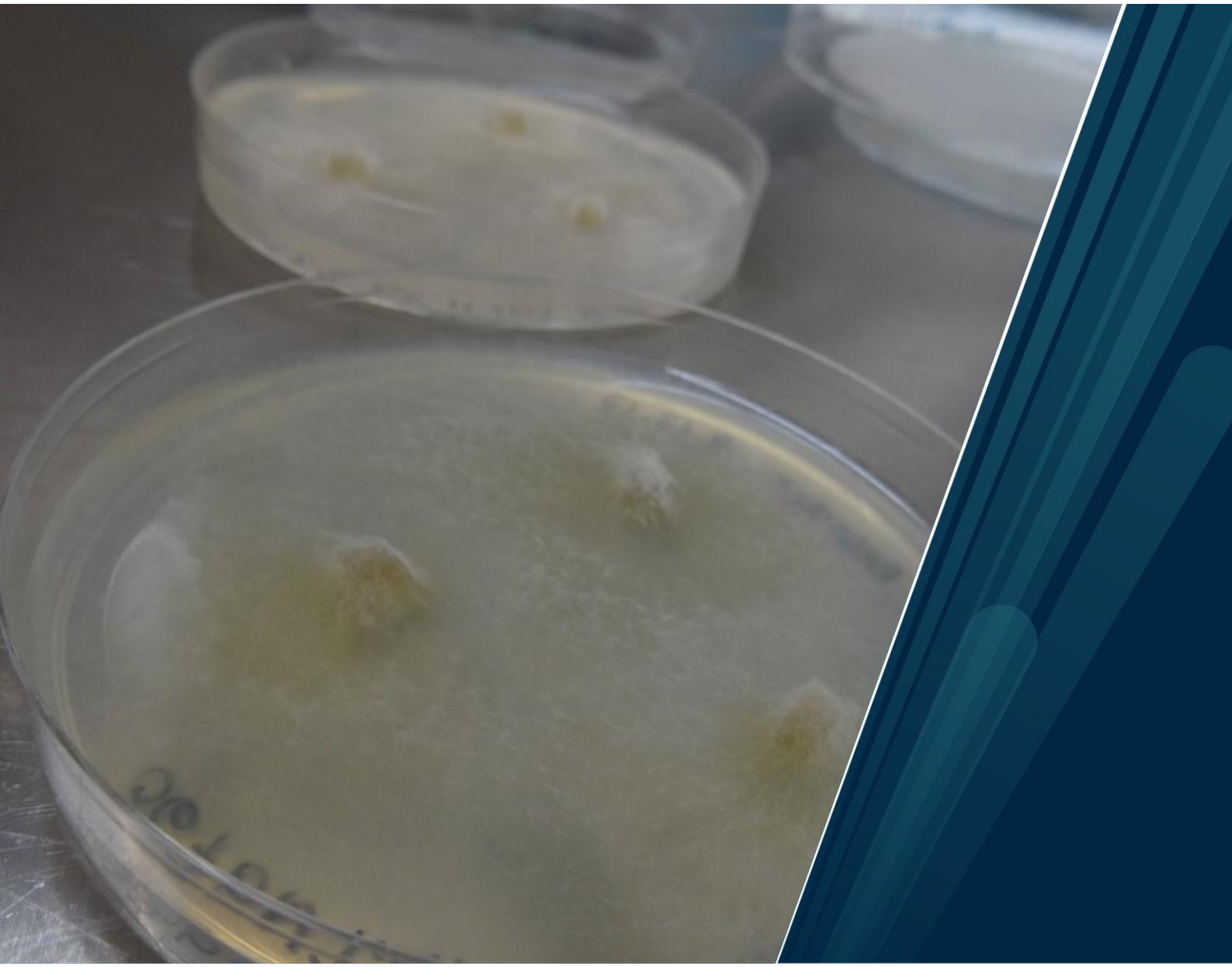

Bioprospecting of marine microorganisms for the discovery of antibacterial compounds

Isolation, structure elucidation and bioactivity assessment of marine microbial natural products

A dissertation submitted in partial fulfilment of the requirement for the degree of Philosophiae Doctor

Marte Jenssen
Tromsø
February 2022

The work for this thesis was carried out from September 2017 to February 2022 at Marbio, The Norwegian College of Fishery Science, UiT – The Arctic University of Norway. The work was part of the DigiBiotics project funded by the Research Council of Norway (Center for Digital Life Norway), and the AntiBioSpec project funded by UiT the Arctic University of Norway.

Summary

Infectious diseases have been a problem for humans since the beginning of human existence. The "golden age" of antibiotics started at the end of the 1920s, with the discovery of penicillin by Sir Alexander Fleming. This was followed by the discovery of several life-saving antibiotics. The number of new marketed antibiotics has declined, and most pharmaceutical companies are no longer working in antibiotic development. This in itself would be unproblematic, had it not been for the rapid ability of bacteria to become resistant towards previously debilitating agents. The need for new antibiotics is therefore eminent. Natural products have been important contributors for antibiotic drug discovery and development. Microorganisms have been a particularly proliferative source of antibiotics, providing us with among others the penicillins, aminoglycosides, tetracyclines and polymyxins. Most naturally derived pharmaceuticals, including antibiotics, originate from terrestrial organisms. This is mainly because the terrestrial environment historically has been easier to access compared to the marine environment below the intertidal zone. The marine environment is highly diverse, and there is still a huge biodiversity that is yet to be explored. In this project, Arctic and sub-Arctic marine bacteria and fungi were cultivated and studied for their production of natural products. The cultures were extracted and fractionated, and the fractions were tested for bioactivity, mainly focusing on antibacterial activity. Using bioactivity-guided isolation, compounds were isolated and structurally characterized. Finally, the bioactivity of the isolated compounds was broadly evaluated.

In paper I, a known siderophore, serratiochelin A, was isolated from a co-culture of two bacteria, *Serratia* sp. and *Shewanella* sp. The compound was not detected in axenic cultures, indicating that co-cultivation triggered production. The acid-catalyzed degradation of serratiochelin A into serratiochelin C was also observed. Serratiochelin A had weak activity against *Staphylococcus aureus*, melanoma cells and non-malignant lung fibroblasts. No activity was observed for the degradation product serratiochelin C, indicating that the oxazoline moiety in the original compound is essential for the bioactivity.

In paper II, a marine bacterium *Lacinutrix* sp. was cultivated and studied for its ability to produce bioactive natural products. Through bioactivity-guided isolation, two new lyso-ornithine lipids were isolated, and their structures elucidated, showing that they only differed by the length of the hydrocarbon tail. Analysis by UHPLC-HR-MS indicate that the purified solutions are mixtures of isomers, but these were not possible to separate by preparative HPLC-MS. The compounds were evaluated for antibacterial activity and antiproliferative activity against human cells. Compound 1 displayed weak activity against *Streptococcus agalactiae,* while compound 2 had weak activity against melanoma cells.

In paper III, a new dimeric naphthopyrone substituted with a sulphate group was isolated in high yields from cultures of an obligate marine fungus in the family *Lulworthiaceae*. The compound was tested against an extended panel of clinical bacterial isolates and showed potent antibacterial activity against several clinical methicillin-resistant *Staphylococcus aureus* isolates, with MICs down to 1.56 µg/mL. Acid-catalyzed degradation was also observed. The compound also displayed moderate activities against three human cell lines: melanoma, hepatocellular carcinoma, and non-malignant lung fibroblast.

In paper IV, a new chlovalicin variant, chlovalicin B, was isolated from cultures of the obligate marine fungus *Digitatispora marina*. The fungus has previously been studied for its distribution in the marine environment but has not been extensively studied for its biosynthetic potential. The compound was isolated in low yields, and the structure was elucidated by NMR and HRMS experiments. The compound was assessed for a range of bioactivities and had weak antiproliferative activity against human melanoma cells.

Acknowledgements

My years in the Marbio research group, since I started with my master's project in 2016, have been better than I could have ever imagined. I would like to thank my supervisors at Marbio: Prof. Jeanette Hammer Andersen and Prof. Espen Hansen. Thank you for your guidance, help and support, and for the incredible working environment that you have built at Marbio. To Dr. Kine Østnes Hansen, thank you for always being there with knowledge and the best humor.

I would also like to thank the whole DigiBiotics team. It has been interesting to work in such a broad consortium with different research interests. I have learned a lot. A special thanks to "the NMR guys" Johan Isaksson and Philip Rainsford for all the time you spent solving my structures and Eric Juskewitz for your great work with the clinical isolates and "the green one". To Digital Life Norway, for funding our project, but also for giving me many great opportunities for courses and conferences during my PhD period. I am especially thankful for the experiences I got from the DLN industry internship at Xellia Pharmaceuticals, I learned a lot and gained new friendships. Also, the DLN Junior Resource Group: Eric, Simona, Emil and Maria, thank you for all the fun times. We did a lot of interesting and important work, but most importantly, we had fun!

In November 2018, I got to leave winter-Tromsø and travel to summer-Cape Town to work at the Institute for Microbial Biotechnology and Metagenomics at the University of the Western Cape. I would like to thank all the great students and co-workers at IMBM, especially Dr. Lonnie van Zyl for your patience when teaching me about the work with the bacterial genomes.

To the amazing group of people at Marbio and Marbank. Our fantastic engineers: Marte, Kirsti and Chun, thanks for all your help with the bioassays and 16S/ITS sequencing. I would also like to thank Dr. Sara Ullsten-Wahlund, Dr. Ruth Hendus-Altenburger and Dr. Lars Ganzert for all our interesting talks. A special thanks goes out to Dr. Teppo Rämä, for introducing me to the incredible world of marine fungi. My appreciation goes out to my fellow PhD students, all of which are now Drs.! Ole Christian Hagestad, thank you for all our nice discussions and your support, I always know who to ask if I have any bioinformatics or computer issues. My office mate and co-author Venke Kristoffersen, thank you for always lifting my mood and for all our scientific (and non-scientific) conversations. Renate Døving Osvik, thank you for motivating and inspiring me by the way you are! And to my PhD buddy Yannik Schneider, I have learned so much from you and you always make me laugh.

Finally, I would like to thank my family and friends. My mother and father, sisters and brother, thank you for always being there for me. To my nieces and nephews, Johan, Elise, Frida and Sigve, I am the luckiest aunt in the world. To the rest of my family and good friends, thank you.

Tromsø, February 2022

Marte Jenssen

List of abbreviations

ADMET	Absorption, distribution, metabolism, excretion, toxicity
AMR	Antimicrobial resistance
BGC	Biosynthetic gene cluster
BLAST	Basic Local Alignment Search Tool
CBD	Convention on Biological Diversity
ESI	Electrospray ionization
ET-743	Ecteinascidin 743
HMBC	Heteronuclear Multiple-Bond Correlation
HPLC	High performance liquid chromatography
HRMS	High resolution mass spectrometry
HSQC	Heteronuclear Single Quantum Correlation
HTS	High-throughput screening
IR	Infrared
ITS	Internal transcribed spacer
LC	Liquid chromatography
MIC	Minimal inhibitory concentration
MNP	Marine natural product
MS	Mass spectrometry
NCBI	National Center for Biotechnology Information
NMR	Nuclear magnetic resonance
NP	Natural product
NRP	Non-ribosomal peptide
NRPS	Non-ribosomal peptide synthetase
OSMAC	One strain many compounds
PAINS	Pan Assay INterference compoundS
PBP	Penicillin binding protein
PK	Polyketide
PK-NRP	Polyketide-Non-ribosomal peptide
PKS	Polyketide synthase
QTOF	Quadrupole time of flight
SAR	Structure-activity relationship
SARS-CoV-2	Severe acute respiratory syndrome coronavirus 2
SPE	Solid-phase extraction
UHPLC	Ultra-high performance liquid chromatography
UV/Vis	Ultraviolet/visible
WHO	World Health Organization

List of publications

PAPER I:

Yannik Karl-Heinz Schneider*, **Marte Jenssen***, Johan Isaksson, Kine Østnes Hansen, Jeanette Hammer Andersen and Espen Hansen. *shared first authorship.

Bioactivity of Serratiochelin A, a Siderophore Isolated from a Co-Culture of *Serratia* sp. and *Shewanella* sp.

Microorganisms, **2020**, *8*, 1042. doi: 10.3390/microorganisms8071042.

PAPER II:

Venke Kristoffersen, **Marte Jenssen**, Heba Raid Jawad, Johan Isaksson, Espen Hansen, Teppo Rämä, Kine Østnes Hansen and Jeanette Hammer Andersen.

Two Novel Lyso-Ornithine Lipids Isolated from an Arctic Marine *Lacinutrix* sp. Bacterium

Molecules, **2021**, *26*, 5295. doi: 10.3390/molecules26175295.

PAPER III:

Marte Jenssen, Philip Rainsford, Eric Juskewitz, Jeanette Hammer Andersen, Espen Hansen, Johan Isaksson, Teppo Rämä and Kine Østnes Hansen.

Lulworthinone, a New Dimeric Naphthopyrone from a Marine Fungus in the Family Lulworthiaceae with Antibacterial Activity Against Clinical Methicillin-Resistant *Staphylococcus aureus* Isolates

Frontiers in Microbiology, **2021**, *12*, 730740. doi: 10.3389/fmicb.2021.730740.

PAPER IV:

Marte Jenssen, Venke Kristoffersen, Kumar Motiram-Corral, Johan Isaksson, Teppo Rämä, Jeanette Hammer Andersen, Espen Holst Hansen and Kine Østnes Hansen.

Chlovalicin B, a Chlorinated Sesquiterpene Isolated from the Marine Mushroom *Digitatispora marina*.

Molecules, **2021**, *26*, 7560. https://doi.org/10.3390/molecules26247560

Contributions:

	Paper I	**Paper II**	**Paper III**	**Paper IV**
Concept and idea	YS, **MJ**, JA, EH	VK, **MJ**, TR, EH, JA	**MJ**, JA, EH, TR, KH	**MJ**, VK, TR, JA, EH
Study design and methods	YS, **MJ**, JI, KH, JA, EH	VK, **MJ**, KH, EH, JA	**MJ**, JA, EH, JI, TR, KH	**MJ**, VK, TR, JA, EH, KH
Data gathering and interpretation	YS, **MJ**, JI	VK, **MJ**, HJ, JI, KH	**MJ**, PR, EJ, JI	**MJ**, KC, VK, JI, EH, KH
Manuscript preparation	YS, **MJ**, JI, KH, JA, EH	VK, **MJ**, HJ, JI, KH, EH, JA	**MJ**, PR, EJ, JA, EH, JI, TR, KH	**MJ**, KC, JA, EH, KH

EH = Espen Holst Hansen, EJ = Eric Juskewitz, HJ = Heba Raid Jawad, JA= Jeanette Hammer Andersen, JI = Johan Isaksson, KC = Kumar Motiram-Corral, KH = Kine Østnes Hansen, **MJ = Marte Jenssen**, PR = Philip Rainsford, TR = Teppo Rämä, VK = Venke Kristoffersen, YS = Yannik Karl-Heinz Schneider

Table of contents

Paper I – Paper IV

List of tables

List of figures

Cover photo: Fungal isolate 067bN1.2 (family *Lulworthiaceae*), the producer of lulworthinone (photo: Marte Jenssen).

1 Introduction

1.1 Infectious diseases

Humans have been in constant battles with microbes, with possibly the largest battle in modern times (1918-1920) being the Spanish flu pandemic [1]. The Spanish flu was caused by an influenza virus which killed about 5% of the human population [1]. We are also currently in the middle of a pandemic, caused by the severe acute respiratory syndrome coronavirus 2 (SARS-CoV-2) [2]. The Black Death was a plague that lasted from 1346 to 1353 (persisting in Europe until 1750 in epidemic waves) and is considered to be the most fatal pandemic in human history, taking the life of one third of the European population. This plague was caused by bacterial infections of *Yersinia pestis* [3, 4], and was spread by fleas and through person-to-person contact. In fact, this Gram-negative bacterium, is assumed to have caused three plague pandemics, the Justinian's plague (AD 541 – 542), the Black Death, and a third pandemic spreading from the Yunnan region in China in the mid-19th century [3]. In addition to such massive outbreaks, human health is constantly challenged by infectious diseases caused by pathogenic organisms that are persistent in the human population. One of the most problematic bacterial infectious diseases today is tuberculosis, where the causative agent is *Mycobacterium tuberculosis*. In 2016, an estimated 290 000 new cases of tuberculosis and 26 000 deaths were reported in the World Health Organization (WHO) European Region. The European Region does not have the highest incidences of tuberculosis in the world, but has the highest case number of multidrug resistant tuberculosis [5].

1.1.1 Antibiotics and antibiotic resistance

Humans have developed several strategies to prevent and treat pathogenic microorganisms, for example by the development of vaccines and antibiotics, and through increased focus on sanitation. Herein, the focus will be on antibiotics. An antibiotic is a compound that inhibits the growth of (bacteriostatic) or kills (bactericidal) bacteria by specific interactions with bacterial targets [6, 7]. Several targets exist, with the most common affected targets for marketed antibiotics being the bacterial ribosome (protein synthesis), cell wall or lipid membrane, metabolic pathways, and the DNA/RNA synthetic machinery [8]. The inhibition of cell wall assembly is exemplified by β-lactam antibiotics in Box 1. The era of antibiotic drug discovery began with Sir Alexander Fleming's discovery of penicillin produced by the mold *Penicillium rubens* [9], in 1928 [10]. He discovered that the mold, which had serendipitously entered his laboratory through an open window, was able to kill the bacterium *Staphylococcus aureus* growing on a Petri dish, leading to the discovery of penicillin (Figure 1) [10]. Today, the penicillins are still some of the most used antibiotics [8]. The years 1940s-1980s are considered the "golden age" of antibiotic discovery, as most of our life saving antibiotic classes were discovered

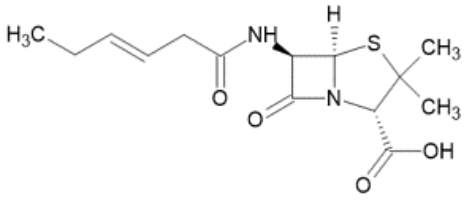

Figure 1: Penicillin F, the first penicillin variant, discovered by Alexander Fleming in 1928. The compound was produced by the mold *Penicillium rubens.*

during this time, for example the aminoglycosides, tetracyclines, polymyxins and macrolides [11]. Unfortunately, the number of new antibacterial drugs have declined since, and most new antibiotics are derivatives from already known drug classes, meaning that they have similar targets and function as the antibiotics discovered during the golden age [6].

The discovery of antibiotics has been a revolution within modern medicine. However, even with the currently available antibiotics there is a huge challenge evolving all over the world: The spread of antibiotic resistant microbes, transforming once treatable diseases into untreatable ones [1]. Antibiotic resistance occurs when bacteria gain the ability to circumvent the mechanism of action of the antibiotic. This is caused by culminations of mutations, or by acquisition of resistance genes through horizontal gene transfer, rendering the bacteria more fit to survive with antibiotics present [1, 6, 12, 13].

Box 1: The β-lactams; mechanism of action and resistance mechanisms

Left - Mechanisms of action of the β-lactams: The β-lactams interfere with the cell wall synthesis by binding to the Penicillin Binding Proteins (PBPs), enzymes that are essential for crosslinking of the peptidoglycan layers. Cell wall formation is inhibited, and the cells die.

Right - Resistance against the β-lactams: The resistant bacterium can alter its PBPs to give reduced affinity towards the β-lactams, while still being able to cross-link the peptidoglycan layers. Some resistance also comes from the production of plasmid-encoded β-lactamases, enzymes that break the amide bond in the β-lactam ring, rendering the antibiotic inactive against the pathogen.

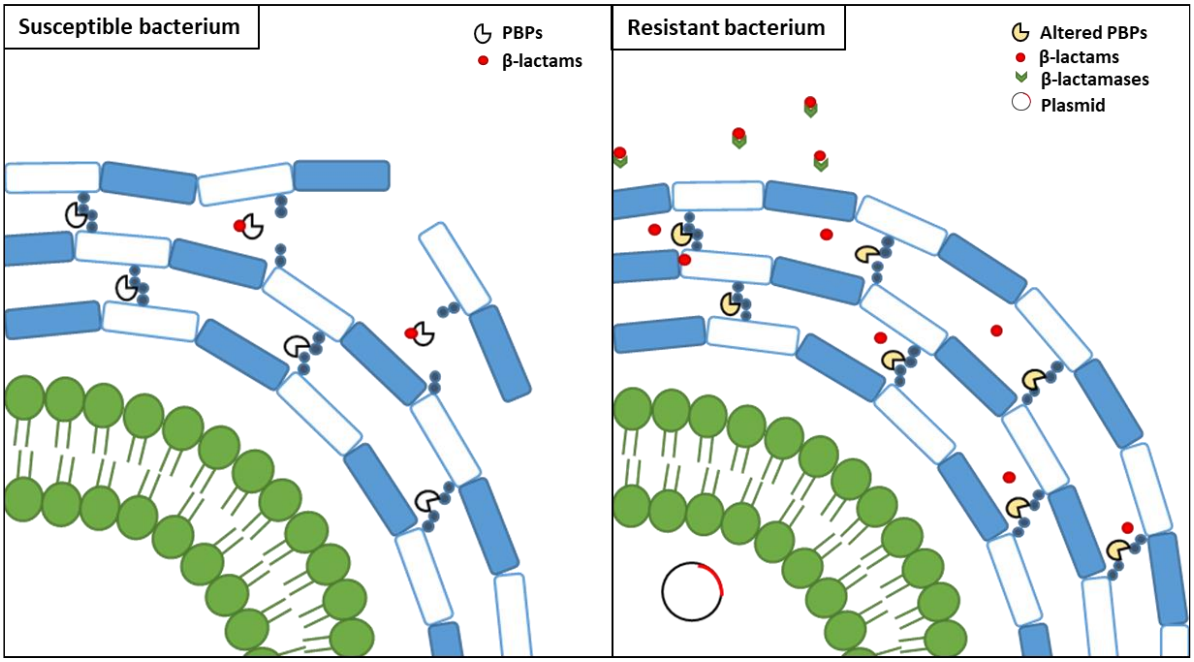

What are the driving factors for development of resistance? The development of antimicrobial resistance (AMR) is a naturally occurring phenomenon, and resistance genes are a part of the natural gene pool and have been so also before the commercial use of antibiotics in human medicine [1]. Some resistance factors are intrinsic to the bacterium [13], for example, the natural resistance of Gram-negative bacteria to glycopeptides due to their impermeable outer membranes, or the formation of biofilms which generally makes the bacterial population much less susceptible to antibiotics. There are indications that excessive use of antibiotics both in human medicine, but also in agriculture, has led to a faster development of resistance due to the steep increase in selective evolutionary pressure imposed on the microbes [8, 14]. However, the severity of the impact from agriculture has been disputed [15, 16]. Infectious diseases are a global societal problem today and are considered to be one of the most pressing health issues in the world [17]. The emergence of multidrug-resistant pathogens is increasing mortality and leading to prolonged illness. It has been estimated that the yearly costs of antimicrobial resistance in the US health system alone is between US $21 to $34 billion dollars, and that it increases the pressure on the health care system by causing an additional 8 million days of hospitalization [18]. It has also been estimated that in total, AMR will cause 10 million deaths yearly by the year 2050 [19].

1.2 Discovery and development of antibiotics

Even though it is generally accepted that antimicrobial resistance is one of the biggest threats to human health, the clinical pipeline of new antimicrobials is dry. One of the reasons for this is the profitability of antibiotic research. The cost of developing an antibiotic drug is currently about US$ 1.5 billion [20, 21], making the expenses associated with their development comparable to drugs developed towards other indications, while the estimated average annual revenue is US$ 46 million [21]. This modest average annual revenue is due to several factors. The retail prices of antibiotics are relatively low compared to drugs marketed towards other indications, and regulations regarding the use of antibiotics to reduce rapid resistance development contributes to making antibiotics a less attractive investment compared to other drugs [21]. In addition, antimicrobials are used in shorter periods and if successful, eliminate the disease and therefore also eliminates further use of the drug. Drugs for chronic diseases and conditions, like cardiovascular disease, mood disorders, pain and high cholesterol, are considerably more profitable [22, 23]. For these reasons, many of the larger pharmaceutical companies have dropped out of the antibiotics race to pursue more profitable avenues of drug development, leaving smaller pharma companies and funding bodies with the great task of antibiotic drug discovery and development [21]. For companies to enter back into antimicrobial research, new incentives are needed that ensure revenue from these projects. The STEDI values have been created to assess the value of antibiotics, not only focusing on their direct economic value, see Box 2 for more information.

Box 2: The STEDI values of antibiotics

There has been an increasing political focus on the financial circumstances (the business model) surrounding antibiotic development and several incentives have been launched. The STEDI values of antibiotics is a relatively new term that has been introduced to assess the actual value of antibiotics with the aim of paying for the value of antibiotics to society (indirect value), not only for their value in sales volume or the value for the patient (primary value) [24]. This is to ensure that the companies are reimbursed for their research once the drug reaches the market and to boost more companies into the lane of antibiotic research once again. STEDI is an abbreviation for five different values of antibiotics to society and these are briefly described below [24]:

1. **Spectrum:** Replacing broad spectrum antibiotics with narrow spectrum agents, to reduce the collateral damage to the microbiome
2. **Transmission:** Avoiding disease transmission of pathogens in the population by effectively treating patients
3. **Enablement:** Enabling other medical treatments, such as surgery (extremely high value to society)
4. **Diversity:** Reducing selection pressure by offering a range of treatment options
5. **Insurance:** Availability of optional agents in case of resistance development to currently used agents

There have been several incentives to help prioritize which microbes are the most important to find new treatments for, to focus the discovery and development of antibiotics on the most severe pathogens that we have today. In 2018 the WHO launched a priority list for research and development of new antibiotics for the treatment of antibiotic resistant bacteria. The list is an initiative to help prioritize research and development of new antibiotics, based on several criteria including mortality, availability of effective therapy, health-care burden and increase in drug resistance. The main conclusion was that the focus should be on multidrug-resistant tuberculosis and Gram-negative bacteria [25]. Another list of "Bad Bugs, No Drugs" is the ESKAPE pathogens, which are both highly infectious and able to develop resistance [26, 27]: *Enterococcus faecium*, *Staphylococcus aureus*, *Klebsiella pneumoniae*, *Acinetobacter baumanii*, *Pseudomonas aeruginosa*, *Enterobacter* sp. The ESKAPE pathogens are often causing nosocomial infections [26].

From 2000 and until October 2019, a total of 38 new antibacterials were launched in the pharmaceutical market. Of these, five were first-in-class drugs: linezolid (oxaxolidinone, 2000), daptomycin (lipopeptide, 2003), retapamulin (pleuromutilin, 2007), fidaxomicin (tiacumicin, 2011) and bedaquiline (diarylquinoline, 2012) [17]. All five antibacterials have Gram-positive activity. Bedaquiline is the first

new class of antibiotics approved for the treatment of tuberculosis infections since 1963 [28]. Figure 2 shows the number of antibacterial compounds in the different clinical development phases in 2011, 2013, 2015 and 2019. As can be seen, there were twice as many antibacterials in phase I clinical trials in 2019 compared to 2015, which is most likely reflecting the increased funding opportunities during the last years [17].

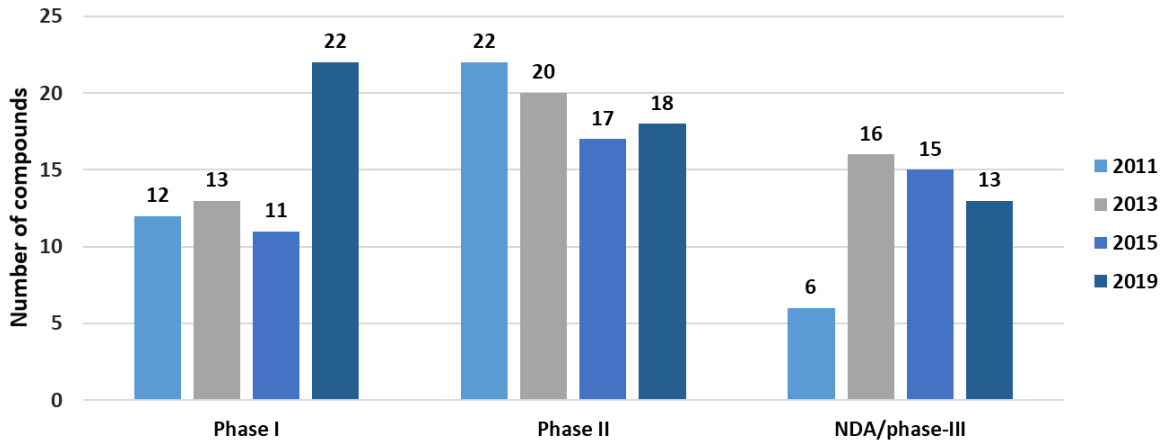

Figure 2: Number of antibacterial compounds in the different clinical development phases as of 2011 [29], 2013 [30], 2015 [31] and 2019 [17]. Modified from [17]. NDA: New Drug Application.

1.3 Bioprospecting and natural products

Bioprospecting is the exploration of biodiversity for new biological resources of social and economic value [11, 32]. It is carried out by a wide variety of industries including pharmaceutical, crop protection, cosmetics, horticulture, agricultural seeds, environmental monitoring, manufacturing, and construction [32, 33]. The end products could be e.g., compounds developed into drugs, enzymes needed for industrial purposes, biological control agents, new species for aquaculture or bioremediation, or active ingredients in cosmetic or nutraceutical products. Most of the currently used antibiotics were discovered through the bioprospecting approach, including β-lactams, aminoglycosides, tetracyclines and the macrolides [11].

"*All we have yet discovered is but a trifle in comparison with what lies hid in the great treasury of nature*" - Antonie van Leeuwenhoek 1680 [34].

1.3.1 Primary and secondary metabolites

In order to survive, grow, reproduce, compete and thrive in their natural environments, all organisms produce a large spectrum of metabolites [35]. Natural products (NPs) can be entire organisms, parts of organisms, extracts or exudates, or compounds produced by an organism [36]. In this thesis the focus will be on compounds. Usually, NP compounds are divided into primary metabolites and secondary metabolites, depending on if their production is necessary for the immediate survival and growth of the organism (primary), or if the NP is produced to bring advantageous properties that are not vital for the organism (secondary) [35]. In other words, secondary metabolites are not needed for the vital processes of life such as growth and reproduction, but they can influence the organism's interaction with the environment and thereby be beneficial for its long-term survival. Examples of primary metabolites are common monosaccharides (e.g., glucose, mannose), disaccharides (e.g., lactose), proteogenic amino acids and membrane lipids (e.g., phospholipids) [35], the components of the basic metabolic pathways that are required for life. When it comes to NP research, especially in the search for new drugs, the secondary metabolites are commonly the ones that are investigated [35]. These compounds are usually rather small (< 2000 Da) and their production is often limited to certain groups of organisms [35]. This distinction between primary and secondary metabolites is rather rough, and naturally, some compounds are difficult to place within one of these groups. In this "grey area" we can find several of the classical primary metabolites, like disaccharides and fatty acids, that are only produced by specific organisms under specific environmental stresses and cues, but also the classic secondary metabolites, like several steroids that are distributed among a large variety of organisms [35]. Since the process of producing secondary metabolites is energy consuming for the organism itself, evolution has favored the survival of organisms that produce secondary metabolites that indeed are beneficial. There are several reasons why organisms produce secondary metabolites, examples being as defense molecules against predating or competing organisms, or as signaling molecules [36, 37]. NPs have shown a diverse range of biological activities that are relevant to human health, including anticancer, antibacterial, antifungal and immunosuppressive activities.

1.3.2 Natural products and drug discovery

Humans have been using NPs for healing and medicine since before Christ, where the use of licorice (*Glycyrrhiza glabra*), myrrh (*Commiphora* species) and poppy capsule latex (*Papaver somniferum*) have been mentioned as medicinal herbs from Mesopotamia in 2600 BC [38]. The first commercial NP was morphine (E. Merck) in 1826, followed by among others the first semi-synthetic drug based on a NP, aspirin (Bayer) in 1899, both used as analgesics [39]. Then came the discovery of penicillin, which was followed by the discovery of several important antibiotics, including the β-lactam cephalosporin C from the *Cephalosporium acremonium* (now *Sarocladium strictum*) fungus, the aminoglycosides

(*Streptomyces* sp.), the tetracyclines (*Streptomyces* sp.), macrolides (*Streptomyces* sp.), and more. All the antibiotics mentioned were produced by microorganisms [38]. Nature has provided a plethora of molecules that have been used to improve human health, and other parts of human life. Of all new drugs approved from 1981 to 2019, only 24.6 % were purely synthetic compounds with no connection to NPs, while the rest were either biological macromolecules, unaltered NPs, botanical drugs, NP derivatives, synthetic drugs with NP pharmacophores, vaccines or mimics of NPs [38]. A complete overview of the different contributions can be seen in the Figure 3, clearly displaying the importance of NPs in drug discovery.

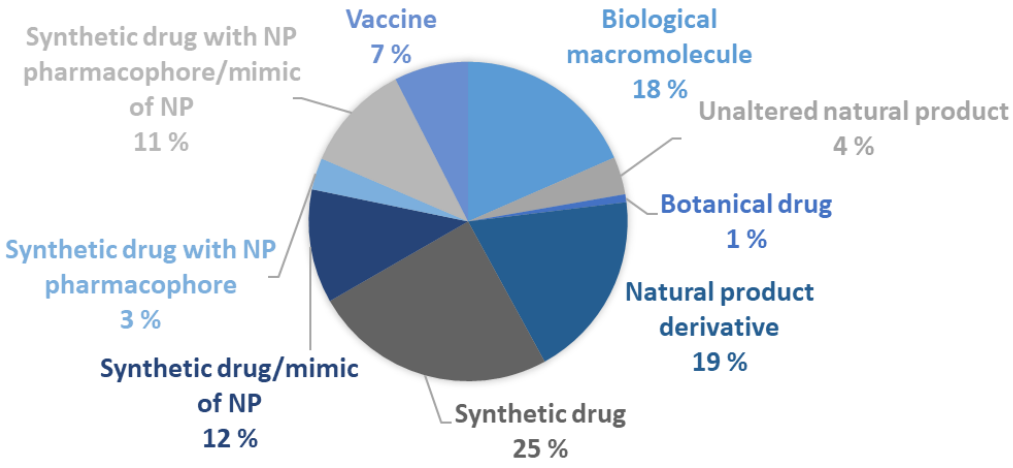

Figure 3: All new approved drugs from 01.01.1981 to 30.09.2019 (adapted from [40]). Only 25 % of all drugs in this period are of direct synthetic origin. The remaining 75 % are all connected to NPs, for examples as derivatives, mimics or by incorporating NP pharmacophores.

Common issues in NP drug discovery, such as low yields and re-discovery of known compounds, led to a shift from NP drug discovery and into synthetic chemistry/combinatorial chemistry during the 1980s. More knowledge of relevant molecular targets and the development of high throughput screening (HTS) methods also fed into this shift, as design and synthesis of compounds could be target-focused and could provide a large panel of compounds to screen [41-43]. However, the shift to combinatorial chemistry and HTS did not yield the expected increase in number of new drugs, which might be partially due to unrealistic expectations [41]. In contrast to synthetic compounds, NPs have developed through evolution to interact with their targets and to give some kind of ecological benefit to their producing organism [41]. As most drug targets are proteins or nucleic acids, consisting of the same building blocks as the ecological targets of the NPs and the same building blocks as the biosynthetic enzymes producing NPs, NPs have evolved towards interacting with similar targets [41, 44]. Because of this, NPs occupy a biologically relevant chemical space making them good starting points for drug discovery [42].

1.3.3 Classification and chemical properties of natural products

Natural products can be classified in several ways based on e.g., structural or functional properties, biosynthetic production pathway or source organism. However, with the complexity of NP structures, many compounds fit into several classes, so called hybrids, like the polyketide – non-ribosomal peptide (PK-NRP) hybrids. Even though NPs are highly variable in structure, the main building blocks in their biosynthesis is somewhat limited, with examples being isoprene units (terpenoids and steroids) and acetyl co-enzyme A (polyketides and fatty acids). The following classification of secondary metabolites is based on Hanson (2003) [45]:

- Polyketides and fatty acids: combine acetate units, derived from acetyl co-enzyme A
- Terpenoids and steroids: formed by isoprenoid C_5 units
- Phenylpropanoids: contains phenylpropanoid (C_6-C_3) units
- Alkaloids: large group built by different constituents, all containing nitrogen, often derived from amino acids such as lysine and tryptophan. Many contain piperidine, isoquinoline or indole structures
- Specialized amino acids and peptides: built by amino acids (regular and special)
- Specialized carbohydrates: different building blocks. Often attached to natural products, producing for example glycopeptides

Even though the NPs stem from a limited group of building blocks, the subsequent enzymatic modifications, such as cyclization, methylation and halogenation, is resulting in a high chemical diversity with different chemical scaffolds. Figure 4 shows some examples of NPs from the different structural classes. As shown in the figure, NPs have a wide diversity of structures and sizes. Compared to compounds from synthetic screening libraries, natural products often have higher molecular weight, higher oxygen content, contain fewer nitrogen, halogens and sulphur atoms, and contain a higher number of ring structures and chiral centers. NPs are more sterically complex than synthetic compounds [46, 47], and drugs based on NPs occupy a larger chemical space compared to synthetic drugs [48]. This chemical complexity of NPs is difficult to reproduce in synthetical compound libraries, and these features make NPs difficult to work with (e.g., complex structures and difficult synthesis), but it is also these features that make NPs relevant in drug discovery and development.

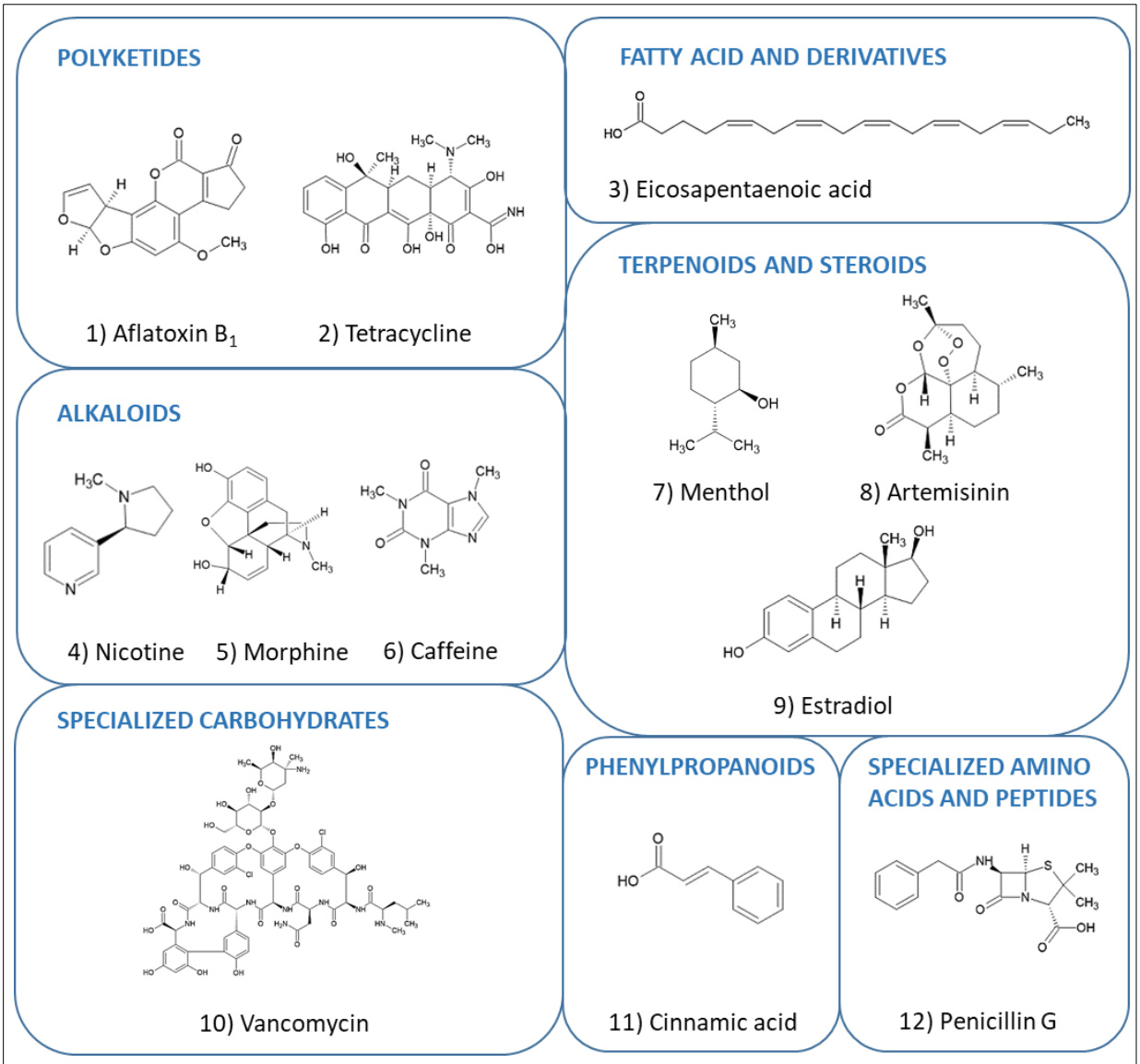

Figure 4: Examples of natural products and their importance to human life [45].

Polyketides: 1) The aflatoxins are polyketides that are highly toxic, produced by *Aspergillus* spp. molds. Here represented with the highly carcinogenic aflatoxin B_1. 2) The tetracycline antibiotics are produced by *Streptomyces* spp. bacteria, here represented with tetracycline.

Fatty acids and derivatives: 3) Eicosapentaenoic acid is a marine omega-3 fatty acid, often introduced to the human diet via oily fish or fish oil supplements, as it is believed to reduce the chances of cardiovascular disease.

Alkaloids: 4) The toxic alkaloid nicotine, produced by the tobacco plant *Nicotiana tabacum*, is the major neuroactive component of tobacco smoke. 5) Morphine, produced by the poppy plant (*Papaver somniferum*), is used in pain medication by affecting the central nervous system. 6) Caffeine, produced by the *Coffea* plant, is a stimulant of the central nervous system and is the causative agent of coffee which has beneficial properties like reducing drowsiness.

Terpenoids and steroids: 7) Many essential oils are terpenoids, among them is menthol, found in field mint (*Mentha arvensis*), which has local anaesthetic and refreshing effects. 8) Artemisinin, from the plant *Artemisia annua*, and semisynthetic derivatives are used to treat malaria caused by *Plasmodium falciparum*. 9) The steroids are derived from tetracyclic triterpenes. The estrogen steroid hormone estradiol is the major female sex hormone, and it is essential for female sexual characteristics and female reproduction.

Specialized carbohydrates: Most sugars are typical primary metabolites, but often sugars are attached to NPs forming glycosides, such as glycopeptides and glycolipids. 10) The glycopeptide antibiotic vancomycin, produced by *Amycolatopsis orientalis* is used in the treatment of different infections such as bloodstream infections and meningitis.

Phenylpropanoids: 11) Cinnamic acid is produced by a number of plants, and is used as a flavor additive, in the perfume industry and it is the precursor for the sweetener aspartame which is commonly used in diet soda.

Specialized amino acids and peptides: Many important compounds arise from the specialized amino acids and peptides, and several of these are today used as drugs. 12) The penicillins are a group of antibiotics, usually obtained from different *Penicillium* species, here represented with penicillin G.

1.3.4 Protection of natural resources

As an increasing number of countries are getting involved in bioprospecting activities, more and more areas of the earth are being investigated, and the world is progressing towards a bio-based economy. Laws and legislations have been put into place to maintain fairness between the user and the provider, and to facilitate safe use of natural resources [32]. Two of these incentives will be mentioned here: the Convention on Biological Diversity (CBD) [49] and the Nagoya Protocol on Access to Genetic Resources and the Fair and Equitable Sharing of Benefits Arising from their Utilization to the Convention on Biological Diversity [50] (Nagoya Protocol for short), which were implemented in 1993 and 2014, respectively. The CBD and the Nagoya Protocol have been implemented to ensure fair and equitable sharing of the benefits arising from the utilization of biological resources and traditional knowledge. The main objectives of the CBD are as follows [49]:

1. The conservation of biological diversity
2. The sustainable use of its components
3. The fair and equitable sharing of benefits arising from the utilization of genetic resources

The Nagoya Protocol is regarded as a supplementary agreement to the CBD, with the aim of advancing the implementation of the third objective, by providing a stronger basis for legal certainty and transparency with regards to genetic resources, both for the user and the provider. The protocol also aims to ensure that when traditional knowledge from indigenous and local communities are utilized, this should bring back benefit to these communities [50].

1.4 The marine environment

The ocean is one of the most diverse and largest habitats on Earth, covering about 70% of the Earth's surface. Life in the oceans has evolved for 3.7 billion years [51]. It has been estimated that there exist about 2.2 million (range 0.3-10 million) eukaryotic [51-53], and between 1 million to 3.0 x 10^{27} prokaryotic [51] species in the ocean. Of the 34 major animal phyla, 33 can be found in the ocean, in comparison to the 12 phyla that have been recorded in terrestrial habitats [51]. Still, many marine organisms are yet to be discovered, due to issues of both sampling and access (caused by the harsh realities of the ocean habitat with e.g., extreme depths) and low cultivability of marine microorganisms. It has been estimated that marine microorganisms account for approximately 70% of the total marine biomass, with the remaining 30% mainly being arthropods and fish [54]. Our knowledge on biomass distribution is limited by our ability to sample biomass in certain environments, such as the deep subsurface environments, and there still are major gaps in our understanding of the biosphere [54]. Even though the marine environment is highly diverse, it is still largely unexplored, also when it comes to bioprospecting for interesting molecules and products [6, 55].

Investigating unexplored ecosystems enhances the chances of finding novel organisms producing novel compounds, like new antibiotics [6, 11]. With the oceanic environments there is another effect to take into consideration, the dilution effect. It is believed that because the marine NPs (MNPs) are released into the ocean and are highly diluted, the MNPs have to be especially potent to have the desired effects on their targets [6, 56]. There are many factors in the marine environment that makes it a special habitat, including areas with either high and low temperatures, osmotic and hydrostatic pressure, availability of sunlight, radiation, oxidative stress, nutrient availability etc. Psychrophilic organisms that thrive and proliferate at low temperatures have several challenges that they need to tackle because of the nature of their cold habitat. These include decreased membrane fluidity, decreased rates of cellular processes like transcription, translation and cell division, and reduced enzyme activity. To survive these challenges, cold-adapted organisms have evolved features to overcome this to enable their growth in this extreme environment [57].

1.5 Microbes as producers of natural products

As exemplified by the antimicrobial drugs, microbes have been important contributors to NP discovery. In addition, many of the compounds that have been isolated and reported from macroorganisms in the past are now believed to be produced by symbiotic microorganisms [58-60]. Ecteinascidin 743 (ET-743, Yondelis), a chemotherapeutic NP was isolated from the Caribbean mangrove tunicate *Ecteinascidia turbinata*. After suspicions that the compound had a bacterial producer, metagenomic DNA was isolated from the tunicate, revealing the bacterium *Candidatus Endoecteinascidia frumentensis* as the true producer of ET-743 [61, 62]. Supply of sufficient amounts of compound is a common issue in NP discovery. Due to low production yields, ET-743 is now produced semi-synthetically, using cyanosafracin B, a fermentation product of *Pseudemonas fluorescens*, as the starting point [63]. Often, large amounts of biomass are needed to obtain enough of NPs for thorough investigation. An advantage of NP discovery from microorganisms is the possibility to continuously produce more of the compound(s) of interest, if the microbe is in fact cultivable in the laboratory.

One of the biggest issues with microbes in NP discovery is that many of them are difficult to grow under standard laboratory conditions, leading to only a small proportion of the microbial diversity being studied for their biosynthetic potential. This challenge is related to *the great plate count anomaly* that describes the discrepancy between the number of cells from natural environments that form colonies on agar media and the number of cells countable by microscopic examination or from studies on sequencing environmental DNA [64, 65]. It has been estimated that in the marine ecosystems, only 0.01 to 0.1 % of all bacterial cells produce colonies by standard plating techniques [64, 66]. Different microorganisms need different factors to grow, for example specific nutrients, pH conditions, incubation temperatures or signaling molecules [64, 67]. One way to increase the biodiversity of isolated microorganisms is to

limit overgrowth of fast-growing microbes that are not of interest. Using sub-minimal inhibitory concentrations (sub-MIC) of antibiotics in the media used for isolation of the microorganisms is one way of doing this [68]. Laboratory cultivation techniques need to be targeted and adjusted towards the microorganisms that we are interested in studying.

1.5.1 Marine microorganisms as producers of natural products

In 2019, 1490 new marine natural products (MNPs) were described in a total of 440 papers. Almost half of the new MNPs isolated in 2019 were isolated from marine fungi [69]. Figure 5 shows the number of new compounds per year from different marine sources for the period 2015 to 2019 [69], clearly showing a trend with marine fungi as the biggest source of reported MNPs over the last couple of years. For marine-sourced bacteria, the number of new metabolites has stabilized at around 240 per year, with the greatest source of new metabolites being the genus *Streptomyces*, representing 62.5% of the total bacterial MNPs reported in 2019 [69]. For the marine fungi, the genera *Aspergillus* and *Penicillium* have proven to be highly prolific regarding new MNPs [69-71].

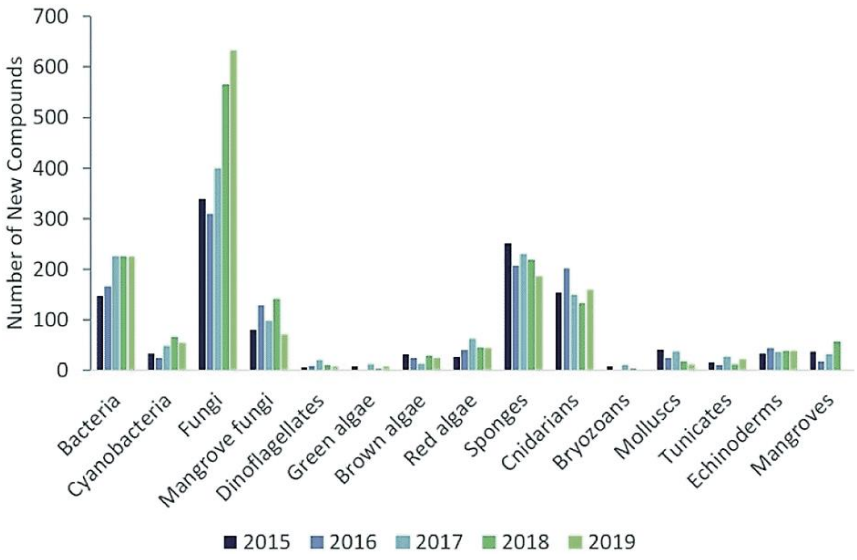

Figure 5: Numbers of new marine natural products from 2014 to 2019, and their sources (modified from [69]).

1.5.2 Biosynthetic gene clusters

Biosynthetic gene clusters (BGCs) are gene clusters that encode large, multi-domain and multi-modular enzymes [72]. The BGCs commonly encode genes for a set of biosynthetic enzymes that perform enzymatic reactions, leading to the production of a compound [42]. Herein, two compound classes commonly produced by such biosynthetic enzymes in microorganisms will be mentioned, the polyketides (PKs) and the non-ribosomal peptides (NRPs). **The PKs** is a major biosynthetic compound

class within microbial natural products. Examples of PKs include compounds that have been beneficial for humankind (e.g., the antibiotic erythromycin A and the cholesterol lowering agent lovastatin) and others that are not suitable for human consumption (e.g., aflatoxin B_1, which is a highly carcinogenic compound, and the cytotoxic compound maitotoxin). Characteristics for these compounds are high degrees of oxygenation, containing several ring systems and conjugated systems. The biosynthesis is performed by large multidomain enzyme complexes, polyketide synthases (PKSs), that form an assembly line of elongation and catalyze other reactions (e.g., reductions, oxidations, alkylation). The enzyme complexes are comprised of several domains, which each have different modules or enzymes with different functions that connect and modify the building blocks that eventually gives the final polyketide. For the PKs specifically, the starter building block is usually acetyl-CoA, and the elongation building block is usually malonyl-CoA, but some PKSs are also able to incorporate other building blocks [73]. This variation in modules and building blocks, together with the other catalytic reactions leads to a large variation in PKs produced in nature.

Like the PKs, the **non-ribosomal peptides (NRPs)** are synthesized by large multidomain enzymes, the non-ribosomal peptide synthetases (NRPSs) in an assembly line fashion [74]. The NRPSs do not depend on messenger RNA (mRNA) for peptide synthesis. Another difference between ribosomal and non-ribosomal peptide synthesis is the building blocks. While the ribosomes are restricted to 20 proteinogenic amino acids, the NRPSs can incorporate more than 500 different building blocks into the NRPs [75]. The NRPSs need carrier protein domains, the peptidyl carrier protein, for activation and attachment of the specific amino acid and for transport of the peptide intermediated between the different catalytic domains. The incorporation and modification of residues is performed by the catalytic domains found in the modules. Some key catalytic domains are the adenylation domain and the condensation domain, which are responsible for activating and catalyzing peptide bond formation. In the final module, the thioesterase domain cleave of the final product. NRPs are often highly modified, which can be done by additional integrated domains, or after the NRPS process has finished. Some examples of modifications are epimerizations (transformations of L- amino acids to D- amino acids) and methylations [74]. NRPs have been important in treatment of human diseases and infections, with examples like vancomycin (antibacterial), bleomycin (antitumoral) and cyclosporine (immunosuppressant) [76]. The main producers of NRPs are bacteria and fungi. It was thought that some higher-order organisms could produce these compounds, but this hypothesis has been weakened due to presence of symbiotic microbes that are the true producers [76]. Genome sequencing has revealed the *Actinobacteria* as the most prolific contributors, followed by *Firmicutes*, *Cyanobacteria* and some classes of *Proteobacteria*. In the fungal world, the members of the phylum *Ascomycota* are the most prolific NRPs producers [76]. In addition to the PKs and the NRPs, there are examples of PK-NRP hybrids, giving rise to compounds like rapamycin, bleomycin and the mycotoxin fusarin C [77]. Figure 6 shows the domain architecture and the structure of the antifungal PK-NRP hybrid dihydromaltophilin.

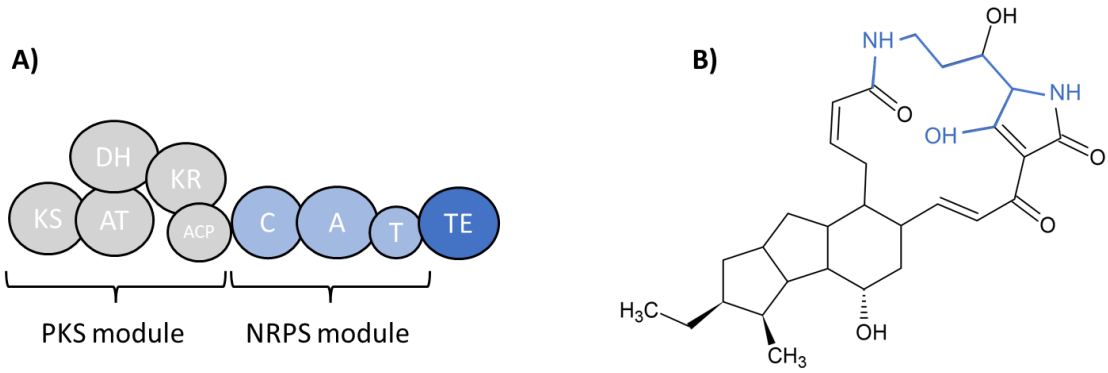

Figure 6: Domain architecture of the bacterial iterative hybrid PKS-NRPS(**A**) and the final biosynthesis product dihydromaltophilin (**B**) (modified from [78]). Dihydromaltophilin was first isolated from a *Streptomyces* sp. bacterium [79], but has also been produced by *Lysobacter enzymogenes* [80]. The compound has antifungal activity [79] against several fungal species, caused by the disruption of sphingolipid biosynthesis [80]. Abbreviated domains: KS – ketosynthase, AT – acyltransferase, DH – dehydratase, KR – ketoreductase, ACP – acyl carrier protein, C – condensation domain, A – adenylation domain, T – thiolation domain (also called PCP – peptidyl carrier domain), TE – thioesterase. Incorporated amino acids are shown in blue (**B**).

1.5.3 The One Strain Many Compounds (OSMAC) approach

The production of NPs is highly regulated, and NPs are often only produced under certain conditions. Since many of these conditions often are not used in standard laboratory cultivation, these clusters are silenced, meaning that the compounds are not produced in the laboratory cultures. There are several strategies that have been used to trigger expression of these clusters. The one strain, many compounds (OSMAC) approach is one such strategy. The OSMAC approach was introduced by Bode and colleagues, and it was defined as "*the systematic alteration of easily accessible cultivation parameters in order to increase the number of secondary metabolites available from one microbial source*" [81]. This can be achieved by alterations in the cultivation framework (e.g., media composition, temperature and culturing vessel), or by for example mimicking the natural environmental conditions from which the microorganism was isolated [81]. Another approach to trigger the expression of more gene clusters is by co-cultivation of two or more microorganisms, or microorganisms together with a macroorganism. An example of the OSMAC approach from the marine world is the study on chitin-degrading *Vibrionaceae* bacteria, often found in association with chitin-containing organisms [82]: The transcriptome and metabolite profile of two antibiotic-producing bacteria from the *Vibrionaceae* family were studied by comparing cultures where the carbon sources were either glucose or chitin. The transcriptomics data showed that genes involved in chitin metabolism and genes involved in secondary metabolism were upregulated, they also saw that the two antibiotics andrimid and holomycin were produced in larger amounts in cultures grown with chitin as the carbon source [82]. This is a typical example of how ecological perspectives can be used to aid in the development of a cultivation strategy for the activation of BGCs. Through co-culturing of a marine-derived *Aspergillus versicolor* with *Bacillus subtilis*, four new and thirty known compounds were isolated, of which none were found in the

axenic cultures [83], showing the potential of co-cultivation as a technique for induction of secondary metabolite production.

1.6 Marine natural products as drugs

In 2016, 1277 new natural products with promising biomedical applications were described from the marine environment [84]. In a recent study by Voser and co-authors (2021), structural similarities between MNPs and terrestrial NPs were investigated, showing that 76.7% of the compounds isolated from marine microorganisms were closely related to compounds from the terrestrial counterparts (Figure 7) [44]. The authors also highlight that targeting the understudied marine phyla results in a higher likelihood of discovering marine-specific compounds [44]. Sea water has high contents of halogens, and marine organisms often tend to incorporate these into their MNPs [85, 86], therefore, halogenation (mainly bromination and chlorination) has become a common distinguishing feature of MNPs [44, 87]. However, it seems that this might not be as apparent for MNPs produced by marine microorganisms. The study showed that the bromine and chlorine content of the microbial MNPs was rather similar to that of their terrestrial counterparts, indicating that halogenation might not be such a distinguishing feature of microbially produced MNPs as it is for MNPs produced by macroorganisms [44].

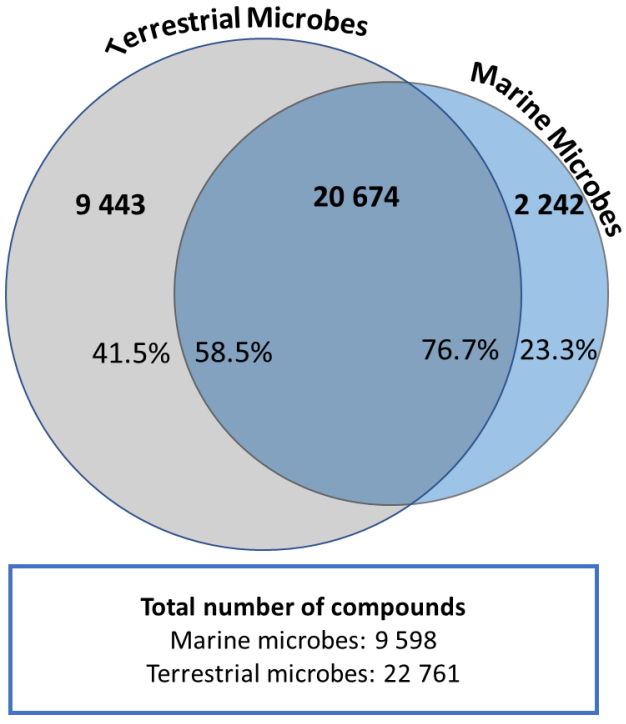

Figure 7: Visual representation of the overlap between marine (blue) and terrestrial (grey) microbial NPs (modified from [44]), with a total of 22 761 NPs from terrestrial microorganisms and 9 598 from marine microorganisms. The numbers shown in bold show the total number of NPs in each section. Percentages refer to the proportion of NPs from each biome, meaning that out of the 9,598 NPs isolated from marine microbes, 76.7% are closely related to terrestrial NPs.

Several MNPs have made their way from the laboratory into the clinic. According to the marine pharmacology clinical pipeline, there are 17 approved marine drugs (as of February 2022). Cytarabine and vidarabine were the first marine drugs to be approved for clinical use in the years 1969 and 1976 (FDA approval), respectively. Both are isolated from sponges and used in cancer treatment (Cytosar-U®, leukemia) and as an antiviral (Arsena A®, Herpes Simplex). The most recently approved marine drugs are belantamab mafodotin (brand name Blenrep™, isolated from mollusk/cyanobacterium), lurbinectedin (ZepZelca™, tunicate), disitamab vedotin (Aidixi™, mollusk/cyanobacterium) and tisotumab vedotin (TIVDAK™, mollusk/cyanobacterium), all used in cancer treatment [88]. There are currently no approved marine antibacterials on the marked, and most of the approved MNP drugs are used against chronic diseases, like certain types of cancer and hypertriglyceridemia. None of the approved drugs stem from marine fungi, but several originate from cyanobacteria [88]. In phase 3 clinical trials, there are two compounds originating from marine microorganisms: Plinabulin, isolated from a fungus and salinosporamide A (Marizomib) from a bacterium, both in clinical trials against cancer [89]. Also, in phase 3 clinical trials is plitidepsin, a depsipeptide isolated from a tunicate, which is currently in clinical phase III for treatment of covid-19 [89]. There are no marine antibacterial drugs in the clinical pipeline (phase 1-3) [89-91].

2 Aims of the thesis

The work in this thesis has been part of the DigiBiotics project (Box 3), with the overall aim of discovering antimicrobial molecules from Arctic marine resources. This PhD project was part of work package 1 – Biodiscovery, with the aim to isolate and characterize antimicrobial NPs produced by marine microorganisms. A selection of marine fungi and bacteria were cultivated under different conditions to induce production of interesting NPs. The secondary objectives of the project were to:

1. Identify extracts and fractions from cultures of marine microorganisms with antimicrobial bioactivity
2. Identify and dereplicate potentially bioactive compounds
3. Isolate compounds and elucidate their structures
4. Assess bioactivity of isolated compounds

Box 3: The DigiBiotics project

The DigiBiotics project is funded through Digital Life Norway (Research Council of Norway) and started in 2017. It is a research consortium at UiT working with digital discovery of antimicrobial molecules from marine Arctic resources with reduced risk of triggering resistance. The project is divided into six work packages:

- WP1: Biodiscovery
- WP2: Organic synthesis
- WP3: Optical spectroscopy and *ab initio* calculations
- WP4: NMR spectroscopy
- WP5: Molecular dynamics simulations
- WP6: Activity and resistance studies

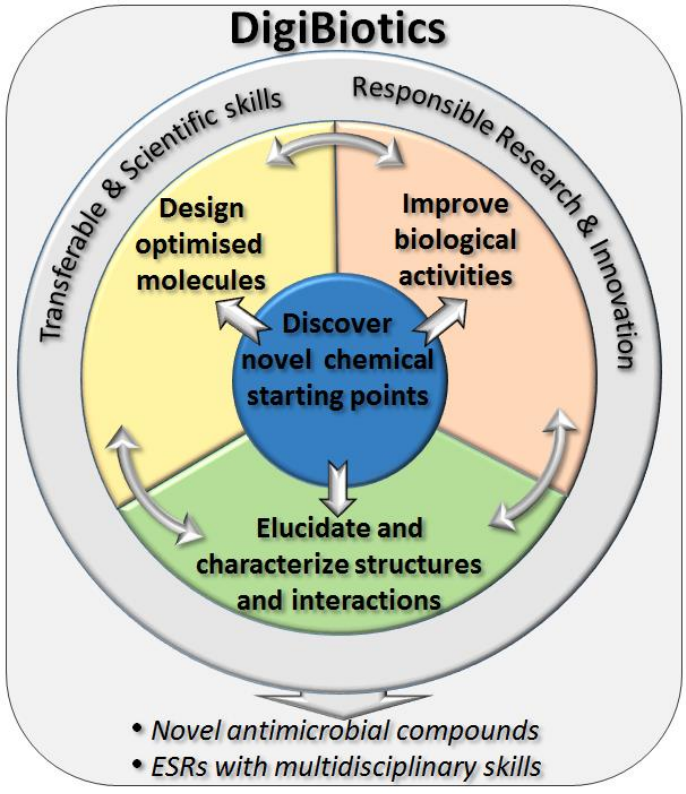

https://site.uit.no/antibiotics/sample-page/

3 Methods and techniques for bioprospecting of marine microorganisms

The general bioprospecting pipeline for marine microorganisms is illustrated in Figure 8. In the following sections, commonly used techniques and processes involved in NP discovery are described, focusing on the methods used in this thesis. This thesis is focused in the first steps of the NP discovery pipeline, the discovery phase, with hit identification and further characterization of the hit compounds. Some of the following processes in the pipeline, like mode-of-action studies, ADMET properties investigations and lead optimization will also be mentioned.

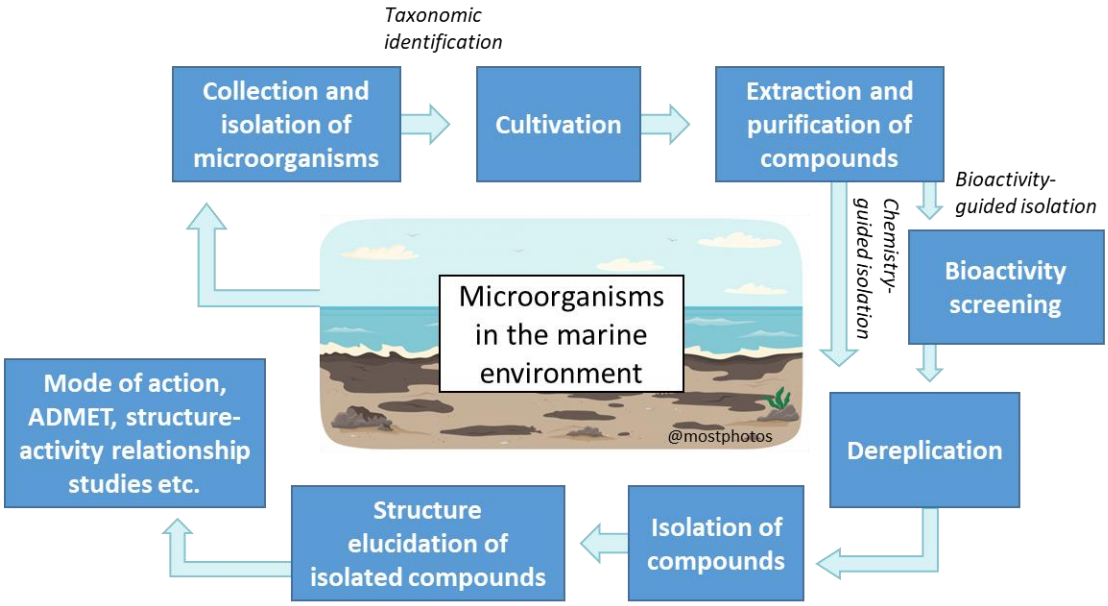

Figure 8: The pipeline for bioprospecting of marine microorganisms.

3.1 Isolation, identification, and cultivation of marine microorganisms

The microorganisms used in this project were provided by the Norwegian national marine biobank Marbank (bacterial isolates) and by Dr. Teppo Rämä (fungal isolates). The microorganisms were isolated from different marine substrates, like driftwood, macroorganisms and sediments, and preserved for further use in the bioprospecting pipeline. Different isolation techniques will select for different microbes. For example, by heating the sample to 60ºC, one can select for spore-forming bacteria like the *Actinobacteria* [92]. For taxonomic identification of the microorganisms, both in the initial isolation process and as a control during the pipeline, the 16S rRNA (bacteria) and internal transcribed spacer (ITS, fungi) regions were sequenced and compared to existing sequences in databases such as the National Center for Biotechnology Information (NCBI) non-redundant database, using the Basic Local

Alignment Search Tool (BLAST) [93]. Such regions, used for taxonomic placement, are often referred to as DNA barcoding regions. For bacteria 16S rRNA is the most commonly used barcoding region, and for fungi it is the ITS region which is most commonly used [68, 94, 95]. In this study, the microbes were cultivated under different conditions to induce expression of interesting gene clusters, including different media, static/non-static incubation, solid or liquid cultures etc. The parameters that can be altered are many, as mentioned in section 1.5.3 about the OSMAC approach. The aim of the cultivation is to trigger the production of compounds with interesting bioactivities that can be detected and brought further in the bioprospecting pipeline. The cultivation conditions that led to the isolation of compounds are mentioned in the publications that are included as part of this thesis. In addition to the published cultivation conditions, other tested conditions include different temperatures, different media (testing different carbon and nitrogen sources), culturing with wooden sticks (for fungi isolated from wood), static conditions vs. shaking, and solid vs. liquid cultivation media.

3.2 Extraction and purification of compounds

The next step in the pipeline is to extract compounds from the cultures. There are several ways of doing this, liquid-liquid extraction and liquid solid-phase extraction (SPE) being the most common ones. The choice of extraction method depends on which parts of the culture that should be extracted, and what types of compounds that are of interest. The microbial extract is a complex mixture of compounds, and prior to bioactivity testing, a pre-fractionation step can be performed to reduce the complexity of the sample. This is beneficial both because it can increase the concentration of the active compounds and it will make the following chemical investigation easier, with fewer candidates possibly responsible for any observed bioactivity [36, 37, 58]. In this study, pre-fractionation was done using flash chromatography, a high capacity and low-pressure liquid chromatography (LC) method [96]. LC techniques are used to separate compounds in a mixture based on different properties e.g., polarity, size or charge. One of the advantages of flash chromatography, compared to high-performance liquid chromatography (HPLC), is the high sample volume/amount that can be applied to the column, but the separation is much lower compared to HPLC. For the purpose of initial reduction of complexity, flash chromatography is an effective method. For the isolation of compounds, preparative HPLC is one of the most commonly used methods [97].

In this project, flash chromatography and reversed-phase preparative HPLC ultraviolet/visible – mass spectrometry (UV/vis-MS) were used for the isolation of compounds. HPLC-UV/vis-MS is a hyphenated technique, meaning that a separation technique (HPLC) is coupled to a spectroscopic or spectrometric detection technique (UV/vis and MS) [98]. This gives the opportunity to both separate compounds in a mixture and obtain information regarding their structure [98]. The isolation process can be based on different approaches, among them are bioactivity-guided isolation and chemistry-guided

isolation. In bioactivity-guided isolation (also called bioassay-guided isolation or fractionation), it is the bioactivity of an extract or a fraction that is guiding the dereplication and isolation [99, 100]. In chemistry-guided isolation, it is the discovery of interesting chemical moieties or features that is guiding the isolation [101]. To determine whether or not to isolate a compound, dereplication is an important step. This will be described in the following section.

3.3 Mass spectrometry and dereplication

As mentioned above, the use of hyphenated techniques (such as HPLC-MS) gives both separation of compounds in a mixture and information about the compounds. This is useful in NP discovery as it can provide information about the compounds in the extract or fraction, regarding for example novelty, prior to compound isolation [98]. For efficient NP discovery, an accurate and effective dereplication step is necessary. Dereplication is the process of eliminating further work on compounds that have already been studied [58]. The process usually combines a chromatographic (e.g., HPLC) separation with a spectroscopic/spectrometric detection of compounds in a mixture (e.g., MS), followed by database searches [102] of relevant NP databases such as the Dictionary of Natural Products and MarinLit [58]. In this way, one can avoid spending time on the re-isolation of well characterized compounds, and rather focus on the discovery of new ones. One of the most common set-ups for dereplication is by HPLC - high resolution MS (HRMS), which can provide the accurate mass and isotope pattern, used to calculate the elemental composition of a given molecular ion [102].

In this work, the dereplication step was performed using a Quadrupole Time-of-Flight (QToF) MS coupled to an ultra-high performance LC-system (UHPLC). The sample is first separated on the reversed phase UHPLC column. The compounds eluting from the column enter the ion source of the MS, which in this case uses an electrospray ionization (ESI) technique, where the molecules are converted into gas phase ions (both positive and negative ionization is possible) [103]. Usually, because we want to investigate the full complexity of a sample or to determine impurities in a purified sample, we use a method called MS^E [104], which is a data-independent acquisition mode [105]. Using MS^E, the quadrupole remains inactive, while two collision energies are used in the collision cell: low collision energy – ions remain intact, and high collision energy – ions are fragmented. The ions then travel from the collision cell and to the ToF MS, which records both precursor ion spectrum and fragment ion spectrum [104]. The ions are separated based on mass-to-charge (*m/z*) ratios, and the detected signals are used to produce a mass spectrum and a chromatogram. For each given peak in the chromatogram, it is possible to obtain the accurate mass and isotope distribution, which is used to calculate the elemental composition. The fragmentation data can be used for information of sub-structures in the molecule.

There are some common issues and difficulties with accurate dereplication using HPLC-MS [102]. Not all compounds are readily ionized in the MS [106]. Therefore, all compounds are not equally ionized using the different ionization techniques, which may give a flawed picture of the complexity or purity of a sample [102]. In addition, adduct formation is highly compound dependent [107, 108] and adduct determination is not always straight forward, and can lead to incorrect molecular mass assignment, and thereby wrongfully calculated elemental composition [102]. Adduct formation can also differ from instrument to instrument and is concentration dependent [102]. The formation of di- and trimeric ions can complicate molecular mass assignment, providing ions such as $[2M+H]^+$ and $[2M+Na]^+$, which are not always straight forward to detect [102, 108]. However, the presence of multiple adducts of a compound will indeed make it easier to determine its actual neutral mass. Lastly, some compounds are more likely to fragment during ionization (in-source fragmentation), losing for example H_2O, CO_2 or HCOOH, which again leads to wrongful assignment of molecular mass [102, 107, 108].

3.4 Structure elucidation

A combination of analytical techniques are usually applied to elucidate or confirm the structure of a NP. Such techniques include UV/vis spectroscopy, infrared (IR) spectroscopy, nuclear magnetic resonance (NMR) spectroscopy, as well as MS [36]. Briefly, if the compound of interest contains a characteristic chromophore, this can be detected using UV/vis. IR spectroscopy can provide information about the different functional groups present in the molecule, like aromatics, carbonyls and alcohols [36]. For full structure elucidation, MS and NMR experiments are usually needed. The MS will give information of the elemental composition and fragmentation patterns of your molecule, which is usually available from the dereplication of the compound. The NMR experiments give information on the number and types of elements in the molecule (usually focusing on protons and carbons), and how these atoms are connected to each other [36]. In brief, atomic nuclei with ½ spin number have properties making them suitable for NMR analysis. These nuclei include ^{13}C and ^{1}H. The nuclear spin gives the nuclei magnetic properties, and their orientation can be manipulated by an external magnet. ^{12}C and ^{16}O are commonly present in a range of NPs, but as these nuclei do not possess spin, they will not give NMR spectra. Using ^{1}H-NMR as an example: The spinning proton nuclei have magnetic properties, so when an external static magnetic field is applied, the nuclei will align their orientation relative to the applied field (with or against the field of the magnet) [109]. Then, when a radio-frequency signal/pulse is applied to the system, the nuclei get to an excited state (from low-energy state to high-energy state) before they return to the relaxed state (back to low-energy state). The energy released by the different nuclei is recorded and processed into an NMR spectrum [109]. ^{1}H-NMR provides the following information [109]:

- **Chemical shift:** Provides information about the chemical environment of the proton, if it is for example close to an electron negative neighboring element pulling on the electrons, the signal will appear in the down/low field of the spectra.
- **Peak area/integral:** The peak area is proportional to the number of ^{1}H nuclei responsible for one peak.
- **Multiplicity:** The number of peaks present at the same chemical shift (multiplicity) provides information of the number of neighboring protons (n+1 rule).

NMR experiments can be classified into two major categories: One-dimensional NMR techniques, such as ^{1}H NMR and ^{13}C NMR where you study one nucleus, and two-dimensional NMR techniques such as Heteronuclear Single Quantum Correlation (HSQC), which gives information on proton-carbon connectivity and Heteronuclear Multiple-Bond Correlation (HMBC) which gives information on heteronuclear correlation across multiple bonds [36]. The NMR experiments, interpretation, and structure elucidation for the work of this thesis was done by Johan Isaksson and colleagues at the Department of Chemistry at UiT. Once the structure of the compound has been elucidated, the bioactivity must be re-assessed for the pure compound.

3.5 Bioactivity testing

Bioactivity testing is an important step of the bioprospecting pipeline, where the aim is to identify biologically relevant activity of a sample. Testing of bioactivity occurs at several stages in the bioactivity guided isolation pipeline, with testing of extracts, fractions, semi-purified samples and isolated compounds. The activities screened for can be any relevant biological activity, such as anti-cancer, anti-diabetic or antimicrobial. High-throughput screening is a large-scale experiment where a library of compounds is tested for biological activity [110]. There are two main types of assays; phenotypic (also called whole cell or functional assays) or target-based assays (also called receptor-based assays). In phenotypic assays, the effect of the sample is measured on cells, tissues, or whole living organisms, and it is the effect on the whole system that is measured, meaning that you do not know what target is being affected. With target-based assays it is the effect on a specific target e.g., a receptor or an enzyme that is measured. The phenotypic assays will give more information of how the compound will function in a complex system, with active signaling, nutrients and other factors, while target assays can say more specifically which target is affected. Phenotypic assays usually produce more hits than target-based assays [111], which is not unexpected since there can be several different targets in one phenotypic assay. For intracellular targets, the target-based assays will give more information about the effect on the target, while phenotypic assays will say something about the compounds ability to enter the cell.

In bioactivity guided isolation, it is the bioactivity of a given sample that guides compound isolation. Compounds that are active in NP bioactivity screening are **hit compounds** [110]. A hit compound is a compound that has the desired effect in a given assay, the activity is also confirmed by retesting and by generating dose-response curves [112]. The hit compounds are further assessed for important drug-like properties, such as lipophilicity (to assure movement across membranes), toxicity and solubility. Drug-like properties are properties that are crucial for a compound to become a drug, apart from bioactivity [112, 113]. The ADMET properties are a set of properties that are important to consider in drug discovery, and the term covers Absorption, Distribution, Metabolism, Excretion and Toxicity [113]. A successful drug should be able to cross intestinal walls, travel in the blood circulation, reach its target and stay sufficiently long to exert its activity on the target. The drug should also be eliminated from the body, so that it does not accumulate to toxic concentrations [113]. Oral bioavailability is an important property for most drugs, as it makes oral administration possible. The Lipinski Rule of Five were established to evaluate the oral bioavailability of a compound, and a set of properties were summarized as follows: <5 hydrogen-bond donors, <10 hydrogen-bond acceptors, molecular mass <500 Da and an octanol-water partition coefficient (logP) <5. Compound classes that are substrates for biological transporters are exceptions to the rule [111]. In conclusion, the rule-of-five is a way of predicting passive oral absorption [47], and is an approach to estimate solubility and permeability of compounds in the drug discovery and development setting [111]. It was highlighted that many antibiotics, antifungals, vitamins and cardiac glycosides violate the rule-of-five [111]. The reason for this is that natural products are more likely to resemble, or have similar structures, as the actual substrates, and can in that way be taken up by active transportation [47, 114]. It should be highlighted that the rule-of-five is only a guide for oral availability and does not say anything about biological activity of the compounds.

3.6 From hit to lead, and further to a marketed drug

Defining good hits is only the beginning of the developmental pipeline of a potential drug candidate (Figure 9). As part of the early stages of pre-clinical drug development, a hit compound will (most often) be structurally optimized through medicinal chemistry efforts. The resulting analogues are evaluated for their on- and off-target activities and their ADMET properties. This process aims to identify the pharmacophore of the hit and to identify parts of the compound that may be liable to degradation in the body, amongst other parameters. The compound with the most favorable overall properties is selected as the **lead** compound. This process is referred to as the lead generation or hit to lead process. Once a lead compound has been chosen, lead optimization follows. Lead optimization is similar to lead generation, however most of the time more analogs are produced, aiming at improving bioactivity, while also improving (or maintaining) the drug-like properties [112]. Structure-activity relationship (SAR) studies can be performed both in the hit to lead process and during lead optimization.

The goal of SAR investigation is to determine the core structure that is essential for the bioactivity of the compound (the pharmacophore) [112, 115]. During lead optimization, extended studies on the drug-like properties of the analogues is performed, such as studies of microsomal stability which gives information of compound clearance by the liver, or hepatotoxicity which is important as liver toxicity is a common reason for why some drug candidates fail to make it to the clinic [112]. All information about the lead compound is documented in the target candidate profile (also called target product profile), which is important to be allowed to continue with preclinical testing on animals and clinical testing on humans [8, 112]. If the goals for the lead optimization are achieved, the following steps are preclinical testing in animal models to assess *in vivo* safety and efficacy, followed by clinical trials in humans (phase I-III with increasing patient group size). If the compound is successful in the clinical trials and sufficient data is produced, marketing approval by approving agencies such as the Food and Drug Administration can be applied for, followed by marketing of the drug.

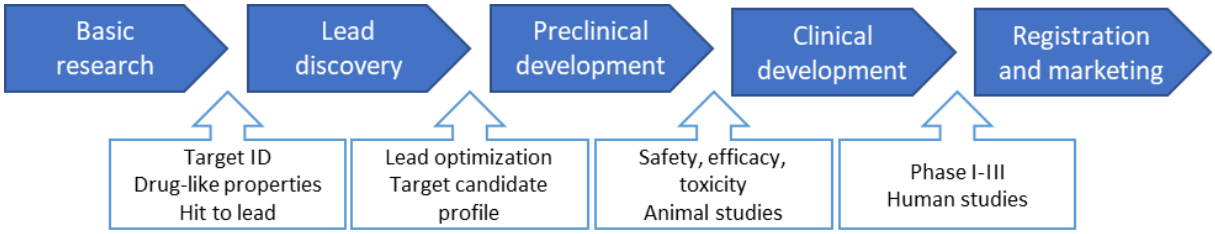

Figure 9: Extended pipeline for drug discovery, from basic research until registration and marketing [112]

4 Results – Summary of papers

4.1 Paper I

Bioactivity of Serratiochelin A, a Siderophore Isolated from a Co-Culture of *Serratia* sp. and *Shewanella* sp.

Yannik Karl-Heinz Schneider*, **Marte Jenssen*,** Johan Isaksson, Kine Østnes Hansen, Jeanette Hammer Andersen and Espen Hansen. *shared first authorship

Microorganisms, **2020**, *8*, 1042.

In this study, we isolated the siderophore serratiochelin A, from a liquid co-culture of marine-derived bacteria of the genera *Serratia* and *Shewanella*. The compound was not identified from axenic cultures of either of the bacteria. Siderophores are compounds with high affinity for ferric iron, and are often produced by bacteria to acquire iron in iron-limited conditions. Serratiochelin A (**1**) was produced in high yields in the co-culture when grown under iron-limiting conditions, and not produced when iron was added to the growth medium. During the isolation process, the degradation of serratiochelin A into serratiochelin C (**2**) was observed. The iron chelating properties of both compounds were assessed by mixing with aqueous $FeCl_3$ solution, which showed that both compounds chelated iron as detected by HRMS. Both compounds were verified by 1D and 2D NMR and HRMS, and the configuration of the threonine moiety in the molecule was established to be L using Marfey's analysis. Serratiochelin A had previously been isolated from cultures of *Serratia* sp., but to our knowledge, the antibacterial and antiproliferative activity of the compound had not yet been published. Both compounds were assessed for antibacterial effect against a selection of pathogenic bacteria and antiproliferative effect against two human cell lines. Antibacterial activity was detected for serratiochelin A against *S. aureus* with a minimal inhibitory concentration (MIC) of 25 µM. No activity was observed against the other assayed bacteria, and no activity was observed for the degraded variant serratiochelin C. Inhibition of biofilm formation by *Staphylococcus epidermidis* was also investigated, and serratiochelin A displayed weak activity (60% inhibition) at 200 µM. No biofilm inhibiting activity was detected for serratiochelin C with concentrations up to 200 µM. The effect on eukaryotic cells was evaluated against a human melanoma cell line (A2058), and a non-malignant lung fibroblast cell line (MRC5) included as a test for general toxicity. Serratiochelin A displayed weak activity against both cell lines, with stronger effect against MRC5 than A2058, but the compound was unable to completely inhibit the growth of the cells at any of the tested concentrations (up to 100 µM). No activity was observed by serratiochelin C against the human cells. In summary, serratiochelin A had activity against *S. aureus* and both human cell lines, while the degradation product serratiochelin C showed no activity in the assays performed. Specifically, the degradation is causing the hydrolyzation of the oxazoline ring in the compound. Oxazoline moieties can be regarded as privileged structures and compounds with such moieties have shown both antibacterial and antiproliferative activities previously.

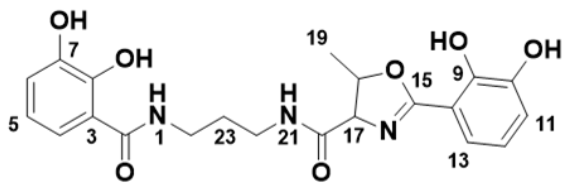

1

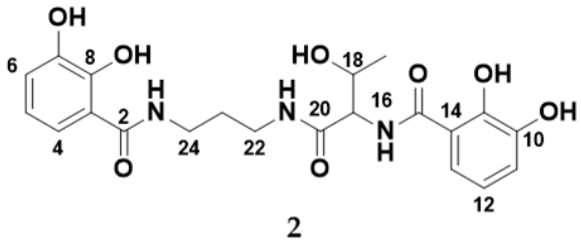

2

4.2 Paper II

Two Novel Lyso-Ornithine Lipids Isolated from an Arctic Marine *Lacinutrix* sp. Bacterium

Venke Kristoffersen, **Marte Jenssen**, Heba Raid Jawad, Johan Isaksson, Espen Hansen, Teppo Rämä, Kine Østnes Hansen and Jeanette Hammer Andersen.

Molecules, **2021**, *26*, 5295.

The *Lacinutrix* genus consists of 12 marine species isolated from both cold polar waters and warm waters. To the best of our knowledge, this is the first published study on the biosynthetic potential of these bacteria. Through bioactivity-guided isolation, two new lyso-ornithine lipids were isolated from the liquid culture of a *Lacinutrix* sp. bacterium originally isolated from a *Halichondria* sp. sponge collected in the Barents Sea. As the elemental compositions of the two compounds gave no relevant hits in database searches, the compounds were isolated by preparative HPLC-MS. The structures of the lipids were established by MS and NMR experiments and found to be iso-branched lyso-ornithine lipids, only differing in the length of the hydrocarbon tail as suggested by the elemental compositions: $C_{20}H_{40}N_2O_4$ for compound **1** and $C_{21}H_{42}N_2O_4$ for compound **2**. The chemical analysis of the compounds indicated that the bacterium produced different isomers of the lipids, suggesting that the purified solutions are isomer mixtures.

The compounds were assessed for bioactivity against bacteria and human cells. Against the bacteria, **1** had weak activity against *S. agalactiae*, with MIC between 100 and 150 µM. No activity was observed against the other bacteria, and no activity was observed by **2** against any of the bacteria. The cytotoxic effects against the human melanoma cell line A2058 and the non-malignant lung fibroblast cell line MRC5 was assessed, where **2** was active against A2058 with complete inhibition at 100 µM and 23% cell survival at 50 µM. No activity was observed against MRC5, and no activity of **1** was observed against the human cells. Lipoamino acids are reported to have various bioactivities, but this observed discrepancy in bioactivity was unanticipated since the compounds are structurally highly similar. This could be caused by the different isomers of the compounds or the difference in length of the fatty acid chain, as previous studies have shown a difference in bioactivity caused by minor differences in fatty acid chain length.

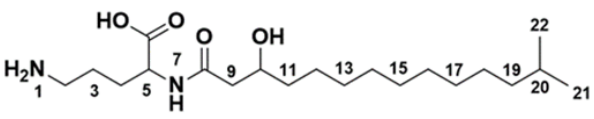

1

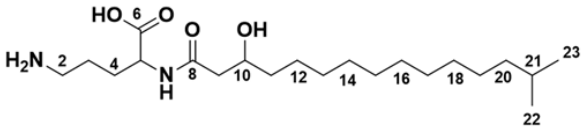

2

4.3 Paper III

Lulworthinone, a New Dimeric Naphthopyrone from a Marine Fungus in the Family Lulworthiaceae with Antibacterial Activity Against Clinical Methicillin-Resistant *Staphylococcus aureus* Isolates

Marte Jenssen, Philip Rainsford, Eric Juskewitz, Jeanette Hammer Andersen, Espen Hansen, Johan Isaksson, Teppo Rämä and Kine Østnes Hansen.

Frontiers in Microbiology, **2021**, *12*, 730740.

Marine fungi *sensu stricto* are under-represented in marine natural product discovery. In this study we describe the isolation of a new dimeric naphthopyrone, lulworthinone (**1**), from the liquid culture of a marine fungi from the strictly marine family *Lulworthiaceae*. Lulworthinone represents the first compound reported from this family of fungi, and to the best of our knowledge the first compound reported from the marine order *Lulworthiales*. The structure of the compound is elucidated by spectroscopic methods, including NMR and HRMS. Acid-catalyzed alterations of the compound was observed during the purification process leading to the identification of the degradation product compound **2**, which made us change our purification strategy to avoid degradation. The NMR experiments also indicated aggregation of lulworthinone (**1**), which was not observed in the presence of acid (**2**). The compound was produced in high yields by the fungus (~45mg/mL) and was isolated using flash chromatography with non-acidified solvents. Lulworthinone was assessed for bioactivity against bacteria, *Candida albicans* and human cells. In the antibacterial growth assay, the compound was tested against reference strains and clinical strains of relevant pathogens. The compound showed high activity against two of the Gram-positive reference strains, *S. aureus* and *S. agalactiae*, and against five clinical MRSA isolates with MICs from 12.5 down to 1.56 µg/mL. Against the two reference strains, it was investigated whether the activity was bacteriostatic or bacteriocidal, which indicated bacteriocidal effect of the compound. The compound was also tested for inhibition of biofilm formation against *S. epidermidis*, and activity was observed, but it was difficult to conclude if the activity was selective against biofilm formation or if it was actually reflecting growth inhibition. No activity was observed against established biofilm. The compound was tested, and had activity, against three of our in-house human cell lines, namely a melanoma cell line (A2058, IC_{50} = 15.5 µg/mL), a hepatocellular carcinoma cell line (HepG2, IC_{50} = 27 µg/mL), and a non-malignant lung fibroblast cell line (MRC5, IC_{50} = 32 µg/mL) which was included as a test for general toxicity. No activity was observed against *C. albicans*. The study shows that it is possible to isolate new compounds in high yields and with interesting bioactivity against some of our most problematic antibiotic resistant bacteria (MRSA is one of the ESKAPE pathogens) from marine fungi *sensu stricto*.

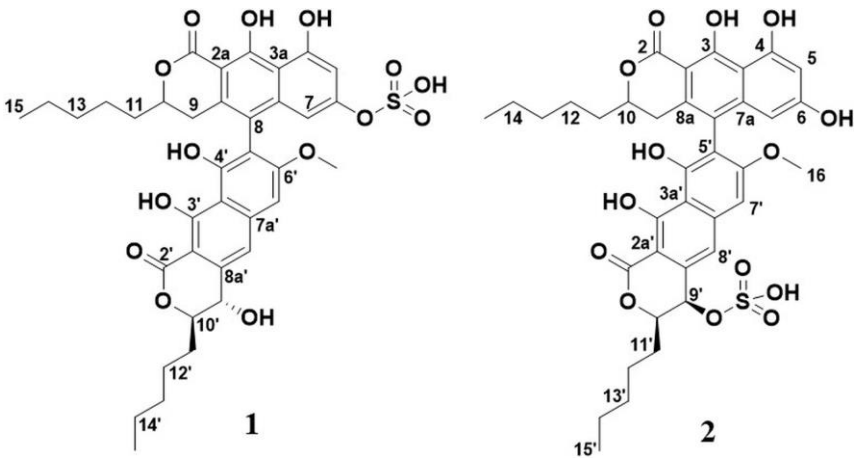

4.4 Paper IV

Chlovalicin B, a Chlorinated Sesquiterpene Isolated from the Marine Mushroom *Digitatispora marina*.

Marte Jenssen, Venke Kristoffersen, Kumar Motiram-Corral, Johan Isaksson, Teppo Rämä, Jeanette Hammer Andersen, Espen Holst Hansen and Kine Østnes Hansen.

Molecules, **2021**, *26*, 7560.

As part of our search for new bioactive compounds from understudied marine fungi *sensu stricto*, *Digitatispora marina*, a marine mushroom was isolated from driftwood, cultivated, and studied for its production of NPs. *D. marina* has previously been studied for its distribution in marine environments, but its biosynthetic potential has not previously been published. A new chlorinated sesquiterpene was identified and isolated from a liquid culture of the fungus, as the elemental composition gave no hits for known compounds in relevant compound databases. The compound structure was established by spectroscopic/spectrometric methods, including NMR and HRMS. The chlorinated compound, named chlovalicin B, shares its molecular scaffold with the previously isolated compound chlovalicin. The structure of chlovalicin B differs from that of chlovalicin by having the C3 position of the cyclohexane ring substituted by a methoxy group, while chlovalicin contains a hydroxyl group. To the best of our knowledge, chlovalicin is the first published metabolite isolated from *D. marina.* Chlovalicin B was assayed for a range of bioactivities including antibacterial activity, ability to inhibit biofilm formation, antifungal activity, and cytotoxic activity against human cells. The compound displayed weak cytotoxic activity against the human melanoma cell line A2058, ~50 % survival at 50 µM, otherwise no activity was detected.

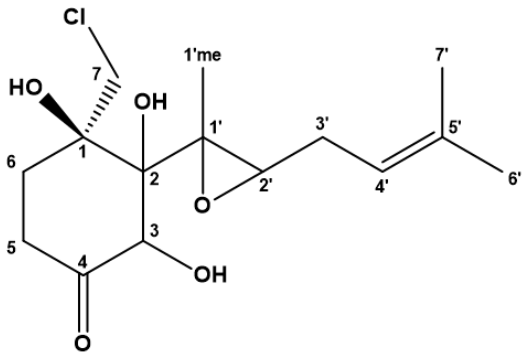

4.5 Graphical summary of papers

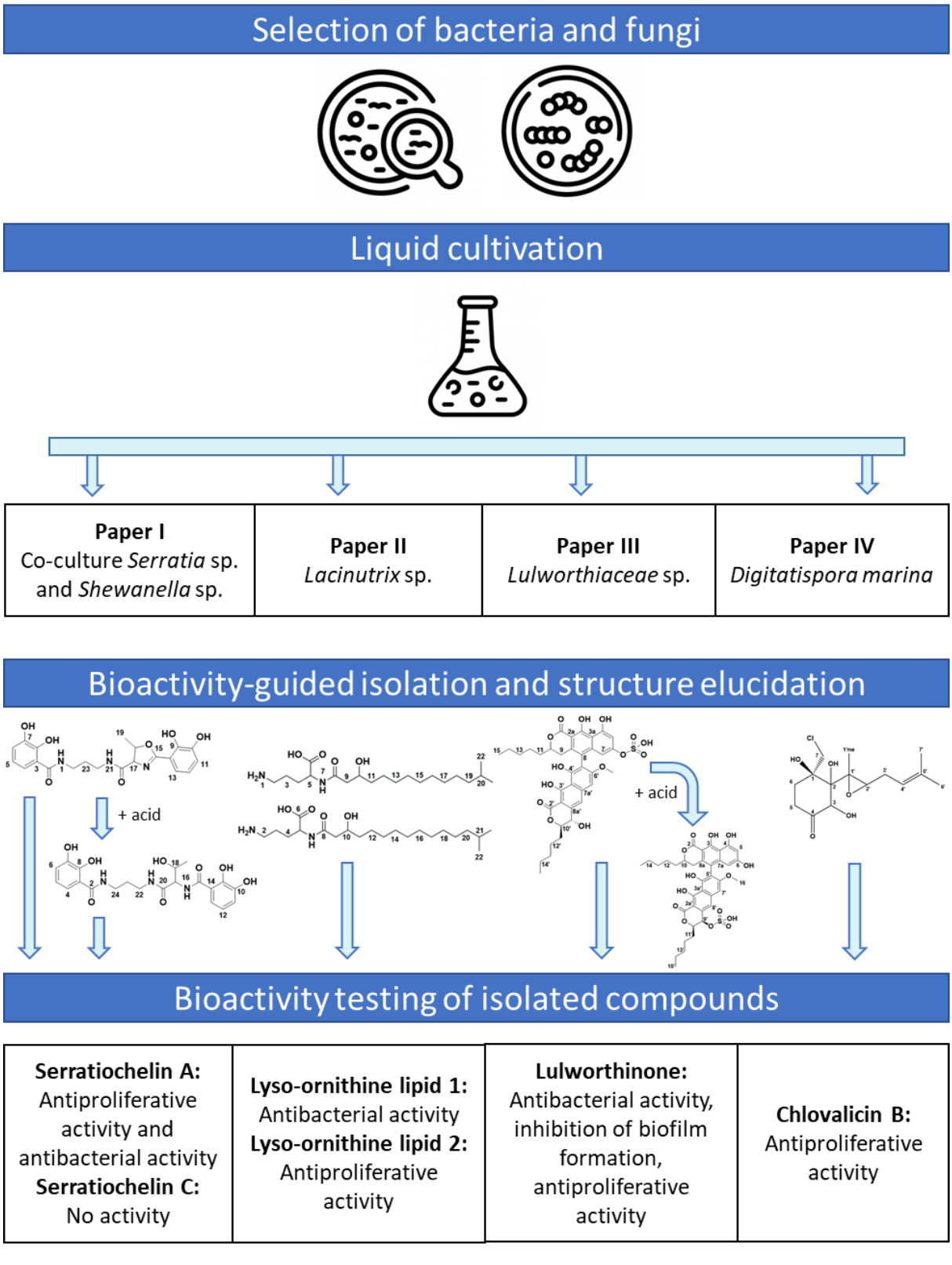

*Graphics from Mostphotos.com

5 Discussion

Throughout history, microorganisms have proven themselves as proliferative producers of bioactive NPs, in particular within the field of antimicrobials. The marine environment is rich in understudied microorganisms with high biosynthetic potential. Thus, the probability of isolating novel antimicrobial compounds from these organisms is high. Still, there are many hurdles and bottlenecks in the bioprospecting of marine microorganisms and in biodiscovery in general. The aim of this study was to isolate and characterize antimicrobial NPs produced by marine microorganisms. Marine bacteria and fungi isolated from Arctic and sub-Arctic regions were cultivated in an attempt to induce production of novel bioactive NPs. The cultures were extracted and fractionated, and the fractions were screened for bioactivity, mainly using antibacterial activity assays. The results from the antibacterial screening and chemical dereplication were used to guide the selection of compounds for purification. Following compound isolation and structural elucidation, purified compounds were assayed for relevant bioactivities. In the following section, some of the most common issues in bioprospecting of marine microorganisms, which have also been encountered in this project, are discussed. Some future perspectives on antibiotic development are also discussed.

5.1 Exploitation of microbial biodiversity

One strategy for increasing the chances to discover novel NPs through bioprospecting is by studying underexplored microorganisms. Many marine microorganisms are yet to be discovered and explored for biosynthetic potential. But what is a marine microorganism? Especially in the fungal realm, there is a lot of discussion surrounding the definition of marine fungi and what separates them from the terrestrial fungi. Has it been isolated from the marine environment, or is it dependent on, for example high salt contents for survival? The term “marine-derived” is popular, and its use has increased in natural product research. This term only indicates that a fungus has been isolated from the marine environment but does not specify whether it could also exist in terrestrial habitats. As fungi from different environments can end up in the sea, by for example river run-offs or by air currents, several common terrestrial fungi can naturally be found in the sea. The term “marine-derived” can give the impression that the marine aspect is vital for the survival of the fungus, and that it is essential to produce specific MNPs. Only rarely has it been investigated whether a microbe is dependent on the marine environment for survival, or if the NP is only produced under marine-like conditions. Several other terms have been used to describe the degree of dependence to the marine environment: marine fungi *sensu lato*, obligate marine, facultative marine, primary marine, secondary marine. The term marine fungi *sensu stricto* (synonymous to obligate marine) is a restrictive definition; fungi that exclusively carry out their life cycles in marine or estuarine habitats [116]. It represents an ecological group of fungi, spread across different parts of the fungal kingdom, which has not been thoroughly studied regarding their biosynthetic potential [116, 117].

Perhaps the question is not really whether a fungus is strictly marine, but rather if the full biodiversity of marine fungi is utilized in natural product research today. Most studies focus on a small group of fungi, mainly the genera *Aspergillus* and *Penicillium*, and to an extent *Fusarium* and *Cladosporium* [71]. The same can be said for the utilization of the full biodiversity of bacteria, where the by far most investigated bacterial genera are *Streptomyces* and *Bacillus* [118]. Maybe the biosynthetic potential of the microorganism is more important than from where it has been isolated [44, 118]? Obviously, the large phylogenetic diversity of marine microorganisms has not yet been extensively studied, especially the fungi that are regarded as marine fungi *sensu stricto* [44, 71, 116]. In 2014, only approximately 80 of more than 1000 isolated fungal MNPs were isolated from marine fungi *sensu stricto* [116], which supports the statement that the phylogenetic diversity of marine microorganisms remains understudied.

When combining data from two large NP databases, MarinLit and the NPAtlas, and assigning each compound to either marine microorganism or terrestrial microorganism, it became apparent that some groups of microorganisms are highly under-represented in NP research in general, and in marine discovery in particular [44]. The study showed that *Ascomycota* and *Actinobacteria* yielded 22 835 of the total 32 359 microbial NPs included in the analysis, and that of these 39.4% (*Ascomycota*) and 26.8% (*Actinobacteria*) were isolated from the marine environment [44]. This is not surprising, as the most studied microorganisms fall into these phyla [44, 71, 118]. On the other side, the fungal phylum *Basidiomycota* were the producers of only 3 766 compounds in the dataset, of which only 2.2% were isolated from the marine environment [44], indicating that marine *Basidiomycota* remain understudied. It might also be reflecting that *Basidiomycota* are less abundant, considering the number of different species in marine environments, compared to *Ascomycota* [119]. In this project, two marine fungi *sensu stricto* were studied for their biosynthetic potential, one *Basidiomycota* and one *Ascomycota*, and new compounds were isolated. This is covered in paper III and paper IV, with the discovery of lulworthinone from a fungus in the *Lulworthiaceae* family (phylum *Ascomycota*) and chlovalicin B from *Digitatispora marina* (phylum *Basidiomycota*). To the best of my knowledge, no compounds have previously been reported from either of these fungi. Due to the lack of focus on these groups of fungi, the access to barcode sequences and whole genomes are highly limited. This can make accurate identification difficult, as seen for the *Lulworthiaceae* fungus, where we chose to restrain from identifying the fungus to species or even genus. Some of the marine fungi *sensu stricto* have especially slow growth rates, like *Lulworthiaceae* sp. (paper III) and *Digitatispora marina* (paper IV), which were cultivated for more than 100 days prior to extraction. The studies on these two fungi show that marine fungi *sensu stricto* are capable of producing compounds with interesting chemistry and bioactivity, even in high yields, and that patience might be needed for their cultivation.

The bacteria responsible for the production of serratiochelin A (*Serratia* sp., paper I) and the two new lyso-ornithine lipids (*Lacinutrix* sp., paper II) belong to the phyla *Proteobacteria* and *Bacteroidetes*,

respectively. *Lacinutrix* sp. bacteria are exclusively isolated from marine sources, and no NPs have been reported from the genus before. Serratiochelin A was produced in a liquid co-culture of *Shewanella* sp. and *Serratia* sp., with *Serratia* being the most probable producer as the compound was previously isolated from this genus [120, 121]. *Serratia* sp. is omnipresent in nature, and is found in both terrestrial and marine environments [122]. Regarding the productivity of their phyla, *Proteobacteria* and *Bacteroidetes* produced 1938 and 151 NPs in the total 32 359 NP dataset, with 22.2% and 33.1% being isolated from marine microbes [44].

5.2 Sample supply and compound yield

In bioprospecting, gaining access to sufficient biomass to enable the isolation of NPs in amounts which allows structural and biological characterization can be challenging [37]. The anticancer compound halichondrin B, initially isolated from a sponge, was isolated in such poor yields that a synthetic route of production was chosen [123, 124]. After identifying that only specific fragments of the compound were needed to sustain the bioactivity (through SAR studies), eribulin was developed and is currently marketed under the tradename Halaven® (Figure 10) [125, 126]. Sustainable sampling to obtain sufficient amounts of biomass might not be possible without being highly intrusive and destructive to the ecosystem. Re-collection of invertebrate biomass is often not straight forward as it requires substantial economical investment to conduct a research cruise or excursion [37], and sample collection in the same area does not guarantee recollection of the same species. Furthermore, if the same species is collected, seasonal and other environmental differences may have altered the NP production of the invertebrate (or symbiotic microorganism), hindering re-isolation. Using cultivable microorganisms, one can circumvent this problem as the sample supply can be controlled under laboratory conditions. Still, in many cases the yield of the targeted compound is so low that isolation is not a feasible process.

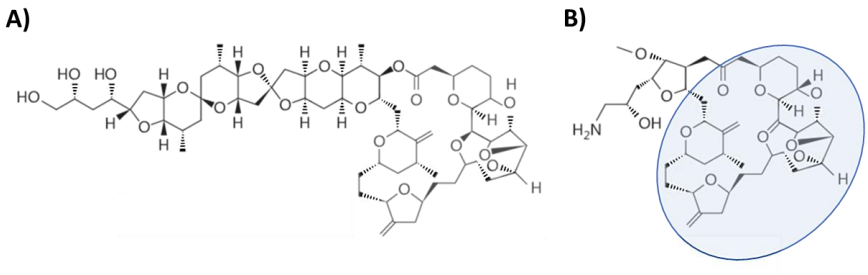

Figure 10: The structures of halichondrin B (**A**) and the anticancer drug eribulin (**B**) (modified from [127]). The blue circle shows the fragment of halichondrin B which was used to produce eribulin.

Five compounds were isolated as part of this PhD project, serratiochelin A (paper I), two lyso-ornithine lipids (1 and 2, paper II), lulworthinone (paper III) and chlovalicin B (paper IV). Table 1 gives an overview of the volumes of cultures, amounts and yields of each individual isolated compound, ranging

from lulworthinone with the highest yield of 45.6 mg/L to chlovalicin B with 0.02 mg/L yield. The isolation process has an impact on the obtained compound yield. For example, lulworthinone (paper III) bound strongly to the column material used in the preparative HPLC-MS system and eluted over several minutes. The compound also degraded/changed under acidic conditions, such as those used in preparative HPLC-MS. Because of this, the compound was instead isolated using flash chromatography. Serratiochelin A was also isolated using flash chromatography, due to degradation into serratiochelin C under acidic conditions. Chlovalicin B and the lyso-ornithine lipids were isolated using preparative HPLC-MS. Both displayed lower yields, and higher culture volumes were needed for isolation of sufficient compound amounts. Isolation of lulworthinone and serratiochelin A was possible using flash chromatography because of the high compound content in the respective samples, which was not the case for the other compounds, therefore isolation by flash chromatography would have been difficult. This shows that the isolation process must be adapted to each individual compound.

Table 1: Yields of compounds isolated as part of this PhD project

Compound (paper)	**Producing organism**	**Volume (L)**	**Amount (mg)**	**Yield (mg/L)**
Serratiochelin A (I)	Co-culture, *Serratia* sp. and *Shewanella* sp.	3.6	50.9	14.1
Lyso-ornithine lipid 1 (II)	*Lacinutrix* sp.	38.4	28.3	0.75
Lyso-ornithine lipid 2 (II)	*Lacinutrix* sp.	38.4	5.5	0.14
Lulworthinone (III)	*Lulworthiaceae* sp.	1.4	63.8	45.6
Chlovalicin B (IV)	*Digitatispora marina*	30	0.6	0.02

It is not only the isolation process that affects the yield of a compound, the cultivation conditions are also important. This is where the OSMAC approach and other cultivation schemes, such as co-cultivation, become relevant. In paper I, the siderophore serratiochelin A was only produced when the bacteria were grown under iron-limited conditions, and the compound was only produced in co-culture. This highlights the importance of cultivation conditions when studying a microorganism for its biosynthetic potential, and when optimizing compound production for isolation. As more and more microbial genomes are being sequenced, the use of genome-based approaches for NP discovery is increasing. See Box 4 for a brief description of top-down vs. bottom-up approaches in MNP discovery from microorganisms [128].

Box 4: Overview of top-down and bottom-up approaches to MNP discovery from microorganisms.

Top-down: The approach starts with the collection and isolation of microorganisms from the marine environment. The microorganisms are cultivated, and metabolites are produced, giving the metabolome. Compounds are then isolated through for example bioactivity- or chemistry-guided isolation, providing marine natural products.

Bottom-up: Also here, it starts with the marine environment, either through collection and sequencing of environmental DNA or by sequencing of isolated microorganisms from the environment, providing us with genomes (or other types of genomic sequences). Through genome mining, BGCs are identified. Interesting BGCs are expressed, either by heterologous expression or by genome editing approaches, providing us with the MNPs.

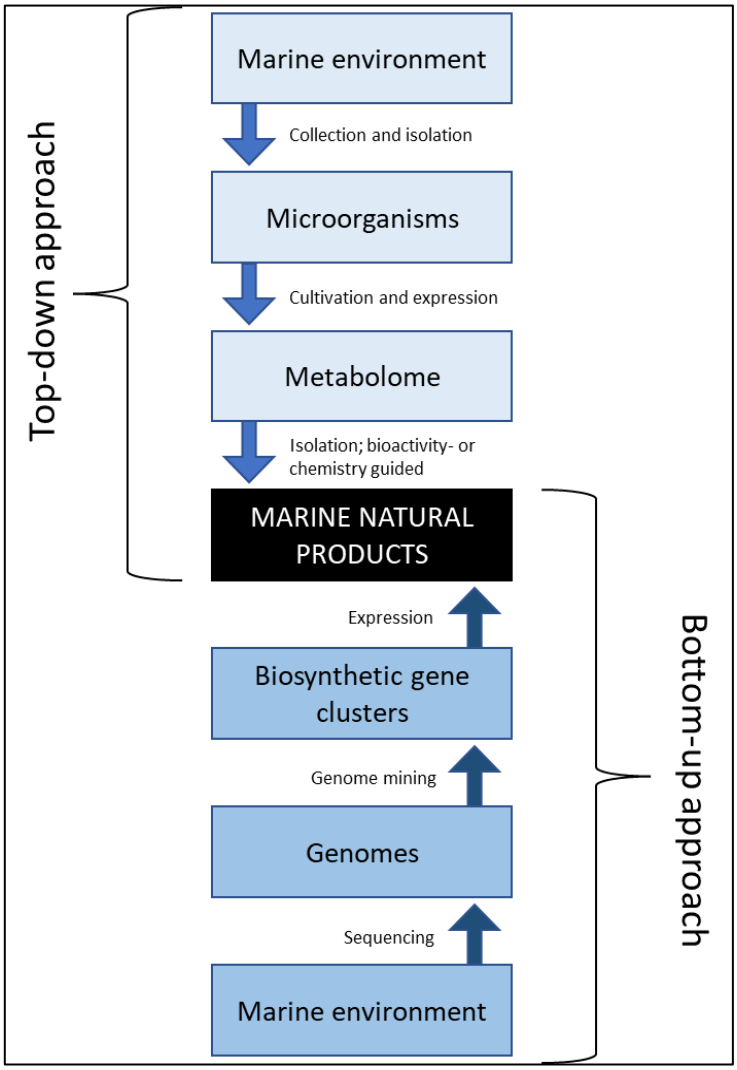

5.3 Chemical and biological characterization of NPs – errors in dereplication, natural product artifacts and PAINS

There are several steps in the chemical and biological characterization of NPs where you can end up getting misleading (or false) results. Dereplication is an essential step in NP discovery, as it helps to avoid re-investigation of known compounds [58]. The process of dereplication can be divided into two major steps: 1) Using an analytical technique to get information about the compound, HR-MS is often used for this purpose, giving the elemental composition of the compound. 2) Searching databases to investigate if the compound is known. As mentioned previously, there are some limitations to the dereplication process. During the dereplication of serratiochelin A (paper I), the compound lost one H_2O in the analysis process on the UHPLC-HR-MS (in-source fragmentation), which led to the assignment of the wrong molecular mass, followed by incorrect calculated elemental composition, which made the structure elucidation process more challenging.

Natural product artifacts that are generated in the extraction and isolation processes is a common issue in biodiscovery. This was observed in the isolation of the serratiochelins and lulworthinone (paper I and paper III) where acid-induced degradation of the compounds happened. The treatment and handling of NPs in the process of isolation can lead to the production of "un-natural products", so-called natural product artifacts [129]. The changes can be caused by small alterations in pH or temperature, exposure to light etc., and very often these changes are not recognized or highlighted in publications. In natural product discovery, there are many steps where the NP can be exposed to acidic conditions, for example during extraction, isolation, handling, and storage. For example, acidification of solvents used during isolation is very common, also some solvents can become acidic over time (e.g., DMSO). It is important to take into consideration what conditions the sample has been exposed to in the preparation steps and during chemical and biological analysis. Could it be that the compound is an artifact produced during sample preparation? If possible, it should be attempted to perform the operations at neutral conditions, reduce use of excessive heat and exposure to direct sunlight, but this is often not possible [129]. The reaction can also happen in the NMR tube, as seen with the conversion of euryspongin A, which after exposure to $CDCl_3$ in the NMR tube was dehydrated into dehydroeuryspongin A [130]. These artifacts are under-reported in literature, and possibly often misinterpreted as actual NPs. The knowledge of conditions that produce artifacts can also be used to generate new analogues, which can be used in SAR investigations [129], as was done for the serratiochelins (paper I). We observed that the hydrolyzation of the oxazoline moiety in the molecule made the compound lose its bioactivity against *S. aureus* and the human melanoma cells (A2058), meaning that the oxazoline structure was essential for bioactivity. Such information is important to determine structural elements that could be relevant in drug discovery and development. Going back to the example of euryspongin A: The artifact dehydroeuryspongin A inhibited protein tyrosine phosphatase 1B, which is a target enzyme for treatment of type II diabetes and obesity, while none of the "natural" euryspongins (A-C) had inhibiting effect on the enzyme [130]. Investigating the chemical samples at all stages of preparation (extract, fraction, isolated compound) can eliminate or reduce the chances of "missing" this formation. If the compound is not present in the original extract, it is highly likely that it is an artifact, though, the conversion could have happened already during extraction. Of course, the production of these artifacts can also take place in nature, as non-enzymatic transformation by, for example, acidic environments could lead to the production of the same compounds under natural conditions.

Bioactivity screening is a crucial step in bioactivity-guided isolation of NPs. Pan Assay INterference compoundS (PAINS) are compounds that give false hits in bioassays [131], where the activity is not caused by specific interaction between the molecule and its target [132]. This can for example be compounds that have non-specific activities and are therefore not interesting for drug discovery purposes. Such compounds will often have activity on different cells and against different targets and display promiscuous activity by acting on several unrelated targets. In our work, we have observed this

several times, with the identification of known compounds such as phosphocholines and rhamnolipids [133] in microbial samples. These compounds are known to have promiscuous bioactivity, and their activity might be caused by a membrane bilayer-mediated mechanism, indicating that their mechanism of action is caused by cell membrane perturbation, not specific protein binding. With proper dereplication, such promiscuous compounds should be identified, and further work terminated. Another example is metal binding compounds, whose activity might be caused by the sequestration of metal ions, which are essential for the function of several proteins, and not by actual interaction with any disease-related targets [132]. This might be the case for serratiochelin A (paper I), a known iron chelator, where we observed that the compound had activity against human melanoma cells (A2058) and the non-malignant lung fibroblasts (MRC5) but did not completely inhibit cell survival at any tested concentrations. Aggregation formation of compounds in aqueous solution (most bioassays are run in aqueous solutions) is also a problem, which can give false positives in the screens due to sequestration and nonspecific inhibition of enzymes by the colloid-like aggregates [134-136]. Compounds that form aggregates can lose activity if buffers or detergents such as Triton is added to the solution [134, 135]. In paper III, we discovered through the NMR experiments that lulworthinone formed aggregates. Further studies on how this might affect the antibacterial activity of the compound are being performed. Prior to choosing a compound for lead optimization, it is important to be certain that activity comes from specific and selective interactions with molecular targets [137].

5.4 The development of antibiotics

The road from hit to lead, and to an actual drug is long. One of the biggest problems of antibiotic discovery and development today is that if you develop a new antibiotic there is a dramatically low return of investment (if any), which has caused big pharma to leave this area of research. We need new incentives to take the bioactive compounds from the lab bench and into the clinic. A few countries are now in the forefront by launching pilot programs and passing bills to make the antibiotic business model more inviting [24]. In 2019, a UK pilot was launched, where two new antibiotics will be rewarded based on their value to society, not based on the volume sold, a so called Market Entry Reward [24]. A different pilot was launched in Sweden in where an annual amount is paid to the developers/producers if they fulfil specific requirements, like the effectiveness of a drug against multidrug resistant microbes etc. In this way, the developers are paid, even if zero packs of antibiotics have been sold and the countries have access to the antibiotic when needed [24, 138]. The PASTEUR act in the US is a subscription solution which also ensures revenue, even if the drug is not in use. In Norway, no similar actions have been taken yet, and today the financial model for antibiotics is based on prescription volume and unit price. During the “Trontaledebatt” in 2020 the government passed a unanimous call to the parliament to establish suggestions for new economic models for development of new and effective antibiotics which rewards

development, not sale and use, where different reward mechanisms (such as reduced fees and taxes) should be considered. All these incentives are indicating a worldwide political shift on the policies and regulations that affect antibiotic development, and hopefully it will lead to new antibiotics being introduced into the clinical pipeline during the near future. The number of antibacterials in phase I clinical trials in 2019 might indicate that these incentives are starting to have an effect, as there were twice as many antibacterials in phase I clinical trials in 2019 compared to 2015 [17].

The ESKAPE pathogen list, has been established to help focus the antibacterial discovery towards the infectious diseases that we struggle the most with today. Lulworthinone (paper III) showed potent activity against one of the ESKAPE pathogens, *S. aureus*. *S. aureus* is becoming an increasing problem due to increasing rates of infections by methicillin resistant *S. aureus* (MRSA). Lulworthinone was tested against several clinical MRSA isolates and had activity against all with MICs down to 1.56 µg/mL. The mode of action of lulworthinone is currently being investigated. Serratiochelin A (paper I) showed activity against *S. aureus*, with an MIC of 25 µM, but interestingly it was not active against the tested MRSA isolate. No activity was observed against Gram-negative bacteria during this project; not extracts, fractions nor isolated compounds have had any antibacterial activity against Gram-negative bacteria. Reduced treatment options of infections caused by Gram-negative pathogens is possibly the biggest problem we have in infectious disease treatment today, in addition to infections caused by *M. tuberculosis* [25]. It is the extra outer membrane of the Gram-negative bacteria that makes them more difficult to treat using antibiotics, as it functions as a permeability barrier, making it difficult for the antibiotics to penetrate the cell [13, 139, 140]. To stimulate the production of compounds with antibacterial activity against specifically Gram-negative bacteria, co-cultivation with either Gram-negative pathogens or Gram-negative bacteria isolated from the same environment could be tested. Also, addition of lipopolysaccharide, an important component of the Gram-negative outer membrane, might also be an option to stimulate production of such compounds. Addition of lipopolysaccharide in the cultivation medium has been shown to activate and enhance secondary metabolite production in fungi [141]. Currently, there are no approved antibacterials from marine sources on the market [88] and most of the MNPs that have been developed into drugs are for chronic diseases. This is a trend that is not exclusive for marine sourced drugs, but for drug development in general. With the increasing number of isolated MNPs with promising biomedical applications [84], the increased knowledge on isolation and cultivation of marine microorganisms, and the increased funding opportunities for antibacterial discovery, there is hope that new marine sourced antibiotics (and other drugs) will be taken to marked in the near future.

6 Future prospects

As shown by the four papers included as part of this thesis, marine microorganisms represent a good source for the discovery of novel bioactive compounds. In the study of serratiochelin A (paper I), we observed that it was the oxazoline moiety that was essential for the bioactivity of the compound, as the acid degraded variant serratiochelin B (oxazoline ring hydrolyzed) did not have any bioactivity in the performed assays. Compounds containing oxazole and oxazoline moieties in their structures have shown both antibacterial and antiproliferative effects [142, 143]. In NP discovery, it is not only the discovery of novel compounds that is of importance, but also uncovering structural motifs that are responsible for the observed bioactivity (privileged structures) is important for the development of nature-derived or nature-inspired compounds that can be developed for pharmaceutical use. As serratiochelin A is known and published, no further work on this particular compound will be prioritized. Serratiochelin A was only detected in samples from the co-culture, and not in axenic cultures. The work with co-culturing as a technique to trigger the production of secondary metabolites will continue, as this study clearly shows that co-culturing can induce secondary metabolite production. In paper II, we observed that the lyso-ornithine lipid samples contained several isomers. We attempted to separate the isomers, but this was not possible due to limited chromatographic resolution of the preparative column. As the compounds did not have any potent bioactivity and are common metabolites that are rather well studied, further studies will not be prioritized for these two lipids. Interestingly, the two lipids showed very different bioactivities, while being highly structurally similar only differing in the length of the hydrocarbon tail. Compound **1** showed antibacterial activity against *S. agalactiae* and compound **2** had activity against the human melanoma cell line (A2058). It could be that the difference in activity is indeed caused by the length of the hydrocarbon tail, but it might also be related to the fact that the samples were composed of a mixture of several isomers. These were to my knowledge the first published NPs from the marine bacterial genus *Lacinutrix*. Further work with this isolate should be considered, as it has not been thoroughly studied for its biosynthetic potential. Several *Lacinutrix* sp. isolates have been whole genome sequenced and analyzed for the presence of BGCs. Of the genomes available in the Joint Genome Institute Genome Portal, it appears that most of these bacteria have below 5 predicted BGCs, which might indicate that the biosynthetic potential of *Lacinutrix* sp. bacteria is rather limited.

In paper III we isolated a novel sulphated dimeric naphthopyrone from a marine fungus *sensu stricto* of the family *Lulworthiaceae*. Due to unresolved systematics within the order *Lulworthiales* including morphologically similar cryptic species and relatively few available barcoding sequences from morphologically identified isolates, the studied isolate was only taxonomically placed in the family *Lulworthiaceae*, and the genus was not determined. For further taxonomic placement of the fungus, sequencing of several barcoding regions could be performed, but this would not solve the issue with few barcoding sequences available in the databases. To know more about the biosynthetic potential of the

fungus, and possibly coupling it to the production of lulworthinone, whole genome sequencing of the isolate should be done. As very few fungi in this order have been fully sequenced (closest sequenced relative *Lindra thalassiae*, also in the family *Lulworthiaceae*), whole genome sequencing would provide valuable information of this highly understudied group of marine fungi. The compound showed potent antibacterial activity against clinical MRSA isolates with MICs down to 1.56 µg/mL. Further studies to determine the mode of action are ongoing. We are also investigating the aggregation that was observed, and how this potentially influences bioactivity, as we know that aggregation can cause false positives in bioactivity screens [134-136]. As the compound has potent activity against MRSA, one of the most difficult human pathogens we have today, it is of high priority to gain more knowledge of this compound, regarding mode of action and drug-like properties. From another marine fungus *sensu stricto*, *Digitatispora marina* (paper IV), we isolated chlovalicin B. The compound did not show potent bioactivity in the tested assays but had weak antiproliferative activity against the melanoma cell line A2058 to about 50% cell survival at 50 µM. No further studies of the compound are prioritized due to low yields, limited bioactivity in the tested assays and the fact that several similar compounds have been extensively studied and published. The fungus on the other hand has not been extensively studied regarding its biosynthetic potential, and because of this the fungus will be prioritized for further cultivation studies. In our work with *D. marina*, we observed other compounds during dereplication that were prioritized for isolation. Because of difficulties in separating the compounds from other components in the fraction and very low yields we didn't obtain sufficient amounts of the compounds for structure elucidation. By exposing the fungus to different cultivation schemes, hopefully we can find a suitable cultivation method for this fungus to induce the production of interesting metabolites in higher yields. The fungus has also been whole genome sequenced, and the genome is currently being investigated for the presence of interesting biosynthetic gene clusters and enzymes.

7 Conclusions

The aim of this thesis was to isolate and characterize bioactive NPs produced by marine microorganisms, with special focus on antimicrobial compounds. Fungi and bacteria collected in marine environments were cultivated, compounds were isolated, and the compounds were chemically and biologically characterized. Different cultivation conditions were used to trigger metabolite production, such as changes in media composition, length of cultivation and co-cultivation. This yielded five compounds, four new and one known, published in four papers (paper I – paper IV). The most potent bioactivity was seen for lulworthinone, which had antibacterial activity against several MRSA isolates and is being further investigated for mode of action and for its aggregating properties. Luckily, the compound was isolated in such high yields, that proper characterization of these properties is possible. We also experienced some of the common issues in NP discovery, such as low yields of compound, acid-induced degradation and compound aggregation. The work presented as part of this thesis shows that marine microorganisms are a good source of new bioactive compounds and structures that can be used in pharmaceutical development of MNP inspired molecules. It also shows that even though some of the understudied and slow-growing microbes can be difficult to work with, they can provide us with interesting and bioactive natural products that may help us solve some of the societal challenges we face today, such as antimicrobial resistance.

8 References

1. Strachan, C.R. and Davies, J., The whys and wherefores of antibiotic resistance. *Cold Spring Harbor Perspectives in Medicine*, **2017**. *7*: p. 1-6.
2. Zhou, F., et al., Clinical course and risk factors for mortality of adult inpatients with COVID-19 in Wuhan, China: a retrospective cohort study. *Lancet*, **2020**. *395*: p. 1054-1062.
3. Haensch, S., et al., Distinct clones of *Yersinia pestis* caused the Black Death. *PLOS Pathogens*, **2010**. *6*: p. 1-8.
4. Bos, K.I., et al., A draft genome of *Yersinia pestis* from victims of the Black Death. *Nature*, **2011**. *478*: p. 506-510.
5. World Health Organization - Regional Office for Europe., *Tuberculosis*. **2021**. Available from: https://www.euro.who.int/en/health-topics/communicable-diseases/tuberculosis/tuberculosis-read-more (cited 13.12.2021).
6. Hughes, C.C. and Fenical, W., Antibacterials from the sea. *Chemistry – A European Journal*, **2010**. *16*: p. 12512-12525.
7. Baquero, F. and Levin, B.R., Proximate and ultimate causes of the bactericidal action of antibiotics. *Nature Reviews Microbiology*, **2021**. *19*: p. 123-132.
8. Hughes, D. and Karlén, A., Discovery and preclinical development of new antibiotics. *Upsala Journal of Medical Sciences*, **2014**. *119*: p. 162-169.
9. Houbraken, J., Frisvad, J.C., and Samson, R.A., Fleming's penicillin producing strain is not *Penicillium chrysogenum* but *P. rubens*. *IMA Fungus*, **2011**. *2*: p. 87-95.
10. Fleming, A., On the antibacterial action of cultures of a *Penicillium*, with special reference to their use in the isolation of *B. influenzæ*. *British Journal of Experimental Pathology*, **1929**. *10*: p. 226-236.
11. Cushnie, T.P.T., et al., Bioprospecting for antibacterial drugs: A multidisciplinary perspective on natural product source material, bioassay selection and avoidable pitfalls. *Pharmaceutical Research*, **2020**. *37*: p. 1-24.
12. Stone, M.J. and Williams, D.H., On the evolution of functional secondary metabolites (natural products). *Molecular Microbiology*, **1992**. *6*: p. 29-34.
13. Blair, J.M., et al., Molecular mechanisms of antibiotic resistance. *Nature Reviews Microbiology*, **2015**. *13*: p. 42-51.
14. Hoelzer, K., et al., Antimicrobial drug use in food-producing animals and associated human health risks: what, and how strong, is the evidence? *BMC Veterinary Research*, **2017**. *13*: p. 1-38.
15. Chang, Q., et al., Antibiotics in agriculture and the risk to human health: how worried should we be? *Evolutionary Applications*, **2015**. *8*: p. 240-247.
16. Cox Jr., L.A. and Popken, D.A., Quantifying potential human health impacts of animal antibiotic use: Enrofloxacin and macrolides in chickens. *Risk Analysis*, **2006**. *26*: p. 135-146.
17. Butler, M.S. and Paterson, D.L., Antibiotics in the clinical pipeline in October 2019. *The Journal of Antibiotics*, **2020**. *73*: p. 329-364.
18. World Health Organisation., *Antimicrobial resistance: Global report on surveillance*. **2014**. Available from: https://apps.who.int/iris/handle/10665/112642.
19. O'Neill, J., *Antimicrobial resistance: tackling a crisis for the health and wealth of nations*. **2014**. Available from: https://amr-review.org/sites/default/files/AMR%20Review%20Paper%20-%20Tackling%20a%20crisis%20for%20the%20health%20and%20wealth%20of%20nations_1.pdf

20. Towse, A., et al., Time for a change in how new antibiotics are reimbursed: Development of an insurance framework for funding new antibiotics based on a policy of risk mitigation. *Health Policy*, **2017**. *121*: p. 1025-1030.
21. Plackett, B., No money for new drugs. *Nature*, **2020**. *586*: p. S50-S52.
22. Hassan, M., et al., Natural antimicrobial peptides from bacteria: characteristics and potential applications to fight against antibiotic resistance. *Journal of Applied Microbiology*, **2012**. *113*: p. 723-736.
23. Spellberg, B., et al., Trends in antimicrobial drug development: Implications for the future. *Clincal Infectious Diseases*, **2004**. *38*: p. 1279-1286.
24. Outterson, K. and Rex, J.H., Evaluating for-profit public benefit corporations as an additional structure for antibiotic development and commercialization. *Translational Research*, **2020**. *220*: p. 182-190.
25. Tacconelli, E., et al., Discovery, research, and development of new antibiotics: the WHO priority list of antibiotic-resistant bacteria and tuberculosis. *The Lancet Infectious Diseases*, **2018**. *18*: p. 318-327.
26. Rice, L.B., Federal funding for the study of antimicrobial resistance in nosocomial pathogens: No ESKAPE. *The Journal of Infectious Diseases*, **2008**. *197*: p. 1079-1081.
27. Boucher, H.W., et al., Bad bugs, no drugs: no ESKAPE! An update from the Infectious Diseases Society of America. *Clinical Infectious Diseases*, **2009**. *48*: p. 1-12.
28. Medecins Sans Frontiers. *Bedaquiline: First new tuberculosis drug in 50 years*. **2012**. Available from: https://www.msf.org/bedaquiline-first-new-tuberculosis-drug-50-years (cited 19.01.2022).
29. Butler, M.S. and Cooper, M.A., Antibiotics in the clinical pipeline in 2011. *The Journal of Antibiotics*, **2011**. *64*: p. 413-425.
30. Butler, M.S., Blaskovich, M.A., and Cooper, M.A., Antibiotics in the clinical pipeline in 2013. *The Journal of Antibiotics*, **2013**. *66*: p. 571-591.
31. Butler, M.S., Blaskovich, M.A.T., and Cooper, M.A., Antibiotics in the clinical pipeline at the end of 2015. *The Journal of Antibiotics*, **2017**. *70*: p. 3-24.
32. Artuso, A., Bioprospecting, benefit sharing, and biotechnological capacity building. *World Development*, **2002**. *30*: p. 1355-1368.
33. Beattie, A., et al., *New products and industries from biodiversity*, in *Ecosystems and Human Well-Being: Current State and Trends*. **2005**, Island Press. p. 271-296.
34. Beattie, A.J., et al., Ecology and bioprospecting. *Austral Ecology*, **2011**. *36*: p. 341-356.
35. Dewick, P.M., *Secondary metabolism: The building blocks and construction mechanisms*, in *Medicinal Natural Products*, **2009**, John Wiley & Sons. p. 7-38.
36. Sarker, S.D. and Nahar, L., *An Introduction to Natural Products Isolation*, in *Natural Products Isolation*, **2012**, Humana Press. p. 1-25.
37. Beutler, J.A., Natural products as a foundation for drug discovery. *Current Protocols in Pharmacology*, **2009**. *46*: p. 1-30.
38. Newman, D.J., Cragg, G.M., and Snader, K.M., The influence of natural products upon drug discovery. *Natural Product Reports*, **2000**. *17*: p. 215-234.
39. Grabley, S. and Thiericke, R., Bioactive agents from natural sources: trends in discovery and application. *Advances in Biochemical Engineering/Biotechnology*, **1999**. *64*: p. 101-154.
40. Newman, D.J. and Cragg, G.M., Natural products as sources of new drugs over the nearly four decades from 01/1981 to 09/2019. *Journal of Natural Products*, **2020**. *83*: p. 770-803.
41. Ortholand, J.-Y. and Ganesan, A., Natural products and combinatorial chemistry: back to the future. *Current Opinion in Chemical Biology*, **2004**. *8*: p. 271-280.

42. Montaser, R. and Luesch, H., Marine natural products: A new wave of drugs? *Future Medicinal Chemistry*, **2011**. *3*: p. 1475-1489.
43. Harvey, A.L., Natural products in drug discovery. *Drug Discovery Today*, **2008**. *13*: p. 894-901.
44. Voser, T.M., Campbell, M.D., and Carroll, A.R., How different are marine microbial natural products compared to their terrestrial counterparts? *Natural Product Reports*, **2021**. *39*: p. 7-19.
45. Hanson, J.R., *The classes of natural product and their isolation*, in *Natural Products: The Secondary Metabolites*, **2003**, The Royal Society of Chemistry. p. 1-34.
46. Henkel, T., et al., Statistical investigation into the structural complementarity of natural products and synthetic compounds. *Angewandte Chemie International Edition*, **1999**. *38*: p. 643-647.
47. Ganesan, A., The impact of natural products upon modern drug discovery. *Current Opinion in Chemical Biology*, **2008**. *12*: p. 306-317.
48. Stratton, C.F., Newman, D.J., and Tan, D.S., Cheminformatic comparison of approved drugs from natural product versus synthetic origins. *Bioorganic & Medicinal Chemistry Letters*, **2015**. *25*: p. 4802-4807.
49. Convention on Biological Diversity. *The Convention on Biological Diversity*. **2021**. Available from: https://www.cbd.int/convention/ (cited 01.12.2021).
50. Convention on Biological Diversity. *The Nagoya Protocol on access and benefit-sharing*. **2021**. Available from: https://www.cbd.int/abs/ (cited 01.12.2021).
51. Blasiak, R., et al., The ocean genome and future prospects for conservation and equity. *Nature Sustainability*, **2020**. *3*: p. 588-596.
52. Louca, S., et al., A census-based estimate of Earth's bacterial and archaeal diversity. *PLOS Biology*, **2019**. *17*: p. 1-30.
53. Mora, C., et al., How many species are there on earth and in the ocean? *PLOS Biology*, **2011**. *9*: p. 1-8.
54. Bar-On, Y.M., Phillips, R., and Milo, R., The biomass distribution on Earth. *Proceedings of the National Academy of Sciences*, **2018**. *115*: p. 6506-6511.
55. Stincone, P. and Brandelli, A., Marine bacteria as source of antimicrobial compounds. *Critical Reviews in Biotechnology*, **2020**. *40*: p. 306-319.
56. Haefner, B., Drugs from the deep: marine natural products as drug candidates. *Drug Discovery Today*, **2003**. *8*: p. 536-544.
57. D'Amico, S., et al., Psychrophilic microorganisms: challenges for life. *EMBO Reports*, **2006**. *7*: p. 385-389.
58. Gerwick, W.H. and Moore, B.S., Lessons from the past and charting the future of marine natural products drug discovery and chemical biology. *Chemistry & Biology Review*, **2012**. *19*: p. 85-98.
59. Piel, J., Metabolites from symbiotic bacteria. *Natural Product Reports*, **2009**. *26*: p. 338-362.
60. Simmons, T.L., et al., Biosynthetic origin of natural products isolated from marine microorganism–invertebrate assemblages. *Proceedings of the National Academy of Sciences*, **2008**. *105*: p. 4587-4594.
61. Schofield, M.M., et al., Identification and analysis of the bacterial endosymbiont specialized for production of the chemotherapeutic natural product ET-743. *Environmental Microbiology*, **2015**. *17*: p. 3964-3975.
62. Rath, C.M., et al., Meta-omic characterization of the marine invertebrate microbial consortium that produces the chemotherapeutic natural product ET-743. *ACS Chemical Biology*, **2011**. *6*: p. 1244-1256.

63. Cuevas, C., et al., Synthesis of ecteinascidin ET-743 and phthalascidin Pt-650 from cyanosafracin B. *Organic Letters*, **2000**. *2*: p. 2545-2548.
64. Connon, S.A. and Giovannoni, S.J., High-throughput methods for culturing microorganisms in very-low-nutrient media yield diverse new marine isolates. *Applied and Environmental Microbiology*, **2002**. *68*: p. 3878-3885.
65. Staley, J.T. and Konopka, A., Measurement of *in situ* activities of nonphotosynthetic microorganisms in aquatic and terrestrial habitats. *Annual Review of Microbiology*, **1985**. *39*: p. 321-346.
66. Kogure, K., Shimizu, U., and Taga, N., A tentative direct microscopic method for counting living marine bacteria. *Canadian Journal of Microbiology*, **1979**. *25*: p. 415-420.
67. Vartoukian, S.R., Palmer, R.M., and Wade, W.G., Strategies for culture of 'unculturable' bacteria. *FEMS Microbiology Letters*, **2010**. *309*: p. 1-7.
68. Salim, A.A., et al., Methods in microbial biodiscovery. *Marine Drugs*, **2021**. *19*: p. 1-25.
69. Carroll, A.R., et al., Marine natural products. *Natural Product Reports*, **2021**. *38*: p. 362-413.
70. Carroll, A.R., et al., Marine natural products. *Natural Product Reports*, **2020**. *37*: p. 175-223.
71. Imhoff, J.F., Natural products from marine fungi--still an underrepresented resource. *Marine Drugs*, **2016**. *14*: p. 1-19.
72. Demain, A.L., *Valuable secondary metabolites from fungi*, in *Biosynthesis and Molecular Genetics of Fungal Secondary Metabolites*, **2014**, Springer. p. 1-16.
73. Gomes, E.S., Schuch, V., and de Macedo Lemos, E.G., Biotechnology of polyketides: new breath of life for the novel antibiotic genetic pathways discovery through metagenomics. *Brazilian Journal of Microbiology*, **2014**. *44*: p. 1007-1034.
74. Miller, B.R. and Gulick, A.M., *Structural biology of nonribosomal peptide synthetases*, in *Nonribosomal Peptide and Polyketide Biosynthesis: Methods and Protocols*, **2016**, Springer. p. 3-29.
75. Walsh, C.T., O'Brien, R.V., and Khosla, C., Nonproteinogenic amino acid building blocks for nonribosomal peptide and hybrid polyketide scaffolds. *Angewandte Chemie International Edition*, **2013**. *52*: p. 7098-7124.
76. Süssmuth, R.D. and Mainz, A., Nonribosomal peptide synthesis—principles and prospects. *Angewandte Chemie International Edition*, **2017**. *56*: p. 3770-3821.
77. Boettger, D. and Hertweck, C., Molecular diversity sculpted by fungal PKS–NRPS hybrids. *ChemBioChem*, **2013**. *14*: p. 28-42.
78. Fisch, K.M., Biosynthesis of natural products by microbial iterative hybrid PKS–NRPS. *RSC Advances*, **2013**. *3*: p. 18228-18247.
79. Graupner, P.R., et al., Dihydromaltophilin; a novel fungicidal tetramic acid containing metabolite from *Streptomyces* sp. *The Journal of Antibiotics*, **1997**. *50*: p. 1014-1019.
80. Yu, F., et al., Structure and biosynthesis of heat-stable antifungal factor (HSAF), a broad-spectrum antimycotic with a novel mode of action. *Antimicrobial Agents and Chemotherapy*, **2007**. *51*: p. 64-72.
81. Bode, H.B., et al., Big Effects from small changes: Possible ways to explore nature's chemical diversity. *ChemBioChem*, **2002**. *3*: p. 619-627.
82. Giubergia, S., et al., Growth on chitin impacts the transcriptome and metabolite profiles of antibiotic-producing *Vibrio coralliilyticus* S2052 and *Photobacterium galatheae* S2753. *mSystems*, **2017**. *2*: p. 1-12.
83. Abdel-Wahab, N.M., et al., Induction of secondary metabolites from the marine-derived fungus *Aspergillus versicolor* through co-cultivation with *Bacillus subtilis*. *Planta Medica*, **2019**. *85*: p. 503-512.
84. Blunt, J.W., et al., Marine natural products. *Nat Prod Rep*, **2018**. *35*: p. 235-294.

85. Rocha-Martin, J., et al., Emerging strategies and integrated systems microbiology technologies for biodiscovery of marine bioactive compounds. *Marine Drugs*, **2014**. *12*: p. 3516-3559.
86. Butler, A. and Walker, J.V., Marine haloperoxidases. *Chemical Reviews*, **1993**. *93*: p. 1937-1944.
87. Gribble, G.W., The natural production of organobromine compounds. *Environmental Science and Pollution Research*, **2000**. *7*: p. 37-49.
88. Marine Pharmacology. *Approved Marine Drugs*. **2022.** Available from: https://www.marinepharmacology.org/approved (cited 03.02.2022).
89. Marine Pharmacology. *Phase 3 Clinical Status*. **2021**. Available from: https://www.marinepharmacology.org/phase-3-drugs (cited 03.02.2022).
90. Marine Pharmacology. *Phase 2 Clinical Status*. **2021**. Available from: https://www.marinepharmacology.org/phase-2-drugs (cited 03.02.2022).
91. Marine Pharmacology. *Phase 1 Clinical Status*. **2022**. Available from: https://www.marinepharmacology.org/phase-1-drugs (cited 03.02.2022).
92. Abdelfattah, M.S., et al., Isolation and characterization of marine-derived actinomycetes with cytotoxic activity from the Red Sea coast. *Asian Pacific Journal of Tropical Biomedicine*, **2016**. *6*: p. 651-657.
93. Altschul, S.F., et al., Basic local alignment search tool. *Journal of Molecular Biology*, **1990**. *215*: p. 403-410.
94. Schoch, C.L., et al., Nuclear ribosomal internal transcribed spacer (ITS) region as a universal DNA barcode marker for fungi. *Proceedings of the National Academy of Sciences*, **2012**. *109*: p. 6241-6246.
95. Yang, B., Wang, Y., and Qian, P.-Y., Sensitivity and correlation of hypervariable regions in 16S rRNA genes in phylogenetic analysis. *BMC Bioinformatics*, **2016**. *17*: p. 1-8.
96. Reid, R.G. and Sarker, S.D., *Isolation of natural products by low-pressure column chromatography*, in *Natural Products Isolation - Methods in Molecular Biology*, **2012**, Humana Press. p. 155-187.
97. Latif, Z. and Sarker, S.D., *Isolation of natural products by preparative high performance liquid chromatography (Prep-HPLC)*, in *Natural Products Isolation - Methods in Molecular Biology*, **2012**, Humana Press. p. 255-274.
98. Sarker, S.D. and Nahar, L., *Hyphenated techniques and their applications in natural products analysis*, in *Natural Products Isolation - Methods in Molecular Biology*, **2012**, Humana Press. p. 301-340.
99. Koehn, F.E. and Carter, G.T., The evolving role of natural products in drug discovery. *Nature Reviews Drug Discovery*, **2005**. *4*: p. 206-220.
100. Camp, D., et al., Guiding principles for natural product drug discovery. *Future Medicinal Chemistry*, **2012**. *4*: p. 1067-1084.
101. Jeon, H., et al., Chemical assay-guided natural product isolation via solid-supported chemodosimetric fluorescent probe. *Chemical Science*, **2015**. *6*: p. 2806-2811.
102. Nielsen, K.F., et al., Dereplication of microbial natural products by LC-DAD-TOFMS. *Journal of Natural Products*, **2011**. *74*: p. 2338-2348.
103. El-Aneed, A., Cohen, A., and Banoub, J., Mass spectrometry, review of the basics: electrospray, MALDI, and commonly used mass analyzers. *Applied Spectroscopy Reviews*, **2009**. *44*: p. 210-230.
104. Waters, *An overview of the principles of MSE, the engine that drives MS performance*. 2011. Available from: https://www.waters.com/waters/library.htm?cid=10160596&lid=134644867&locale=en_NO

105. Guo, J. and Huan, T., Comparison of full-scan, data-dependent, and data-independent acquisition modes in liquid chromatography–mass spectrometry based untargeted metabolomics. *Analytical Chemistry*, **2020**. *92*: p. 8072-8080.
106. Nielsen, K.F., et al., Trichothecene production by *Trichoderma brevicompactum. Journal of Agricultural and Food Chemistry*, **2005**. *53*: p. 8190-8196.
107. Fredenhagen, A., Derrien, C., and Gassmann, E., An MS/MS library on an ion-trap instrument for efficient dereplication of natural products. Different fragmentation patterns for $[M + H]^+$ and $[M + Na]^+$ ions. *Journal of Natural Products*, **2005**. *68*: p. 385-391.
108. Nielsen, K.F. and Smedsgaard, J., Fungal metabolite screening: database of 474 mycotoxins and fungal metabolites for dereplication by standardised liquid chromatography–UV–mass spectrometry methodology. *Journal of Chromatography A*, **2003**. *1002*: p. 111-136.
109. Hart, D.J., et al., *Spectroscopy and structure determination*, in *Organic Chemistry - a Brief Course*. 2012, CENGAGE Learning Custom Publishing. p. 356-389.
110. Thorne, N., Auld, D.S., and Inglese, J., Apparent activity in high-throughput screening: origins of compound-dependent assay interference. *Current Opinion in Chemical Biology*, **2010**. *14*: p. 315-324.
111. Lipinski, C.A., et al., Experimental and computational approaches to estimate solubility and permeability in drug discovery and development settings. *Advanced Drug Delivery Reviews*, **1997**. *23*: p. 3-25.
112. Hughes, J.P., et al., Principles of early drug discovery. *British Journal of Pharmacology*, **2011**. *162*: p. 1239-1249.
113. Ntie-Kang, F., et al., "Drug-likeness" properties of natural compounds. *Physical Sciences Reviews*, **2019**. *4*: p. 1-14.
114. Harvey, A.L., Edrada-Ebel, R., and Quinn, R.J., The re-emergence of natural products for drug discovery in the genomics era. *Nature Reviews Drug Discovery*, **2015**. *14*: p. 111-129.
115. Cannell, R.J.P., Sarker, S.D., and Nahar, L., *Follow-up of natural products isolation*, in *Natural Products Isolation - Methods in Molecular Biology*, **2012**, Humana Press. p. 473-514.
116. Overy, D.P., et al., An assessment of natural product discovery from marine (*sensu strictu*) and marine-derived fungi. *Mycology*, **2014**. *5*: p. 145-167.
117. Overy, D.P., et al., The neglected marine fungi, *sensu stricto*, and their isolation for natural products' discovery. *Marine Drugs*, **2019**. *17*: p. 1-20.
118. Hernandez, A., et al., The need to innovate sample collection and library generation in microbial drug discovery: a focus on academia. *Natural Product Reports*, **2021**. *38*: p. 292-300.
119. Jones, E.B.G., et al., Classification of marine Ascomycota, Basidiomycota, Blastocladiomycota and Chytridiomycota. *Fungal Diversity*, **2015**. *73*: p. 1-72.
120. Ehlert, G., Taraz, K., and Budzikiewicz, H., Serratiochelin, a new catecholate siderophore from *Serratia marcescens. Zeitschrift für Naturforschung C*, **1994**. *49*: p. 11-17.
121. Seyedsayamdost, M.R., et al., Mixing and matching siderophore clusters: structure and biosynthesis of serratiochelins from *Serratia* sp. V4. *Journal of the American Chemical Society*, **2012**. *134*: p. 13550-13553.
122. Barman, S., Bhattacharya, S.S., and Chandra Mandal, N., *Chapter 3 - Serratia*, in *Beneficial Microbes in Agro-Ecology*, **2020**, Academic Press. p. 27-36.
123. Pettit, G.R., et al., Antineoplastic agents. 219. Isolation and structure of the cell growth inhibitory constituents from the western Pacific marine sponge *Axinella* sp. *Journal of Medicinal Chemistry*, **1991**. *34*: p. 3339-3340.
124. Aicher, T.D., et al., Total synthesis of halichondrin B and norhalichondrin B. *Journal of the American Chemical Society*, **1992**. *114*: p. 3162-3164.

125. Swami, U., et al., Eribulin—A review of preclinical and clinical studies. *Critical reviews in Oncology/Hematology*, **2011**. *81*: p. 163-184.
126. Dabydeen, D.A., et al., Comparison of the activities of the truncated halichondrin B analog NSC 707389 (E7389) with those of the parent compound and a proposed binding site on tubulin. *Molecular Pharmacology*, **2006**. *70*: p. 1866-1875.
127. Cragg, G.M. and Pezzuto, J.M., Natural products as a vital source for the discovery of cancer chemotherapeutic and chemopreventive agents. *Medical Principles and Practice*, **2016**. *25*: p. 41-59.
128. Luo, Y., Cobb, R.E., and Zhao, H., Recent advances in natural product discovery. *Current Opinion in Biotechnology*, **2014**. *30*: p. 230-237.
129. Capon, R.J., Extracting value: mechanistic insights into the formation of natural product artifacts – case studies in marine natural products. *Natural Product Reports*, **2020**. *37*: p. 55-79.
130. Yamazaki, H., et al., Absolute structures and bioactivities of eurysponginsand eurydiene obtained from the marine sponge *Euryspongia* sp. collected at Iriomote Island. *Bioorganic & Medicinal Chemistry*, **2015**. *23*: p. 797-802.
131. Aldrich, C., et al., The ecstasy and agony of assay interference compounds. *Journal of Medicinal Chemistry*, **2017**. *60*: p. 2165-2168.
132. Baell, J. and Walters, M.A., Chemistry: Chemical con artists foil drug discovery. *Nature*, **2014**. *513*: p. 481-483.
133. Kristoffersen, V., et al., Characterization of rhamnolipids produced by an Arctic marine bacterium from the *Pseudomonas fluorescence* Group. *Marine Drugs*, **2018**. *16*: p. 1-19.
134. McGovern, S.L., et al., A common mechanism underlying promiscuous inhibitors from virtual and high-throughput screening. *Journal of Medicinal Chemistry*, **2002**. *45*: p. 1712-1722.
135. Feng, B.Y., et al., High-throughput assays for promiscuous inhibitors. *Nature Chemical Biology*, **2005**. *1*: p. 146-148.
136. Coan, K.E.D. and Shoichet, B.K., Stoichiometry and physical chemistry of promiscuous aggregate-based inhibitors. *Journal of the American Chemical Society*, **2008**. *130*: p. 9606-9612.
137. Simeonov, A., et al., Fluorescence spectroscopic profiling of compound libraries. *Journal of Medicinal Chemistry*, **2008**. *51*: p. 2363-2371.
138. Public Health Agency of Sweden. *Availability of antibiotics*. **2020**. Available from: https://www.folkhalsomyndigheten.se/the-public-health-agency-of-sweden/communicable-disease-control/antibiotics-and-antimicrobial-resistance/availability-of-antibiotics/ (cited 09.11.2021).
139. Exner, M., et al., Antibiotic resistance: What is so special about multidrug-resistant Gram-negative bacteria? *GMS Hygiene and Infection Control*, **2017**. *12*: p. 1-24.
140. Silhavy, T.J., Kahne, D., and Walker, S., The bacterial cell envelope. *Cold Spring Harbor Perspectives in Biology*, **2010**. *2*: p. 1-16.
141. Khalil, Z.G., Kalansuriya, P., and Capon, R.J., Lipopolysaccharide (LPS) stimulation of fungal secondary metabolism. *Mycology*, **2014**. *5*: p. 168-178.
142. Chiacchio, M.A., et al., Oxazole-based compounds as anticancer agents. *Current Medicinal Chemistry*, **2019**. *26*: p. 7337-7371.
143. Zhang, H.-Z., Zhao, Z.-L., and Zhou, C.-H., Recent advance in oxazole-based medicinal chemistry. *European Journal of Medicinal Chemistry*, **2018**. *144*: p. 444-492.

Paper I

microorganisms

MDPI

Article

Bioactivity of Serratiochelin A, a Siderophore Isolated from a Co-Culture of *Serratia* sp. and *Shewanella* sp.

Yannik Schneider [1,*,†], Marte Jenssen [1,*,†], Johan Isaksson [2], Kine Østnes Hansen [1], Jeanette Hammer Andersen [1] and Espen H. Hansen [1]

1 Marbio, Faculty for Fisheries, Biosciences and Economy, UiT—The Arctic University of Norway, Breivika, N-9037 Tromsø, Norway; kine.o.hanssen@uit.no (K.Ø.H.); jeanette.h.andersen@uit.no (J.H.A.); espen.hansen@uit.no (E.H.H.)

2 Department of Chemistry, Faculty of Natural Sciences, UiT—The Arctic University of Norway, Breivika, N-9037 Tromsø, Norway; johan.isaksson@uit.no

* Correspondence: yannik.k.schneider@uit.no (Y.S.); marte.jenssen@uit.no (M.J.); Tel.: +47-7764-9267 (Y.S.); +47-7764-9275 (M.J.)

† These authors contributed equally to the work.

Received: 15 June 2020; Accepted: 10 July 2020; Published: 14 July 2020

Abstract: Siderophores are compounds with high affinity for ferric iron. Bacteria produce these compounds to acquire iron in iron-limiting conditions. Iron is one of the most abundant metals on earth, and its presence is necessary for many vital life processes. Bacteria from the genus *Serratia* contribute to the iron respiration in their environments, and previously several siderophores have been isolated from this genus. As part of our ongoing search for medicinally relevant compounds produced by marine microbes, a co-culture of a *Shewanella* sp. isolate and a *Serratia* sp. isolate, grown in iron-limited conditions, was investigated, and the rare siderophore serratiochelin A (**1**) was isolated with high yields. Compound **1** has previously been isolated exclusively from *Serratia* sp., and to our knowledge, there is no bioactivity data available for this siderophore to date. During the isolation process, we observed the degradation product serratiochelin C (**2**) after exposure to formic acid. Both **1** and **2** were verified by 1-D and 2-D NMR and high-resolution MS/MS. Here, we present the isolation of **1** from an iron-depleted co-culture of *Shewanella* sp. and *Serratia* sp., its proposed mechanism of degradation into **2**, and the chemical and biological characterization of both compounds. The effects of **1** and **2** on eukaryotic and prokaryotic cells were evaluated, as well as their effect on biofilm formation by *Staphylococcus epidermidis*. While **2** did not show bioactivity in the given assays, **1** inhibited the growth of the eukaryotic cells and *Staphylococcus aureus*.

Keywords: Serratiochelin A; Serratiochelin C; *Serratia* sp.; siderophore; iron; anticancer; natural products; microbial biotechnology; degradation; antibacterial; *S. aureus*

1. Introduction

Iron is the fourth most abundant metal in the Earth's crust and is an absolute requirement for life [1]. Iron is an essential nutrient vital for several biological processes, such as respiration, gene regulation, and DNA biosynthesis [1,2]. Despite its abundance, iron is a growth-limiting factor for organisms in many environments [1]. To tackle this, microorganisms produce a vast range of iron-chelating compounds, called siderophores. Siderophores are compounds of low molecular weight (<1000 Da) that have high affinity and selectivity for ferric iron (iron(III)) [1], with the function of mediating iron uptake by microbial cells [3]. Siderophore production is commonly regulated by the iron concentration in the surroundings [4]. The siderophores are accumulated by membrane-bound iron receptors and brought inside the cell by active transport. Subsequently, the iron is normally reduced from iron(III) to

iron(II). Since the affinity towards iron(II) is much lower than to iron(III), the iron is released from the iron-siderophore complex and can be utilized by the microorganism [4]. One of the major functional groups of siderophores is catecholate. Many siderophores of the catecholate type contain building blocks consisting of dihydroxybenzoic acid coupled to an amino acid [3]. The first catecholate-type siderophore, a glycine conjugate of 2,3-dihydroxybenzoic acid, was identified in 1958. The compound was produced by *Bacillus subtilis* under iron-poor conditions [5].

The genus *Serratia* is part of the family *Enterobacteriaceae*, whose type species is *Serratia marcescens* [6,7]. Species of the genus *Serratia* have been detected in diverse habitats, such as soil, humans, invertebrates, and water. For *Serratia plymuthica*, water appears to be the principal habitat [6]. Bacteria from this genus are also problematic in health care, as *Serratia marcescens* is an opportunistic pathogen causing infections in immunocompromised patients. One of the pathogenicity factors of the bacterium is its production of potent siderophores. Several different siderophores are produced by bacteria of this genus [8], one example being the serratiochelins produced by *Serratia* sp. V4 [9,10].

The serratiochelins are catecholate siderophores produced by *Serratia* sp. [9,10]. In a paper from 2012 by Seyedsayamdost and co-authors, a new siderophore biosynthetic pathway was proposed for the production of the serratiochelins [10]. The new pathway consisted of genes originating and recombined from two known siderophore biosynthetic clusters: The clusters for enterobactin (*Escherichia coli*) and vibriobactin (*Vibrio cholera*). The study mentions three different serratiochelins, serratiochelin A (**1**), B, and C (**2**); the structures of **1** and **2** can be seen in Figure 1. In the study from 2012, only two of the three compounds, **1** and serratiochelin B, were found in the untreated culture extracts, while **2** is a hydrolysis product of **1**, which was produced in the presence of formic acid. Sayedsayamdost et al. indicated that **1** and serratiochelin B were the native compounds produced by the bacterium [10].

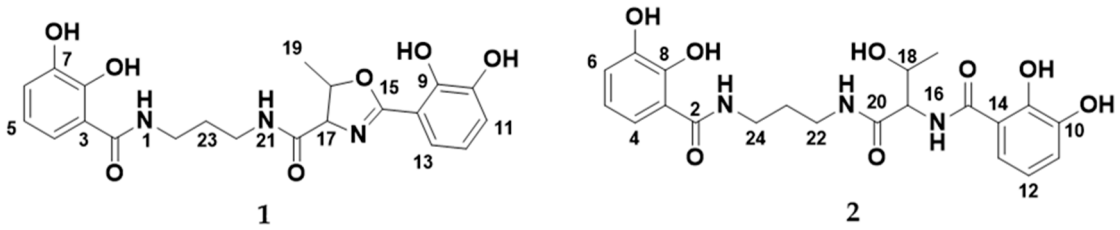

Figure 1. The structures of serratiochelin A (**1**) and C (**2**).

Siderophores are of pharmaceutical interest. They can be used in their native form to treat iron overload diseases, like sickle cell disease. Desferal® (Deferoxamine) is a siderophore-based drug used to treat iron poisoning and thalassemia major, a disease that leads to iron overload, which can lead to severe organ damage [11,12]. Siderophores can furthermore be used to facilitate active uptake of antibiotics by bacteria, and by the production of siderophore-antibiotic drug conjugates (SADCs). For some antibiotics, this strategy can reduce the minimal inhibitory concentration (MIC) by 100-fold, compared to an unbound antibiotic that enters the bacterial cell by passive diffusion [13]. The sideromycins are one example of SADCs. Albomycin, which belongs to this group, enters via the ferrichrome transporter, and has broad-spectrum antibiotic activity and is active against different Gram-negative bacteria [4,14]. The main problem with the use of SADCs is that most pathogenic bacteria have different routes for iron uptake, which could lead to higher frequency in resistance [4].

Due to the important role of *Shewanella* sp. and *Serratia* sp. in the environmental iron cycle, we were intrigued by observing a compound in high yields in an iron-limited co-culture of the two bacteria, which was not found in cultures supplemented with iron nor in axenic cultures of the bacteria. Here, we report the isolation of **1** from a co-culture of *Shewanella* sp. and *Serratia* sp. The degradation of **1** into **2** in the presence of acid was confirmed. To our knowledge, there is no published data regarding the bioactivity of these compounds. In this study, **1** and **2** were tested against a panel of bacterial and human cells, and for their ability to inhibit biofilm formation of the biofilm-producing bacterium *S. epidermidis*.

2. Materials and Methods

2.1. Bacterial Isolates

Compound **1** was isolated from bacterial cultures started from a non-axenic glycerol stock. The bacterial glycerol stock originally contained a *Leifsonia* sp. isolate. The stock was found to be contaminated with both *Shewanella* sp. and *Serratia* sp. after several steps of cultivation and production of new glycerol stock solutions. The non-axenic glycerol stock was inoculated onto three different agar plates, in order to gather information of the different isolates present. Originally, the *Leifsonia* sp. isolate was provided as an axenic culture by The Norwegian Marine Biobank (Marbank, Tromsø, Norway) (Reference number: M10B719). The bacterium was isolated from the intestine/stomach of an Atlantic hagfish (*Myxine glutinosa*) collected by benthic trawl in Hadselfjorden (Norwegian Sea, 16th of April, 2010). The bacterium was grown in liquid FMAP medium (15 g Difco Marine Broth (Becton Dickinson and Company, Franklin Lakes, NJ, USA), 5 g peptone from casein, enzymatic digest (Sigma, St. Louis, MS, USA), 700 mL ddH_2O, and 300 mL filtrated sea water) until sufficient turbidity, and cryo-conserved at −80 °C with 30% glycerol (Sigma). Filtration of sea water was done through a Millidisk® 40 Cartridge with a Durapore® 0.22-µm filter membrane (Millipore, Burlington, MA, USA).

2.2. PCR and Identification of the Strains

The glycerol stock was plated onto three different types of agar: FMAP agar (FMAP medium with 15 g/L agar), DVR1 agar (6.7 g malt extract (Sigma), 11.1 g peptone from casein, enzymatic digest (Sigma), 6.7 g yeast extract (Sigma), 0.5 L filtered sea water, 0.5 L ddH_2O), and potato glucose agar (Sigma). The plates with bacteria were incubated at 10 °C until sufficient growth, and transferred to 4 °C for temporary storage. This plating experiment resulted in the discovery of three different bacterial isolates, based on bacterial morphology and sequencing of the 16S rRNA gene. Clear colonies were picked from the plates, and inoculated into 100 µL of autoclaved ddH_2O. The samples were stored at −20 °C until PCR amplification. The characterization of the bacterial strains was done with sequencing of the 16S rRNA gene through colony PCR and Sanger sequencing. The primer set used for amplification of the gene was the 27F primer (forward primer; 5'-AGAGTTTGATCMTGGCTCAG) and the 1429R primer (reverse primer; 5'-TACCTTGTTACGACTT), both from Sigma. Prior to the amplification PCR, the bacterial samples were vortexed and diluted 1:100 and 1:1000 in UltraPure Water (BioChrom GmbH, Berlin, Germany). For PCR, 1 µL of the diluted bacterial sample was combined in a 25-µL PCR reaction, together with 12.5 µL DreamTaq Green PCR Master Mix (2×) (Thermo Scientific, Vilnius, Lithuania), 10.5 µL ultrapure water, and 0.5 µL of the forward and reverse primers (10 µM) mentioned above. The amplification was done using a Mastercycler ep gradient S (Eppendorf AG, Hamburg, Germany) with the following program: 95 °C initial denaturation for 3 min, followed by 35 cycles of 95 °C for 30 s, 47 °C for 30 s, and 72 °C for 1 min. Final extension was 72 °C for 10 min. The success and purity of the PCR reaction was analyzed on a 1.0% agarose gel (Ultrapure™ Agarose, Invitrogen, Paisley, UK) with Gel-Red® Nucleic Acid Gel Stain (Biotium, Fremont, CA, USA), and the results were documented using a Syngene Bioimaging system (Syngene, Cambridge, UK). Successfully amplified samples were purified by the A'SAP PCR clean up kit (ArcticZymes, Tromsø, Norway). The purified PCR product was used for sequencing PCR, using 1 µL PCR product, 2 µL BigDye™ 3.1 (Applied Biosystems, Foster City, CA, USA), 2 µL 5× sequencing buffer (Applied Biosystems, Foster City, CA, USA), 4 µL of UltraPure water, and 1 µL of primer (1 µM of 27F primer or 1429R primer). The program for the sequencing PCR was as follows: 96 °C initial denaturation for 1 min, followed by 30 cycles of 96 °C for 10 s, 47 °C for 5 s, and 60 °C for 2 min. The PCR product was sequenced at the University Hospital of North Norway (Tromsø, Norway).

The forward and reverse sequences obtained were assembled using the Geneious Prime® 2020.0.5 software (https://www.geneious.com). The sequences were assembled by using the built-in Geneious assembler. Prior to assembly, the sequences were trimmed using a 0.05 error probability limit. Sequence homology comparison was conducted using the built-in Basic Local Alignment Search

Tool (BLAST) [15] in Geneious, excluding environmental samples, metagenomes, and uncultured microorganisms, for phylogenetic identification of the strains.

To identify which strain was responsible for the production of **1**, the three bacterial strains were isolated on separate agar plates and inoculated in small cultures of DVR1 medium (for media contents, see below). The bacteria were pelleted by centrifugation, and the supernatant was diluted 1:1 in methanol and ran on the UHPLC-HR-MS for identification of the compound.

2.3. Fermentation and Extraction of Bacterial Cultures

For extraction of compounds, the bacteria were cultivated in 1000-mL flasks containing 300 mL DVR1 medium (6.7 g malt extract (Sigma), 11.1 g peptone from casein, enzymatic digest (Sigma), 6.7 g yeast extract (Sigma), 0.5 L filtered sea water, and 0.5 L ddH_2O) cultures for 16 days, at 10 °C and 130 rpm. A total of 12 flasks were inoculated, giving 3.6 L of culture. The medium was autoclaved for 30 min at 120 °C prior to inoculation. Cultures were started by loop inoculation from the non-axenic glycerol stock solution.

Extraction of metabolites from the liquid media was done with Diaion® HP-20 resin (Supelco, Bellefonte, PA, USA). The resin was activated by incubation in methanol for 30 min, followed by washing with ddH_2O for 15 min, and added to the cultures (40 g/L). The cultures were incubated with resin for 3 days prior to compound extraction. For extraction, the resin beads were separated from the liquid by vacuum filtration through a cheesecloth mesh (Dansk Hjemmeproduktion, Ejstrupholm, Denmark), the resin was washed with ddH_2O, and finally extracted two times with methanol. The extract was vacuum filtered through a Whatman No. 3 filter paper (Whatman plc, Maidstone, UK), and dried under reduced pressure at 40 °C.

2.4. Fractionation by FLASH Chromatography

Due to the degradation of **1** in the presence of acid, the culture extract was fractionated for bioactivity testing and structure verification, using FLASH chromatography (Biotage SP4™ system, Uppsala, SE), removing the use of acid in the purification process. The extract (3667.9 mg) was re-dissolved in 90% methanol, before adding Diaion® HP20-SS resin (Supelco) in a ratio of 1:1.5 (resin:dry extract, *w*/*w*) and drying under reduced pressure at 40 °C. Due to the high amount of the extract, it was fractionated in two rounds. FLASH columns were prepared with 6.5 g activated Diaion® HP-20SS resin per column. The dried extract was applied to the column, and ran with a water: methanol gradient from 5–100% methanol over 36 min at a flow rate of 12 mL/min. This resulted in 15 fractions per run. The fractions eluting at 100% methanol were analyzed on the UHPLC-HR-MS, and the purest fraction (fraction no 13, >95% pure based on UV/Vis) was used and dried under reduced pressure at 40 °C. The fraction yielded 50.9 mg and was used for the bioactivity testing.

2.5. UHPLC-HR-MS and Dereplication

UHPLC-HR-MS data for dereplication and to analyze the various experiments was recorded using an Acquity I-class UPLC (Waters, Milford, MA, USA) coupled to a PDA detector and a Vion IMS QToF (Waters). The chromatographic separation was performed using an Acquity C-18 UPLC column (1.7 µm, 2.1 mm × 100 mm) (Waters). Mobile phases consisted of acetonitrile (HiPerSolv, VWR, Radnor, PA, USA) for mobile phase B and ddH_2O produced by the in-house Milli-Q® system (Millipore, Burlington, MA, USA) as mobile phase A, both containing 1% formic acid (*v*/*v*) (33015, Sigma). The gradient was run from 10% to 90% B in 12 min at a flow rate of 0.45 mL/min. Samples were run in ESI+ and ESI- ionization mode. The data was processed and analyzed using UNIFI 1.9.4 (Waters). Exact masses and isotopic distributions were calculated using ChemCalc (https://www.chemcalc.org).

2.6. Purification by Preparative HPLC

Initially, the purification of **1** and **2** was done by preparative HPLC-MS using a 600 HPLC pump, a 3100 mass spectrometer, a 2996 photo diode array detector, and a 2767 sample manager (Waters).

For infusion of the eluents into the ESI-quadrupole-MS, a 515 HPLC pump (Waters) and a flow splitter were used and 80% methanol in ddH_2O (*v/v*) acidified with 0.2% formic acid (Sigma) as make-up solution at a flow rate of 0.7 mL/min. The columns used for isolation were a Sunfire RP-18 preparative column (10 µm, 10 mm × 250 mm) and XSelect CSH preparative fluoro-phenyl column (5 µm, 10 mm × 250mm), both columns were purchased from Waters. The mobile phases for the gradients were A (ddH_2O with 0.1% (*v/v*) formic acid) and B (acetonitrile with 0.1% (*v/v*) formic acid), flow rate was set to 6 mL/min. Acetonitrile (Prepsolv®, Merck, Darmstad, Germany) and formic acid (33015, Sigma) were purchased in appropriate quality, ddH_2O was produced with the in-house Milli-Q® system. The collected fractions were reduced to dryness at 40 °C in vacuo and freeze drying using an 8L laboratory freeze dryer (Labconco, Fort Scott, KS, USA).

2.7. NMR analysis

NMR spectra were acquired in DMSO-d_6 on a Bruker Avance III HD spectrometer (Bruker, Billerica, MA, USA) operating at 600 MHz for protons, equipped with an inverse TCI cryo probe enhanced for ^{1}H, ^{13}C, and ^{2}H. All NMR spectra were acquired at 298 K, in 3-mm solvent-matched Shigemi tubes using standard pulse programs for proton, carbon, HSQC, HMBC, COSY, and ROESY with gradient selection and adiabatic versions where applicable. $^{1}H/^{13}C$ chemical shifts were referenced to the residual solvent peak (DMSO-d_6: $\delta H = 2.50$, $\delta C = 39.51$).

2.8. Cultivation Study

Due to the hypothesis that the compound had iron-chelating properties for the bacteria, a cultivation study with and without the addition of iron to the medium was conducted. To investigate if the production was temperature specific, the bacteria were also grown at two different temperatures. The bacteria were grown in DVR1 medium and DVR2 medium (DVR1 with added 5.5 mL $FeSO_4$ 7 H_2O (8 g/L stock, ≙ 28.8 mM Fe)), at room temperature and at 10 °C with 130 rpm shaking. Samples were taken from the cultures, under sterile conditions, after 7, 14, and 21 days, for chemical analysis by UHPLC-HR-MS. From the cultures, 5 mL of sample were taken and centrifuged to pellet the bacteria, 1 mL of the supernatant was transferred to a new tube and centrifuged again, before sterile filtration using an Acrodisc syringe filter 0.2 µm, supor membrane (Pall Corp., East Hills, NY, USA) The filtered sample was mixed 1:1 with methanol prior to injecting on the UHPLC-HR-MS for investigation.

2.9. Marfey's Amino Acid Analysis

A small quantity of **1** was dissolved in 1 mL of 6N HCL and incubated for 6 h at 110 °C using 1.5-mL reaction tubes and a thermoblock. After cooling down to room temperature, the reaction was reduced to dryness by vacuum centrifugation at 40 °C. The dry sample after hydrolysis was re-dissolved in 100 µL of H_2O. The derivatization was carried out by mixing the re-dissolved hydrolystate with 180 µL FDAA in acetone (Marfey's reagent, Sigma), N_α-(2,4-Dinitro-5-fluorophenyl)-L-alaninamide), and 20 µL 1N $NaHCO_3$. The reaction was incubated at 40 °C using a thermoblock. After incubation, the reaction was acidified with 30 µL of 1N HCl and diluted with 2.5 mL of methanol. Then, 0.1 mg of L-threonine and D-threonine dissolved in 100 µL water were used to prepare standards of the amino acids using the same derivatization procedure as described for the sample hydrolysate. The standards and sample diluted in methanol were analyzed using UHPLC-MS/MS as described above.

2.10. Iron Chelation Experiment

For testing the capability of **1** and **2** to chelate iron, a chelation assay was performed. The molecule was dissolved in water (0.2 mg/mL) and 75 µL of the molecule were mixed with 25 µL of 10 mg/mL $FeCl_3 \times 6\ H_2O$. The preparation was done in HPLC vials, the reaction was thoroughly mixed by vortexing, centrifuged, and subsequently analyzed by UHPLC-MS/MS.

2.11. Hydrolyzation with Formic Acid

For testing the liability for hydrolyzation, a 1-mg sample of **1** was dissolved in 1 mL 10% (*v/v*) DMSO *aq*. and incubated for 24 h at room temperature with formic acid concentrations of 0% (control), 0.1%, 1.0%, 5.0%, and 10% (*v/v*). The reaction product was analyzed by UHPLC-MS/MS.

2.12. Production of Serratiochelin C

For testing the bioactivity of **2** in comparison to **1**, a sample of non-degraded **1** was hydrolyzed by adding 10% (*v/v*) formic acid and incubation over 24 h at room temperature. The formic acid was removed by vacuum centrifugation at 40 °C and subsequent freeze drying using a laboratory freeze dryer (Labconco).

2.13. Bioactivity Testing

2.13.1. Growth Inhibition Assay

To determine antimicrobial activity, a bacterial growth inhibition assay was executed. Compounds **1** and **2** were tested against *Staphylococcus aureus* (ATCC 25923), *Escherichia coli* (ATCC 259233), *Enterococcus faecialis* (ATCC 29122), *Pseudomonas aeruginosa* (ATCC 27853), *Streptococcus agalactiae* (ATCC 12386), and Methicillin-resistant *Staphylococcus aureus* (MRSA) (ATCC 33591), all strains from LGC Standards (Teddington, London, UK). *S. aureus*, MRSA, *E. coli*, and *P. aeruginosa* were grown in Muller Hinton broth (275730, Becton). *E. faecalis* and *S. agalactiae* were cultured in brain hearth infusion broth (53286, Sigma). Fresh bacterial colonies were transferred to the respective medium and incubated at 37 °C overnight. The bacterial cultures were diluted to a culture density representing the log phase and 50 µL/well were pipetted into a 96-well microtiter plate (734-2097, Nunclon™, Thermo Scientific, Waltham, MA, USA). The final cell density was 1500–15,000 colony forming units/well. The compound was diluted in 2% (*v/v*) DMSO (Dimethyl sulfoxide) in ddH_2O, and the final assay concentration was 50% of the prepared sample, since 50 µL of sample in DMSO/water were added to 50 µL of bacterial culture. After adding the samples to the plates, they were incubated over night at 37 °C and the growth was determined by measuring the optical density at λ = 600 nm (OD_{600}) with a 1420 Multilabel Counter VICTOR3™ (Perkin Elmer, Waltham, MA, USA). A water sample was used as the reference control, growth medium without bacteria as a negative control, and a dilution series of gentamycin (32 to 0.01 µg/mL, A2712, Merck) as the positive control and visually inspected for bacterial growth. The positive control was used as a system suitability test and the results of the antimicrobial assay were only considered valid when the positive control was passed. The final concentration of DMSO in the assays was ≤2% (*v/v*), known to have no effect in the tested bacteria. The data was processed using GraphPad Prism 8 (GraphPad, San Diego, CA, USA).

2.13.2. Cell Proliferation Assay

The inhibitory effect **1** and **2** was tested using an MTS in vitro cell proliferation assay against two cell lines: The human melanoma cell line A2058 (ATCC, CLR-1147™), and for general cytotoxicity assessment, the non-malignant MRC5 lung fibroblast cells (ATCC CCL-171™) were employed. The cells were cultured and assayed in Roswell Park Memorial Institute medium (RPMI-16040, FG1383, Merck) containing 10% (*v/v*) fetal bovine serum (FBS, 50115, Biochrom, Holliston, MA, USA). The cell concentration was 4000 cells/well for the lung fibroblast cells and 2000 cells/well for the cancer cells. After seeding, the cells were incubated for 24 h at 37 °C and 5% CO_2. The medium was then replaced with fresh RPMI-1640 medium supplemented with 10% (*v/v*) FBS and gentamycin (10 µg/mL, A2712, Merck). After adding 10 µL of sample diluted in 2% (*v/v*) DMSO in ddH_2O, the cells were incubated for 72 h at 37 °C and 5% CO_2. For assaying the viability of the cells, 10 µL of CellTiter 96® AQueous One Solution Reagent (G3581, Promega, Madison, WI, USA) containing tetrazolium [3-(4,5-dimethylthiazol-2-yl)-5-(3-carboxymethoxyphenyl)-2-(4-sulfophenyl)-2*H*-tetrazolium, inner salt] and phenazine ethosulfate was added to each well and incubated for one hour. The tests were executed

with three technical replicates. The plates were read using a DTX 880 plate reader (Beckman Coulter, CA, USA) by measuring the absorbance at λ = 485 nm. The cell viability was calculated using the media control. As a negative control, RPMI-1640 with 10% (*v/v*) FBS and 10% (*v/v*) DMSO (Sigma) was used as a positive control. The data was processed and visualized using GraphPad Prism 8.

2.13.3. Biofilm Inhibition Assay

For testing the inhibition of biofilm formation, the biofilm-producing *Staphylococcus epidermidis* (ATCC 35984) was grown in Tryptic Soy Broth (TSB, 105459, Merck, Kenilworth, NJ, USA) overnight at 37 °C. The overnight culture was diluted in fresh medium with 1% glucose (D9434, Sigma) before being transferred to a 96-well microtiter plate; 50 µL/well were incubated overnight with 50 µL of the test compound dissolved in 2% (*v/v*) DMSO aq. added in duplicates. The bacterial culture was removed from the plate and the plate was washed with tap water. The biofilm was fixed at 65 °C for 1 h before 70 µL of 0.1% crystal violet (115940, Millipore) were added to the wells for 10 min of incubation. Excess crystal violet solution was then removed and the plate dried for 1 h at 65 °C. Seventy microliters of 70% ethanol were then added to each well and the plate incubated on a shaker for 5–10 min. Biofilm formation inhibition were assessed by the presence of violet color and was measured at 600-nm absorbance using a 1420 Multilabel Counter VICTOR3™. Fifty microliters of a non-biofilm-forming *Staphylococcus haemolyticus* (clinical isolate 8-7A, University Hospital of North Norway Tromsø, Norway) mixed in 50 µL of autoclaved Milli-Q water was used as a control; 50 µL of *S. epidermidis* mixed in 50 µL of autoclaved Milli-Q water was used as the control for biofilm formation; and 50 µL of TSB with 50 µL of autoclaved Milli-Q water was used as a medium blank control.

3. Results

Compound **1** was isolated from a co-culture of *Serratia* sp. and *Shewanella* sp. when cultivated in an iron-limited medium. The bacteria were also cultivated in iron-supplemented media, where **1** was not detected. Compound **1** was only produced in co-cultures started directly from the glycerol stock by loop inoculation, and not found in any axenic cultures. The cultures were extracted, and the extracts were fractionated using FLASH chromatography to isolate serratiochelin A (**1**), a siderophore previously isolated exclusively from a *Serratia* sp., also when grown under iron-limited conditions [10]. During preparative HPLC-MS isolation, it was observed that the compound was degraded, and the degradation product was found to be serratiochelin C (**2**), which corresponds to previous observations [10]. A study of the iron binding of the compounds and a degradation study with formic acid was conducted. The structures of the compounds were verified by 1-D and 2-D NMR and MS experiments, and Marfey's analysis was used to find the configuration of the threonine moiety of the molecule. Compound **1** and **2** were tested for their antibacterial activities, their abilities to inhibit the formation of biofilm, and their toxicity towards human cells. This is the first study on the bioactivity of **1** since its original discovery in 1994 [9].

3.1. Identification of Co-Culture and Serratiochelin A Production Strain

When streaking out the glycerol stock onto three different agar plates, three morphologically different bacterial colonies were observed (Figure S14). The 16S rRNA gene of these bacteria was amplified and sequenced by Sanger sequencing, showing that the stock solution contained *Leifsonia* sp. (original isolate in stock), *Shewanella* sp., and *Serratia* sp. The 16S rRNA sequences for the three isolates can be found in the Supplementary Material (Texts S15–S17). *Shewanella* sp. and *Serratia* sp. are assumed to be of marine origin, as strains of the same genera have been cultivated at the same time as the *Leifsonia* sp. isolate, and the 16S rRNA sequences are similar to two strains of the Marbank strain collection (*Shewanella* sp. M10B851 and *Serratia* sp. M10B861, Marbank ID). In order to investigate if all bacteria were able to co-exist in the liquid culture started from the glycerol stock, a 450-mL culture of DVR1 was inoculated with the glycerol stock (identically as was done with the culture from which **1** was isolated) and the culture was streaked out on agar after 3 and 10 days of cultivation.

After three days of cultivation, the colony forming units (CFUs) of both *Shewanella* sp. and *Serratia* sp. were observed on the plates (Figure S14), proven by morphological identification and sequencing of the 16S rRNA gene. After 10 days of culturing, no CFUs of *Shewanella* sp. were observed from the culture, and the experiment detected exclusively CFUs of *Serratia* sp. No *Leifsonia* colonies were observed from the liquid cultures, not after 3 nor 10 days of cultivation. This indicates that the *Serratia* sp. isolate outgrow the other two isolates in the cultivation done in this study. After re-streaking the three bacterial isolates present in the glycerol stock to obtain pure cultures, the different isolates were cultivated separately in 50-mL cultures in DVR1 to identify the actual producer of **1**. Compound **1** was only produced in co-cultures started directly from the glycerol stock, and not by any of the cultures started from axenic colonies from agar plates.

3.2. Dereplication and Isolation

Serratiochelin A (**1**) was obtained as a brown powder. The bacterial extracts and fractions were analyzed using UHPLC-IMS-MS and **1** was detected at *m/z* 430.1594 ($[M+H]^+$) in ESI+ eluting at 4.45 min. The calculated elemental composition was $C_{21}H_{23}N_3O_7$ (Calc. *m/z* 430.1614 $[M+H]^+$), corresponding to 12 degrees of unsaturation. The elemental composition gave several hits for natural products in available databases, including serratiochelin A (**1**). As **1** had been previously isolated from *Serratia* sp., we saw it as a clear possibility that we had a positive identification of the compound. However, to confirm this, isolation and structure elucidation was necessary. After the first round of isolation using preparative HPLC, we detected two species of the product, one at RT= 4.45 min (**1**) and another at RT = 2.07 min (**2**), both having the same *m/z* and elemental composition in ESI+. We later confirmed that the *m/z* of **2** in ESI+ was not the *m/z* of the molecular ion due to neutral water loss in the ion source. The masses of **1** and **2** are thus not equivalent, which was later confirmed by ESI-ionization, which confirmed the mass of **2** to be equal to that of **1**+H_2O.

It was not possible to obtain **1** as a pure compound after the purification, as it was always accompanied by **2**, indicating a possible degradation of **1**. Compound **2,** on the other hand, was obtained as a pure compound after using preparative HPLC for isolation. To distinguish between the two molecules, the collision cross section (CCS) and drift time of the compounds were compared, and the samples were also investigated in ESI- (see Table 2 for the respective values, the high- and low-energy MS spectra, as well as UV/Vis spectra for **1** and **2** that are given in Figures S11 and S12). For isolating **1,** FLASH chromatography was used, since there was no **2** detected using this protocol, where no acid was employed. The collected fractions were assayed individually using UHPLC-MS and the first fraction eluting at 100% methanol was found to be sufficiently pure for structure elucidation via NMR and further bioactivity testing (results of the purity assay are given in Figure 2), yielding 50.9 mg **1** from 3667.9 mg of extract. Compound **1** was not readily dissolved in water and methanol but it dissolved in DMSO. Solutions of **1** were prepared in 100% DMSO and further diluted in water. The same was done with **2,** which also dissolved in methanol.

Serratiochelin C (**2**) was obtained as a brown powder, after acid-catalyzed degradation of **1**. From the ESI-, it was possible to elucidate the elemental composition of **2**. Compound **2** was detected, with *m/z* 446.1568 ($[M-H]^-$) in ESI- eluting at 2.07 min. The calculated elemental composition was $C_{21}H_{25}N_3O_8$ (Calc. *m/z* 446.1563 $[M-H]^-$), corresponding to 11 degrees of unsaturation.

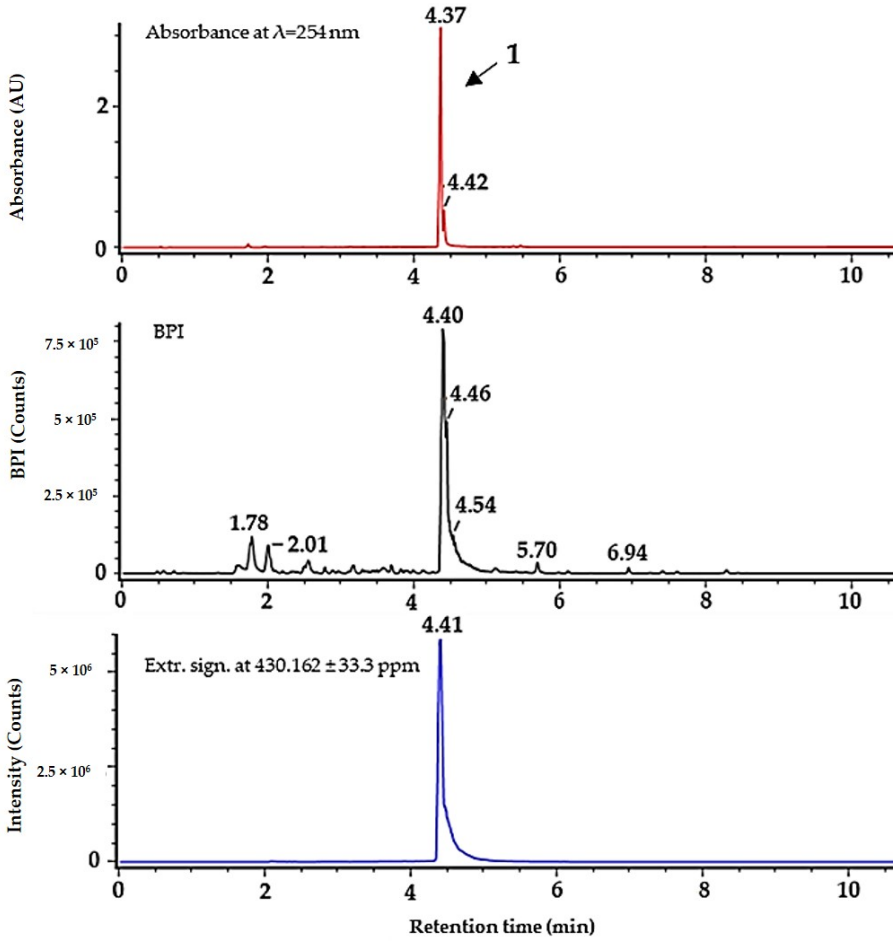

Figure 2. Purity of serratiochelin A (**1**) after isolation using FLASH chromatography, analyzed by UHPLC-MS. Top (in red) absorbance at 254 nm, middle (black) BPI chromatogram, bottom (blue) extracted signal for *m/z* = 430.162 (±33.3 ppm). ΔRT for UV/Vis detector is ~−0.05 min.

3.3. Structure Elucidation

Close inspection of 1-D (^{1}H and ^{13}C, Table 1) and 2-D (HSQC, HMBC, COSEY, and ROESY) NMR data of **1** confirmed that we isolated the previously reported compound serratiochelin A (**1**). All NMR spectra can be seen in the Supplementary Material (Figures S1–S5). Key COSY and HMBC correlations used to assign the structure of **1** can be seen in Figure 3.

In preparations treated with formic acid, we detected a third molecule eluting at 2.60 min. According to its signal, fragments, and retention time, we concluded it was serratiochelin B [10]. Serratiochelin B was not isolated or verified by NMR. Serratiochelin B and **2** were not present within the crude extract or within fractions obtained by FLASH chromatography but were detected after treatment with acid. The conformation of threonine was found to be L by Marfey's method, which is in compliance what has been published previously [10]. Results are given within the Supplementary Material (Figure S13).

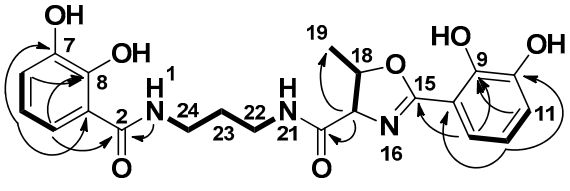

Figure 3. Key COSY (bold) and HMBC (arrow) correlations for serratiochelin A (**1**).

Table 1. ^{1}H- and ^{13}C-NMR data for serratiochelin A (**1**) and C (**2**) in DMSO-d_6.

NMR Data	Serratiochelin A (1)		Serratiochelin C (2)	
Position	δ_C, Type	δ_H (*J* in Hz)	δ_C, Type	δ_H (*J* in Hz)
1		8.30, t (5.9)		8.01, t (5.9)
2	169.6, C		169.73, C	
3	114.9, C		114.92, C	
4	117.1, CH	7.25, dd (8.1, 1.5)	117.04, CH	7.25, dd (8.2, 1.5)
5	117.8, CH	6.67, t (7.9)	117.84, CH	6.66, t (8.0)
6	118.7, CH	6.9, dd (7.8, 1.4)	118.65, CH	6.89, dd (7.8, 1.5)
7	146.3, C		146.27, C	
8	149.8, C		149.81, C	
9	148.3, C		146.12, C	
10	145.7, C		148.27, C	
11	119.4, CH	6.96, dd (7.8, 1.6)	118.18, CH	6.92, dd (7.7, 1.5)
12	118.7, CH	6.73, t (7.9)	117.77, CH	6.69, t (7.9)
13	117.9, CH	7.07, dd (7.9, 1.6)	118.92, CH	7.37, dd (8.1, 1.6)
14	110.3, C		116.77, C	
15	165.7, C		168.01, C	
16				8.66, s
17	73.7, CH	4.45, d (87.3)	59.18, CH	4.34, dd (8.0, 4.4)
18	78.8, CH	4.86, p (6.4)	66.38, CH	4.10, qd (6.1, 4.7)
19	20.7, CH_3	1.45, d (6.3)	20.30, CH_3	1.09, d (6.4)
20	169.8, C		169.99, CH	
21		8.81, s		8.78, t (5.3)
22	36.7, CH_2	3.30, m	36.58, CH_2	3.29, q (6.7)
23	28.9, CH_2	1.72, p (7.0)	28.96, CH_2	1.67, p (7.0)
24	36.6, CH_2	3.18, m	36.41, CH_2	3.20–3.08, m

The structure of serratiochelin C (**2**) was confirmed in a similar manner to that of **1**. All NMR spectra can be seen in the Supplementary Material (Figures S6–S10).

3.4. Detection of Iron Chelation

Compounds **1** and **2** were mixed with aqueous $FeCl_3$ solution to investigate if the compounds were able to chelate iron. Both **1** and **2** chelated iron, and the mass spectrometric data given in Table 2 indicate chelation of iron by the loss of three protons through coordination, as published previously [10]. The calculated exact mass for chelation of **1** was *m/z* 483.0729 ($[M+Fe-2H]^+$) and for **2** and serratiochelin B *m/z* 501.0835 ($[M+Fe-2H]^+$). In ESI-, the calculated *m/z* ratios were *m/z* 481.0572 ($[M+Fe-4H]^+$) for **1** and *m/z* 499.0678 ($[M+Fe-4H]^+$) for **2**.

Table 2. IMS and MS data for the apo- and ferrylspecies of serratiochelin A (**1**), serratiochelin B, and serratiochelin C (**2**).

Compounds	Form	Ionization	RT * [min]	*m/z*	CCS ** [A^2]	Drift Time [ms]
Serratiochelin C (earliest eluting)	apo	ESI+	2.07	430.1610 ***	202.88	7.00
	apo	ESI-	2.05	446.1568 ***	198.35	6.94
	ferri	ESI+	2.09	501.0844	208.06	6.75
	ferri	ESI-	2.11	499.0680	203.54	7.12
Serratiochelin B (middle eluting)	apo	ESI+	2.64	448.1714	210.99	6.84
	apo	ESI-	2.60	446.1573	199.52	6.98
	ferri	ESI+	2.61	501.0822	211.91	6.89
	ferri	ESI-	2.62	499.0673	201.16	7.04
Serratiochelin A (late eluting)	apo	ESI+	4.45	430.1611	202.85	6.99
	apo	ESI-	4.37	428.1466	201.47	7.05
	ferri	ESI+	4.46	483.0723	206.88	6.70
	ferri	ESI-	4.39	481.5058	208.50	7.30

* Retention time, ** Collision cross section, *** Loss of water of apo-serratiochelin C (**2**) in ESI+, not in ESI-, and not for the ferri-siderophores.

3.5. Degradation Study with Formic Acid

The study confirmed that the degradation was triggered by formic acid. In order to obtain a pure sample of **1**, we used FLASH fraction no. 13, which predominantly contained **1** since during the extraction process and the FLASH chromatography, no formic acid or acidic solution is used that could induce degradation. This sample was used for the degradation study. Formic acid at concentrations of 0.1%, 1.0%, 5.0%, and 10% (*v*/*v*) were tested and compared to the control (no acid), as can be seen in Figure 4. It was found that the degradation correlates with the concentration of formic acid. The degradation takes place not only in the presence of formic acid. When incubated with 1% (*v*/*v*) hydrochloric acid or acetic acid, we observed degradation to approximately the same extent (data not shown). The acid-catalyzed degradation mechanism turning **1** into **2** via intermediates **1a**–**e** can be seen in Figure 5.

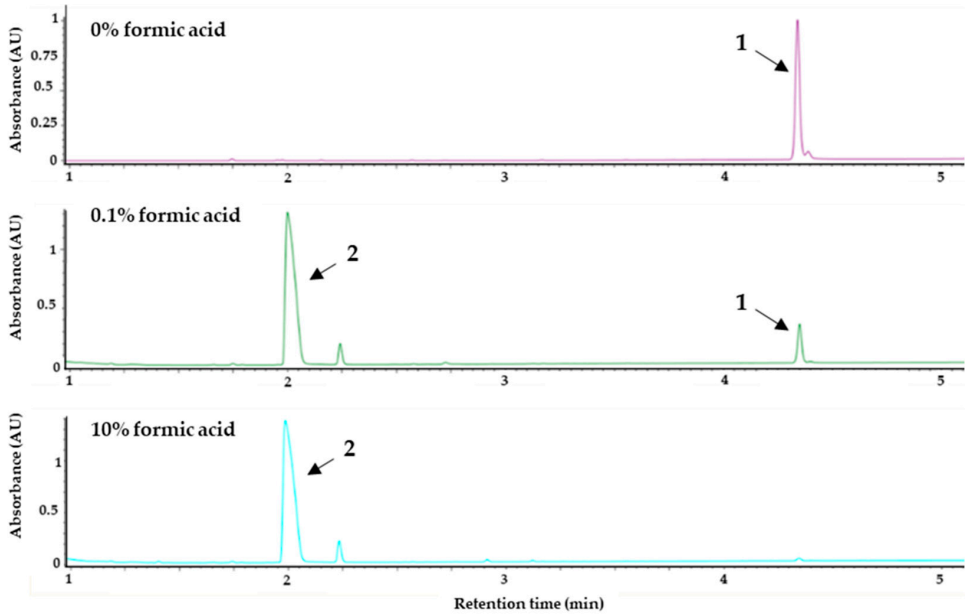

Figure 4. UV-max plot chromatogram. Degradation study showing the effect of formic acid on serratiochelin A (**1**). The purified sample of **1** was treated with different concentrations of formic acid (% (*v*/*v*)) for 24 h at room temperature and subsequently analyzed via UHPLC-PDA-MS. The chromatograms of the control (0% formic acid), 0.1% formic acid, and 10% formic acid are given above. The degradation of **1** (RT = 4.45 min) into serratiochelin C (**2**) (RT = 2.07 min) corresponds to the amount of formic acid used.

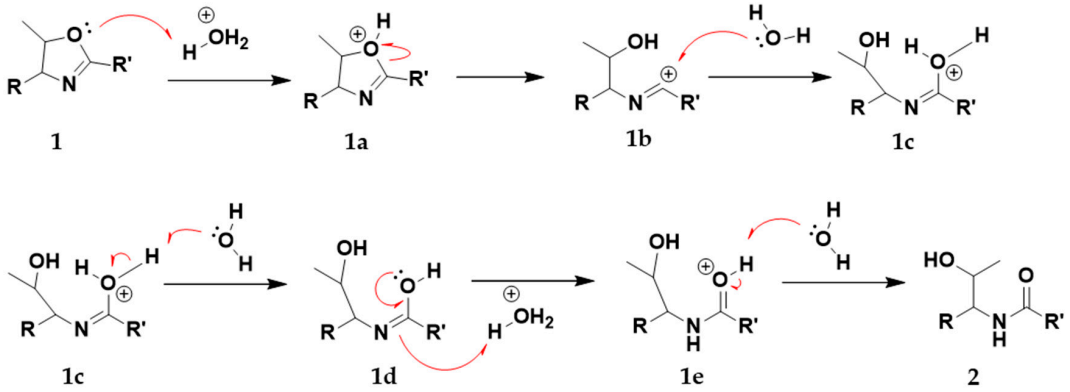

Figure 5. The proposed acid-catalyzed degradation reaction of the central methylated oxazoline ring of **1**, turning **1** into **2** via intermediates **1a** to **1e**.

3.6. Cultivation Study

The cultivation study revealed that **1** was only produced in the iron-deficient co-cultures, as can be seen in Figure 6. Cultures grown in media supplemented with 160 µM $FeSO_4$ did not produce **1** after 7, 14, and 21 days when grown at room temperature nor when grown at 10 °C (Figure 6). Within the iron-deficient cultures, **1** was detected after 7, 14, and 21 days cultivation at 10 °C as well as when cultivated at room temperature. Additionally, when extracting two cultures grown for 14 days at 10 °C using solid-phase extraction, there was no **1** present within the iron-supplemented media while it was a major component in the extract of the iron-deficient culture. Serratiochelin B and **2** were not detected in the cultures, nor in crude extracts after solid-phase extraction.

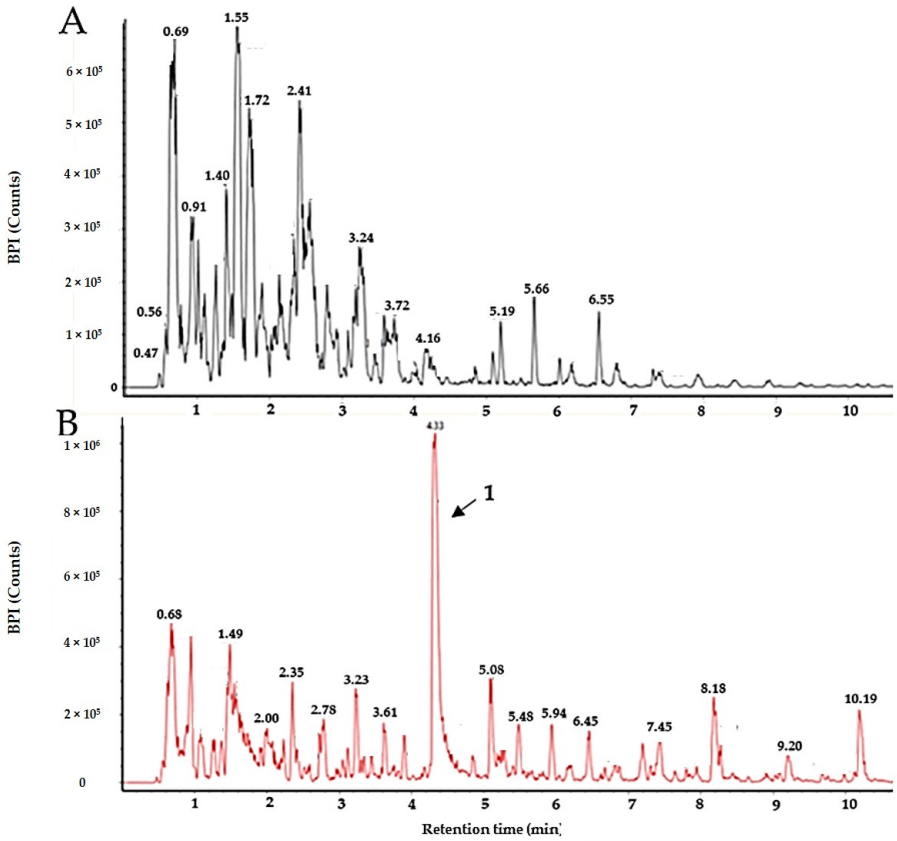

Figure 6. BPI chromatograms of the extracts of two co-cultures. (**A**) The extract of a 14-day culture (10 °C) supplemented with 160 µM Fe(III). (**B**) The extract of a 14-day culture (10 °C) grown in iron-deficient media. The peak of serratiochelin A (**1**) is indicated by the black arrow.

3.7. Bioassays

The growth-inhibiting properties of **1** and **2** were tested against several Gram-positive and Gram-negative strains. The antimicrobial assay detected an effect of **1** on *S. aureus*. Interestingly, there was no effect of **2** on *S. aureus* detected in the assay. There was no antimicrobial effect of **1** and **2** against *S. agalactiae*, *P. aeruginosa*, *E. coli*, *E. faecalis*, and MRSA observed. The results against all the test strains can be seen in Figure 7. The antimicrobial assay with *S. aureus* was repeated to verify the effect of **1**. Among the tested concentrations, 25 µM was the lowest concentration of **1**, which completely inhibited the growth of *S. aureus*, as displayed in Figure 8. Compound **1** and **2** were also tested for their ability to inhibit biofilm formation by *S.epidermidis* in concentrations up to 200 µM. Compound **1** showed some weak effects (assay result of ~ 40%, meaning 60% inhibition, normal cut-off used for further investigation is minimum 70% inhibition) at 200 µM. Compound **2** showed no visible effect up to 200 µM.

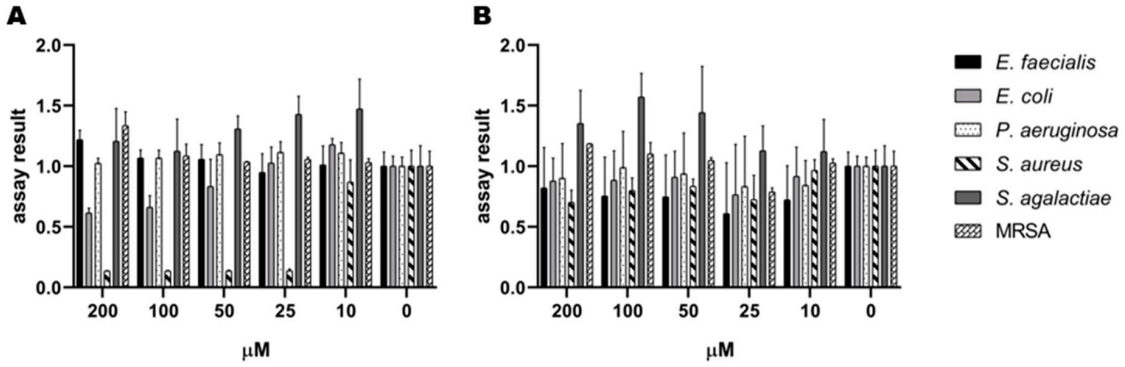

Figure 7. Initial screen of antibacterial activity of (**A**) serratiochelin A (**1**) and (**B**) serratiochelin C (**2**) on *E. faecialis*, *E. coli*, *P. aeruginosa*, *S. agalactiae*, and MRSA, normalized assay results. The experiment was executed twice with two technical replicates each.

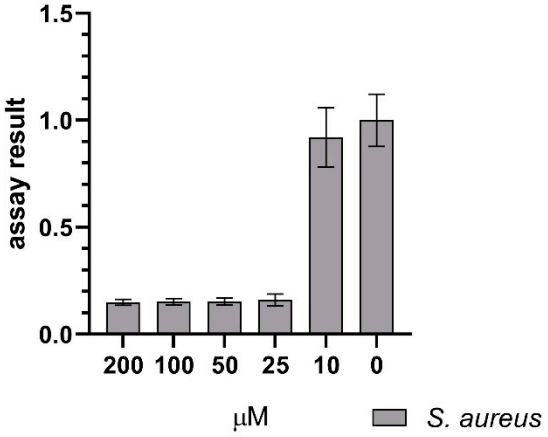

Figure 8. Effect of serratiochelin A (**1**) on *S. aureus* showing inhibition of growth down to 25 µM, normalized assay results. The assay was executed in four experiments with 3 × 2 and 1 × 3 technical replicates.

The effects of the compounds on eukaryotic cells was evaluated using the human melanoma cell line A2058 and the non-malign lung fibroblast cell line MRC5, see Figure 9. The effect of **2** on both cell lines is insufficient, while **1** reduces the cell proliferation of both MRC5 and A2058 cells. The effect of **1** is stronger against MRC5 cells than against A2058.

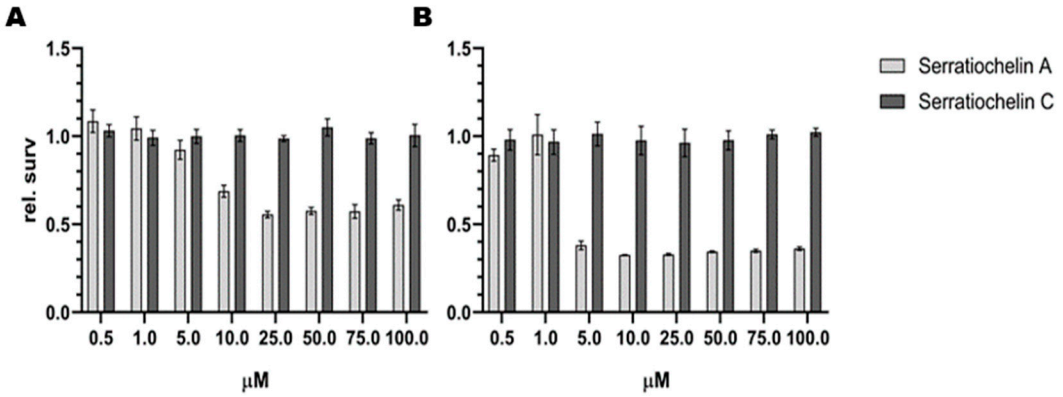

Figure 9. Antiproliferative effect of serratiochelin A (**1**) and C (**2**) on (**A**) A2058 (melanoma) and (**B**) MRC-5 (non-malignant lung fibroblasts) cell lines. The experiments were repeated twice with three technical replicates.

4. Discussion

In this study, a siderophore was isolated from a co-culture of a *Shewanella* sp. and *Serratia* sp. bacteria, both of which come from bacterial genera that are important for environmental iron metabolism. Bacteria from the genus *Shewanella* are known for their important role in iron metabolism, especially in aquatic environments. Previously, several siderophores have been isolated from bacteria of the genus *Serratia*, among these serratiochelin A (**1**).

Shewanella is a genus of Gram-negative rod-shaped γ-proteobacteria, within the order Alteromonadales, found mostly in aquatic habitats [16]. Bacteria from this genus have been isolated from several aquatic sources, both marine and freshwater [17–20]. The genus was established in 1985 [21], after a reconstruction of the *Vibrionaceae* family. *Shewanella* is part of the monogeneric family Shewanellaceae [16], which consists only of this one genera. The genus has high respiratory diversity, with the capability to respire approximately 20 different compounds, including toxic compounds and insoluble metals, one example being reducing Fe(III) chelate and Fe(III) oxide to produce soluble Fe(II) [22]. Bacteria from this genus are often involved in the iron metabolism in their environment, and several iron chelators (siderophores) have been isolated from this genus. Putrebactin is a cyclic dihydroxamate siderophore, produced and isolated from *S. putrefaciens* [23].

To investigate if the three bacterial isolates present in the glycerol stock co-exist in the liquid DVR1 cultures, the culture was streaked out on several agar plates after 3 and 10 days of incubation. The *Shewanella* colonies appeared first, followed by *Serratia* forming colonies on top of the *Shewanella* sp. colonies (Figure S14). After 10 days, there were only colony forming units of *Serratia* sp. present from the liquid co-culture, and the *Shewanella* could not be detected when streaked out on agar. Serratiochelins have previously only been isolated from the *Serratia* genus, and are considered to be rare siderophores [10]. As *Serratia* completely dominates the *Serratia-Shewanella* co-culture after 10 days, and based on data reported regarding previous isolation of **1** [**9**,**10**], it seems to be reasonable to hypothesize that *Serratia* is the true producer of **1** in this co-culture and that it is outcompeting *Shewanella* because of its specific iron acquisition. As **1** was not observed in axenic cultures of *Shewanella* or *Serratia*, we assume that the co-culturing is inducing the production of the compound, possibly due to the competition for iron in the culture.

Compound **1** was isolated from the co-culture after modifying the purification protocol. The degradation of **1** to **2** was triggered by formic acid used in the mobile phase during chromatographic isolation of the compounds. We confirmed that the degradation correlates with the concentration of formic acid as previously published [10]. In addition, the same acidic hydrolyzation of an oxazoline ring was also observed for the compound agrobactin after exposure to hydrochloric acid [24]. We also confirmed the chelation of iron in a hexadecanoate coordination indicated by the loss of three protons, observed in HR-MS experiments [10]. Compound **1** was only produced when no additional iron was added to the co-culture. In the presence of iron, **1** was not detected in the bacterial culture media. We did not detect serratiochelin B and **2** in the culture media, extract, or FLASH fractions (where no acid was used). Previously, it was reported that **1** and serratiochelin B are the initial biosynthetic products of *Serratia* [10]. For our isolate, the results strongly indicate that **1** is the only biosynthetic product, while serratiochelin B and **2** are degradation products of **1**. To obtain **1**, its liability for acid degradation is a significant disadvantage. The FLASH liquid chromatography represents a rather inefficient method for isolation since we were taking only the fraction with the highest purity. Thus, a considerable amount of compound eluted before and after together with other impurities, which diminished the yield of pure **1** significantly, and the purification protocol was not optimized regarding yields but for obtaining **1** without its degradation product. We assume that within the producer isolates' natural environment, **1** is, however, most likely not degrading into **2** due to the rather alkaline pH of seawater [25].

The acid-free isolation enabled us to isolate **1** for bioactivity testing. Since there is no bioactivity data present for **1** and **2,** and the purpose of our investigation was to find new bioactive molecules, it was prioritized for isolation. The testing of both compounds revealed some interesting insights into their bioactivity. Compound **2** displayed no activity in the tested assays and at the tested concentrations,

while **1** had antibacterial activity against *S. aureus* and toxic effects on both eukaryotic cell lines tested. Its antibacterial effect was specific towards *S. aureus*, while not having an effect on the other bacteria, including MRSA. Its cytotoxic effect was evaluated against the melanoma cell line (A2058), as we frequently observed that it is the most sensitive cancer cell line in our screening of extracts and compounds. The non-malignant lung fibroblasts (MRC5) was included as a general control of toxicity. The observed effect was stronger on lung fibroblasts than melanoma cells. Of interest to us was the observed difference in activity between **1** and **2** despite the fact that the two structures are closely related. It is questionable if the antiproliferative effect of **1** is caused by iron deprivation as observed for other siderophores [26] or by another effect. The same applies for the observed antibacterial effect on *S.aureus*, while the lack of effect on the other bacteria might indicate a specific target. Both molecules are capable of chelating iron, so either **1** has a higher affinity to iron than **2**, or it has another mode of action. The species-specific antibacterial effect indicates the latter. Gokarn and co-authors investigated the effect of iron chelation by exochelin-MS, mycobactin S, and deferoxiamine B on mammalian cancer cell lines and an antiproliferative effect was observed at concentrations between 0.1 to 1.0 mg/mL. Only HEPG2 cells have shown 23% cell survival at 20 µg/mL for mycobactin S. They observed a different sensitivity among the tested cell lines and siderophores [26]. Compound **1** had an effect at concentrations of <43 µg/mL (40% cell survival was detected at 2.15 µg/mL of **1** against MRC5). Therefore, testing of **1** against more cell lines and testing of **2** at higher concentrations would be an approach for further studies on the antiproliferative effects of **1** and **2**. Some siderophores are known to have additional functions, such as a virulence factor and modulation of the host of a pathogen [27]. Assuming another mode of action than iron chelation, the most relevant structural difference would be the 5-methyl-2-oxazoline heterocycle in **1**, which is hydrolyzed in **2**. Oxazole and oxazoline moieties are structural motives present in molecules with an antibacterial and antiproliferative effect [28,29]. They are ligands to a number of different protein targets and can be regarded as "privileged structures" [29,30]. Further bioactivity elucidation of the two serratiochelins and the mode of action studies of **1** will be the subject of further investigation.

5. Conclusions

We proved the production of **1** in high yields by a co-culture of *Serratia* sp. and *Shewanella* sp., while the compound was not observed in axenic cultures. We confirmed the iron chelation, as well as the degradation of **1** to **2**. We did not observe the production of any compound that could be related to serratiochelin B in the bacterial cultures nor in the extract, but we observed its generation in traces during acid-induced degradation, which gives rise to the assumption that serratiochelin B and **2** are both hydrolyzation products of **1** in this study.

While **1** showed antiproliferative activity on human cancer cells but also on non-malignant lung fibroblasts, and a specific antimicrobial effect on *S. aureus*, **2** did not show any bioactivity in the assays conducted in this study. Since **1** and **2** differ in the presence of a structural motif that can be seen as a privileged structure, we hypothesize that the hydrolyzation of the 5-methyl-2-oxazoline explains the difference in bioactivity. The liability for hydrolyzation, however, represents a strong disadvantage for developing this candidate further as a drug lead.

Supplementary Materials: The following are available online at http://www.mdpi.com/2076-2607/8/7/1042/s1, Figure S1: ^{1}H NMR (600 MHz, DMSO-d_6) spectrum of **1**; Figure S2: ^{13}C (151 MHz, DMSO-d_6) spectrum of **1**; Figure S3: HSQC + HMBC (600 MHz, DMSO-d_6) spectrum of serratiochelin A; Figure S4: COSY (600 MHz, DMSO-d_6) spectrum of **1**; Figure S5: ROESY (600 MHz, DMSO-d_6) spectrum of **1**; Figure S6: ^{1}H NMR (600 MHz, DMSO-d_6) spectrum of **2**; Figure S7: ^{13}C (151 MHz, DMSO-d_6) spectrum of **2**; Figure S8: HSQC + HMBC (600 MHz, DMSO-d_6) spectrum of **2**; S9: HSQC + HMBC (600 MHz, DMSO-d_6) spectrum of **2** (**2**), zoomed in crowded area; Figure S10: COSY (600 MHz, DMSO-d_6) spectrum of **2**; Figure S11: Mass spectra of **1** and **2**; Figure S12: UV/Vis spectra of **1**and **2**; Figure S13: Chromatograms of Marfey's analysis of **1**; Figure S14: Isolation of the bacteria and co-culture of *Serratia* sp. and *Shewanella* sp., Text S15: Consensus sequence of *Shewanella* sp.; Text S16: Consensus sequence of *Serratia* sp.; Text S17: Consensus sequence of *Leifsonia* sp.

Author Contributions: Conceptualization, J.H.A., Y.S. and M.J.; investigation, M.J. and Y.S.; structure elucidation J.I.; writing—original draft preparation, M.J., K.Ø.H. and Y.S.; writing—review and editing, J.I., J.H.A. and E.H.H. All authors have read and agreed to the published version of the manuscript.

Funding: This project received funding from the following projects: The Marie Skłodowska-Curie Action MarPipe of the European Union and from UiT-The Arctic University of Norway (grant agreement GA 721421 H2020-MSCA-ITN-2016), The DigiBiotics project of the Research Counsil of Norway (project iD 269425) and the AntiBioSpec project of UiT the Arctic University of Norway (Cristin iD 20161326). The publication charges for this article have been funded by a grant from the publication fund of UiT-The Arctic University of Norway.

Acknowledgments: Yannik Schneider has been supported by the MarPipe Project, and Marte Jenssen by the DigiBiotics project and the AntiBioSpec project. Kirsti Helland and Marte Albrigtsen are gratefully acknowledged for executing the bioactivity assays and Chun Li for his help with identifying the strains. We want to acknowledge our colleagues of The Norwegian Marine Biobank (Marbank) for sampling and isolation of the bacterial strains.

Conflicts of Interest: The authors declare no conflict of interest.

References

1. Andrews, S.C.; Robinson, A.K.; Rodríguez-Quiñones, F. Bacterial iron homeostasis. *FEMS Microbiol. Rev.* **2003**, *27*, 215–237. [CrossRef]
2. Sandy, M.; Butler, A. Microbial iron acquisition: marine and terrestrial siderophores. *Chem. Rev.* **2009**, *109*, 4580–4595. [CrossRef]
3. Winkelmann, G. Microbial siderophore-mediated transport. *Biochem. Soc. Trans.* **2002**, *30*, 691–696. [CrossRef]
4. Hider, R.C.; Kong, X. Chemistry and biology of siderophores. *Nat. Prod. Rep.* **2010**, *27*, 637–657. [CrossRef] [PubMed]
5. Ito, T.; Neilands, J.B. Products of "low-iron fermentation" with bacillus subtilis: Isolation, characterization and synthesis of 2, 3-dihydroxybenzoylglycine. *J. Am. Chem. Soc.* **1958**, *80*, 4645–4647. [CrossRef]
6. Dworkin, M.; Falkow, S.; Rosenberg, E.; Schleifer, K.-H.; Stackebrandt, E. *The Genus Serratia*; Springer: New York, NY, USA, 2006; pp. 219–244. [CrossRef]
7. Martinec, T.; Kocur, M. The taxonomic status of Serratia marcescens Bizio. *Int. J. Syst. Evol. Microbiol.* **1961**, *11*, 7–12. [CrossRef]
8. Khilyas, I.; Shirshikova, T.; Matrosova, L.; Sorokina, A.; Sharipova, M.; Bogomolnaya, L. Production of siderophores by Serratia marcescens and the role of MacAB efflux pump in siderophores secretion. *BioNanoScience* **2016**, *6*, 480–482. [CrossRef]
9. Ehlert, G.; Taraz, K.; Budzikiewicz, H. Serratiochelin, a new catecholate siderophore from Serratia marcescens. *Z. Nat.* **1994**, *49*, 11–17. [CrossRef]
10. Seyedsayamdost, M.R.; Cleto, S.; Carr, G.; Vlamakis, H.; João Vieira, M.; Kolter, R.; Clardy, J. Mixing and matching siderophore clusters: Structure and biosynthesis of serratiochelins from *Serratia* sp. V4. *J. Am. Chem. Soc.* **2012**, *134*, 13550–13553. [CrossRef]
11. Modell, B.; Letsky, E.A.; Flynn, D.M.; Peto, R.; Weatherall, D.J. Survival and desferrioxamine in thalassaemia major. *Br. Med. J.* **1982**, *284*, 1081–1084. [CrossRef] [PubMed]
12. Saha, M.; Sarkar, S.; Sarkar, B.; Sharma, B.; Bhattacharjee, S.; Tribedi, P. Microbial siderophores and their potential applications: A review. *Environ. Sci. Pollut. Res.* **2015**, *23*, 3984–3999. [CrossRef] [PubMed]
13. Braun, V.; Pramanik, A.; Gwinner, T.; Koberle, M.; Bohn, E. Sideromycins: Tools and antibiotics. *Biometals* **2009**, *22*, 3–13. [CrossRef]
14. Pramanik, A.; Stroeher, U.H.; Krejci, J.; Standish, A.J.; Bohn, E.; Paton, J.C.; Autenrieth, I.B.; Braun, V. Albomycin is an effective antibiotic, as exemplified with Yersinia enterocolitica and Streptococcus pneumoniae. *Int. J. Med. Microbiol.* **2007**, *297*, 459–469. [CrossRef]
15. Altschul, S.F.; Gish, W.; Miller, W.; Myers, E.W.; Lipman, D.J. Basic local alignment search tool. *J. Mol. Biol.* **1990**, *215*, 403–410. [CrossRef]
16. Ivanova, E.P.; Flavier, S.; Christen, R. Phylogenetic relationships among marine Alteromonas-like proteobacteria: Emended description of the family Alteromonadaceae and proposal of Pseudoalteromonadaceae fam. nov., Colwelliaceae fam. nov., Shewanellaceae fam. nov., Moritellaceae fam. nov., Ferrimonadaceae fam. nov., Idiomarinaceae fam. nov. and Psychromonadaceae fam. nov. *Int. J. Syst. Evol. Microbiol.* **2004**, *54*, 1773–1788. [CrossRef]

17. Lee, O.O.; Lau, S.C.; Tsoi, M.M.; Li, X.; Plakhotnikova, I.; Dobretsov, S.; Wu, M.C.; Wong, P.K.; Weinbauer, M.; Qian, P.Y. *Shewanella irciniae* sp. nov., a novel member of the family Shewanellaceae, isolated from the marine sponge Ircinia dendroides in the Bay of Villefranche, Mediterranean Sea. *Int. J. Syst. Evol. Microbiol.* **2006**, *56*, 2871–2877. [CrossRef] [PubMed]
18. Ivanova, E.P.; Nedashkovskaya, O.I.; Sawabe, T.; Zhukova, N.V.; Frolova, G.M.; Nicolau, D.V.; Mikhailov, V.V.; Bowman, J.P. *Shewanella affinis* sp. nov., isolated from marine invertebrates. *Int. J. Syst. Evol. Microbiol.* **2004**, *54*, 1089–1093. [CrossRef]
19. Kizhakkekalam, K.V.; Chakraborty, K.; Joy, M. Antibacterial and antioxidant aryl-enclosed macrocyclic polyketide from intertidal macroalgae associated heterotrophic bacterium Shewanella algae. *Med. Chem. Res.* **2019**, *29*, 145–155. [CrossRef]
20. Bowman, J.P.; McCammon, S.A.; Nichols, D.S.; Skerratt, J.H.; Rea, S.M.; Nichols, P.D.; McMeekin, T.A. *Shewanella gelidimarina* sp. nov. and *Shewanella frigidimarina* sp. nov., novel Antarctic species with the ability to produce eicosapentaenoic acid (20:5 omega 3) and grow anaerobically by dissimilatory Fe(III) reduction. *Int. J. Syst. Evol. Microbiol.* **1997**, *47*, 1040–1047. [CrossRef]
21. MacDonell, M.T.; Colwell, R.R. Phylogeny of the Vibrionaceae, and recommendation for two new genera, Listonella and Shewanella. *Syst. Appl. Microbiol.* **1985**, *6*, 171–182. [CrossRef]
22. Hau, H.H.; Gralnick, J.A. Ecology and biotechnology of the genus Shewanella. *Annu. Rev. Microbiol.* **2007**, *61*, 237–258. [CrossRef] [PubMed]
23. Ledyard, K.M.; Butler, A. Structure of putrebactin, a new dihydroxamate siderophore produced by Shewanella putrefaciens. *J. Biol. Inorg. Chem.* **1997**, *2*, 93–97. [CrossRef]
24. Ong, S.A.; Peterson, T.; Neilands, J.B.; Ong, S.A. Agrobactin, a siderophore from Agrobacterium Tumefaciens. *J. Biol. Chem.* **1979**, *254*, 1860–1865. [PubMed]
25. Halevy, I.; Bachan, A. The geologic history of seawater pH. *Science* **2017**, *355*, 1069–1071. [CrossRef]
26. Gokarn, K.; Sarangdhar, V.; Pal, R.B. Effect of microbial siderophores on mammalian non-malignant and malignant cell lines. *BMC Complement. Altern. Med.* **2017**, *17*, 145. [CrossRef]
27. Behnsen, J.; Raffatellu, M. Siderophores: More than stealing iron. *MBio* **2016**, *7*, e01906–e01916. [CrossRef]
28. Chiacchio, M.A.; Lanza, G.; Chiacchio, U.; Giofrè, S.V.; Romeo, R.; Iannazzo, D.; Legnani, L. Oxazole-based compounds as anticancer agents. *Curr. Med. Chem.* **2019**, *26*, 7337–7371. [CrossRef]
29. Zhang, H.-Z.; Zhao, Z.-L.; Zhou, C.-H. Recent advance in oxazole-based medicinal chemistry. *Eur. J. Med. Chem.* **2018**, *144*, 444–492. [CrossRef]
30. Kim, J.; Kim, H.; Park, S.B. Privileged structures: Efficient chemical "navigators" toward unexplored biologically relevant chemical spaces. *J. Am. Chem. Soc.* **2014**, *136*, 14629–14638. [CrossRef]

Bioactivity of Serratiochelin A, a Siderophore Isolated from a Co-Culture of *Serratia* sp. and *Shewanella* sp.

Yannik Schneider [1†*], Marte Jenssen [1†*], Johan Isaksson [2], Kine Ø. Hansen [1], Jeanette Hammer Andersen [1] and Espen H. Hansen [1]

[1] Marbio, Faculty for Fisheries, Biosciences and Economy, UiT—The Arctic University of Norway, Breivika, N-9037 Tromsø, Norway; kine.o.hanssen@uit.no (K.Ø.H.); espen.hansen@uit.no (E.H.H.); jeanette.h.andersen@uit.no (J.H.A.)

[2] Department of Chemistry, Faculty of Natural Sciences, UiT—The Arctic University of Norway, Breivika, N-9037 Tromsø, Norway; johan.isaksson@uit.no (J.I.)

* Correspondence: yannik.k.schneider@uit.no; Tel.: +47-77649267; marte.jenssen@uit.no; Tel.: +47-77649275

† Authors contributed equally to the work

Supplemental Information Table of Contents

Results chemistry and mass spectrometry

Figure S11 Mass spectra of serratiochelin A (**1**) and serratiochelin C (**2**)

Figure S12 UV/Vis spectra of serratiochelin A (**1**) and serratiochelin C (**2**)

Figure S13 Chromatograms of Marfey's analysis of serratiochelin A (**1**)

Pictures of culture plates

Figure S14 Isolation of the bacteria and co-culture of *Serratia* sp. and *Shewanella* sp.

Consensus sequences of the bacterial isolates

Text S15: Consensus sequence of *Shewanella* sp.

Text S16: Consensus sequence of *Serratia* sp.

Text S17: Consensus sequence of *Leifsonia* sp

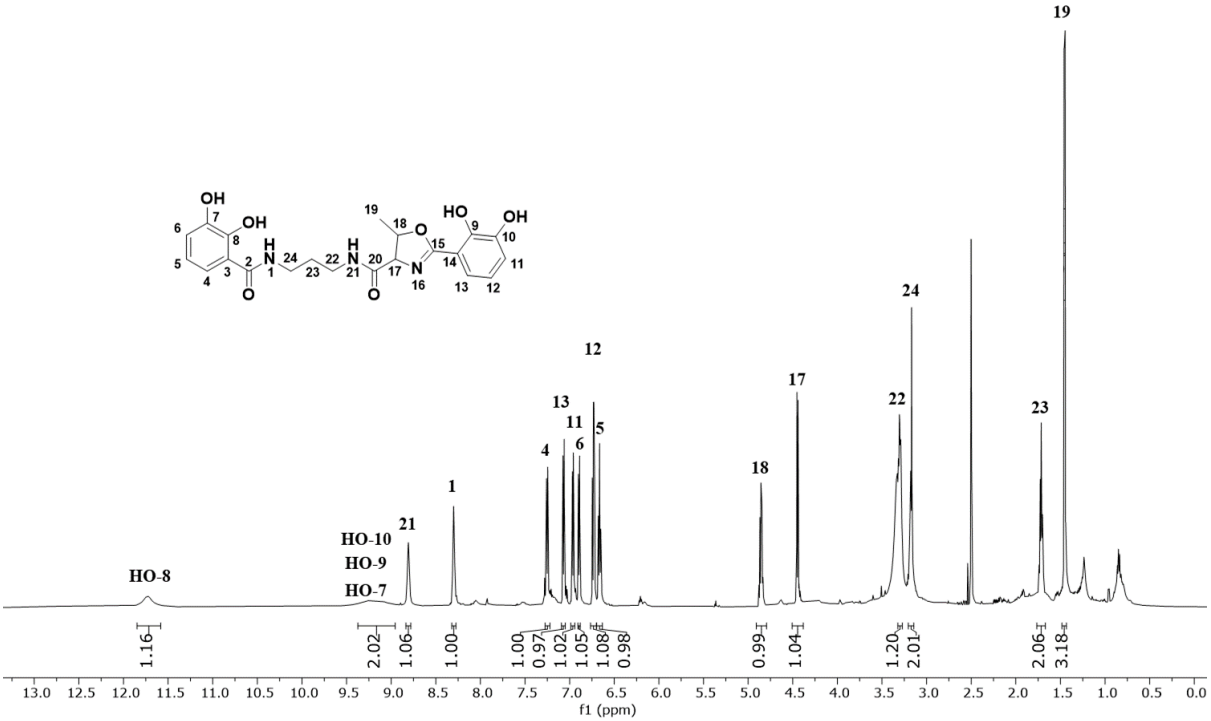

S1. ^{1}H NMR (600 MHz, DMSO-d_6) spectrum of serratiochelin A (**1**)

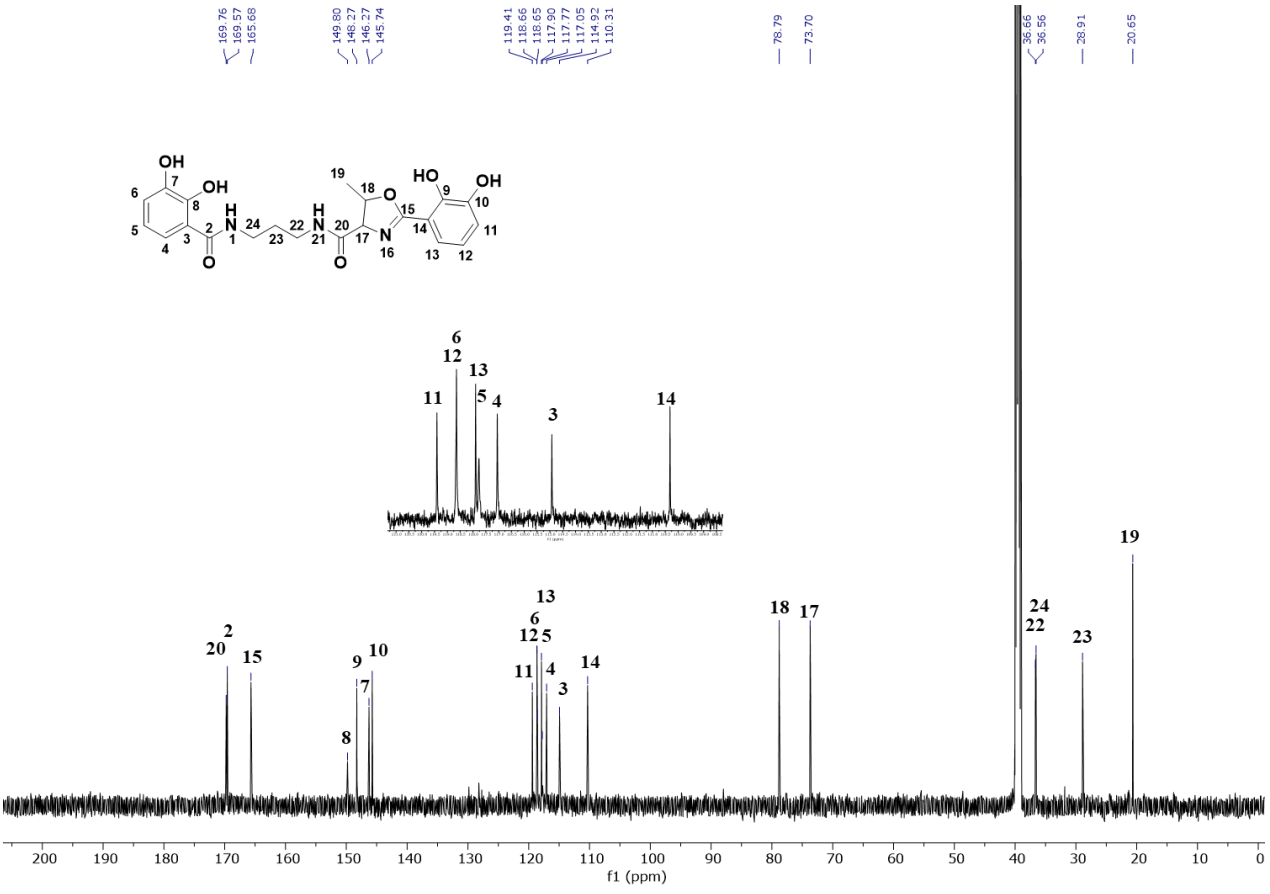

S2. ^{13}C (151 MHz, DMSO-d_6) spectrum of serratiochelin A (**1**)

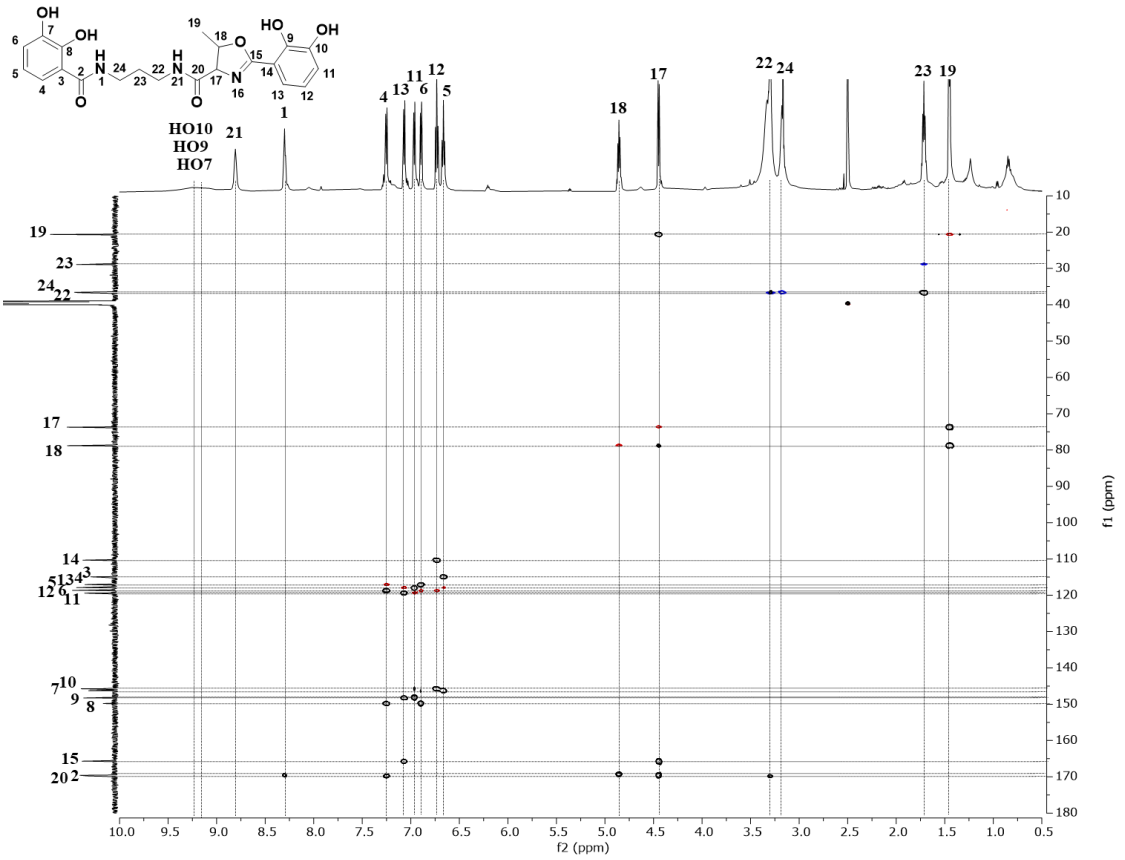

S3. HSQC + HMBC (600 MHz, DMSO-d_6) spectrum of serratiochelin A (**1**)

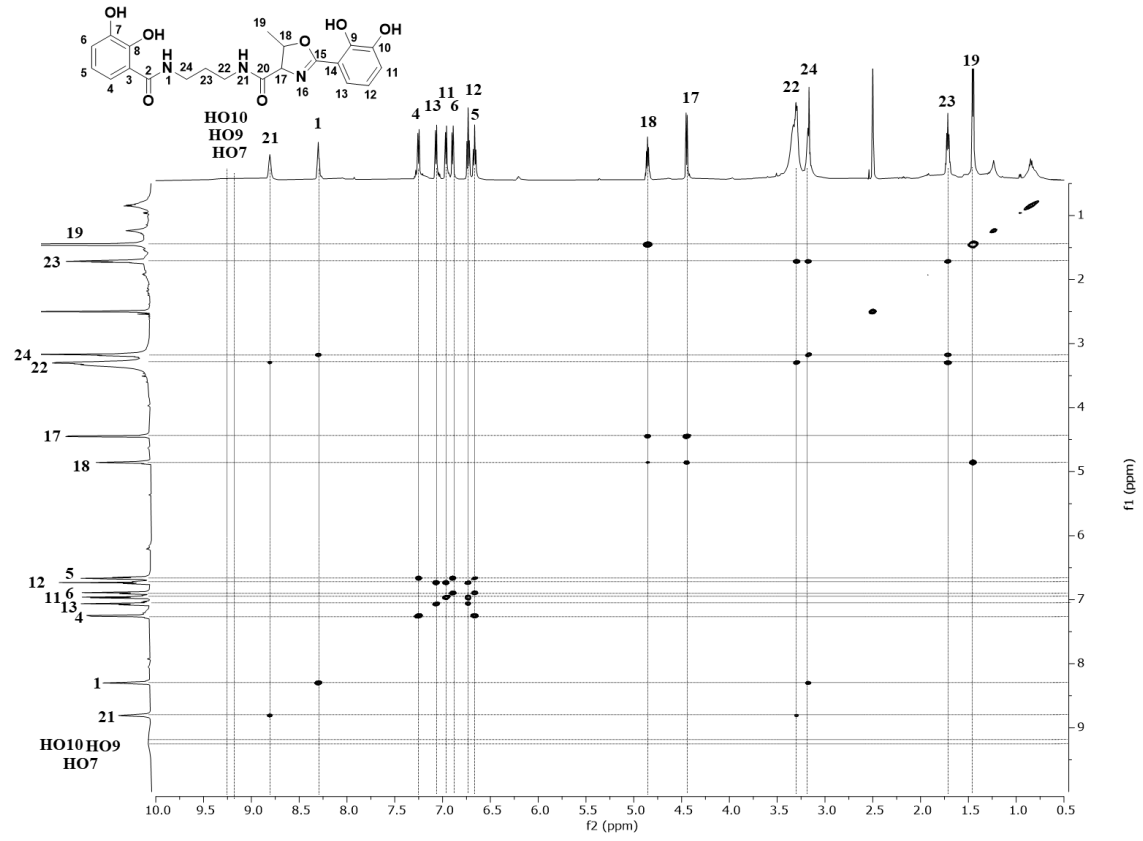

S4. COSY (600 MHz, DMSO-d_6) spectrum of serratiochelin A (**1**)

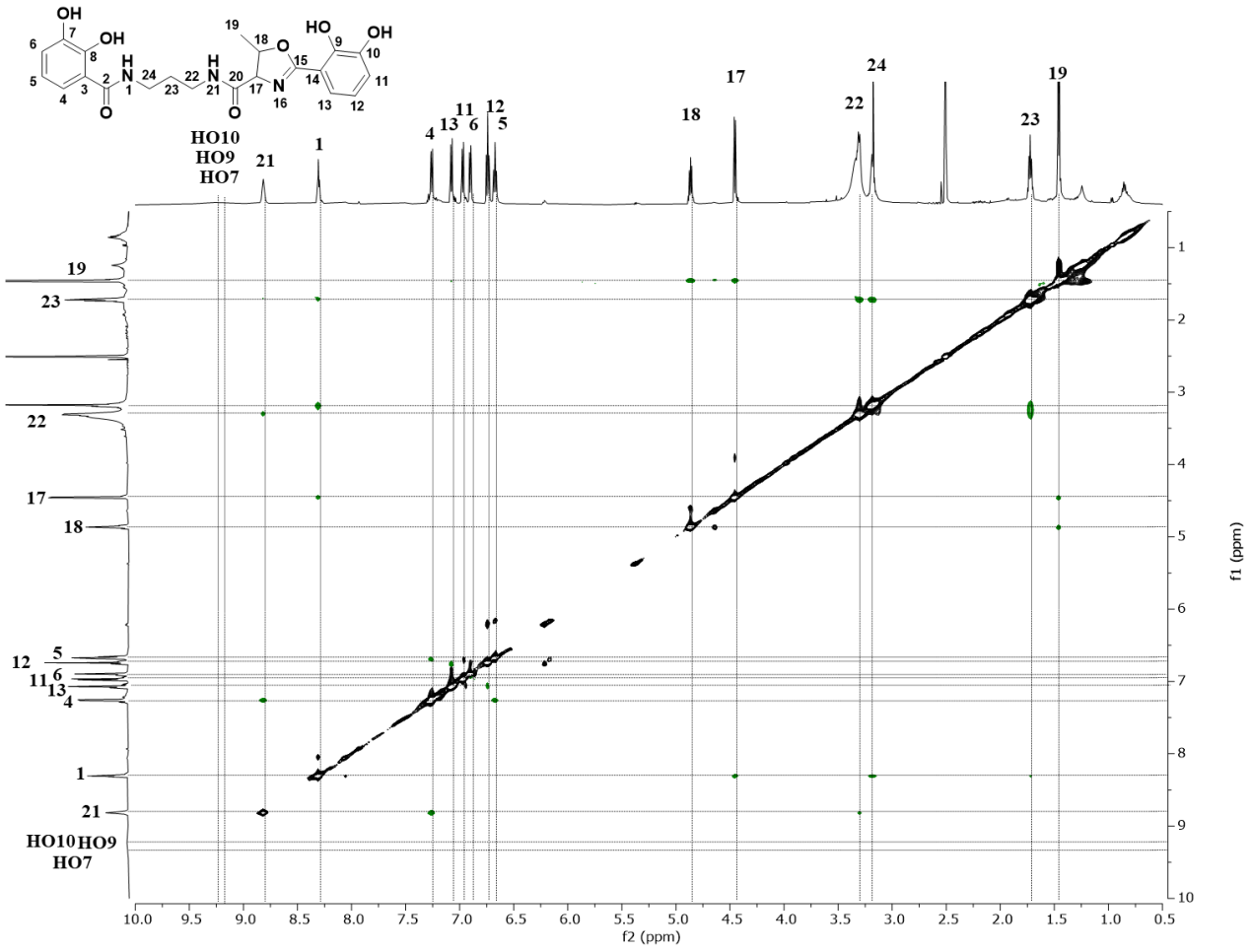

S5. ROESY (600 MHz, DMSO-d_6) spectrum of serratiochelin A (**1**)

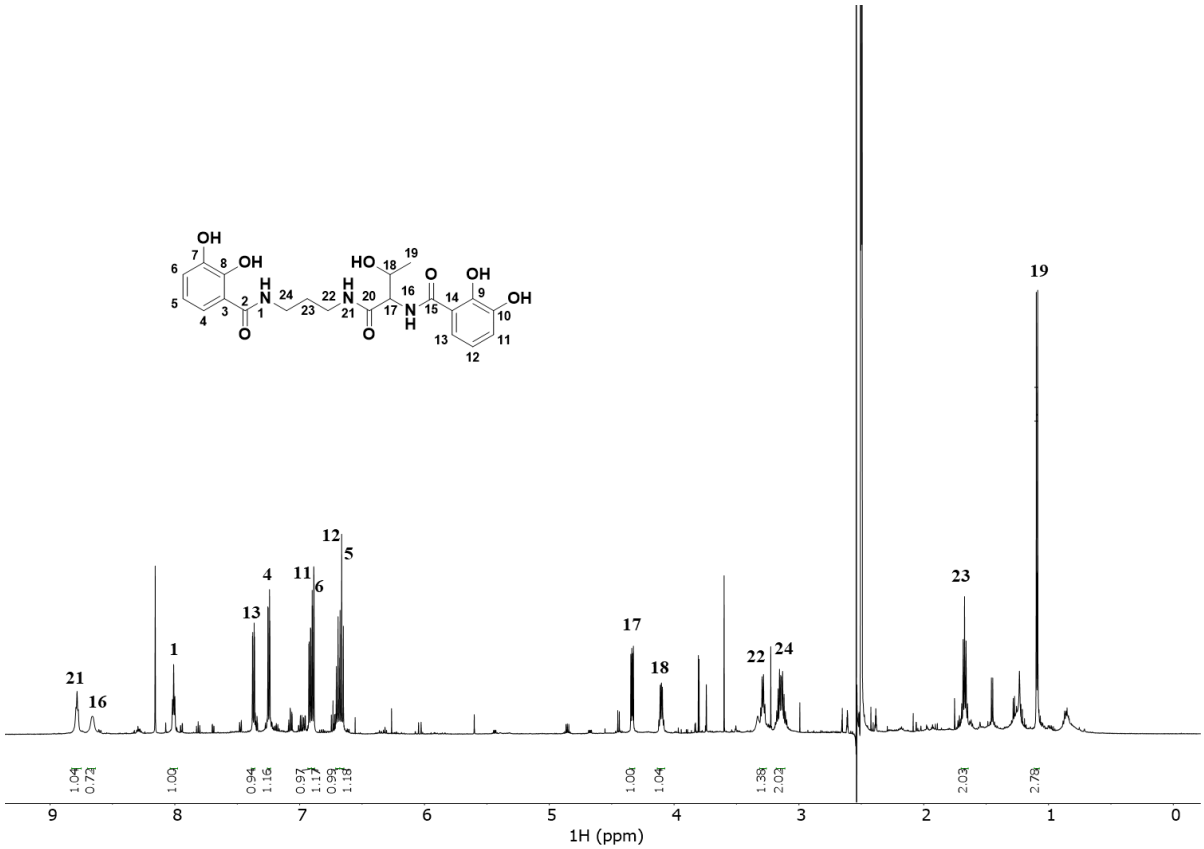

S6. ^{1}H NMR (600 MHz, DMSO-d_6) spectrum of serratiochelin C (**2**)

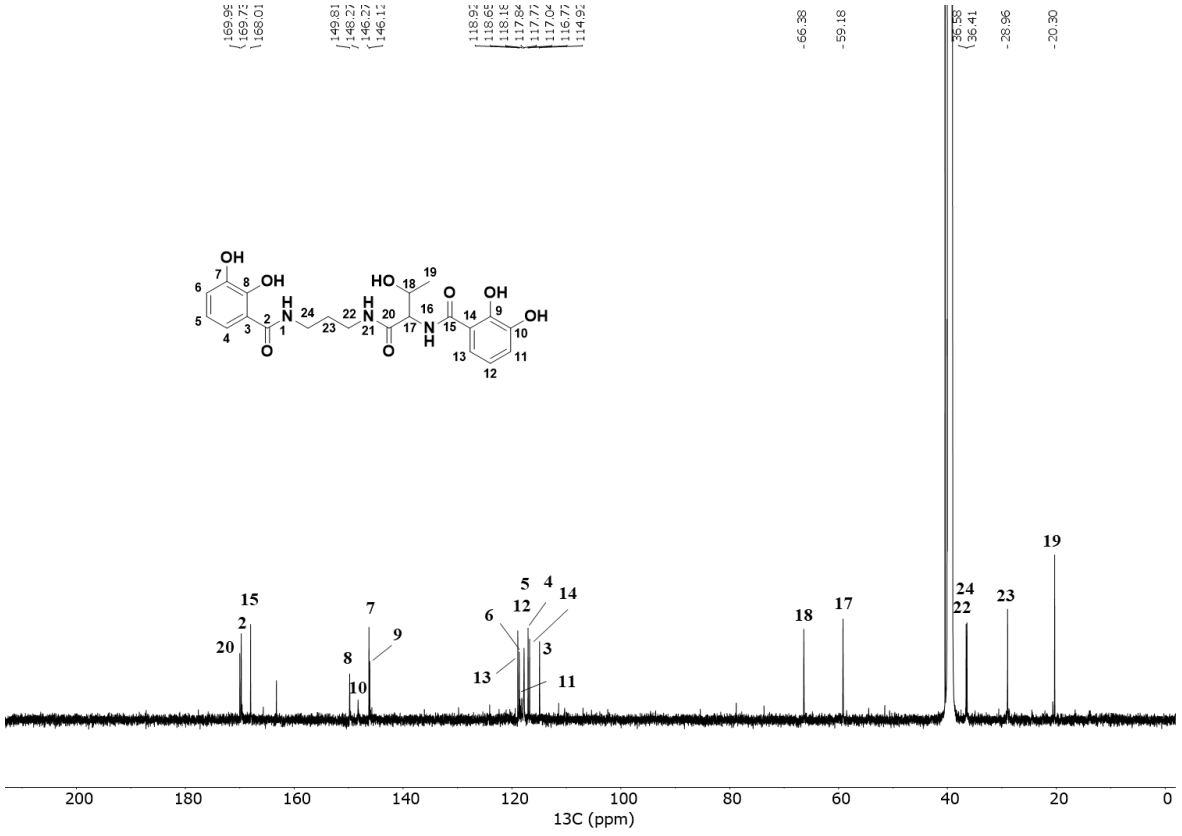

S7. ^{13}C (151 MHz, DMSO-d_6) spectrum of serratiochelin C (**2**)

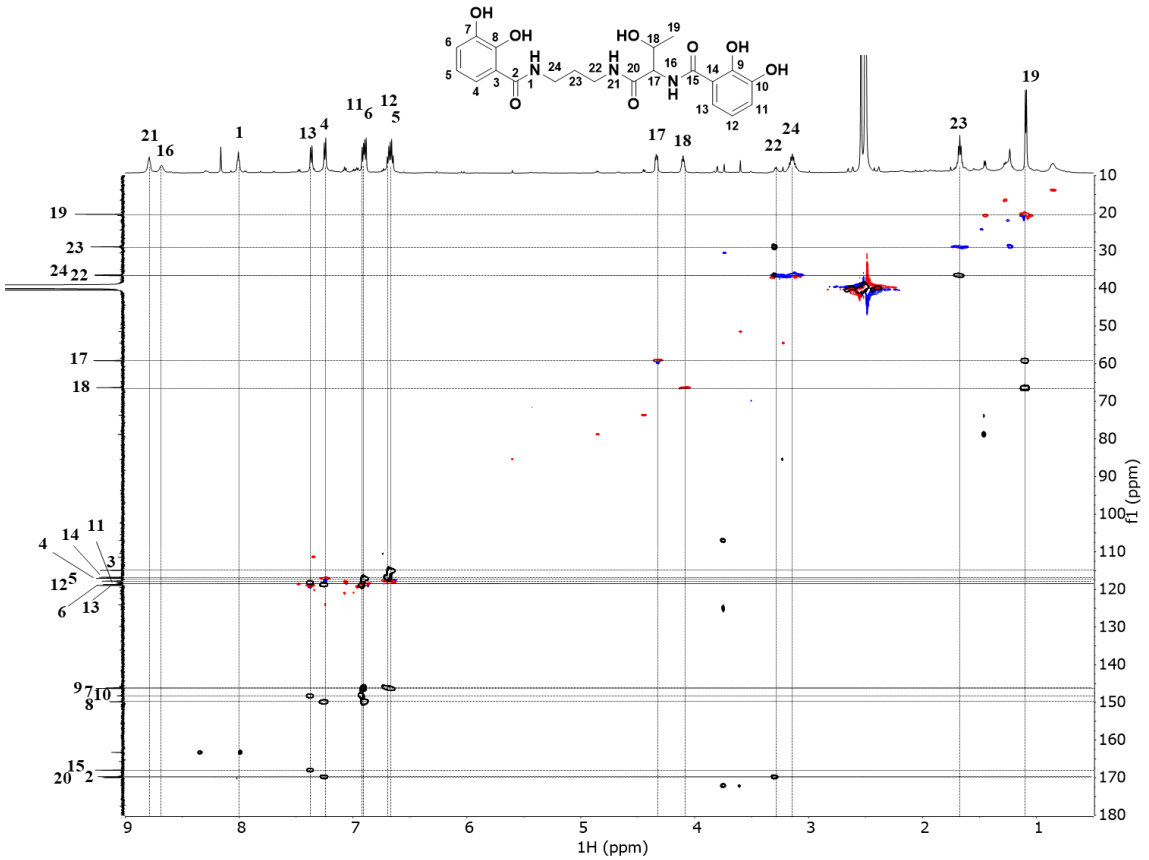

S8. HSQC + HMBC (600 MHz, DMSO-d_6) spectrum of serratiochelin C (**2**)

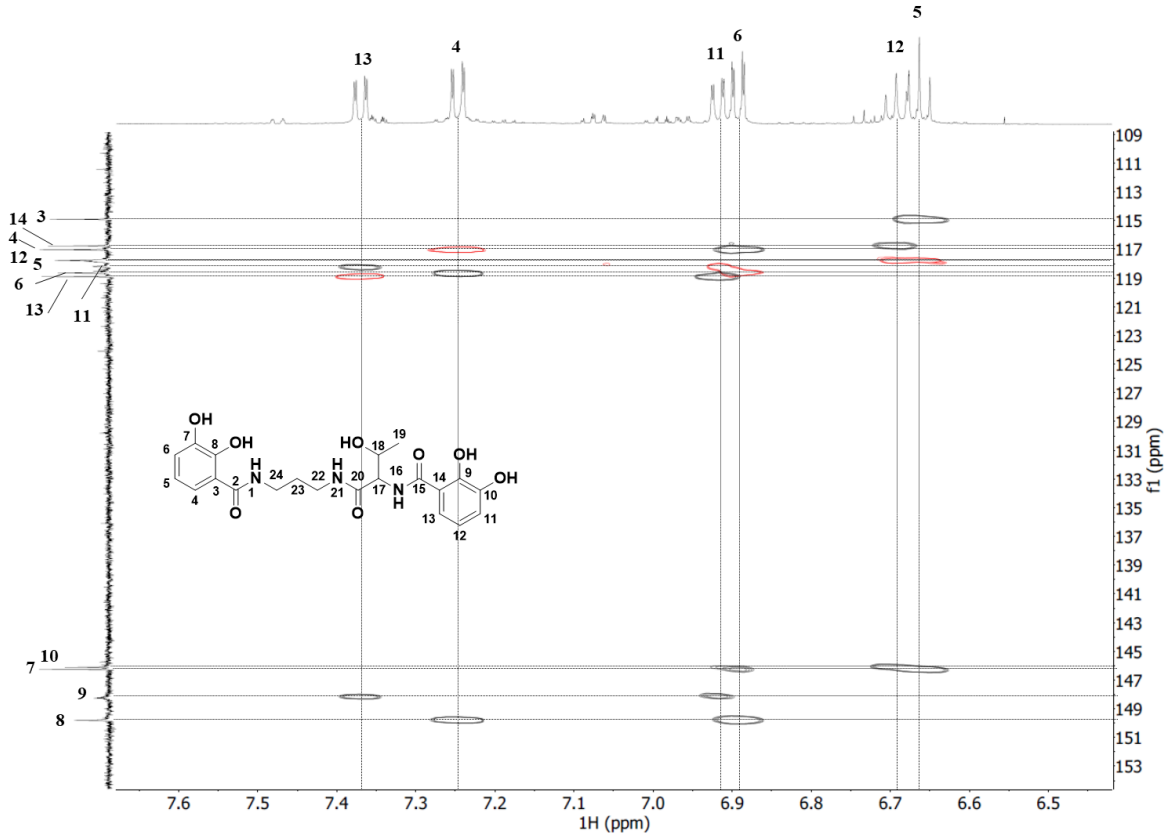

S9. HSQC + HMBC (600 MHz, DMSO-d_6) spectrum of serratiochelin C (**2**), zoomed in crowded area

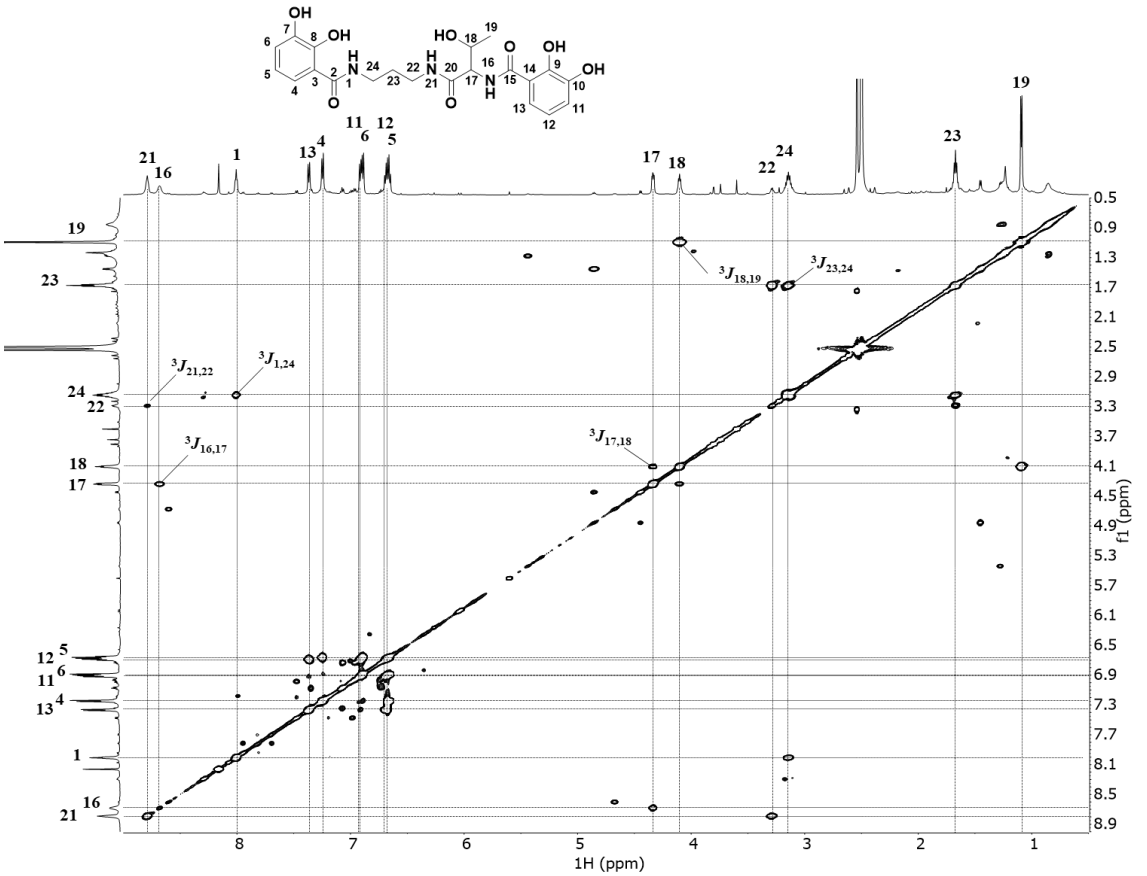

S10. COSY (600 MHz, DMSO-d_6) spectrum of serratiochelin C (**2**)

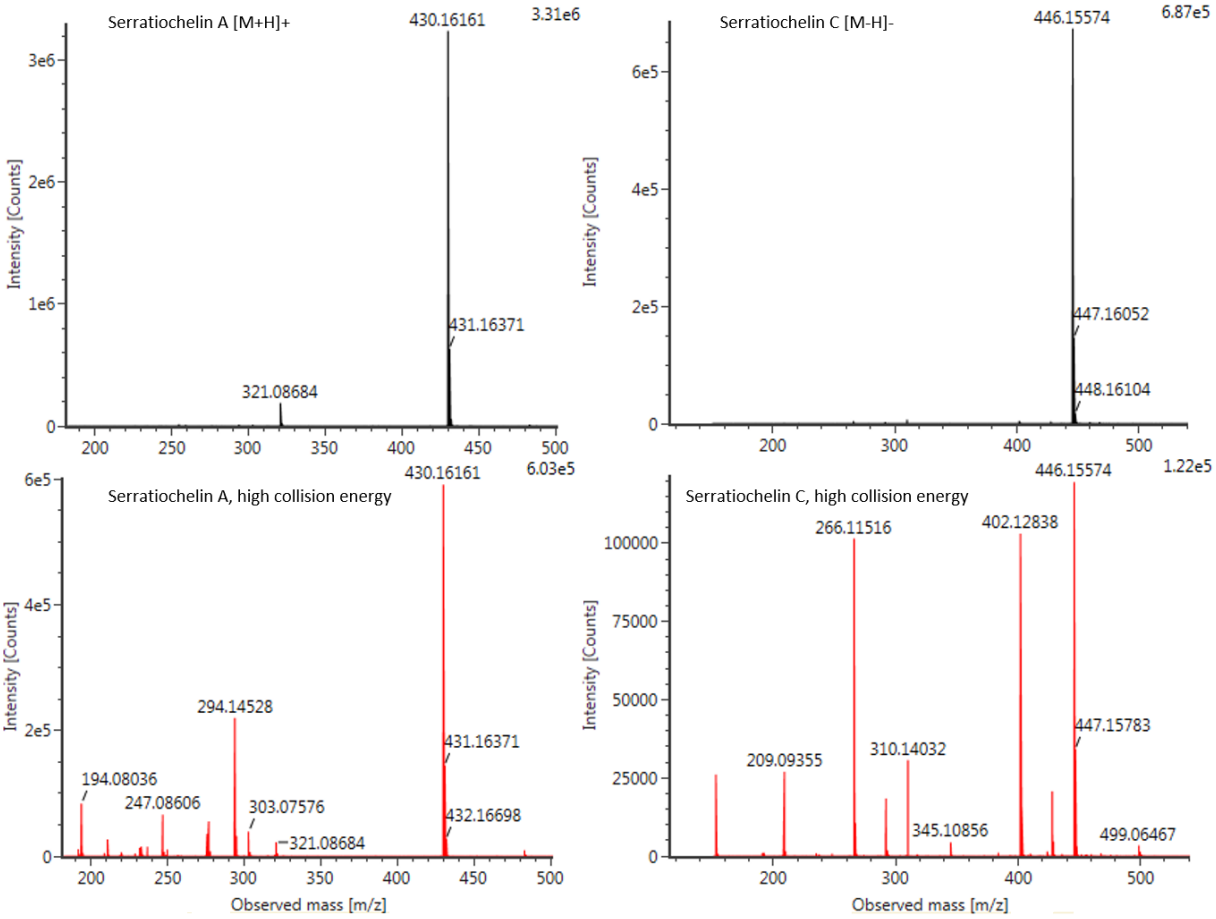

S11. Mass spectra of Serratiochelin A (**1**) (ESI+, left) and Serratiochelin C (**2**) (ESI-, right). The low-collision energy spectra are given in black and the high-collision energy spectra (20-80 eV ramp) in red below.

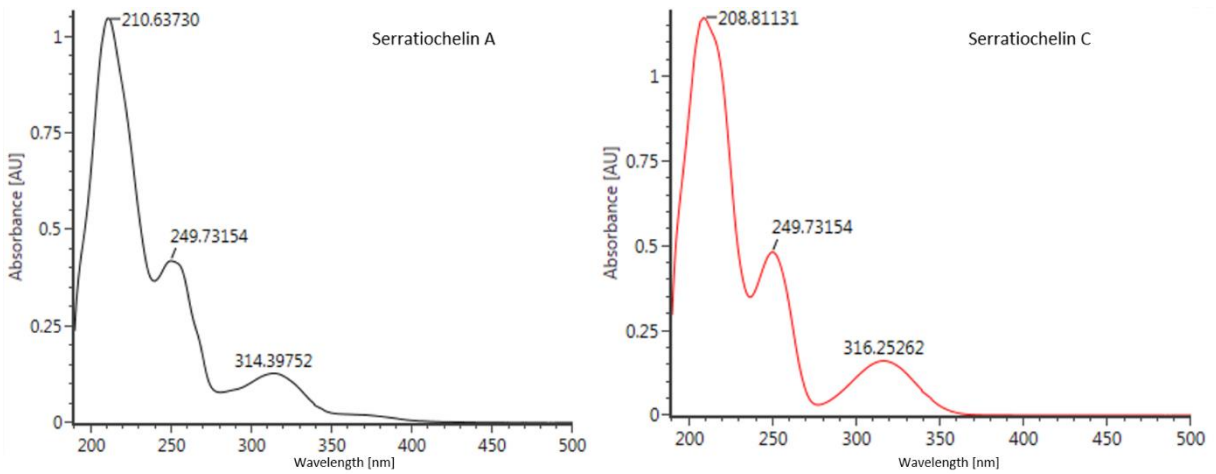

S12. UV/Vis spectra of Serratiochelin A (**1**) and C (**2**) in acetonitrile:water +1% (v/v) formic acid.

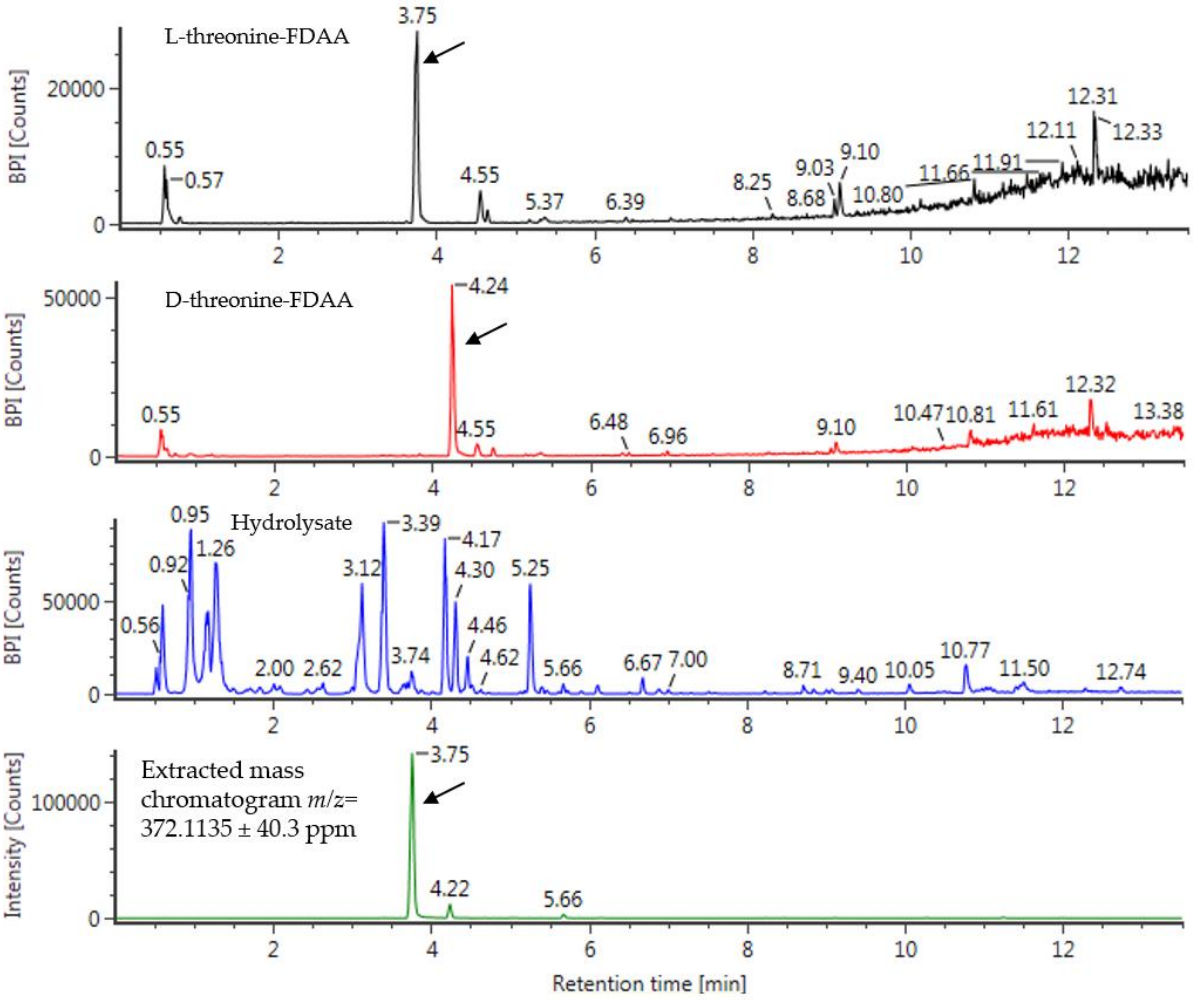

S13. Results of the threonine derivatisation using FDAA. The reactions were analysed using UHPLC-IMS-MS. At the top of the figure in black the chromatogram of L-threonine and below in red D-threonine is given. The chromatogram of the derivatised hydrolysate of serratiochelin A is given in blue (3rd from the top) and at the bottom, the extracted mass-chromatogramm for FDAA-threonine adduct ($C_{13}H_{17}N_5O_8$, calculated monoisotopic mass: 371.1077 u) from the derivatised hydrolysate is given. Comparing the retention times of the L-and D-threonine references we conclude that L-threonine is the present configuration of threonine in serratiochelin A (**1**). The FDAA-threonine peaks are indicated by the black arrows.

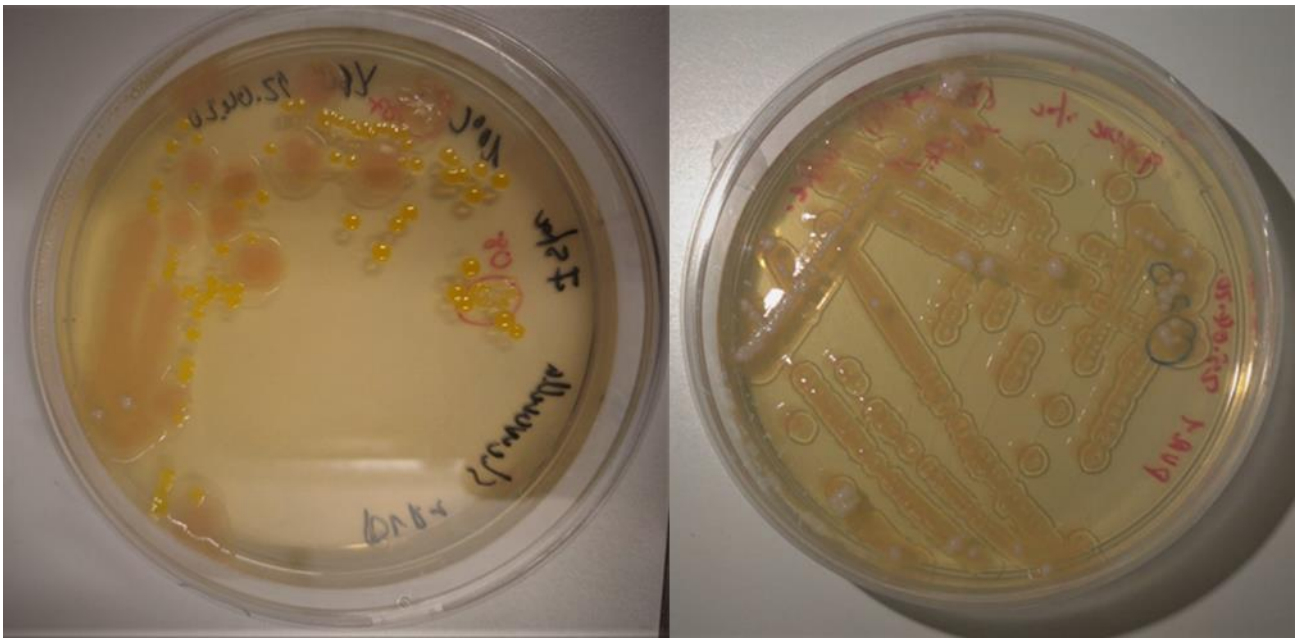

S14. Left: Non-axenic glycerol stock streaked on DVR1 agar displaying three morphologically different bacteria. Through 16S rRNA sequencing the colonies were shown to be *Leifsonia* sp. (yellow colonies), *Shewanella* (pink colonies) and *Serratia* sp. (white colonies). Right: Streak-out of liquid culture (3 days) started by the non-axenic glycerol stock showed *Serratia* sp. (white colonies) growing on top of the *Shewanella* sp. (light pink colonies).

S15. Consensus sequence of *Shewanella* sp.

Multiple sequences of forward and reverse reads were assembled, and the assembly was manually corrected where this was possible. The consensus sequence was used to conduct a Nucleotide BLAST with the nucleotide collection (nr/nt) database, excluding uncultured/environmental sample sequences was conducted giving exclusively hits for *Shewanella* sp. bacteria. The best match (date 20.05.20) was *Shewanella* sp. strain DZ-02-04-aga 16S ribosomal RNA gene, partial sequence (Accession number MK577329), with 100% identity.

>Shewanella_consensus
TGCAGTCGAGCGGTAACACAAGGGAGCTTGCTCCTGAGGTGACGAGCGGCGGACGGGTGAGTAATGCCTAG
GGATCTGCCCAGTCGAGGGGGATAACAGTTGGAAACGACTGCTAATACCGCATACGCCCTACGGGGGAAAGG
AGGGGACCTTCGGGCCTTCCGCGATTGGATGAACCTAGGTGGGATTAGCTAGTTGGTGAGGTAATGGCTCAC
CAAGGCGACGATCCCTAGCTGTTCTGAGAGGATGATCAGCCACACTGGGACTGAGACACGGCCCAGACTCCTA
CGGGAGGCAGCAGTGGGGAATATTGCACAATGGGGGAAACCCTGATGCAGCCATGCCGCGTGTGTGAAGAA
GGCCTTCGGGTTGTAAAGCACTTTCAGTAGGGAGGAAAGGTAGCGTGTTAATAGCACGTTACTGTGACGTTAC
CTACAGAAGAAGGACCGGCTAACTCCGTGCCAGCAGCCGCGGTAATACGGAGGGTCCGAGCGTTAATCGGAA
TTACTGGGCGTAAAGCGTGCGCAGGCGGTTTGTTAAGCCAGATGTGAAATCCCCGGGCTCAACCTGGGAATTG
CATTTGGAACTGGCGAACTAGAGTCTTGTAGAGGGGGGTAGAATTCCAGGTGTAGCGGTGAAATGCGTAGAT
ATCTGGAGGAATACCGGTGGCGAAGGCGGCCCCCTGGACAAAGACTGACGCTCATGCACGAAAGCGTGGGG
AGCAAACAGGATTAGATACCCTGGTAGTCCACGCCGTAAACGATGTCTACTCGGAGTTTGGTGACTTAGTCAC
TGGGCTCCCAAGCTAACGCATTAAGTAGACCGCCTGGGGAGTACGGCCGCAAGGTTAAAACTCAAATGAATTG
ACGGGGGCCCGCACAAGCGGTGGAGCATGTGGTTTAATTCGATGCAACGCGAAGAACCTTACCTACTCTTGAC

ATCCACAGAAGAGACCAGAGATGGACTTGTGCCTTCGGGAACTGTGAGACAGGTGCTGCATGGCTGTCGTCA
GCTCGTGTTGTGAAATGTTGGGTTAAGTCCCGCAACGAGCGCAACCCCTATCCTTATTTGCCAGCACGTAATGG
TGGGAACTCTAGGGAGACTGCCGGTGATAAACCGGAGGAAGGTGGGGACGACGTCAAGTCATCATGGCCCTT
ACGAGTAGGGCTACACACGTGCTACAATGGCGTATACAGAGGGTTGCAAAGCCGCGAGGTGGAGCTAATCTC
ACAAAGTACGTCGTAGTCCGGATCGGAGTCTGCAACTCGACTCCGTGAAGTCGGAATCGCTAGTAATCGTGGA
TCAGAATGCCACGGTGAATACGTTCCCGGGCCTTGTACACACCGCCCGTCACACCATGGGAGTGGGCTGCAAA
AGAAGTGGGTAGTTTAACCTTCGGGAGAACGCTC

S16. Consensus sequence of *Serratia* sp.

Multiple sequences of forward and reverse reads were assembled, and the assembly was manually corrected where this was possible. The consensus sequence was used to conduct a Nucleotide BLAST with the nucleotide collection (nr/nt) database, excluding uncultured/environmental sample sequences was conducted giving exclusively hits for *Serratia* sp. bacteria. The best match (date 20.05.20) was *Serratia plymuthica* PRI-2C chromosome, complete genome (Accession number CP015613), with 100% identity.

>Serratia_consensus
AAGCGCCCTCCCGAAGGTTAAGCTACCTACTTCTTTTGCAACCCACTCCCATGGTGTGACGGGCGGTGTGTACA
AGGCCCGGGAACGTATTCACCGTAGCATTCTGATCTACGATTACTAGCGATTCCGACTTCATGGAGTCGAGTTG
CAGACTCCAATCCGGACTACGACGTACTTTATGAGGTCCGCTTGCTCTCGCGAGTTCGCTTCTCTTTGTATACGC
CATTGTAGCACGTGTGTAGCCCTACTCGTAAGGGCCATGATGACTTGACGTCATCCCCACCTTCCTCCGGTTTAT
CACCGGCAGTCTCCTTTGAGTTCCCGACCGAATCGCTGGCAACAAAGGATAAGGGTTGCGCTCGTTGCGGGAC
TTAACCCAACATTTCACAACACGAGCTGACGACAGCCATGCAGCACCTGTCTCAGAGTTCCCGAAGGCACTAA
GCTATCTCTAGCGAATTCTCTGGATGTCAAGAGTAGGTAAGGTTCTTCGCGTTGCATCGAATTAAACCACATGC
TCCACCGCTTGTGCGGGCCCCCGTCAATTCATTTGAGTTTTAACCTTGCGGCCGTACTCCCCAGGCGGTCGATTT
AACGCGTTAGCTCCGGAAGCCACGCCTCAAGGGCACAACCTCCAAATCGACATCGTTTACAGCGTGGACTACC
AGGGTATCTAATCCTGTTTGCTCCCCACGCTTTCGCACCTGAGCGTCAGTCTTTGTCCAGGGGGCCGCCTTCGC
CACCGGTATTCCTCCAGATCTCTACGCATTTCACCGCTACACCTGGAATTCTACCCCCCTCTACAAGACTCTAGC
TTGCCAGTTTCAAATGCAGTTCCCACGTTAAGCGCGGGGATTTCACATCTGACTTAACAAACCGCCTGCGTGCG
CTTTACGCCCAGTAATTCCGATTAACGCTTGCACCCTCCGTATTACCGCGGCTGCTGGCACGGAGTTAGCCGGT
GCTTCTTCTGCGAGTAACGTCAATGCAATGTGCTATTAACACATTACCCTTCCTCCTCGCTGAAAGTGCTTTACA
ACCCTAAGGCCTTCTTCACACACGCGGCATGGCTGCATCAGGCTTGCGCCCATTGTGCAATATTCCCCACTGCT
GCCTCCCGTAGGAGTCTGGACCGTGTCTCAGTTCCAGTGTGGCTGGTCATCCTCTCAGACCAGCTAGGGATCGT
CGCCTAGGTGAGCCATTACCCCACCTACTAGCTAATCCCATCTGGGCACATCTGATGGCGTGAGGCCCGAAGG
TCCCCCACTTTGGTCCGTAGACGTTATGCGGTATTAGCTACCGTTTCCAGTAGTTATCCCCCTCCATCAGGCAGT
TTCCCAGACATTACTCACCCGTCCGCCGCTCGTCACCCAGAGAGCAAGCTCTCCTGTGCTACCGCTCGACTTGC
AT

S17. Consensus sequence of *Leifsonia* sp.

Multiple sequences of forward and reverse reads were assembled, and the assembly was manually corrected where this was possible. The consensus sequence was used to conduct a Nucleotide BLAST with the nucleotide collection (nr/nt) database, excluding uncultured/environmental sample sequences was conducted giving hits for bacteria of different genera, mainly *Salinibacterium* sp., *Leifsonia* sp., *Agreia* sp., and other un-identified bacteria of marine origin and Actinobacteria, all with % identity above 99%. The best hit (date 20.05.20) was surprisingly found to be *Pseudomonas* sp. AW15 16S ribosomal RNA gene, partial sequence (Accession number FJ362501, 99.93% identity), but the identity

of this sequence is questionable as it has no hits for other *Pseudomonas* sp. through BLAST. The second best hit for our sequence was for *Salinibacterium* sp. strain DZ-02-03-aga 16S ribosomal RNA gene, partial sequence (Accession number MK577334, 99.86% identity).

>Leifsonia_consensus

TGCAGTCGAACGATGAAGCTGGAGCTTGCTCTGGTGGATTAGTGGCGAACGGGTGAGTAACACGTGAGTAAC
CTGCCCTTGACTCTGGAATAAGCGTTGGAAACGACGTCTAATACCGGATACGAGCTTCCGCCGCATGGTGAGG
AGCTGGAAAGAATTTCGGTCAAGGATGGACTCGCGGCCTATCAGGTAGTTGGTGAGGTAATGGCTCACCAAG
CCTACGACGGGTAGCCGGCCTGAGAGGGTGACCGGCCACACTGGAACTGAGACACGGTCCAGACTCCTACGG
GAGGCAGCAGTGGGGAATATTGCACAATGGGCGCAAGCCTGATGCAGCAACGCCGCGTGAGGGACGACGGC
CTTCGGGTTGTAAACCTCTTTTAGTAGGGAAGAAGCGAAAGTGACGGTACCTGCAGAAAAAGCACCGGCTAAC
TACGTGCCAGCAGCCGCGGTAATACGTAGGGTGCAAGCGTTATCCGGAATTATTGGGCGTAAAGAGCTCGTA
GGCGGTTTGTCGCGTCTGCTGTGAAAACTGGGGGCTCAACCCCCAGCCTGCAGTGGGTACGGGCAGACTAGA
GTGCGGTAGGGGAGATTGGAATTCCTGGTGTAGCGGTGGAATGCGCAGATATCAGGAGGAACACCAATGGC
GAAGGCAGATCTCTGGGCCGTTACTGACGCTGAGGAGCGAAAGCATGGGGAGCGAACAGGATTAGATACCCT
GGTAGTCCATGCCGTAAACGTTGGGAACTAGATGTAGGGGCCATTCCACGGTTTCTGTGTCGCAGCTAACGCA
TTAAGTTCCCCGCCTGGGGAGTACGGCCGCAAGGCTAAAACTCAAAGGAATTGACGGGGGCCCGCACAAGCG
GCGGAGCATGCGGATTAATTCGATGCAACGCGAAGAACCTTACCAAGACTTGACATATACGAGAACGGGCTA
GAAATAGTTCACTCTTTGGACACTCGTAAACAGGTGGTGCATGGTTGTCGTCAGCTCGTGTCGTGAGATGTTG
GGTTAAGTCCCGCAACGAGCGCAACCCTCGTTCTTTGTTGCCAGCACGTAATGGTGGGAACTCAAAGGAGACT
GCCGGGGTCAACTCGGAGGAAGGTGGGGATGACGTCAAATCATCATGCCCCTTATGTCTTGGGCTTCACGCAT
GCTACAATGGCCGATACAAAGGGCTGCAATACCGCGAGGTAGAGCGAATCCCAAAAAGTCGGTCTCAGTTCG
GATTGAGGTCTGCAACTCGACCTCATGAAGTCGGAGTCGCTAGTAATCGCAGATCAGCAACGCTGCGGTGAAT
ACGTTCCCGGGCCTTGTACACACCGCCCGTCAAGTCATGAAAGTCGGTAACACCCGAAGCCAGTGGCCTAACC
CGCAAG

Paper II

molecules

MDPI

Article

Two Novel Lyso-Ornithine Lipids Isolated from an Arctic Marine *Lacinutrix* sp. Bacterium

Venke Kristoffersen [1,*], Marte Jenssen [1], Heba Raid Jawad [1], Johan Isaksson [2], Espen H. Hansen [1], Teppo Rämä [1], Kine Ø. Hansen [1] and Jeanette Hammer Andersen [1]

[1] Marbio, Faculty for Fisheries, Biosciences and Economy, UiT-The Arctic University of Norway, Breivika, N-9037 Tromsø, Norway; marte.jenssen@uit.no (M.J.); heba_jr@hotmail.com (H.R.J.); espen.hansen@uit.no (E.H.H.); teppo.rama@uit.no (T.R.); kine.o.hanssen@uit.no (K.Ø.H.); jeanette.h.andersen@uit.no (J.H.A.)

[2] Department of Chemistry, Faculty of Natural Sciences, UiT-The Arctic University of Norway, Breivika, N-9037 Tromsø, Norway; johan.isaksson@uit.no

* Correspondence: venke.kristoffersen@uit.no

Abstract: The *Lacinutrix* genus was discovered in 2005 and includes 12 Gram-negative bacterial species. To the best of our knowledge, the secondary metabolite production potential of this genus has not been explored before, and examination of *Lacinutrix* species may reveal novel chemistry. As part of a screening project of Arctic marine bacteria, the *Lacinutrix* sp. strain M09B143 was cultivated, extracted, fractionated and tested for antibacterial and cytotoxic activities. One fraction had antibacterial activity and was subjected to mass spectrometry analysis, which revealed two compounds with elemental composition that did not match any known compounds in databases. This resulted in the identification and isolation of two novel isobranched lyso-ornithine lipids, whose structures were elucidated by mass spectrometry and NMR spectroscopy. Lyso-ornithine lipids consist of a 3-hydroxy fatty acid linked to the alpha amino group of an ornithine amino acid through an amide bond. The fatty acid chains were determined to be iso-C15:0 (**1**) and iso-C16:0 (**2**). Compound **1** was active against the Gram-positive *S. agalactiae*, while **2** showed cytotoxic activity against A2058 human melanoma cells.

Keywords: marine bacteria; lipoamino acid; secondary metabolites; amphiphilic compounds; antibacterial; cytotoxic; anti-cancer

Citation: Kristoffersen, V.; Jenssen, M.; Jawad, H.R.; Isaksson, J.; Hansen, E.H.; Rämä, T.; Hansen, K.Ø.; Andersen, J.H. Two Novel Lyso-Ornithine Lipids Isolated from an Arctic Marine *Lacinutrix* sp. Bacterium. *Molecules* **2021**, *26*, 5295. https://doi.org/10.3390/molecules26175295

Academic Editors: Magdalena Ligor and Aleksandra Szydłowska-Czerniak

Received: 2 July 2021
Accepted: 27 August 2021
Published: 31 August 2021

1. Introduction

Bacteria are the producers of many secondary metabolites that have been developed into drugs, including the tetracycline and aminoglycoside classes of antibiotics [1,2], that has paved the way for better health for millions of people around the world. Most of the bacterial secondary metabolites have been isolated from terrestrial organisms [3], suggesting that the chemical diversity of natural products can be expanded by investigating bacteria from other habitats.

The Arctic marine environment is home to numerous microorganisms thriving in cold water under the stark seasonal changes from midnight sun to polar darkness. Compared to terrestrial microorganisms, the bacteria living under these conditions must be adapted to cold saline water. It is therefore believed that these bacterial species have specialized metabolic systems tailored for survival in this niche environment. Today there are several marketed drugs originating from the marine environment [4]. While most of them were isolated from invertebrates, the true producers of many of these secondary metabolites are now known to be symbiotic bacteria, showing that marine bacteria is a promising source of new bioactive secondary metabolites [5,6]. To increase the likelihood of discovering novel bioactive compounds, one strategy is to search in underexplored places and sources. As

the Arctic water is less investigated than warmer waters and terrestrial environments, it represents a potential source for the discovery of novel bioactive bacterial compounds.

The *Lacinutrix* genus belongs to the family *Flavobacteriaceae*, which is the largest family in the Bacteroidetes phylum [7]. The genus consists of Gram-negative marine bacteria that have been isolated from both cold polar waters and warm waters. This genus was first described in 2005 by Bowman and Nichols, when *L. copepodicola* was isolated from an Antarctic marine calanoid copepod [8]. Today the genus includes 12 marine species, five isolated from polar waters and seven from warm waters. In addition to *L. copepodicola*, the polar species includes *L. mariniflava*, *L. algicola* [9] and *L. jangbogonensis* isolated from the Antarctic [10], and *L. himadriensis* isolated from the Arctic [11]. Species isolated from warm waters include *L. iliipiscaria* and *L. gracilariae* isolated from China [12–14], *L. cladophorae* and *L. chionocetis* from Japan [13,15], *L. venerupis* from Spain [16] and *L. undariae* and *L. salivirga* isolated from South Korea [17,18]. To date, the studies of *Lacinutrix* sp. have mainly focused on describing novel species; analyzing their genomic and cellular fatty acid content [10,16,19], while their ability to produce secondary metabolites has not yet been assessed.

As part of the current study, two new lyso-ornithine lipids were isolated and characterized. Lyso-ornithine lipids are known to be precursors of ornithine lipids, which are the most common lipoamino acids found in the bacterial membrane. Ornithine lipids are widely distributed in Gram-negative bacteria, but are also present in Gram-positive bacteria. The biosynthesis of ornithine lipids occurs in two steps, where the first step is the formation of lyso-ornithine-lipids from ornithine and 3-hydroxy fatty acyl-acyl carrier protein. Ornithine lipids are formed in the next step by the transfer of an acyl group from fatty acyl-acyl carrier protein to lyso-ornithine [20–22].

In the present work, the Arctic marine *Lacinutrix* sp. strain M09B143 was isolated from a *Halichondria* sp. sponge collected in the Barents Sea. The potential of the bacterium to produce bioactive metabolites was evaluated. It was cultivated and the secreted metabolites were extracted from the fermentation broth. The extract was fractionated into six fractions that were tested for antibacterial and cytotoxic activity. Fraction 5 was active against Gram-positive bacteria and was therefore selected for further chemical analysis. This resulted in the isolation and identification of two novel iso-branched lyso-ornithine lipids that were tested for antibacterial and cytotoxic activities.

2. Results

2.1. Isolation and Identification

Lacinutrix sp. strain M09B143 was isolated from a *Halichondria* sp. sponge collected in the Barents Sea. It was identified as a *Lacinutrix* sp. using 16S rRNA sequencing and Basic Local Alignment Search Tool (BLAST) searches against reference sequences in GenBank. The 16S rRNA gene sequence analysis confirmed that M09B143 was affiliated with the genus *Lacinutrix*, a member of the family *Flavobacteriaceae* and phylum Bacteroidetes, corresponding to the information provided by the Norwegian Marine Biobank Marbank. The bacterium clustered separately on its own branch with *L. algicola* (NR_043592), and sister taxon for this branch was *L. mariniflava* (NR_043592). *L. algicola* and *L. mariniflava* are both isolated from a red alga of the family *Gigartinaceae* [9]. Figure 1 shows the results from the phylogenetic analysis using PhyML. The phylogenetic analysis was also run using the MrBayes 3.2.6 plug-in in Geneious, and the results of this analysis are shown in Supplementary Information Figure S1. There were some differences between the Bayesian Inference tree and the Maximum Likelihood tree, caused by different placement of non-supported nodes in ML and Bayesian analyses and especially the polytomy at one basal node in the tree from MrBayes. The clade consisting of *Lacinutrix* M09B143, *L. algicola*, *L. mariniflava* and *L. jangbogonensis* was statistically supported and topologically similar using both methods.

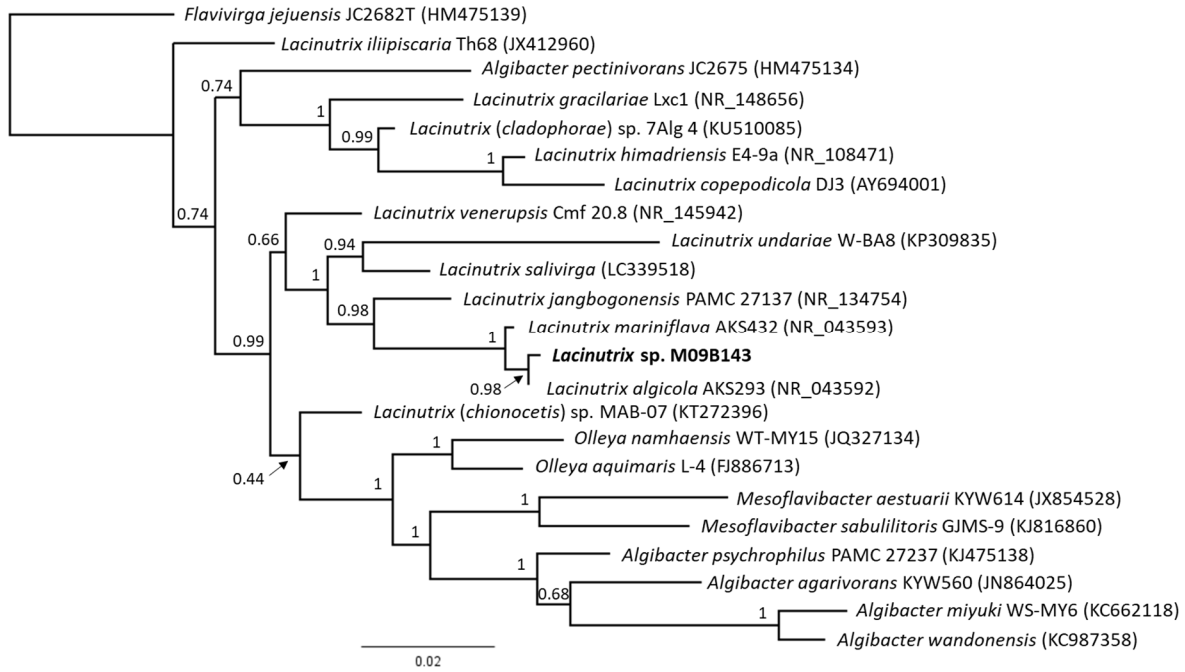

Figure 1. Maximum likelihood tree based on 16S rRNA gene sequences and showing the phylogenetic placement of the strain M09B143 (in bold) within Bacteroidetes. The tree was rooted with *Flavivirga jejuensis* as the outgroup. Branch support is given as aLRT values.

2.2. Bioactivity of Fractionated Extract

The M09B143 strain was fermented in 2 × 200 mL M19 medium in 1 L flasks. Secondary metabolites excreted into the medium were extracted with Diaion® HP20 resin and eluted with methanol. The bacterial extract was fractionated into six fractions by flash column chromatography and the fractions were tested for antibacterial and cytotoxic activities at 50 µg/mL. Only flash fraction 5, eluting at 100% methanol was active. It was active against the Gram-positive bacteria *Streptococcus agalactiae*, *Enterococcus faecalis* and *Staphylococcus aureus* (Figure 2). The activity appeared to be most potent against *S. agalactiae*, followed by *E. faecalis*. The six fractions were not active against the Gram-negative bacteria *Escherichia coli* and *Pseudomonas aeruginosa*, or against the A2058 human melanoma cells (Figure S2).

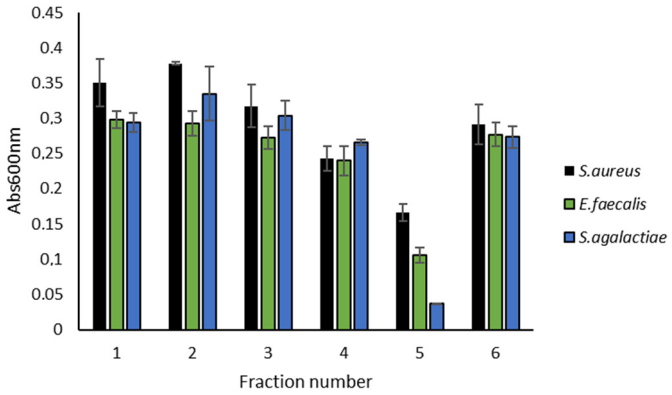

Figure 2. Antibacterial effect of flash fractions 1–6 from M09B143 extract against Gram-positive bacteria tested at 50 µg/mL in a growth inhibition assay (two technical replicates). Fraction 5 was active and was selected for further analysis with UHPLC-HR-MS to identify the compound(s) responsible for the observed activity.

2.3. Dereplication

Based on the observed antibacterial activity, fraction 5 was subjected to UHPLC-HR-MS analysis. The resulting data were compared to the equivalent data recorded for the inactive fractions 4 and 6 to identify compounds that were exclusively present, or present in higher amounts in fraction 5. The dereplication led to the identification of two compounds, **1**, with elemental composition $C_{20}H_{40}N_2O_4$ and **2**, with elemental composition $C_{21}H_{42}N_2O_4$. Compound **1** was the major peak, and **2** was among the most prominent peaks in the MS chromatogram of fraction 5 (Figure S3). Both compounds were only present in very small amounts in the inactive fractions 4 and 6. All other major peaks in the UHPLC-HR-MS chromatogram of fraction 5 were determined to be either media components, or compounds present in comparable amounts in the inactive fractions 4 and 6. Consequently, **1** and **2** were suspected to be responsible for the observed bioactivity of fraction 5. Fragmentation patterns in the UHPLC-HR-MS analysis indicated that they were lipoamino acids, and from their elemental composition and relatively similar retention time, it was assumed that the two compounds differed from each other with a methylene group in the lipid chain. Searches in relevant databases, such as ChemSpider, did not provide any hits that matched the two compounds. Moreover, the dereplication analysis revealed that **1** eluted in three peaks and **2** as two peaks. This indicated that different isomers of both compounds were produced by the bacterium (Figure S4). The three peaks recorded for sample **1** all had the same elemental composition, and the two peaks for sample **2** had the same elemental composition. Fragmentation patterns from MS/MS on the UHPLC-HR-MS were also identical for the different peaks. This strongly indicates that **1** was a mixture of three stereoisomers and that **2** was a mixture of two stereoisomers.

2.4. Isolation of Compound *1* and *2*

For purification of the two compounds, upscale cultivation of *Lacinutrix* sp. M09B143 and isolation were performed in two rounds using a preparative HPLC-MS system. The strain was fermented in 64 × 250 mL in round one, which resulted in 25.0 g of dry extract. Fractionation of the extract yielded 515.0 mg of fraction 5. Extensive efforts were put into separating the isomeric variants of each compound from each other. However, due to the lower chromatographic resolution of the preparative column, it was not possible to do so. Therefore, the three variants of **1** were isolated and further processed together, and so were the two variants of **2**. In the text below, compound **1** refers to the sample containing the three variants of **1**, and compound **2** refers to the sample containing the two variants of **2**.

The first isolation step of the two compounds in round one yielded 8.0 mg of **1** and 5.0 mg of **2**. After the second purification step, the yield of **1** was 1.5 mg and 0.6 mg of **2**.

Fermentation and isolation in round two included 56 × 400 mL cultures, which resulted in 28.02 g of dry extract that was fractionated and yielded 1021.2 mg of fraction 5. First purification step of the two compounds with preparative HPLC-MS gave 26.8 mg of **1** and 23.2 mg of **2**. Compound **2** was subjected to a second purification step, resulting in 4.9 mg of **2**.

The two compounds were isolated as light brown waxes; total yield was 28.3 mg of **1** and 5.5 mg of **2**. The purity of the isolated compounds was checked using UHPLC-HR-MS. This revealed that **1** and **2** were completely separated from each other and that the samples only contained minor impurities.

2.5. Structure Elucidation

The structures of **1** and **2** (Figure 3) were elucidated using 1D (^{1}H and ^{13}C, Table 1) and 2D (HSQC, HMBC, HSQC-TOCSY and COSY, COSY only recorded for **2**). NMR experiments in methanol-d_3 and UHPLC-HR-MS analysis. The compounds were determined to consist of a polar ornithine head group linked to a mono-hydroxylated 15:0 (**1**)/16:0 (**2**) iso-fatty acid through an amide bond. The structures of the individual variants of **1** and **2** could not be determined individually, but the presence of two stereoisomers in the

5-position could be observed as two near isochronous C-5 resonances and an unresolvable H-5 multiplet pattern.

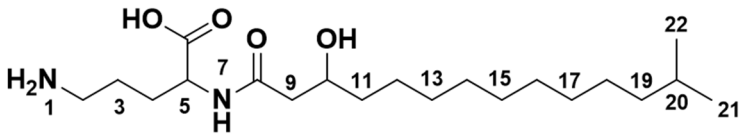

1

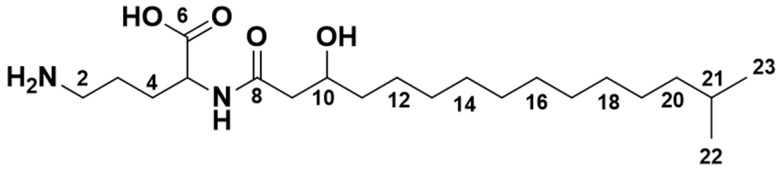

2

Figure 3. Structures of lyso-ornithine lipids isolated from *Lacinutrix* sp. (**1**): $C_{20}H_{40}N_2O_4$, (**2**): $C_{21}H_{42}N_2O_4$.

Table 1. ^{1}H and ^{13}C assignments for **1** and **2**.

	(1)		**(2)**	
position	δ_C, type	δ_H (*J* in Hz)	δ_C, type	δ_H (*J* in Hz)
2	40.2, CH_2	2.95, t (7.3)	40.2, CH_2	2.95, t (7.3)
3	24.6, CH_2	1.71, dtd (17.1, 9.5, 8.5, 4.2)	24.6, CH_2	1.77–1.64, m [e]
4	30.9, CH_2	1.91, ddd (10.0, 8.4, 4.8)	30.9, CH_2	1.90, m
5	54.8, C	4.28, dq (9.9, 3.9, 2.6)	54.8, CH	4.28, d (5.4)
6	178.0, C	-	178.0, C	-
7	-	7.63, d (8.0)	-	7.62, d (8.0)
8	173.7, C	-	173,7, C	-
9a	45.0, CH_2	2.39, dd (14.3, 3.9)	45.0, CH_2	2.39, dd (14.4, 4.0)
9b		2.30, dd (14.4, 9.2)		2.30, dd (14.4, 9.2)
10	69.9, CH	3.95, ddt (8.9, 5.8, 3.1)	69.9, CH	3.95, m
11	38.4, CH_2	1.49, m [b]	38.4, CH_2	1.52, m
12	26.6, CH_2	1.35, m [c]	26.6, CH_2	1.48, dq (7.1, 4.4, 3.9)
13	30.7–30.6, CH_2 [a]	1.40–1.22, m [c]	30.7–30.6, CH_2 [d]	1.40–1.22, m [f]
14	30.7–30.6, CH_2 [a]	1.40–1.22, m [c]	30.7–30.6, CH_2 [d]	1.40–1.22, m [f]
15	30.7–30.6, CH_2 [a]	1.40–1.22, m [c]	30.7–30.6, CH_2 [d]	1.40–1.22, m [f]
16	30.7–30.6, CH_2 [a]	1.40–1.22, m [c]	30.7–30.6, CH_2 [d]	1.40–1.22, m [f]
17	30.7–30.6, CH_2 [a]	1.40–1.22, m [c]	30.7–30.6, CH_2 [d]	1.40–1.22, m [f]
18	28.4, CH_2	1.40–1.22, m [c]	30.7–30.6, CH_2 [d]	1.40–1.22, m [f]
19	40.1, CH_2	1.16, qd (7.5, 4.2)	28.4, CH_2	1.40–1.22, m [f]
20	29.0, CH	1.52, m [b]	40.1, CH_2	1.17, q (7.1)
21	22.9, CH_3	0.86, dd (10.9, 6.7)	29.0, CH	1.77–1.64, m [e]
22			23.6, CH_3	0.87, d (6.8)
23	-	-		

[a–f] Signals are overlapping.

The molecular formula of **1** was calculated to be $C_{20}H_{40}N_2O_4$ (*m*/*z* 373.3055, $[M + H]^+$, calcd 373.3066) by HRESIMS, corresponding to two degrees of unsaturation. The ornithine substructure (atoms 1 to 7) of **1** was assembled through correlations found in the HMBC spectrum (Figures 4 and S5). Deshielding of carbon atom CH_2-2 (δ_C 40.2) places the NH_2 group at the delta carbon of the amino acid. The carbonyl group was determined to be located at C-6 (δ_C 178.0). The fatty acid chain was found to be linked to the polar head group through an amide bond between NH-7 (δ_H 7.63) and C-8 (δ_C 173.3) based

on a HMBC correlation between the two. Furthermore, carbon atoms C-9 to C-13, and C-17 to C-23 were linked through HSQC-TOCSY experiments (Figures 4 and S6), where the C-13 to C-17 resonances overlap in both dimensions. A hydroxy group was placed at carbon atom CH-10 (δ_C 69.9) based on HSQC data (Figure S5) and the deshielded shift value of the carbon atom. In agreement with previously reported data for similar compounds [23,24], the central methines (CH_2-13 to CH_2-17) could not be individually assigned due to complete signal overlap (Figures S7 and S8). The two equivalent CH_3 groups (CH_3-21 and CH_3-22) of the iso-terminal of the fatty acid were assigned based on ^{1}H and HMBC spectrum analysis, and were furthermore linked to a -CH-CH_2-CH_2- fragment (CH-20 (δ_C 29.0), CH_2-19 (δ_C 40.1) and CH_2-18 (δ_C 28.4)) through HMBC and HSQC-TOCSY correlations. Consequently, the structure of **1** was assigned as 5-amino-2-(3-hydroxy-13-methyltetradecanamido) pentanoic acid.

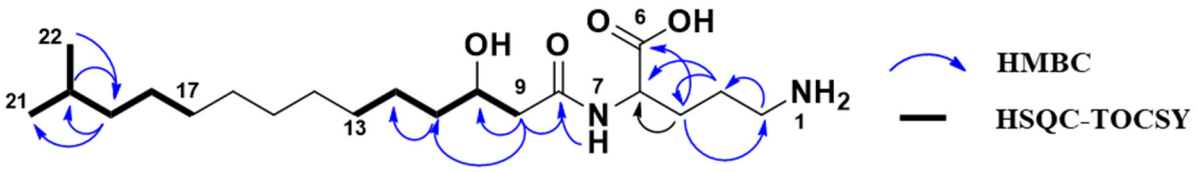

Figure 4. Selected 2D NMR correlations obtained for **1**.

Through HRESIMS analysis, **2** was determined to have a molecular formula of $C_{21}H_{42}N_2O_4$ (*m*/*z* 387.3212 $[M + H]^+$, calcd 387.3223). The structure of **2** (Figure 3) was assigned by analyzing the data from ^{1}H, ^{13}C, HSQC, HMBC, HSQC-TOCSY and COSY NMR experiments (Figures S9–S13). The structure of **2** was unambiguously assigned in a similar manner as described above for **1** and was found to have an extension of the fatty acid chain by a CH_2-group compared to **1** and was consequently assigned as 5-amino-2-(3-hydroxy-14-methylpentadecanamido) pentanoic acid.

2.6. Bioactivity Testing of Isolated Compounds

2.6.1. Antibacterial Assay

The two lyso-ornithine lipids were tested for antibacterial activity against the Gram-positive bacteria *S. agalactiae*, *E. faecalis* and *S. aureus*, and against the Gram-negative bacteria *E. coli* and *P. aeruginosa* in a growth inhibition assay in three biological replicates, each containing three technical replicates. The compounds were tested at 10, 50, 100 and 150 µM. As shown in Figure 5, **1** was active against *S. agalactiae*, while **2** showed no activity. A dose-response curve was observed for **1**, with minimum inhibitory concentration between 100 and 150 µM. Compound **1** also had modest effect against *E. faecalis* and *S. aureus* at the highest concentrations, but visible growth was observed in the wells at all concentrations, so complete growth inhibition was not achieved (Figure S14). Neither of the compounds were active against the Gram-negative bacteria (Figure S15).

2.6.2. Cytotoxic Effect of Isolated Lyso-Ornithine Lipids

The cytotoxicity of the two lyso-ornithine lipids was evaluated against human melanoma cell line A2058 and the non-malignant lung fibroblasts MRC-5 cell line at the concentrations 10, 25, 50, 100 and 150 µM. Some cytotoxic activity against the A2058 cell line was observed for **2**, with 23% cell survival at 50 µM, and ~0% cell survival at 100 and 150 µM (Figure 6). Compound **1** showed no activity against A2058 cells. Neither of the compounds were active against MRC-5 cells (Figure S16). The compounds were tested in three biological replicates with at least eight technical replicates in total.

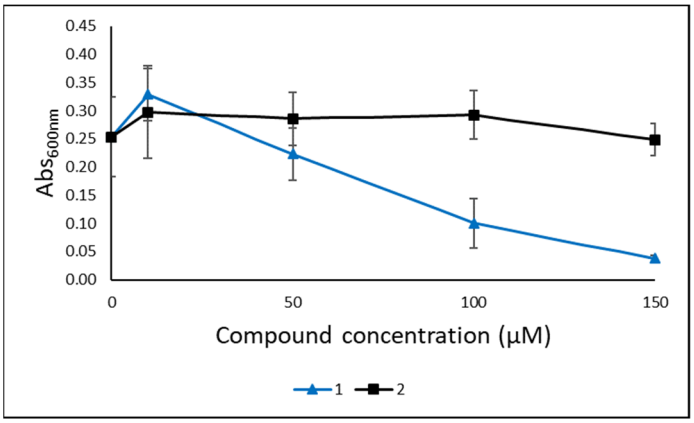

Figure 5. Antibacterial activity of **1** and **2** tested in a growth inhibition assay against the Gram-positive *S. agalactiae*. The assay was performed in three independent experiments, each with three technical replicates.

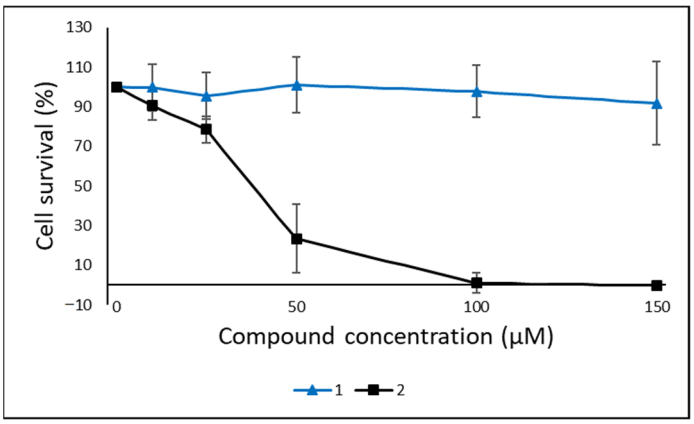

Figure 6. Cytotoxic activity of **1** and **2** against A2058 human melanoma cells. The compounds were tested in three experiments with at least eight technical replicates in total.

3. Discussion

The antibacterial activity of a fractionated extract from the Arctic marine bacterium *Lacinutrix* sp. led to the identification of two novel lyso-ornithine lipids, **1** and **2**.

Lyso-ornithine lipids are amphiphilic due to their nonpolar fatty acid chain and their polar amino acid head group. Previous studies from our group have identified amphiphilic compounds with antibacterial and cytotoxic activities [23,25]. This includes Lipid 430, with similar structure as the lyso-ornithine lipids. Lipid 430 and **2** have the same iso-branched fatty acid chain, they differ at the head group where Lipid 430 has two serine amino acids whereas **2** has one ornithine amino acid. Lipid 430 was active against the Gram-positive bacterium *S. agalactiae* and against A2058 human melanoma cells. In addition, lipoamino acids are reported to have various bioactivities, such as antibacterial, insecticidal, hemolytic, coagulant and macrophage activity [26–28]. Hence, it was likely that the two isolated compounds would be bioactive. After isolation, the two compounds were tested for antibacterial and cytotoxic activities. Compound **1** had some effect against Gram-positive bacteria, particularly *S. agalactiae*, and **2** was moderately cytotoxic to A2058 human melanoma cells. Considering the similarities in the structures of **1** and **2**, this discrepancy in bioactivity was unanticipated. As the compounds are mixtures of isomers, this could be a factor for the discrepancy in activity. However, based on our data, the isomers have the same iso-branched fatty acid linked to an ornithine head group, therefore, the differences in observed bioactivity are most likely due to the different length of the fatty

acid chain. The length of the fatty acid chain is known to affect the bioactivity of amphiphilic compounds. For example, Nashida et al. (2018) [29] synthesized mannosylerythritol lipids with various lipid chain length with different antibacterial activity. A study from Tareq et al. (2019) [30] also shows how small differences in the fatty acid chain can affect the bioactivity of amphiphilic compound. They isolated two gageostatins that showed differences in activity against various bacteria and fungi. The only difference between the two isolated gageostatins was a CH_2 in the lipid chain, similar to the differences between **1** and **2** in the present study.

The two isolated lyso-ornithine lipids showed no activity against the Gram-negative bacteria. This is likely due to the lipopolysaccharide on the outer membrane of Gram-negative bacteria, making it harder for the compounds to access the membrane, as the bioactivity of amphiphilic compounds is commonly due to membrane interactions. Tahara et al. (1977) [31] reported a lyso-ornithine lipid with the same molecular formula as **2**, but with an unbranched fatty acid chain instead of an iso-branched chain, that killed the Gram-negative *E. coli* and *P. aeruginosa* in liquid cultures at 360 μg/mL and 480 μg/mL, respectively. These concentrations are 6-9 times higher than the maximum concentration used in our study, and much higher compared to minimum inhibitory concentrations of marketed antibiotics [32], indicating a fairly weak activity against Gram-negative bacteria.

As lyso-ornithine lipids are precursors for ornithine lipids, it was possible that the extract could contain ornithine lipids. The UHPLC-HR-MS data were therefore specifically checked for the presence of such compounds, but no signals that matched the mass and elemental composition of potential ornithine lipids were detected, indicating that no ornithine lipids were produced. This could be due to the growth conditions used in this study, as the membrane lipid composition can be changed as part of the regulation of membrane fluidity. The amount of iso-branched lipids and lipoamino acids in the membrane is affected by temperature and cultivation conditions [33–36]. Some bacteria produce lipoamino acids only under limiting phosphate conditions, while others produce them regularly [37–40].

In the present study we found that lyso-ornithine lipids have some antibacterial and cytotoxic activities. Previous bioactivity studies of lyso-ornithine lipids are limited. In addition to the mentioned study of Tahara et al. (1977), they include a study by Williams et al. (2019) [41], where a lyso-ornithine lipid with good surface activity was described. Surface activity is a feature possessed by surfactants, which are compounds with amphiphilic nature. Biosurfactants (surfactants produced by microorganisms) have the potential to replace chemical surfactants within industrial applications such as remediation of heavy metal and hydrocarbon-contaminated sites, soil washing technology and in cosmetics. In addition, they are known to have various bioactivity properties. These properties include cytotoxicity and antibacterial activity, and are due to their interaction with membranes of target cells, affecting the integrity and stability of the membranes [42–45]. From this, it is likely that the activity of **1** and **2** is a result of the two compounds interacting with the membranes of the bacteria and the human melanoma cells.

The approach used in this study, investigating underexplored Artic marine bacteria for the production of novel compounds resulted in the characterization of two compounds not described before, showing the potential of Arctic marine bacteria as a source for novel compounds. Bioassay-guided isolation was used to identify the two compounds, as the selection of fractions for further analysis was based on the observed activity in the bioassays. The use of phenotypic bioassays resulted in the isolation of two active compounds with unspecific mode of action. The activity places them outside the potency level needed to be considered relevant for further development toward becoming commercially available pharmaceuticals. Despite of being widely studied, with a few exceptions, the use of biosurfactants within the pharmaceutical industry is today limited. Regarding replacing biosurfactants with chemical surfactants, biosurfactants are today used in cosmetics and in food, but in other industrial applications such as bioremediation and antifouling, the

research is still at laboratorial level [46,47]. However, as the research continues, that may change one day.

4. Materials and Methods

4.1. Sampling and Identification of Lacinutrix sp.

The strain was isolated from a *Halichondria* sp. sponge in the Barents Sea at 74°22′12″ N and 19°11′54.2652 E, in January 2009. Glycerol stocks of the bacterium were prepared and provided by Marbank. The bacterial glycerol was plated onto FMAP agar (15 g Difco Marine Broth (Becton Dickinson and Company, Franklin Lakes, NJ, USA), 5 g peptone from casein, enzymatic digest (Sigma, St. Louis, MS, USA), 15 g/L agar, 700 mL ddH_2O, and 300 mL filtrated sea water), and incubated at 10 °C until sufficient growth. The characterization of the bacterial strains was done by sequencing of the 16S rRNA gene through colony PCR and Sanger sequencing as described previously [48]. The primer set used for gene amplification was the 27F primer (forward primer; 5′-AGAGTTTGATCMTGGCTCAG) and the 1429R primer (reverse primer; 5′-TACCTTGTTACGACTT), both from Sigma. The PCR product was sequenced at the University Hospital of North Norway (Tromsø, Norway). The forward and reverse sequences obtained were assembled using the Geneious Prime® 2021.0.3 software (https://www.geneious.com/) (accessed on 2 July 2021), with the built-in Geneious assembler (sequences trimmed using a 0.05 error probability limit). The *Lacinutrix* M09B143 16S rRNA sequence was deposited in Genbank with the following accession number MZ414169. Reference sequences for the phylogenetic analysis were obtained from Genbank and were selected among top BLAST results of the M09B143 sequence and from recent phylogenetic studies on *Lacinutrix* sp. strains (Supplementary Table S1). The multiple sequence alignment of 23 sequences (including the outgroup *Flavivirga jejuensis*) was conducted using the multiple sequence alignment plug-in Clustal Omega 1.2.2 [49] in Geneious, using the default settings. The alignment was manually adjusted, resulting in a final alignment of 1413 bp length.

Phylogenetic analysis was conducted using the online version of PhyML 3.0 (http://www.atgc-montpellier.fr/phyml/) (accessed on 2 July 2021) [50], and Smart Model Selection [51] was used to select the appropriate substitution model, using the Akaike Information Criterion (AIC) as selection criterion and aBayes for branch support. This suggested the following model to be most appropriate for the dataset: GTR + G + I. The tree was rooted with *F. jejuensis*, branch support is given as aLRT (approximate likelihood ratio test) values. In addition, a phylogenetic analysis was conducted on the same alignment, using the MrBayes 3.2.6 [52] plug-in in Geneious. The analysis was run with the GTR substitution model and rate variation gamma, chain length 1,100,000, subsampling frequency 200 and burn-in length 550,000. The resulting consensus tree was built using default settings.

4.2. Fermentation

The M09B143 *Lacinutrix* strain was cultivated in 250 and 400 mL M19 medium in 1 L Erlenmeyer flasks at 10 °C with 140 rpm shaking for 2–3 week until sufficient growth. M19 medium was prepared of 1 L Milli-Q water (Merck Millipore), 20 g D-Mannitol (63560), 20 g Peptone (82303) and 20 g Sea Salt (S9883), all from Sigma-Aldrich. Diaion® HP-20 resin beads (13607, Supelco Analytica) activated in methanol (34860, Sigma-Aldrich) for 20 min and washed with Milli-Q water were added to the cultures to extract compounds secreted into the medium. After 3–4 days the resin was separated from the cultures by filtrating the cultures under vacuum using a mesh cheesecloth (1057, Dansk Hjemmeproduktion, Ejstrupholm, Danmark). Resin collected on the cheesecloth were washed with 100 mL Milli-Q water and compounds adsorbed to the resin was eluted with methanol. The elution was done twice at 140 rpm for 1 h in 150 mL methanol per 40 g resin. The extract was vacuum filtered through Whatman Ø 90 mm No. 3 filter (Whatman plc), dried under reduced pressure at 40 °C and stored at −20 °C.

4.3. Flash Fractionation, Bioactivity Testing of Flash Fractions, and Dereplication

Extract of M09B143 was dissolved in 90% methanol before Diaion® HP20 resin was added and the sample was dried under pressure at 40 °C. For each sample, 2 g of extract, 2 g of resin and 8 mL methanol were used. Flash column (Biotage® SNAP Ultra, Biotage, Uppsala, Sweden) was prepared with 6.5 g resin activated in methanol for 20 min before rinsing with Milli-Q water. The resin was loaded in the column and equilibrated with 5% methanol before the extract sample was loaded on top of the column. Fractionation was performed with a Biotage SP4™ system using first a step-wise gradient from 5–100% methanol over 36 min (the steps were 5, 25, 50 and 75% methanol, 6 min each, and 100% methanol for 12 min). Then a gradient with methanol:acetone (34850, Sigma-Aldrich) for 4 min and 100% acetone for 12 min was used. The flow rate was 12 mL/min, resulting in 27 sub fractions with 24 mL in each tube. Sub fraction 1–3, 4–6, 7–9, 10–12, 13–15 and 16–27 were pooled together to a total of six flash fractions and dried under pressure at 40 °C.

4.4. Dereplication

The samples were analyzed with ESI+ and ESI- ionization mode on a UPLC-QToF-MS for dereplication. The system (all from Waters) consisted of an Acquity UPLC I-class coupled to a PDA detector and a Vion IMS QToF. An Acquity C18 UPLC column (1.7 µm, 2.1 mm × 100 mm) was used for the separation. Milli-Q water was used for mobile phase A and acetonitrile (HiPerSolv, VWR) for mobile phase B, both containing 0.1% formic acid (*v*/*v*) (33015, Sigma). A 12-min gradient increasing from 10% to 90% acetonitrile with flow rate 0.45 mL/min was used. UNIFI 1.9 (Waters) was used to process the data.

*4.5. Purification of **1** and **2***

The compounds were purified in two different isolation rounds.

4.5.1. Purification Round One

A preparative HPLC-system (Waters) with a 600 HPLC pump, a 2996 photo diode array detector, a 3100 mass spectrometer and a 2767 sample manager was used to isolate the two compounds. MassLynx version 4.1 was used to control the system. The mobile phases consisted of A; Milli-Q water and B; acetonitrile (Prepsolv®, Merck), both containing 0.1% formic acid (*v*/*v*), and flow rate was set to 6 mL/min. Atlantis Prep dC18 column (10 µm, 10 mm × 250 mm) (Waters) was used for the initial separation of the two compounds with gradient 10–88% acetonitrile over 13 min. XSelect CSH Prep Fluoro-Phenyl column (5 µm, 10 mm × 250 mm) (Waters) was used for final purification of **1**, gradient 10–76% acetonitrile over 10 min. For the final purification of **2**, XSelect CSH Phenyl-Hexyl prep column (5 µm, 10 mm × 250 mm) (Waters) was used with gradient 10–54% acetonitrile over 11 min.

4.5.2. Purification Round Two

The initial purification of the compounds in the second round was performed with the same preparative HPLC-system described in the previous section, and the same mobile phases and flow rate. A SunFire C18 OBD column (5 µm, 10 mm × 250 mm) with gradient 50–85% acetonitrile over 10 min was used. A second purification step was performed with **2** on a preparative HPLC-system consisting of Acquity Arc Sample Manager FTN-R, Acquity Arc Quaternary Solvent Manager-R, Acquity Arc Column manager, Acquity QDa Detector and Photodiode Array Detector 2998. Masslynx software was used to control the system. An Atlantis T3, C18 column (3 µm, 3 mm × 150 mm) was used. Flow rate was set to 1.5 mL/min, with gradient 35–55% acetonitrile over 12.5 min.

4.6. Antibacterial Activity

Antibacterial activity screening of the fractions and isolated compounds was performed in a growth inhibition assay against the Gram-positive bacteria *S. aureus* (ATCC 25923), *E. faecalis* (ATCC 29122), and *S. agalactiae* (ATCC 12386), and the Gram-negative bac-

teria *E. coli* (ATCC 259233) and *P. aeruginosa* (ATCC 27853). Flash fractions in the primary screening were dissolved in Milli-Q water with 1% dimethyl sulfoxide (DMSO, D4540, Sigma-Aldrich) to 1 mg/mL, further diluted with Milli-Q water and tested in duplicates at final concentration 50 μg/mL. The isolated compounds were dissolved in DMSO to 20 mM. They were further diluted in Milli-Q water and added to the wells at the final concentrations 10, 50, 100, and 150 μM. The assay was performed as previously described by Kristoffersen et al. (2018) [25]. In total, three biological experiments were performed, with three replicates in each experiment.

4.7. Cytotoxic Activity Assay

The cytotoxicity of the fractions in the preliminary screening and of 1 and 2 was tested in an MTS in vitro cell proliferation assay. The fractions and compounds were tested against human melanoma A2058 cells (ATCC, CRL-1147TM). The isolated compounds were in addition tested against normal lung fibroblasts MRC-5 cells (ATCC CCL-171TM). The flash fractions were dissolved in Milli-Q water with 1% DMSO to 1 mg/mL and further diluted in Roswell Park Memorial Institute cell media (FG1383, Merck) with 10% fetal bovine serum (S0115, Biochrom) and tested at 50 μg/mL in three replicates.

Compounds **1** and **2** were dissolved in DMSO to 20 mM, and further diluted in Roswell Park Memorial Institute cell media with 10% fetal bovine serum and tested at the concentrations 10, 25, 50, 100 and 150 μM. One biological experiment with three replicates (test concentration 25 μM was not used here), and two biological experiments with four replicates each were performed. The bioassay was performed as previously described by Kristoffersen et al. (2018) [25].

4.8. NMR Spectroscopy

The structures of **1** and **2** were established by 1D and 2D NMR experiments. NMR spectra were acquired in methanol-d_3 (CD_3OH) and 298 K in a 3 mm shigemi tube on a Bruker Avance III HD spectrometer operating at 600 MHz for protons, equipped with an inverse TCI cryo-probe enhanced for ^{1}H, ^{13}C, and ^{2}H.

5. Conclusions

Lacinutrix sp. was evaluated for its production of bioactive molecules. This resulted in the isolation and characterizing of two novel lyso-ornithine lipids. The bioactive profiling revealed that **1** had some antibacterial activity against the Gram-positive bacterium *S. agalactiae*, with minimum inhibitory concentration between 100 and 150 μM, and that **2** had moderate cytotoxic activity against human melanoma A2058 cells with 23% cell survival at 50 μM, and ~0% cell survival at 100 μM. The length of their lipid chain seemed to affect their activity as (considering the 2-dimentional structure of the two compounds) they only differed with one methylene group in the lipid chain, but showed activity in different bioassays. Should the two compounds be more potent in other bioassays, further studies to determine the structure of the isomers can be performed. This is to our knowledge the first time bioactive molecules have been reported from *Lacinutrix* sp., and the first data describing lyso-ornithine lipids with cytotoxic activity, and with antibacterial activity against Gram-positive bacteria. This shows that exploration of the secondary metabolite content of underexplored bacteria is a viable strategy to discover novel molecules.

Supplementary Materials: The following are available online, Figure S1: Bayesian Inference tree based on 16S rRNA gene sequence similarity. Figure S2: Fractions 1-6 tested against Gram-negative bacteria and human melanoma A2058 cells. Figure S3: UHPLC-HR-MS base peak intensity chromatogram of flash fraction 5. Figure S4: Extracted UHPLC-HR-MS mass chromatogram of **1** and **2.** Figure S5: HSQC + HMBC (600 MHz, CD_3OH) spectrum of **1.** Figure S6: HSQC-TOCSY (600 MHz, CD_3OH) spectrum of **1**. Figure S7: ^{1}H NMR (600 MHz, CD_3OH) spectrum of **1**. Figure S8: ^{13}C (151 MHz, CD_3OH) spectrum of **1**. Figure S9: ^{1}H NMR (600 MHz, CD_3OH) spectrum of **2**. Figure S10: ^{13}C (151 MHz, CD_3OH) spectrum of **2**. Figure S11: HSQC + HMBC (600 MHz, CD_3OH) spectrum of **2**. Figure S12: HSQC-TOCSY (600 MHz, CD_3OH) spectrum of **2**. Figure S13: COSY (600 MHz, CD_3OH)

spectrum of **2**. Figure S14: Antibacterial activity of **1** and **2** against Gram-positive bacteria. Figure S15: Antibacterial activity of **1** and **2** against Gram-negative bacteria. Figure S16: Cytotoxic activity of **1** and **2** against non-malignant lung fibroblast cell line MRC-5. Table S1: 16S rRNA sequences used in the phylogenetic analysis of *Lacinutrix* M09B143.

Author Contributions: Conceptualization, V.K., J.H.A., E.H.H. and T.R.; methodology, V.K. and M.J.; validation, V.K., M.J., J.H.A., K.Ø.H. and E.H.H.; formal analysis and investigation, J.I., K.Ø.H., M.J., V.K. and H.R.J.; resources and funding acquisition, J.H.A.; data curation and writing—original draft preparation, and visualization V.K., M.J. and K.Ø.H.; writing—review and editing and supervision, J.H.A. and E.H.H.; project administration, V.K. All authors have read and agreed to the published version of the manuscript.

Funding: This research was partially funded by The DigiBiotics project of the Research Council of Norway (project iD 269425), the AntiBioSpec project of UiT-The Arctic University of Norway (Cristin iD 20161323) and the Ocean Medicines project (H2020-MSCA-RISE; Grant ID 690944). The publication charges of this article have been funded by a grant from the publication fund of UiT-The Arctic University of Norway.

Institutional Review Board Statement: Not applicable.

Informed Consent Statement: Not applicable.

Data Availability Statement: The data are available within the article and its Supplementary Materials.

Acknowledgments: The authors thank the Norwegian Marine Biobank (Marbank) for isolation of the bacterial strain M09B143, Marbio technicians Marte Albrigtsen and Kirsti Helland for the bioassay experiments, Chun Li for assistance with 16s RNA sequencing and Marbio researcher Yannik Schneider for support with UHPLC-HR-MS experiments.

Conflicts of Interest: The authors declare no conflict of interest.

Sample Availability: Samples of the compounds are not available from the authors.

References

1. Chopra, I.; Roberts, M. Tetracycline antibiotics: Mode of action, applications, molecular biology, and epidemiology of bacterial resistance. *Microbiol. Mol. Biol. Rev.* **2001**, *65*, 232–260. [CrossRef] [PubMed]
2. Krause, K.M.; Serio, A.W.; Kane, T.R.; Connolly, L.E. Aminoglycosides: An Overview. *Cold Spring Harb. Perspect. Med.* **2016**, *6*, a027029. [CrossRef]
3. Kelecom, A. Secondary metabolites from marine microorganisms. *An. Acad. Bras. Ciênc.* **2002**, *74*, 151–170. [CrossRef]
4. Jekielek, K.; Le, H.; Wu, A.; Newman, D.; Glaser, K.; Mayer, A. The Marine Pharmacology and Pharmaceuticals Pipeline in 2020. *FASEB J.* **2021**, *35*. [CrossRef]
5. Debbab, A.; Aly, A.H.; Lin, W.H.; Proksch, P. Bioactive compounds from marine macteria and fungi. *Microb. Biotechnol.* **2010**, *3*, 544–563. [CrossRef]
6. Gerwick, W.H.; Moore, B.S. Lessons from the past and charting the future of marine natural products drug discovery and chemical biology. *Chem. Biol.* **2012**, *19*, 85–98. [CrossRef] [PubMed]
7. McBride, M. The Family *Flavobacteriaceae*. In *The Prokaryotes*; Rosenberg, E., De Long, E.F., Lory, S., Stackebrandt, E., Thompson, F., Eds.; Springer: Berlin/Heidelberg, Germany, 2014; pp. 643–676. [CrossRef]
8. Bowman, J.P.; Nichols, D.S. Novel members of the family *Flavobacteriaceae* from Antarctic maritime habitats including *Subsaximicrobium wynnwilliamsii* gen. nov., sp. nov., *Subsaximicrobium saxinquilinus* sp. nov., *Subsaxibacter broadyi* gen. nov., sp. nov., *Lacinutrix copepodicola* gen. nov., sp. nov., and novel species of the genera *Bizionia*, *Gelidibacter* and *Gillisia*. *Int. J. Syst. Evol. Microbiol.* **2005**, *55*, 1471–1486. [CrossRef]
9. Nedashkovskaya, O.I.; Kwon, K.K.; Yang, S.-H.; Lee, H.-S.; Chung, K.H.; Kim, S.-J. *Lacinutrix algicola* sp. nov. and *Lacinutrix mariniflava* sp. nov., two novel marine alga-associated bacteria and emended description of the genus *Lacinutrix*. *Int. J. Syst. Evol. Microbiol.* **2008**, *58*, 2694–2698. [CrossRef] [PubMed]
10. Lee, Y.M.; Shin, S.C.; Baek, K.; Hwang, C.Y.; Hong, S.G.; Chun, J.; Lee, H.K. Draft genome sequence of the psychrophilic bacterium *Lacinutrix jangbogonensis* PAMC 27137T. *Mar. Genomics* **2015**, *23*, 31–32. [CrossRef]
11. Srinivas, T.N.R.; Prasad, S.; Manasa, P.; Sailaja, B.; Begum, Z.; Shivaji, S. *Lacinutrix himadriensis* sp. nov., a psychrophilic bacterium isolated from a marine sediment, and emended description of the genus *Lacinutrix*. *Int. J. Syst. Evol. Microbiol.* **2013**, *63*, 729–734. [CrossRef]
12. Huang, Z.; Li, G.; Lai, Q.; Gu, L.; Shao, Z. *Lacinutrix gracilariae* sp. nov., isolated from the surface of a marine red alga *Gracilaria* sp. *Int. J. Syst. Evol. Microbiol.* **2016**, *66*, 587–591. [CrossRef] [PubMed]

13. Nedashkovskaya, O.I.; Kim, S.-G.; Zhukova, N.V.; Lee, J.-S.; Mikhailov, V.V. *Lacinutrix cladophorae* sp. nov., a flavobacterium isolated from the green alga *Cladophora stimpsonii*, transfer of *Flavirhabdus iliipiscaria* Shakeela et al. 2015 to the genus *Lacinutrix* as *Lacinutrix iliipiscaria* comb. nov. and emended description of the genus *Lacinutrix*. *Int. J. Syst. Evol. Microbiol.* **2016**, *66*, 4339–4346. [CrossRef]
14. Shakeela, Q.; Shehzad, A.; Zhang, Y.; Tang, K.; Zhang, X.-H. *Flavirhabdus iliipiscaria* gen. nov., sp. nov., isolated from intestine of flounder (*Paralichthys olivaceus*) and emended descriptions of the genera *Flavivirga*, *Algibacter*, *Bizionia* and *Formosa*. *Int. J. Syst. Evol. Microbiol.* **2015**, *65*, 1347–1353. [CrossRef]
15. Kim, H.; Yoon, S.-C.; Choi, K.-H.; Kim, S.-T.; Lee, J.-B.; Kim, D.-S.; Le Han, H.; Bae, K.S.; Park, D.-S. *Lacinutrix chionocetis* sp. nov., isolated from gut of a red snow crab. *Arch. Microbiol.* **2017**, *199*, 597–603. [CrossRef]
16. Lasa, A.; Diéguez, A.L.; Romalde, J.L. Description of *Lacinutrix venerupis* sp. nov.: A novel bacterium associated with reared clams. *Syst. Appl. Microbiol.* **2015**, *38*, 115–119. [CrossRef]
17. Park, S.; Park, J.-M.; Jung, Y.-T.; Kang, C.-H.; Yoon, J.-H. *Lacinutrix undariae* sp. nov., isolated from a brown algae reservoir. *Int. J. Syst. Evol. Microbiol.* **2015**, *65*, 2696–2701. [CrossRef]
18. Yoon, J.; Lee, J.-S.; Lee, K.-C. Description of *Lacinutrix salivirga* sp. nov., a marine member of the family *Flavobacteriaceae* isolated from seawater. *Arch. Microbiol.* **2018**, *200*, 1159–1165. [CrossRef] [PubMed]
19. Lee, Y.M.; Kim, M.-K.; Ahn, D.H.; Kim, H.-W.; Park, H.; Shin, S.C. Comparative analysis of *Lacinutrix* genomes and their association with bacterial habitat. *PLoS ONE* **2016**, *11*, e0148889. [CrossRef] [PubMed]
20. Weissenmayer, B.; Gao, J.-L.; López-Lara, I.M.; Geiger, O. Identification of a gene required for the biosynthesis of ornithine-derived lipids. *Mol. Microbiol.* **2002**, *45*, 721–733. [CrossRef]
21. Gao, J.-L.; Weissenmayer, B.; Taylor, A.M.; Thomas-Oates, J.; López-Lara, I.M.; Geiger, O. Identification of a gene required for the formation of lyso-ornithine lipid, an intermediate in the biosynthesis of ornithine-containing lipids. *Mol. Microbiol.* **2004**, *53*, 1757–1770. [CrossRef] [PubMed]
22. Vences-Guzmán, M.Á.; Geiger, O.; Sohlenkamp, C. Ornithine lipids and their structural modifications: From A to E and beyond. *FEMS Microbiol. Lett.* **2012**, *335*, 1–10. [CrossRef] [PubMed]
23. Schneider, Y.K.-H.; Hansen, K.Ø.; Isaksson, J.; Ullsten, S.; Hansen, E.H.; Hammer Andersen, J. Anti-bacterial effect and cytotoxicity assessment of Lipid 430 isolated from *Algibacter* sp. *Molecules* **2019**, *24*, 3991. [CrossRef]
24. Clark, R.B.; Cervantes, J.L.; Maciejewski, M.W.; Farrokhi, V.; Nemati, R.; Yao, X.; Anstadt, E.; Fujiwara, M.; Wright, K.T.; Riddle, C.; et al. Serine lipids of *Porphyromonas gingivalis* are human and mouse Toll-like receptor 2 ligands. *Infect. Immun.* **2013**, *81*, 3479–3489. [CrossRef] [PubMed]
25. Kristoffersen, V.; Rämä, T.; Isaksson, J.; Andersen, J.H.; Gerwick, W.H.; Hansen, E. Characterization of rhamnolipids produced by an Arctic marine bacterium from the *Pseudomonas fluorescence* group. *Mar. Drugs* **2018**, *16*, 163. [CrossRef]
26. Touré, S.; Desrat, S.; Pellissier, L.; Allard, P.-M.; Wolfender, J.-L.; Dusfour, I.; Stien, D.; Eparvier, V. Characterization, diversity, and structure-activity relationship study of lipoamino acids from *Pantoea* sp. and synthetic analogues. *Int. J. Mol. Sci.* **2019**, *20*, 1083. [CrossRef] [PubMed]
27. Kimura, A.; Otsuka, H. Biological activities of siolipin (ester of lipoamino acid). *Agric. Biol. Chem.* **1969**, *33*, 1291–1294. [CrossRef]
28. Kawai, Y.; Akagawa, K. Macrophage activation by an ornithine-containing lipid or a serine-containing lipid. *Infect. Immun.* **1989**, *57*, 2086–2091. [CrossRef]
29. Nashida, J.; Nishi, N.; Takahashi, Y.; Hayashi, C.; Igarashi, M.; Takahashi, D.; Toshima, K. Systematic and stereoselective total synthesis of mannosylerythritol lipids and evaluation of their antibacterial activity. *J. Org. Chem.* **2018**, *83*, 7281–7289. [CrossRef]
30. Tareq, F.S.; Lee, M.A.; Lee, H.-S.; Lee, J.-S.; Lee, Y.-J.; Shin, H.J. Gageostatins A-C, antimicrobial linear lipopeptides from a marine *Bacillus subtilis*. *Mar. Drugs* **2014**, *12*, 871–885. [CrossRef]
31. Tahara, Y.; Yamada, Y.; Kondo, K. Antimicrobial activity of the ornithine-containing lipid isolated from *Gluconobacter cerinus*. *Agric. Biol. Chem.* **1977**, *41*, 417–418. [CrossRef]
32. Andrews, J.M. Determination of minimum inhibitory concentrations. *J. Antimicrob. Chemother.* **2001**, *48*, 5–16. [CrossRef]
33. Kaneda, T. Iso- and anteiso-fatty acids in bacteria: Biosynthesis, function, and taxonomic significance. *Microbiol. Rev.* **1991**, *55*, 288–302. [CrossRef]
34. Denich, T.J.; Beaudette, L.A.; Lee, H.; Trevors, J.T. Effect of selected environmental and physico-chemical factors on bacterial cytoplasmic membranes. *J. Microbiol. Methods* **2003**, *52*, 149–182. [CrossRef]
35. Bajerski, F.; Wagner, D.; Mangelsdorf, K. Cell membrane fatty acid composition of *Chryseobacterium frigidisoli* PB4T, isolated from Antarctic glacier forefield soils, in response to changing temperature and pH conditions. *Front. Microbiol.* **2017**, *8*. [CrossRef]
36. Rustan, A.C.; Drevon, C.A. Fatty acids: Structures and properties. *eLS* **2005**. [CrossRef]
37. Sohlenkamp, C.; Geiger, O. Bacterial membrane lipids: Diversity in structures and pathways. *FEMS Microbiol. Rev.* **2015**, *40*, 133–159. [CrossRef]
38. Kawai, Y.; Yano, I.; Kaneda, K. Various kinds of lipoamino acids including a novel serine-containing lipid in an opportunistic pathogen *Flavobacterium*. *Eur. J. Biochem.* **1988**, *171*, 73–80. [CrossRef] [PubMed]
39. López-Lara, I.M.; Sohlenkamp, C.; Geiger, O. Membrane lipids in plant-associated bacteria: Their biosyntheses and possible functions. *Mol. Plant. Microbe. Interact.* **2003**, *16*, 567–579. [CrossRef] [PubMed]
40. Asselineau, J. Bacterial lipids containing amino acids or peptides linked by amide bonds. *Fortschr. Chem. Org. Naturst.* **1991**, *56*, 1–85. [CrossRef]

41. Williams, W.; Kunorozva, L.; Klaiber, I.; Henkel, M.; Pfannstiel, J.; Van Zyl, L.J.; Hausmann, R.; Burger, A.; Trindade, M. Novel metagenome-derived ornithine lipids identified by functional screening for biosurfactants. *Appl. Microbiol. Biotechnol.* **2019**, *103*, 4429–4441. [CrossRef] [PubMed]
42. Varvaresou, A.; Iakovou, K. Biosurfactants in cosmetics and biopharmaceuticals. *Lett. Appl. Microbiol.* **2015**, *61*, 214–223. [CrossRef]
43. Pacwa-Płociniczak, M.; Płaza, G.A.; Piotrowska-Seget, Z.; Cameotra, S.S. Environmental applications of biosurfactants: Recent advances. *Int. J. Mol. Sci.* **2011**, *12*, 633–654. [CrossRef] [PubMed]
44. Schreier, S.; Malheiros, S.V.P.; de Paula, E. Surface active drugs: Self-association and interaction with membranes and surfactants. Physicochemical and biological aspects. *Biochim. Biophys. Acta Biomemb.* **2000**, *1508*, 210–234. [CrossRef]
45. Otzen, D.E. Biosurfactants and surfactants interacting with membranes and proteins: Same but different? *Biochim. Biophys. Acta Biomemb.* **2017**, *1859*, 639–649. [CrossRef]
46. Nikolova, C.; Gutierrez, T. Biosurfactants and Their applications in the oil and gas industry: Current state of knowledge and future perspectives. *Front. Bioeng. Biotechnol.* **2021**, *9*, 626639. [CrossRef] [PubMed]
47. Alemán-Vega, M.; Sánchez-Lozano, I.; Hernández-Guerrero, C.J.; Hellio, C.; Quintana, E.T. Exploring antifouling activity of biosurfactants producing marine bacteria isolated from Gulf of California. *Int. J. Mol. Sci.* **2020**, *21*, 6068. [CrossRef]
48. Schneider, Y.; Jenssen, M.; Isaksson, J.; Hansen, K.Ø.; Andersen, J.H.; Hansen, E.H. Bioactivity of serratiochelin A, a siderophore isolated from a co-culture of *Serratia* sp. and *Shewanella* sp. *Microorganisms* **2020**, *8*, 1042. [CrossRef]
49. Sievers, F.; Wilm, A.; Dineen, D.; Gibson, T.J.; Karplus, K.; Li, W.; Lopez, R.; McWilliam, H.; Remmert, M.; Söding, J.; et al. Fast, scalable generation of high-quality protein multiple sequence alignments using Clustal Omega. *Mol. Syst. Biol.* **2011**, *7*, 539. [CrossRef]
50. Guindon, S.; Dufayard, J.-F.; Lefort, V.; Anisimova, M.; Hordijk, W.; Gascuel, O. New algorithms and methods to estimate maximum-likelihood phylogenies: Assessing the performance of PhyML 3.0. *Syst. Biol.* **2010**, *59*, 307–321. [CrossRef]
51. Lefort, V.; Longueville, J.-E.; Gascuel, O. SMS: Smart Model Selection in PhyML. *Mol. Biol. Evol.* **2017**, *34*, 2422–2424. [CrossRef] [PubMed]
52. Huelsenbeck, J.P.; Ronquist, F. MRBAYES: Bayesian inference of phylogenetic trees. *Bioinformatics* **2001**, 754–755. [CrossRef] [PubMed]

Supplementary Materials

Two Novel Lyso-Ornithine Lipids Isolated from an Arctic Marine *Lacinutrix* sp. Bacterium

Venke Kristoffersen [1,*], Marte Jenssen [1], Heba Raid Jawad [1], Johan Isaksson [2], Espen H. Hansen [1], Teppo Rämä [1], Kine Ø. Hansen [1] and Jeanette Hammer Andersen [1]

[1] Marbio, Faculty for Fisheries, Biosciences and Economy, UiT-The Arctic University of Norway, Breivika, N-9037 Tromsø, Norway; marte.jenssen@uit.no (M.J.); heba_jr@hotmail.com (H.R.J.); espen.hansen@uit.no (E.H.H.); teppo.rama@uit.no (T.R.); kine.o.hanssen@uit.no (K.Ø.H); jeanette.h.andersen@uit.no (J.H.A.)

[2] Department of Chemistry, Faculty of Natural Sciences, UiT-The Arctic University of Norway, Breivika, N-9037 Tromsø, Norway; johan.isaksson@uit.no

* Correspondence: venke.kristoffersen@uit.no

Table S1. The names, accession numbers and lengths (bp) of all 16S rRNA sequences used in the phylogenetic analysis of *Lacinutrix* M09B143. All sequences were acquired from Genbank.

Name/Information	Acc.nr	Length (bp)
Algibacter agarivorans strain KYW560 16S ribosomal RNA gene	JN864025	1452
Algibacter miyuki strain WS-MY6 from South Korea 16S ribosomal RNA gene	KC662118	1441
Algibacter pectinivorans strain JC2675 from South Korea 16S ribosomal RNA gene	HM475134	1442
Algibacter psychrophilus strain PAMC 27237 16S ribosomal RNA gene	KJ475138	1510
Algibacter wandonensis 16S ribosomal RNA gene	KC987358	1443
Flavirhabdus (now *Lacinutrix*) *iliipiscaria* strain Th68 16S ribosomal RNA gene	JX412960	1486
Flavivirga jejuensis strain JC2682 from South Korea 16S ribosomal RNA gene, partial sequence (outgroup)	HM475139	1439
Lacinutrix (*chionocetis*) sp. MAB-07 16S ribosomal RNA gene	KT272396	1421
Lacinutrix (*cladophorae*) sp. 7Alg 4 16S ribosomal RNA gene	KU510085	1478
Lacinutrix algicola strain AKS293 16S ribosomal RNA	NR_043592	1496
Lacinutrix copepodicola strain DJ3 16S ribosomal RNA gene	AY694001	1364
Lacinutrix gracilariae strain Lxc1 16S ribosomal RNA	NR_148656	1444
Lacinutrix himadriensis strain E4-9a 16S ribosomal RNA	NR_108471	1488
Lacinutrix jangbogonensis strain PAMC 27137 16S ribosomal RNA	NR_134754	1443
Lacinutrix mariniflava strain AKS432 16S ribosomal RNA	NR_043593	1454
Lacinutrix salivirga gene for 16S ribosomal RNA	LC339518	1460
Lacinutrix sp. strain M09B143 16S ribosomal RNA gene	Must submit	Must submit
Lacinutrix undariae strain W-BA8 16S ribosomal RNA gene	KP309835	1442
Lacinutrix venerupis strain Cmf 20.8 16S ribosomal RNA	NR_145942	1337
Mesoflavibacter aestuarii strain KYW614 16S ribosomal RNA gene	JX854528	1443
Mesoflavibacter sabulilitoris strain GJMS-9 16S ribosomal RNA gene	KJ816860	1446
Olleya aquimaris strain L-4 16S ribosomal RNA gene	FJ886713	1443
Olleya namhaensis strain WT-MY15 16S ribosomal RNA gene	JQ327134	1441

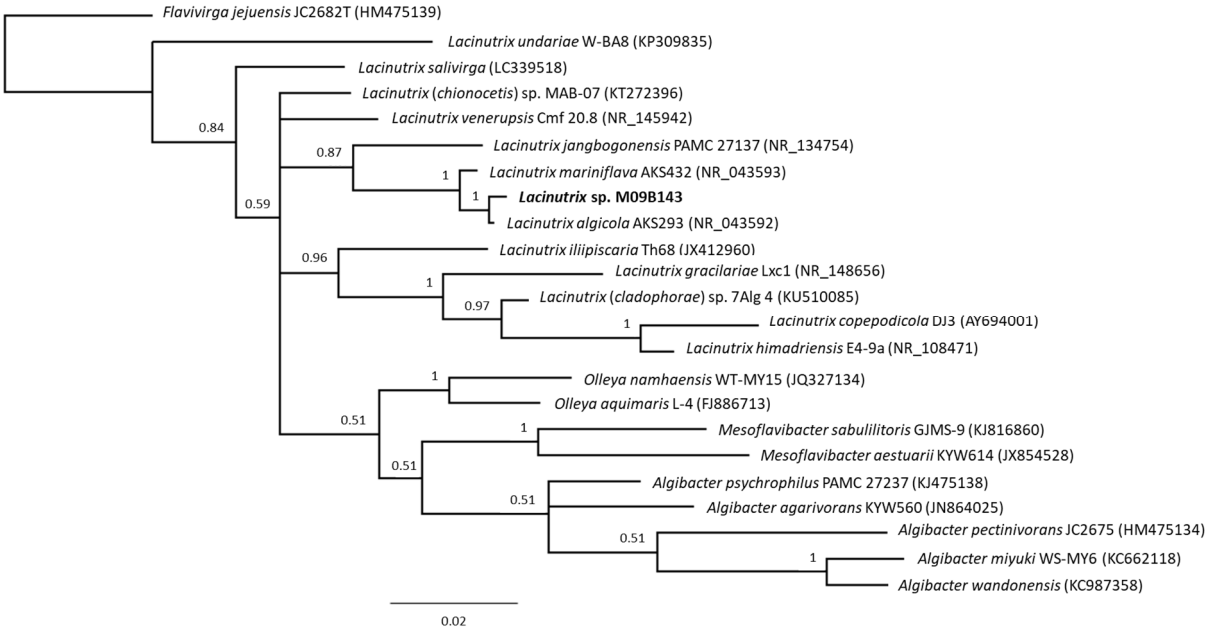

Figure S1. Bayesian Inference tree based on 16S rRNA gene sequence similarity and showing the phylogenetic placement of the isolate M09B143 (in bold) within Bacteroidetes. The tree was rooted with *Flavivirga jejuensis* as the outgroup. Branch support is given Bayesian posterior probability.

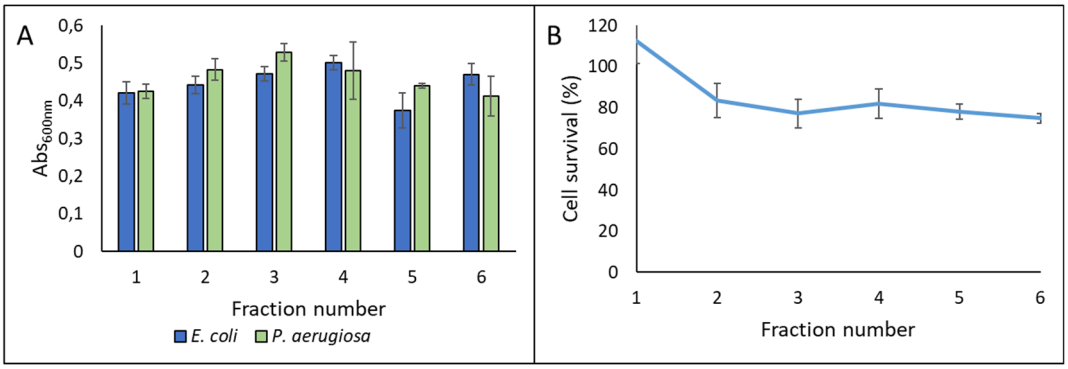

Figure S2. Fractions 1-6 showed no activity against the Gram-negative bacteria *E. coli* and *P. aeruginosa* in the growth inhibition assay, results shown in **A**. There was visible growth in all wells, and the OD values were 0.37 or higher. In comparison, the OD value of fraction 5 was 0.05 when it was active against *S. agalactiae* (Figure 2). The assay was performed in duplicates. Fractions 1-6 showed no activity against human melanoma A2058 cells, results shown in **B**. Cell survival was 75 % or higher for the fractions. The assay was performed with three technical replicates.

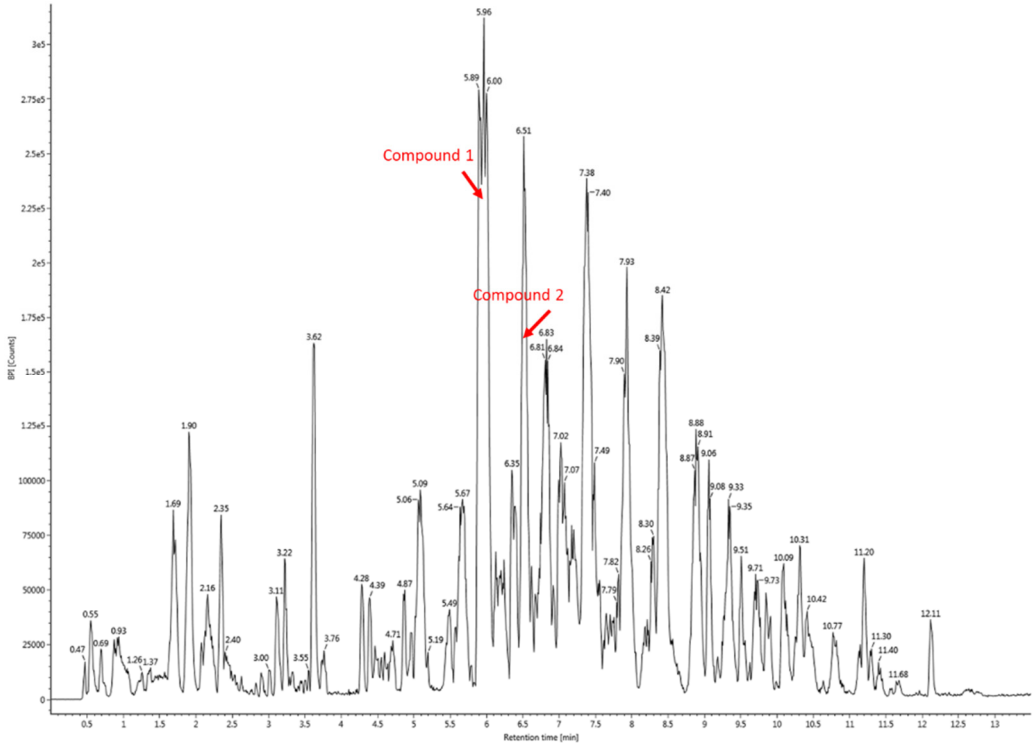

Figure S3. UHPLC-HR-MS base peak intensity chromatogram of fraction 5 of *Lacinutrix* sp., where **1** is the major peak, and **2** among the highest peaks.

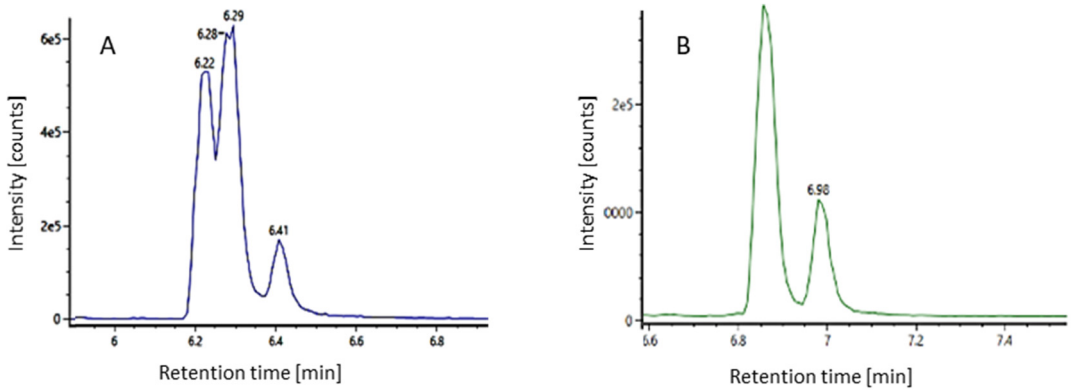

Figure S4. Extracted UHPLC-HR-MS mass chromatogram of **1** shown in **A**, and **2** shown in **B**. Possible isomers were observed, as **1** eluted in three peaks and **2** eluted in two peaks.

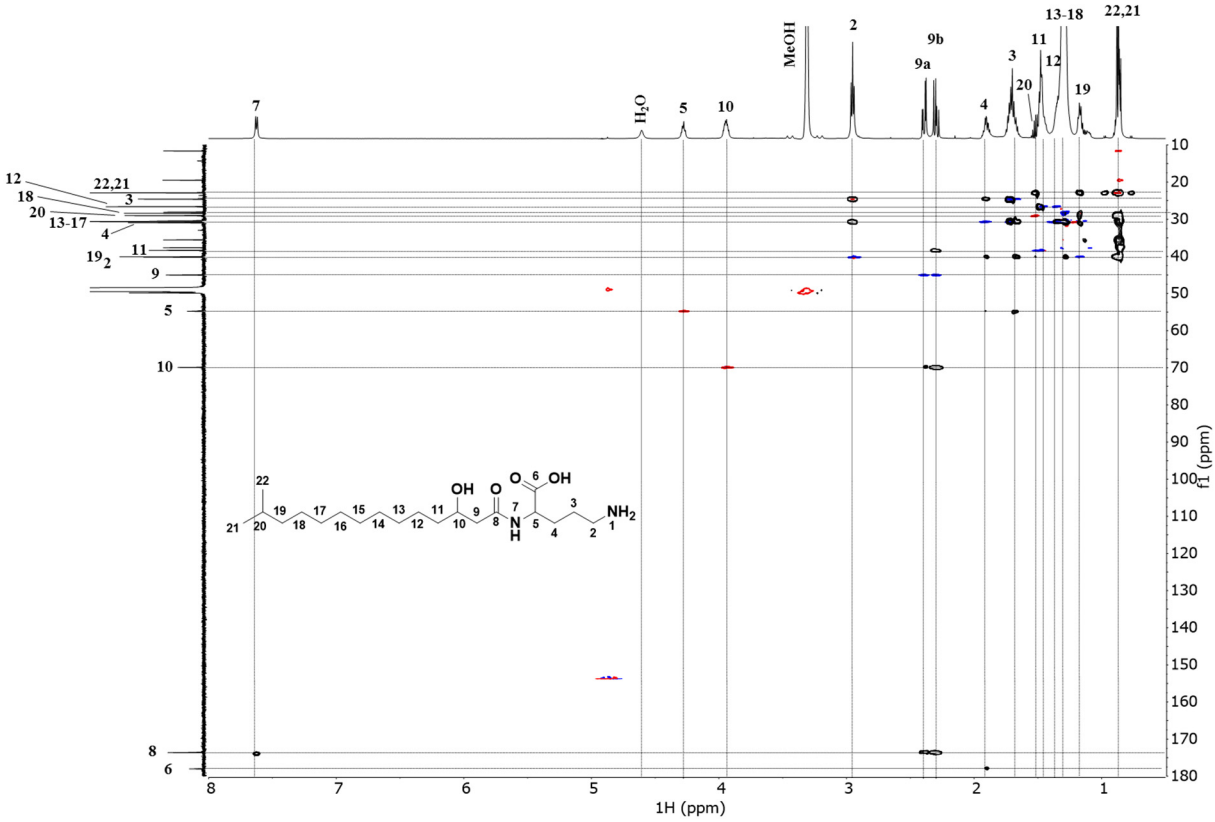

Figure S5. HSQC + HMBC (600 MHz, CD_3OH) spectrum of **1**.

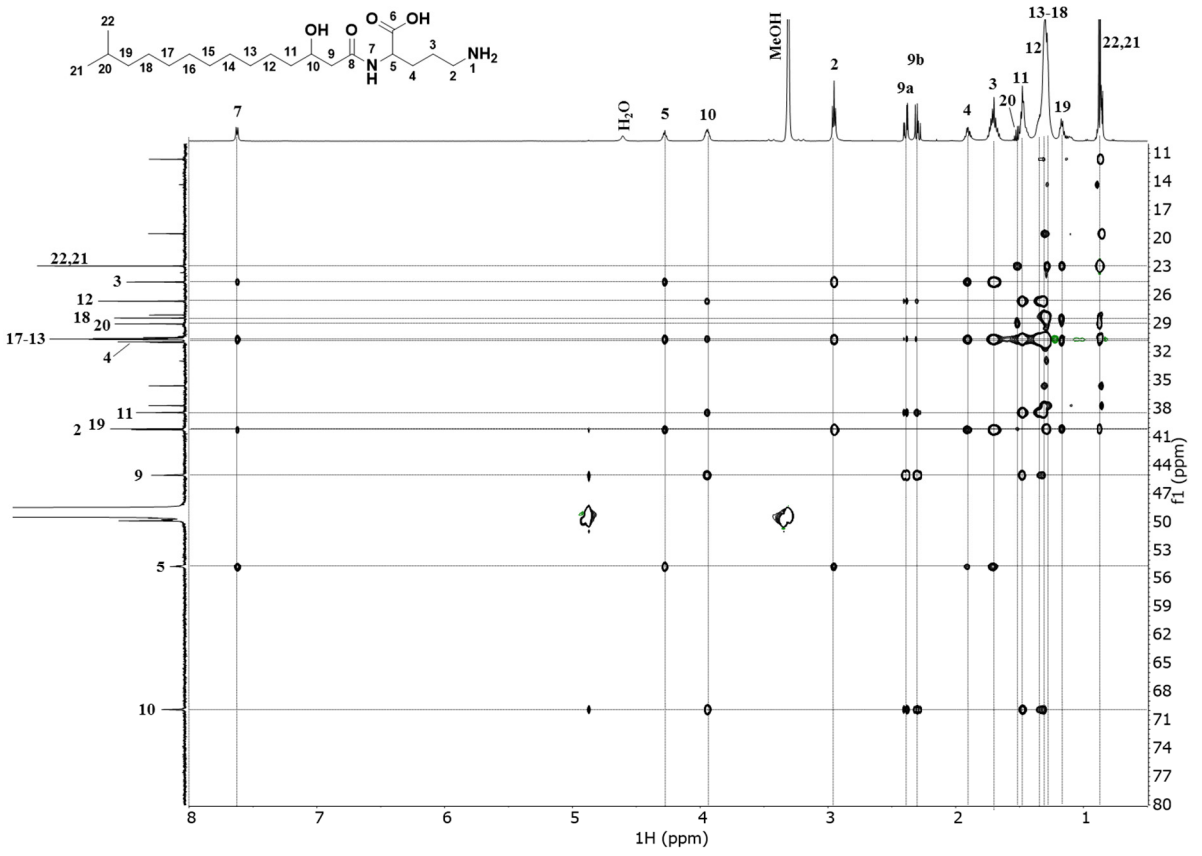

Figure S6. HSQC-TOCSY (600 MHz, CD_3OH) spectrum of **1**.

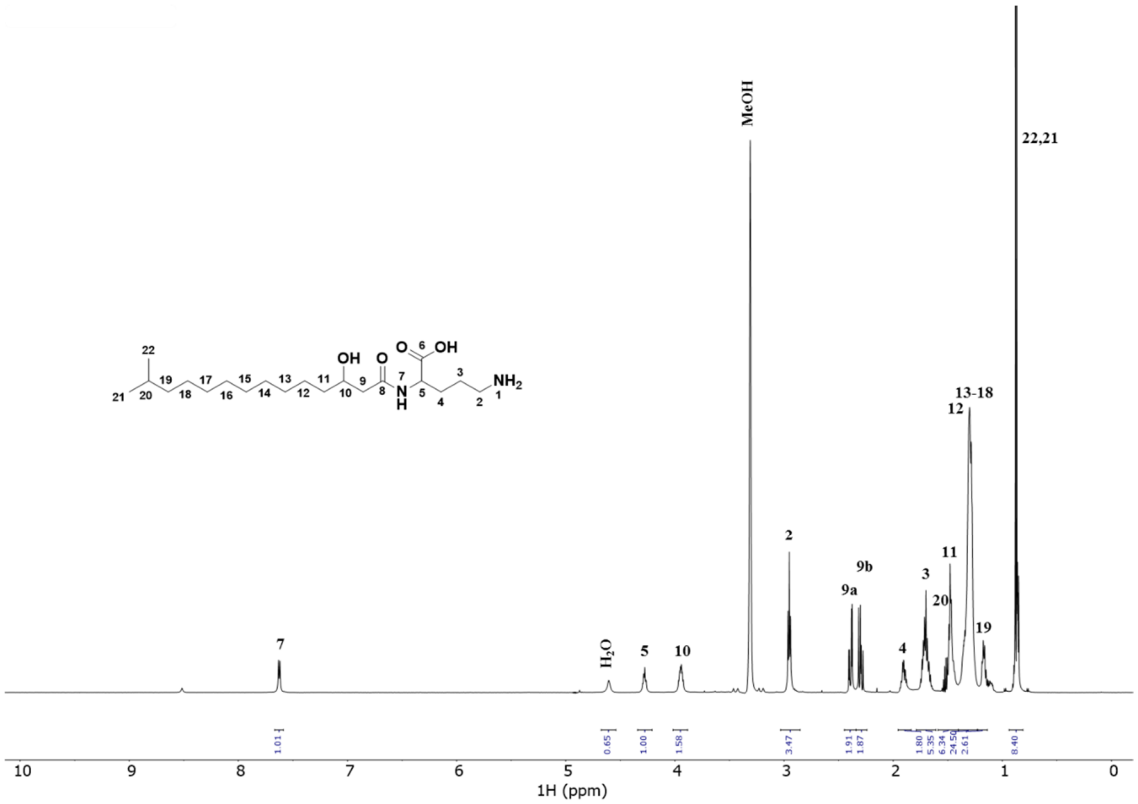

Figure S7. ^{1}H NMR (600 MHz, CD_3OH) spectrum of **1**.

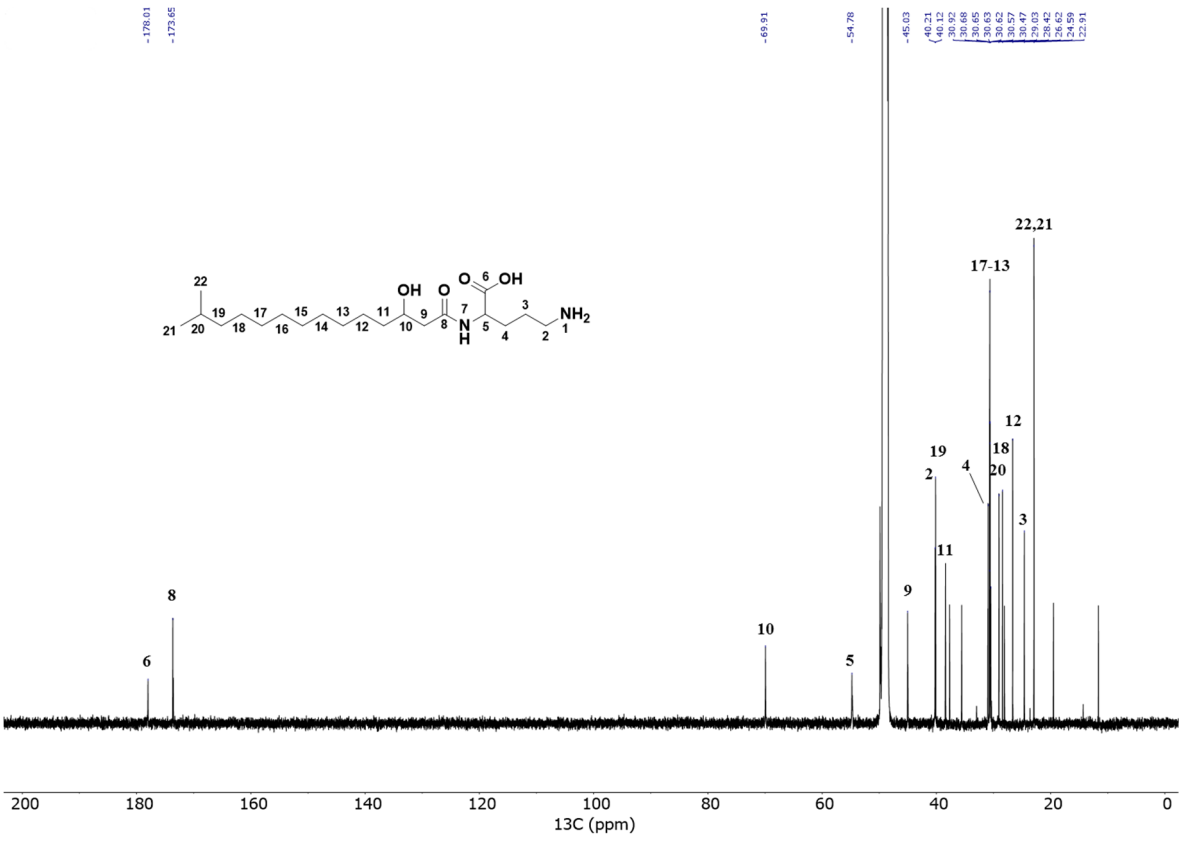

Figure S8. ^{13}C (151 MHz, CD_3OH) spectrum of **1**.

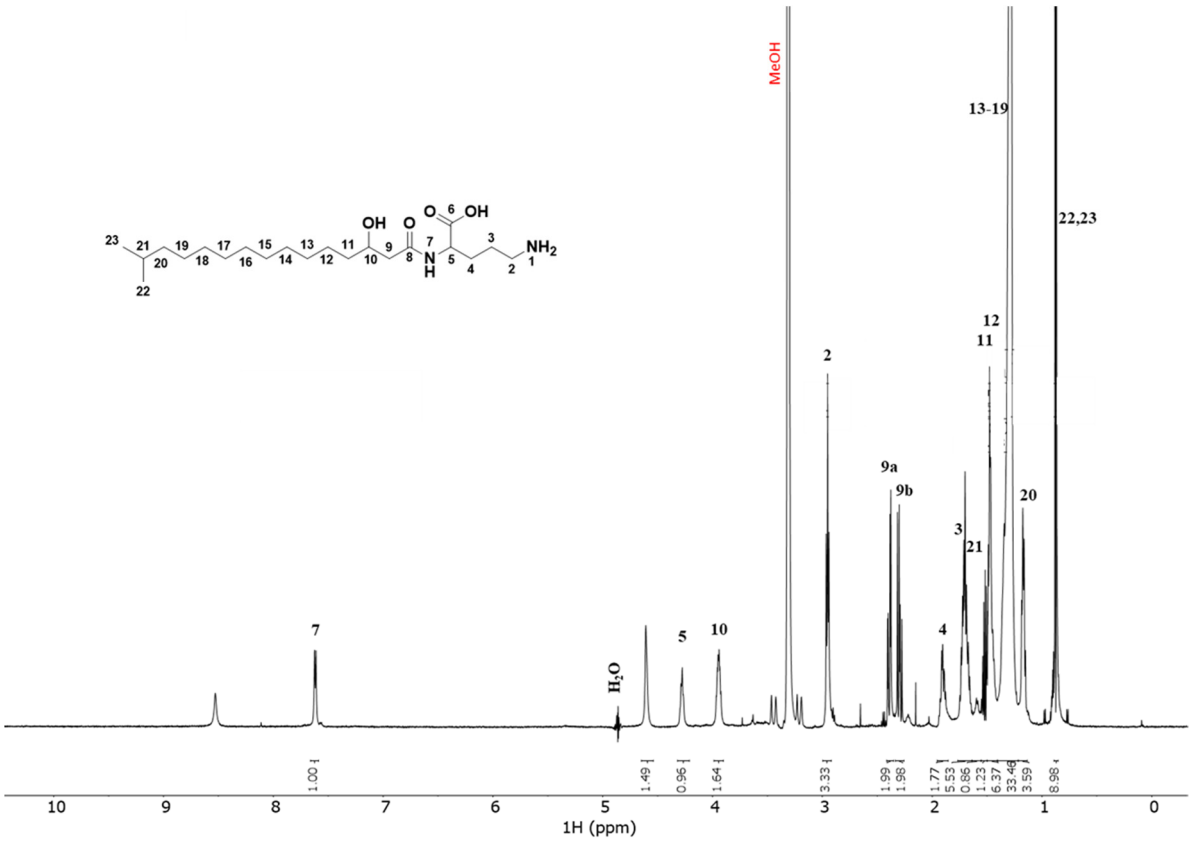

Figure S9. ^{1}H NMR (600 MHz, CD_3OH) spectrum of **2**.

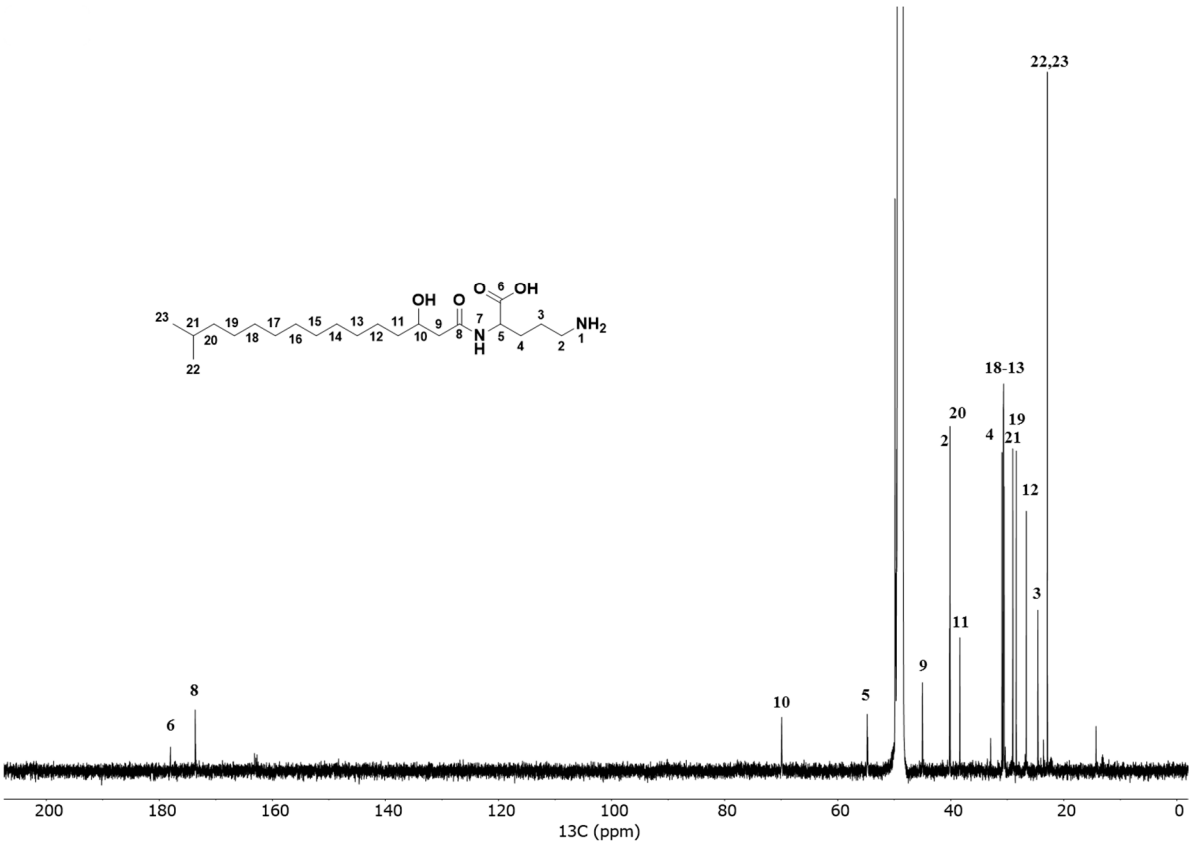

Figure S10. ^{13}C (151 MHz, CD_3OH) spectrum of **2**.

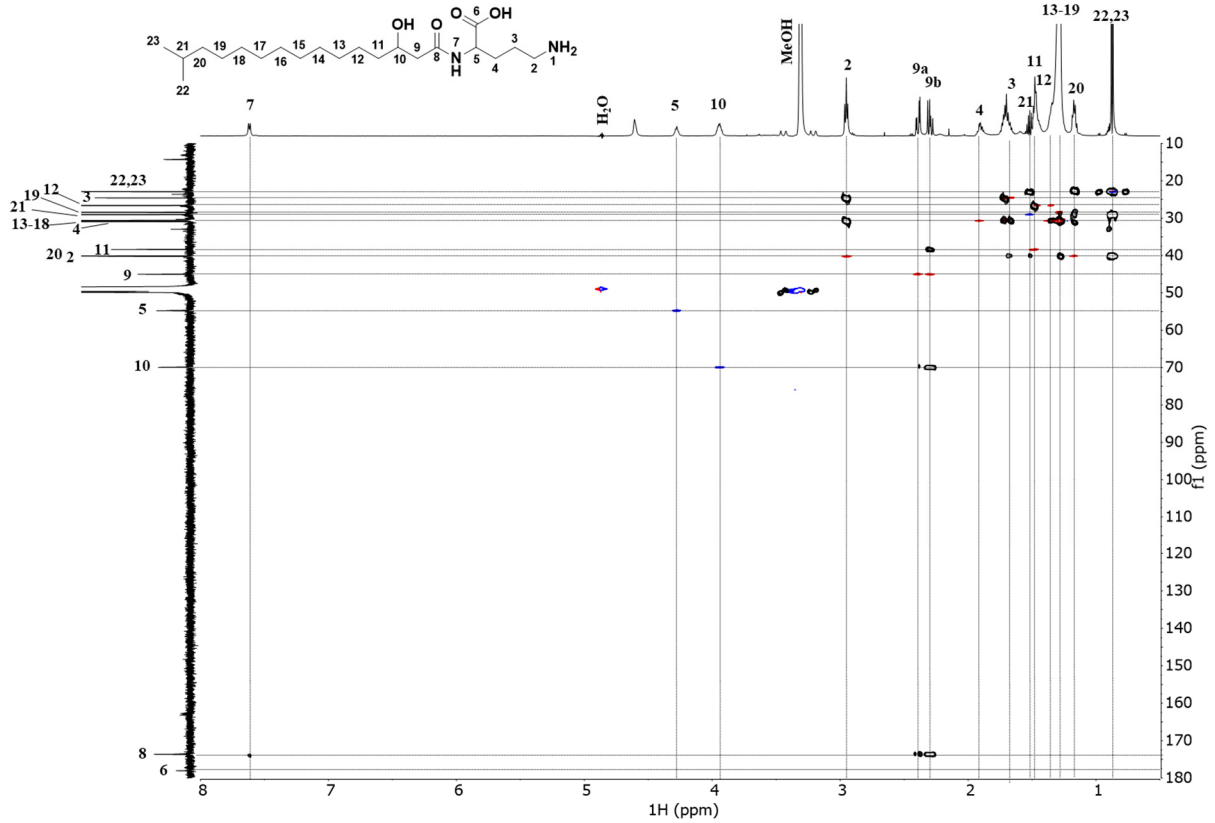

Figure S11. HSQC + HMBC (600 MHz, CD_3OH) spectrum of **2**.

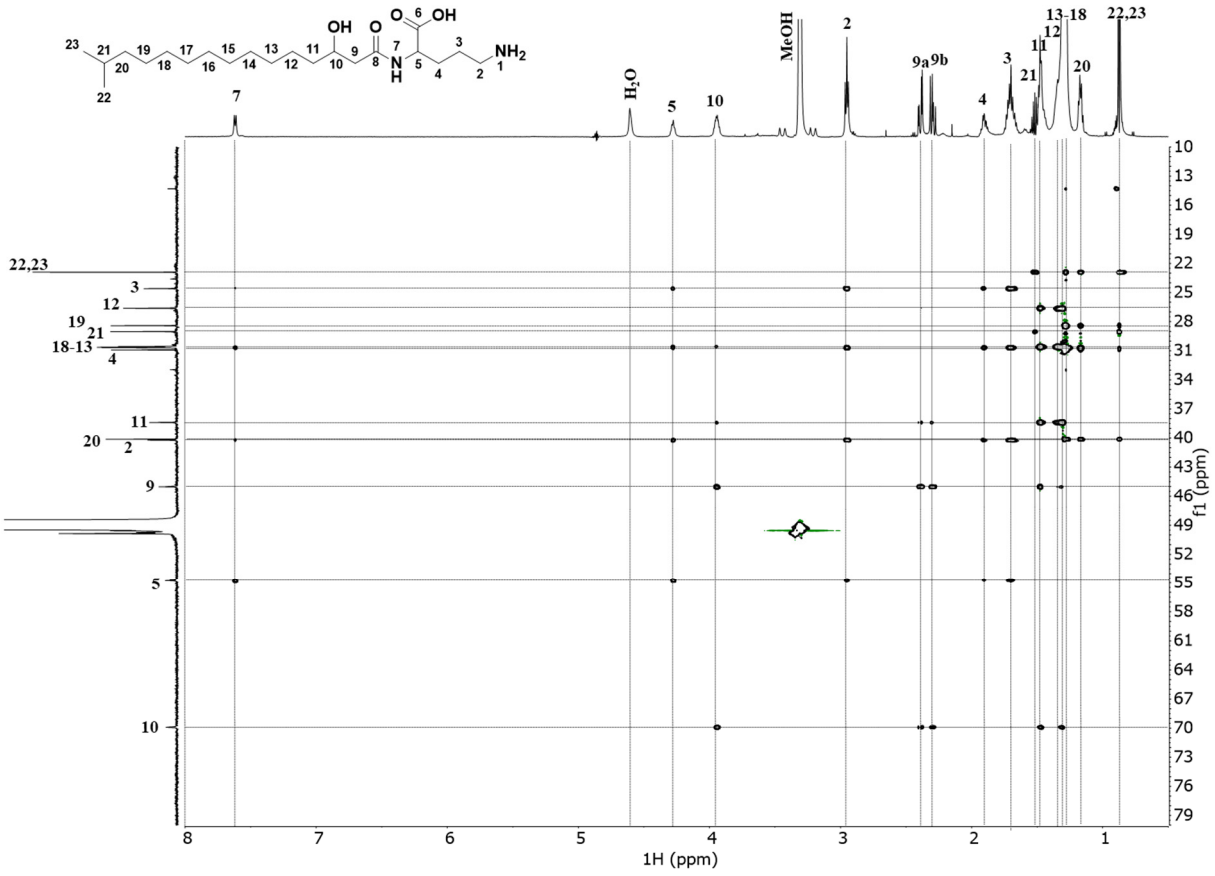

Figure S12. HSQC-TOCSY (600 MHz, CD_3OH) spectrum of **2**.

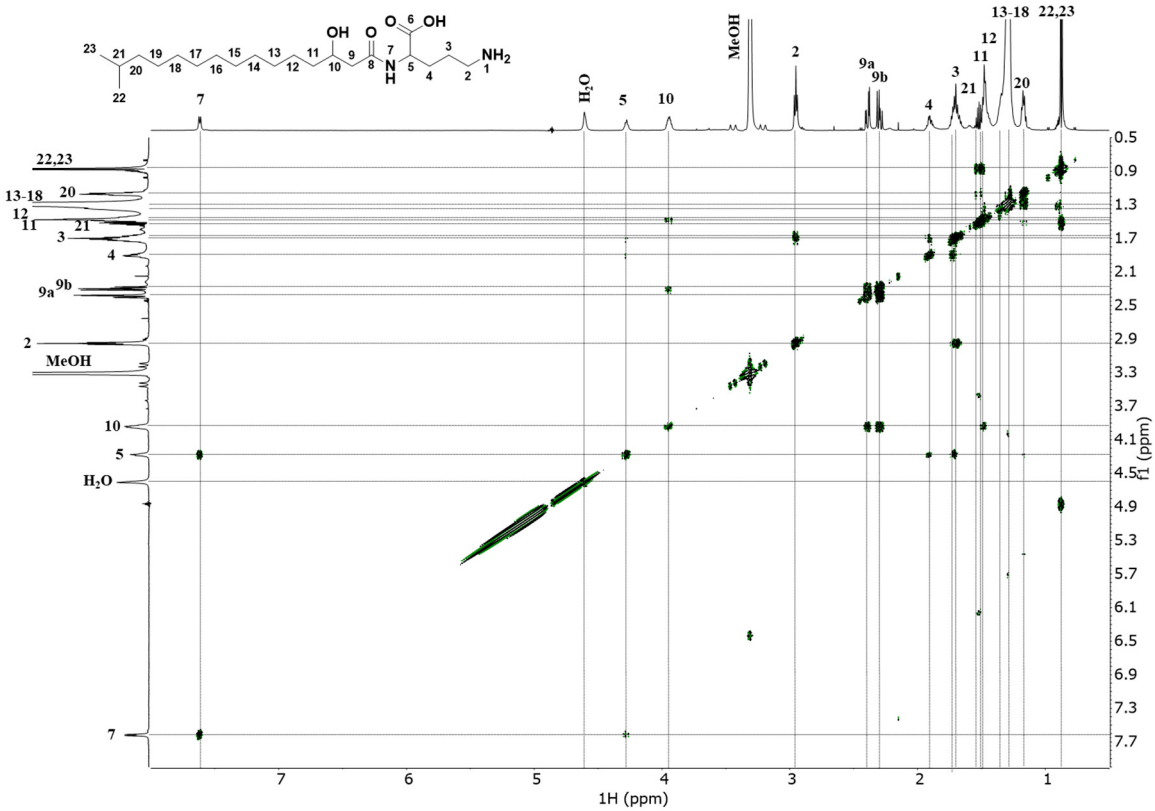

Figure S13. COSY (600 MHz, CD_3OH) spectrum of **2.**

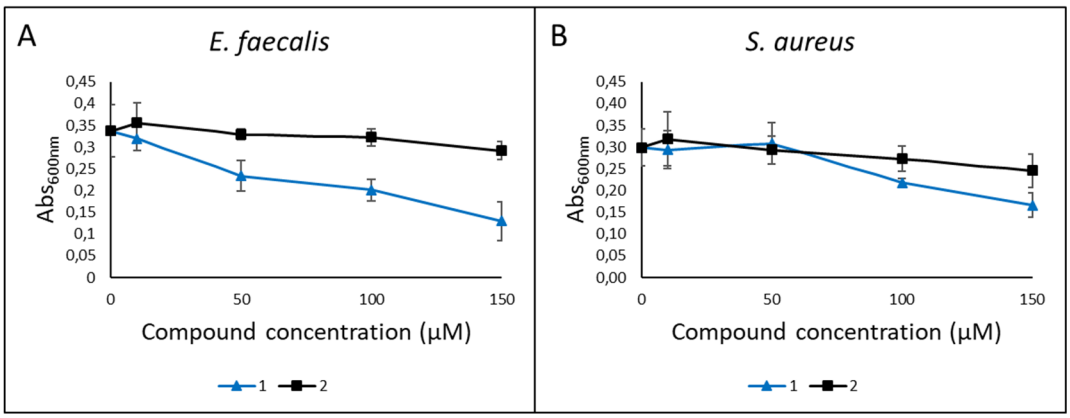

Figure S14. Antibacterial activity of **1** and **2** was tested in a growth inhibition assay. The results are shown for the Gram-positive bacteria *E. faecalis* in A and *S. aureus* in B. The assay was performed in three biological experiments with three technical replicates each.

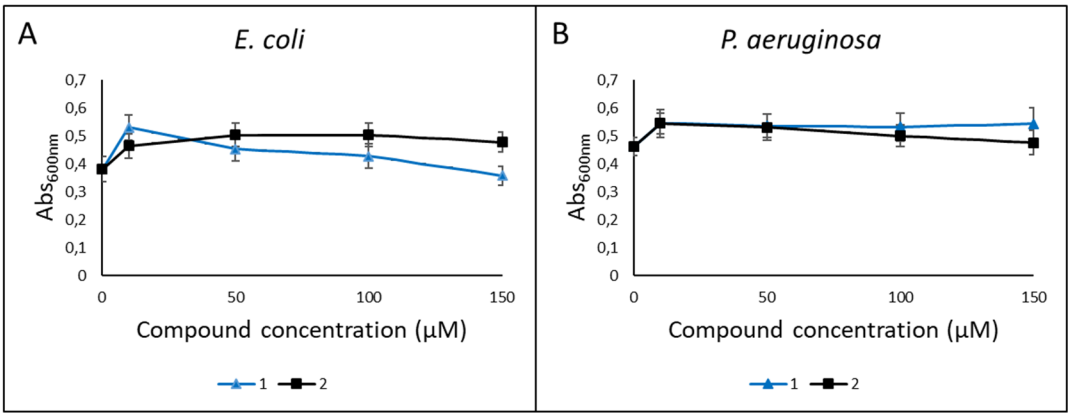

Figure S15. Antibacterial activity of **1** and **2** was tested in a growth inhibition assay. The results are shown for the Gram-negative bacteria *E. coli* in A and *P. aeruginosa* in B. The assay was performed in three biological experiments with three technical replicates each.

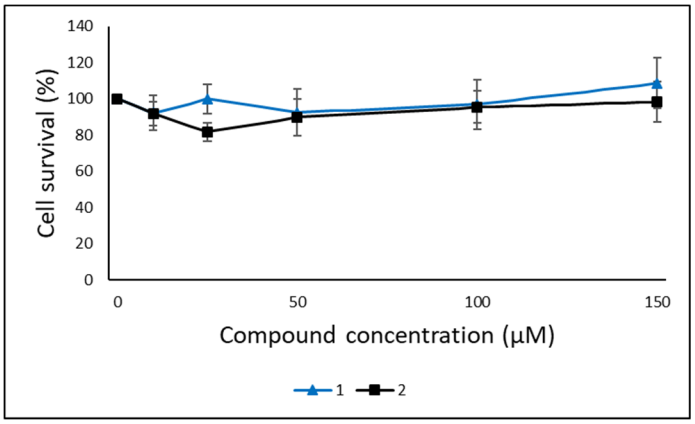

Figure S16. Cytotoxic activity of **1** and **2** was tested against non-malignant lung fibroblasts MRC-5 cells in a viability assay at 10, 25, 50, 100 and 150µM. Three experiments were conducted, one with three replicates (test concentration 25 µM was not used in this setup) and two with four replicates.

Paper III

frontiers in Microbiology

ORIGINAL RESEARCH
published: 01 October 2021
doi: 10.3389/fmicb.2021.730740

Lulworthinone, a New Dimeric Naphthopyrone From a Marine Fungus in the Family Lulworthiaceae With Antibacterial Activity Against Clinical Methicillin-Resistant *Staphylococcus aureus* Isolates

Marte Jenssen[1], Philip Rainsford[2], Eric Juskewitz[3], Jeanette H. Andersen[1], Espen H. Hansen[1], Johan Isaksson[2], Teppo Rämä[1] and Kine Ø. Hansen[1]*

[1] Marbio, The Norwegian College of Fishery Science, Faculty of Biosciences, Fisheries and Economics, UiT the Arctic University of Norway, Tromsø, Norway, [2] Department of Chemistry, Faculty of Science and Technology, UiT the Arctic University of Norway, Tromsø, Norway, [3] Research Group for Host Microbe Interactions, Department of Medical Biology, Faculty of Health Sciences, UiT the Arctic University of Norway, Tromsø, Norway

OPEN ACCESS

Edited by:
Carolina Elena Girometta, University of Pavia, Italy

Reviewed by:
Susan Semple, University of South Australia, Australia
Adelaide Almeida, University of Aveiro, Portugal

***Correspondence:**
Marte Jenssen
marte.jenssen@uit.no

Specialty section:
This article was submitted to Microbiotechnology, a section of the journal Frontiers in Microbiology

Received: *25 June 2021*
Accepted: *06 September 2021*
Published: *01 October 2021*

Citation:
Jenssen M, Rainsford P, Juskewitz E, Andersen JH, Hansen EH, Isaksson J, Rämä T and Hansen KØ (2021) Lulworthinone, a New Dimeric Naphthopyrone From a Marine Fungus in the Family Lulworthiaceae With Antibacterial Activity Against Clinical Methicillin-Resistant Staphylococcus aureus Isolates. Front. Microbiol. 12:730740. doi: 10.3389/fmicb.2021.730740

The emergence of drug-resistant bacteria is increasing rapidly in all parts of the world, and the need for new antibiotics is urgent. In our continuous search for new antimicrobial molecules from under-investigated Arctic marine microorganisms, a marine fungus belonging to the family Lulworthiaceae (Lulworthiales, Sordariomycetes, and Ascomycota) was studied. The fungus was isolated from driftwood, cultivated in liquid medium, and studied for its potential for producing antibacterial compounds. Through bioactivity-guided isolation, a novel sulfated biarylic naphtho-α-pyrone dimer was isolated, and its structure was elucidated by spectroscopic methods, including 1D and 2D NMR and HRMS. The compound, named lulworthinone (**1**), showed antibacterial activity against reference strains of *Staphylococcus aureus* and *Streptococcus agalactiae*, as well as several clinical MRSA isolates with MICs in the 1.56–6.25 μg/ml range. The compound also had antiproliferative activity against human melanoma, hepatocellular carcinoma, and non-malignant lung fibroblast cell lines, with IC_{50} values of 15.5, 27, and 32 μg/ml, respectively. Inhibition of bacterial biofilm formation was observed, but no eradication of established biofilm could be detected. No antifungal activity was observed against *Candida albicans*. During the isolation of **1**, the compound was observed to convert into a structural isomer, **2**, under acidic conditions. As **1** and **2** have high structural similarity, NMR data acquired for **2** were used to aid in the structure elucidation of **1**. To the best of our knowledge, lulworthinone (**1**) represents the first new bioactive secondary metabolite isolated from the marine fungal order Lulworthiales.

Keywords: antibacterial, marine fungi *sensu stricto*, Lulworthiales, lulworthinone, MRSA, natural product, mycology, natural product artifact

INTRODUCTION

Antimicrobial resistance is quickly developing as a worldwide threat, causing problems not only in the general community but also in healthcare facilities. Infections caused by methicillin-resistant *Staphylococcus aureus* (MRSA) has become a worldwide health menace (WHO, 2014). There is an urgent need to develop new antibiotics to fight these resistant microbes. The fungal kingdom has historically played an important role in the discovery and development of antibiotics and other drugs against non-infective diseases (Demain, 2014). The penicillins and cephalosporins are examples of important antibiotics isolated from fungi (Demain, 2014), from the genera *Penicillium* and *Sarocladium* (one syn. *Cephalosporium*), respectively. In marine natural product discovery, the genera *Aspergillus* and *Penicillium* have proven to be the most prolific producers of new compounds with biological activities (Imhoff, 2016). As the focus of marine natural product discovery has been on mold fungi belonging to the few genera mentioned above, the strictly marine clades of fungi remain understudied (Overy et al., 2014).

One of the understudied marine clades include the fungal order Lulworthiales from which no secondary metabolites have been reported since the discovery of the type genus and species, *Lulworthia fucicola*, in the beginning of the twentieth century (Sutherland, 1915). The order Lulworthiales was established in 2000 to accommodate the new family Lulworthiaceae in the class Sordariomycetes (Kohlmeyer et al., 2000). More recently, a new subclass, Lulworthiomycetidae, was described containing the orders Lulworthiales and Koralionastetales (Maharachchikumbura et al., 2015). Lulworthiaceae is the sole family in the Lulworthiales order, and Lulworthiaceae spp. are regarded as strictly marine species, which include the following genera: *Cumulospora*, *Halazoon*, *Hydea*, *Kohlmeyerella*, *Lulwoana*, *Lulworthia*, *Lindra*, *Matsusporium*, and *Moleospora* (Poli et al., 2020). Recently, a novel genus was introduced to the Lulworthiaceae, *Paralulworthia*, with two new species described, *Paralulworthia gigaspora* and *Paralulworthia posidoniae* (Poli et al., 2020). Hyde et al. (2020) also included the following genera in the family: *Haloguignardia*, *Lolwoidea*, *Moromyces*, *Orbimyces*, *Rostrupiella*, and *Sammeyersia*.

Fungi in the family Lulworthiaceae have been isolated from a variety of substrates and environments. Some examples include corals (Góes-Neto et al., 2020), plants located in salt marches (Calado et al., 2019), seagrass (Poli et al., 2020), Portuguese marinas (Azevedo et al., 2017), sandy beaches of the Cozumel island in Mexico (Velez et al., 2015), brown seaweed (Zuccaro et al., 2008), and driftwood (Rämä et al., 2014). The distribution of Lulworthiales fungi in marine habitats has been studied throughout the history of marine mycology (Johnson, 1958; Kohlmeyer et al., 2000; Koch et al., 2007; Rämä et al., 2014; Azevedo et al., 2017; Góes-Neto et al., 2020), but the biosynthetic potential of these fungi has not been investigated, most likely due to the special knowledge required for their isolation (Overy et al., 2019) and low growth rates.

In this paper, we report the isolation of a new antibacterial compound, lulworthinone (**1**), from a liquid culture of a marine fungus belonging to Lulworthiaceae (isolate 067bN1.2). We elucidate the structure of **1** and study its bioactivity against prokaryotic and eukaryotic cells with focus on antibacterial activity against clinical MRSA isolates. Compound **1** represents the first secondary metabolite reported from this order of fungi, and to the best of our knowledge, the first biarylic dimeric naphtho-α-pyrone substituted with a sulfate group. Initially, the compound was isolated using preparative HPLC under acidic conditions. As this procedure caused significant wear and tear to the equipment, the isolation was switched to flash chromatography under neutral conditions. When comparing spectroscopic data from the two samples, one isolated at neutral and one at acidic conditions, structural differences were observed. It was later determined that **1** concerts into the artifact **2** under acidic conditions.

MATERIALS AND METHODS

Biological Material and Phylogenetic Analysis of Isolate 067bN1.2

The marine fungus 067bN1.2 was isolated from a dead pine (*Pinus* sp.) collected in the splash zone in Kongsfjord, Berlevåg Norway in 2010. The isolate grew from a small wooden cube plated onto agar medium (specified below) during a campaign to study wood-inhabiting fungi of 50 intertidal and sea-floor logs along the Northern Norwegian coast, where Lulworthiales was one of the five most frequent orders isolated (Rämä et al., 2014). The fungus was subcultured and DNA sequenced, and the fungus was phylogenetically placed in the Lulworthiales order (isolate TR498 represents 067bN1.2 in Rämä et al., 2014). At the time of the publication (2014), the closest match from Blast, based on a 5.8S/large ribosomal subunit (LSU) dataset, was *Lulworthia medusa* (LSU sequence: AF195637). The following primer pairs were used for the internal transcribed spacer (ITS), LSU and small ribosomal subunit (SSU) sequencing, respectively: ITS5-ITS4 (White et al., 1990), LR0R-LR5 (Vilgalys and Hester, 1990; Rehner and Samuels, 1994), and NS1-NS4 (White et al., 1990). The ITS, LSU, and SSU sequences are deposited in GenBank under the following accessions: MW377595, MW375591, and MW375590. The mycelium of the fungus was preserved on pieces of agar in 20% glycerol solution at −80°C.

To identify the isolate 067bN1.2 growing as an asexual morph in culture and determine its systematic position within the order Lulworthiales, a phylogenetic analysis was run using a dataset consisting of nrSSU, nrITS, and nrLSU sequences. The reference sequences included in the analyses were sampled based on recent phylogenetic studies focusing on Lulworthiales (Azevedo et al., 2017; Poli et al., 2020) and retrieved from Genbank (**Supplementary Table 1**). Sequences for each gene were aligned individually using the E-INS-I and G-INS-I algorithms of MAFFT v7.388 (Katoh et al., 2002; Katoh and Standley, 2013) in Geneious Prime v.11.0.4 followed by manual adjustment. The concatenated dataset consisting of SSU, 5.8S, and LSU sequences and having a length of 2,270 nt was run through PartitionFinder v2.1.1 (Lanfear et al., 2017) to test for best-fit partitioning schemes and evolutionary models with the following settings: models MrBayes, linked branch lengths, greedy search, and AIC

and BIC model selection (Lanfear et al., 2012). This suggested three partitions with varying models: symmetrical model with equal base frequencies and gamma distributed rate variation among sites without (SYM+G) and with (SYM+I+G) invariable sites and general time reversible model with variable base frequencies and gamma distributed rate variation among sites (GTR+G). A phylogenetic analysis was set up applying suggested models using Parallel-MPI MrBayes v3.2.7a with beagle, and was run for 5,000,000 generations or until average standard deviation of split frequencies was below 0.0009 with sampling each of the 2,500 generations (Ronquist et al., 2012). In addition, RAxML in Geneious v10.2.3 was run with the same partitions under GTRCAT and GTRGAMMA using rapid-bootstrapping algorithm with 2,000 replicates with search for best scoring ML tree (Stamatakis, 2006). The resulting MrBayes tree was similar to the RAxML tree, excluding some of the basal nodes within Lulworthiaceae shown as polytomies in the MrBayes tree.

Fungal Cultivation and Extraction

For the purpose of this study, the fungal isolate was plated from glycerol stock and grown on nutrient-poor malt agar with sea salts [4 g/L malt extract (Moss Malt Extrakt, Jensen & Co AS), 40 g/L sea salts (S9883, Sigma-Aldrich), 15 g/L agar (A1296, Sigma-Aldrich) and Milli-Q® H_2O] until the growth covered the entire agar plate (approximately 40 days). Milli-Q® H_2O was produced with the in-house Milli-Q® system. One-half of the agar plate covered in mycelium was used to inoculate each liquid culture, in malt medium with added sea salts (4 g/L malt extract, 40 g/L sea salts). Two cultures of 200 ml were inoculated and incubated for 107 days at static conditions and 13°C. Before the addition of resin for extraction, mycelium was taken from the culture for inoculation of another round of cultures. The second cultivation contained four cultures with 250 ml of malt extract medium supplemented with sea salts and cultivated under the same conditions for 83 days. The total culture volume used for the extraction of **1** was 1.4 L. The cultures were extracted using Diaion HP-20 resin (13607, Supelco) and methanol (20864, HPLC grade, VWR) as described previously (Kristoffersen et al., 2018; Schneider et al., 2020). The extract was dried in a rotary evaporator at 40°C under reduced pressure and stored at −20°C.

Dereplication

As part of our ongoing search for antimicrobial compounds, extracts of marine microorganisms are fractioned into six fractions using flash chromatography, as previously described (Schneider et al., 2020). When we investigated the antibacterial potential of fractions produced from several understudied marine fungi, one fraction from isolate 067bN1.2 piqued our interest due to its antibacterial activity. In the active fraction, **1** was the dominating peak. The monoisotopic mass, calculated elemental composition and fragmentation pattern of **1** was determined using UHPLC-ESI-HRMS. UHPLC-ESI-HRMS was performed with positive ionization mode, using an Acquity I-class UPLC with an Acquity UPLC C18 column (1.7 μm, 2.1 mm × 100 mm), coupled to a PDA detector and a Vion IMS QToF (all from Waters). Compounds were eluted with a gradient over 12 min, from 10 to 90% acetonitrile (LiChrosolv, 1.00029, Supelco) with 0.1% formic acid (Sigma-Aldrich) in Milli-Q H_2O and a flow rate of 0.45 ml/min. Waters UNIFI 1.9.4 Scientific Information System was used to process and analyze the data. Elemental compositions of compounds in the samples were used to search relevant databases, such as Chemspider, in order to identify known compounds. Since the calculated elemental composition gave no hits in database searches, **1** was nominated for isolation.

Isolation of 1

Initial attempts to isolate **1** was performed using mass guided preparative HPLC. This strategy proved difficult due to extensive binding of the compound to an Atlantis Prep C18 (10 μM, 10 × 250 mm) (Waters) column, leading to inefficient isolation and column contamination. The preparative system and mobile phases used were as previously described (Schneider et al., 2020). The resulting sample (referred to as compound **2**) was later used to assist in structure elucidation of compound **1**.

To avoid wear and tear of the preparative HPLC system, attempts were made to isolate **1** using flash chromatography. The dried extract was dissolved in 90% methanol, and 2 g of Diaion HP-20SS (13615, Supelco) was added before removing the solvent under reduced pressure. Flash columns were prepared as previously described (Kristoffersen et al., 2018). The column was equilibrated using 5% methanol, before the dried extract-Diaion HP-20SS mixture was applied to the top of the column (maximum 2 g of extract per round). The fractionation was performed on a Biotage SP4™ system (Biotage) with a flow rate of 12 ml/min and a stepwise gradient from 5 to 100% methanol over 32 min. The following stepwise elution method was used: methanol:water (5:95, 25:75, 50:50, 75:25, 6 min per step, resulting in 12 fractions) followed by methanol (100% over 12 min, resulting in six fractions). The MeOH fractions were analyzed using UHPLC-ESI-HRMS. In the second fraction eluting at 100% MeOH, **1** was the dominating peak and was submitted for NMR and bioactivity analysis. The sample of **1** was therefore produced by pooling the second fraction eluting at 100% MeOH from multiple rounds of flash fractionation and drying the resulting volume under reduced pressure.

Structure Elucidation of 1

The structure of **1** was established by 1D and 2D NMR experiments. NMR spectra were acquired in DMSO-d_6 and methanol-d_3 on a Bruker Avance III HD spectrometer operating at 600 MHz for protons, equipped with an inverse TCI probe cryogenically enhanced for ^{1}H, ^{13}C, and ^{2}H. All NMR spectra were acquired at 298 K, in 3-mm solvent matched Shigemi tubes using standard pulse programs for proton, carbon, HSQC, HMBC, HMQC (J = 4–5 Hz), COSY, NOESY, ROESY and 1,1-ADEQUATE experiments with gradient selection and adiabatic versions where applicable. ^{1}H/^{13}C chemical shifts were referenced to the residual solvent peak (δ_H = 2.50 PPM, δ_C = 39.52 PPM for DMSO). All data were acquired and processed using Topspin 3.5pl7 (Bruker Biospin) including the structure elucidation module CMC-se v. 2.5.1. ^{13}C prediction was done using Mestrelabs MestReNova software version 14.2.0-26256 with the Modgraph NMRPredict Desktop. Optical rotation

data were obtained using an AA-10R automatic polarimeter (Optical Activity LTD).

Lulworthinone (**1**): green colored film. $[\alpha]^{20}_{D}$ -120 ± 0.02 (*c* 0.2 DMSO). ^{1}H and ^{13}C NMR spectroscopic data, **Supplementary Table 3**. HRESIMS *m/z* 741.2204 $[M+H]^{+}$ (calculated for $C_{37}H_{41}O_{14}S$, 741.2217).

Minimal Inhibitory Concentration Determination Against Reference Bacteria

The Minimal Inhibitory Concentration (MIC) of **1** against a panel of Gram-positive and Gram-negative reference bacteria was determined by broth microdilution, at final concentrations 0.2–100 μg/ml (twofold dilution series). The experiments were performed with three technical replicates. The panel of reference bacteria consisted of the following strains: *S. aureus* (ATCC 25923), MRSA (ATCC 33591), *Escherichia coli* (ATCC 25922), *Pseudomonas aeruginosa* (ATCC 27853), *Enterococcus faecalis* (ATCC 29212), and *Streptococcus agalactiae* (ATCC 12386), all strains from LGC Standards (Teddington). Briefly, the bacteria were inoculated from freeze stock onto blood agar plates (University Hospital of North Norway) and transferred to liquid medium for overnight incubation at 37°C. *S. aureus*, *E. coli*, and *P. aeruginosa* were grown in Brain Heart Infusion medium (BHI, 53286, Sigma-Aldrich), and *E. faecalis* and *S. agalactiae* were grown in Difco™ Mueller Hinton medium (MH, 275730, BD Biosciences). After overnight incubation in the respective media, the bacteria were brought to exponential growth by addition of fresh media, and incubated to reach a turbidity of 0.5 McFarland standard. The bacteria were diluted in their respective media 1:1,000 prior to addition. Subsequently, the bacteria were added to 96-well microtiter plates at 50 μl/well. A mixture of 50 μl of autoclaved Milli-Q® H_2O and 50 μl fresh autoclaved media was used as negative control, and 50 μl of autoclaved Milli-Q® H_2O was added to 50 μl of bacteria suspension as growth control. The compound was diluted in DMSO and autoclaved Milli-Q® H_2O (highest concentration of DMSO in the assay was 0.5%), and 50 μl was added to the bacterial suspension. Final volume in the wells was 100 μl. The plates were incubated overnight at 37°C. After incubation, growth was measured by absorbance at 600 nm with 1420 Multilabel Counter VICTOR^{3}™ (Perkin Elmer). Assay controls with gentamicin in a dilution series are routinely run, as well as routine counting of CFUs for each bacterium. For the strains where the compound displayed activity, the MIC was determined with three biological replicates each containing three technical replicates (n = 9). The lowest concentration of **1** that completely inhibited the growth of the bacteria was determined as the MIC.

To investigate if **1** had a bacteriocidal or bacteriostatic effect on *S. aureus* and *S. agalactiae*, the compound was inoculated together with the bacteria, as described above, and after overnight incubation, the inoculum was plated onto agar and incubated overnight at 37°C. The experiment was done with 12.5 and 25 μg/ml concentrations of **1** in triplicate, with two biological replicates (n = 6). Inspired by Zheng et al. (2007), we tested **1**, together with reserpine (broad spectrum efflux pump inhibitor) against the Gram-negative reference strains *E. coli* and *P. aeruginosa*. The assay was conducted as described above, with reserpine (L03506, Thermo Fisher Scientific) added to a final concentration of 20 μg/ml.

Minimal Inhibitory Concentration Determination Against Clinical Bacterial Isolates

Initial testing of **1** was conducted against a panel containing clinically relevant antibiotic-resistant bacteria: Gram-positive MRSA, vancomycin-resistant *Enterococcus faecium* (VRE), and Gram-negative bacteria resistant to extended-spectrum beta-lactamases as well as carbapenemases (ESBL-Carba) (detailed information about the clinical isolates can be found in **Supplementary Table 2**). The initial testing was conducted at one concentration, 100 μg/ml.

The final antibacterial testing of **1** was executed using the five clinical MRSA isolates and the VRE isolates (**Supplementary Table 2**). The isolates were tested by broth microdilution according to the Clinical Laboratory Standard Institute (CLSI) (2012) method MO7-A9. In brief, **1** was solubilized with 100% DMSO and diluted with autoclaved Milli-Q® H_2O to prepare a 200 μg/ml working solution. The final DMSO concentration did not exceed 1% to exclude any artificial influence on the assay. The bacterial inoculum was prepared to contain 1×10^{6} CFU/ml in cationic-adjusted BBL™ Mueller-Hinton II broth (BD). The inoculum was mixed in a 1:1 ratio with the working solution of **1** (twofold dilutions, ranging from 0.2 to 100 μg/ml) for a final amount of 5×10^{5} CFU/ml in each well of a 96-well round-bottom polypropylene plate (Greiner Bio-One GmbH). Growth control (without compound) and sterility control (without bacteria) were included for each strain. Each strain was tested in three independent biological replicates with four technical replicates on consecutive days. As quality assurance for the assay, the protocol was also performed with *E. coli* ATCC 25922 using Gentamicin (Merck Life Science) as a reference antibiotic. The 96-well plates were incubated at 37°C for 24 h without shaking. The MIC values were defined as the lowest concentration of **1** resulting in no visual bacterial growth, determined by visual inspection and 600 nm absorbance measurements with CLARIOstar plate reader (BMG LABTECH).

Inhibition of Biofilm Production and Eradication of Established Biofilm

Inhibition of biofilm production by **1** of *Staphylococcus epidermidis* (ATCC 35984, LGC Standards) was determined at final concentrations 0.2–100 μg/ml (twofold dilution series). Briefly, the bacteria were inoculated from freeze stock onto blood agar plates (University Hospital of North Norway) and transferred to tryptic soy broth (TSB, 22092, Sigma-Aldrich) for overnight incubation at 37°C. The overnight cultures were subsequently diluted 1:100 in fresh TSB with 1% glucose and added to 96-well microtiter plates, 50 μl/well. Positive control was *S. epidermidis* in fresh media with glucose, and negative control was a non-biofilm producing *Staphylococcus haemolyticus* (clinical isolate 8-7A, University Hospital of North Norway) in

fresh media with glucose. The compound was diluted in DMSO and autoclaved Milli-Q® H_2O (highest concentration of DMSO in the assay was 0.5%), and 50 μl was added to the bacterial suspension. Final volume in the wells was 100 μl. The plates were incubated at 37°C overnight. Growth inhibition of the bacterium was determined by visual inspection of the plates prior to further treatment. The bacterial suspension was poured out and the biofilm was fixated by heat, before adding 70 μl of 0.1% crystal violet solution (V5265, Sigma-Aldrich) and staining for 5 min. The crystal violet solution was removed and the wells were washed with water before the plates were dried by heat. The bound crystal violet was dissolved in 70 μl of 70% ethanol, and the presence of violet color, indicating biofilm formation, was measured at 600 nm absorbance using a 1420 Multilabel Counter VICTOR^{3TM} reader. Percent biofilm formation was calculated using the equation below. The data were visualized using GraphPad Prism 8.4.2, and the built-in ROUT method was used to detect and remove outliers from the dataset (Q = 1%).

$$\text{Percent (\%) biofilm formation} = \frac{(\text{absorbance treated wells} - \text{absorbance negative control})}{(\text{absorbance positive control} - \text{absorbance negative control})} \times 100 \quad (1)$$

To determine whether **1** could eradicate biofilm established by *S. epidermidis*, a modified biofilm inhibition assay protocol was performed. Here, the bacteria were grown overnight in a microtiter plate to allow the biofilm to be established prior to the addition of **1**. After addition of **1**, the plates are incubated overnight. Following this, the biofilm was fixated and colored and results were read as stated above. The experiment was conducted once with three technical replicates with concentrations of 0.2–100 μg/ml (twofold dilution series).

Determination of Antiproliferative Activity Toward Human Cell Lines

The antiproliferative activities of **1** was evaluated against the melanoma cell line A2058 (ATCC, CRL-11147^{TM}), the hepatocellular carcinoma cell line HepG2 (ATCC, HB-8065^{TM}), and the non-malignant lung fibroblast cell line MRC5 (ATCC, CCL-171^{TM}) in a MTS *in vitro* cell proliferation assay. The compound was tested in concentrations from 6.3 to 100 μg/ml against all cell lines, with three biological replicates each containing three technical replicates (n = 9). A2058 was cultured and assayed in Dulbecco's Modified Eagle's Medium (D-MEM, D6171, Sigma-Aldrich). HepG2 was cultured and assayed in MEM Earle's (F0325, Biochrom) supplemented with 5 ml of non-essential amino acids (K0293, Biochrom) and 1 mM sodium pyruvate (L0473, Biochrom). MRC5 was cultured and assayed in MEM Eagle (M7278, Sigma-Aldrich) supplemented with 5 ml of non-essential amino acids, 1 mM sodium pyruvate, and 0.15% (w/v) sodium bicarbonate (L1713, Biochrom). In addition, all media were supplemented with 10% fetal bovine serum (FBS, S1810, Biowest), 10 μg/ml gentamicin (A2712, Biochrom), and 5 ml of glutamine stable (200 mM per 500 ml medium, X0551, Biowest). Briefly, the cells were seeded in 96-well microtiter plates (Nunclon Delta Surface, VWR) at 2,000 cells/well for A2058, 4,000 cells/well for MRC5, and 20,000 cells/well for HepG2. After incubation for 24 h in 5% CO_2 at 37°C, the media was replaced and compound was added, generating a total volume of 100 μl/well. A2058 and MRC5 were incubated for 72 h before assaying, and HepG2 for 24 h. Subsequently, 10 μl of CellTiter 96 AQueous One Solution Reagent (G358B, Promega) was added to each well and the plates were incubated for 1 h at 37°C. Following this, the absorbance was measured at 485 nm with a DTX 880 multimode detector (Beckman Coulter). Negative controls were cells assayed with their respective cell media, and positive controls were cells treated with 10% DMSO (D4540, Sigma-Aldrich). Percent cell survival was calculated using the equation below. The data were visualized using GraphPad Prism 8.4.2 and IC_{50} was calculated. The built-in ROUT method was used to detect and remove outliers from the dataset (Q = 1%).

$$\text{Percent (\%) cell survival} : \frac{(\text{absorbance treated wells} - \text{absorbance positive control})}{(\text{absorbance negative control} - \text{absorbance positive control})} \times 100 \quad (2)$$

Minimal Inhibitory Concentration Determination Against *Candida albicans*

The MIC of **1** was determined by broth microdilution against *C. albicans* (ATCC 90028, LGC Standards), at final concentrations of 0.2–100 μg/ml (twofold dilution series). The experiment was performed as one biological replicate, with three technical replicates (n = 3). Briefly, the fungus was inoculated from freeze stock onto potato dextrose agar [24 g/L potato dextrose broth (P6685, Sigma-Aldrich), 15 g/L agar (A1296, Sigma-Aldrich)] and incubated overnight at 37°C. From the overnight culture, five to eight colonies were transferred to 5 ml of sterile 0.9% NaCl, before the cell density was adjusted to 1–5 × 10^6 cells/ml by adding 0.9% NaCl. The cell density was evaluated with 0.5 McFarland standard (Remel 0.5 McFarland Equivalence Turbidity Standard, 10026732, Thermo Fisher Scientific). The fungal suspension was further diluted 1:50, and then 1:20 (1–5 × 10^3 CFU/ml) in RPMI medium (R7755, Sigma-Aldrich) with 0.165 mol/L MOPS (M3183, Sigma-Aldrich) and 10.25 ml of L-glutamine. The compound was added to the microtiter plate together with the fungal suspension (1:1), to a final volume of 200 μl. The final concentration of fungal cells was 0.5–2.5 × 10^3 CFU/ml. Absorbance in the wells was measured with 1420 Multilabel Counter VICTOR^{3TM} right after addition of compound, after 24 h and after 48 h. The plates were incubated at 37°C. Amphotericin B was used as negative control at final concentration 8 μg/ml. Growth control contained fungal suspension and autoclaved Milli-Q® H_2O.

RESULTS

Systematic Placement of the Fungal Isolate 067bN1.2

Due to lack of distinct morphological characters of the cultured asexual morph and closely related reference sequences

in GenBank, the fungus is identified to family level, as Lulworthiaceae sp., for the purpose of this study. A phylogenetic study was carried out with 28 taxa (including outgroups and isolate 067bN1.2), all representing different species, as shown in **Figure 1**. The combined dataset of 5.8S, SSU, and LSU had an aligned length of 2,270 characters, and phylogenetic inference was estimated using both Maximum Likelihood and Bayesian Inference criteria. The isolate producing **1**, 067bN1.2, was placed on its own branch within the Lulworthiaceae, forming a sister clade to the clade including *Halazoon fuscus*, *Lulworthia medusa*, *Lulworthia* cf. *purpurea* and *Halazoon melhae*. Sequences of *Koralionastes ellipticus* were included to exclude the possibility that the isolate 067bN1.2 is part of the family Koralionastetaceae. *Koralionastes ellipticus* was placed outside of Lulworthiaceae.

Isolation and Structure Elucidation

Compound **1** was selected for isolation due to its antibacterial activity in an initial screen of fractions from several understudied marine fungi. Compound **1** was the dominating peak in the active fraction from fungal isolate 067bN1.2 Lulworthiaceae sp., and subsequently the fungus was re-cultivated, cultures were extracted, and the compound was isolated using RP flash chromatography. The extraction of 1.4 L of fungal culture yielded 1,017.2 mg of extract.

Initially, attempts were made to isolate the compound using preparative HPLC. This strategy had several drawbacks, including unfavorable behavior of the compound in the preparative column. This resulted in the compound eluting over several minutes (band broadening) and carryover. A batch of the compound was, however, retrieved using this strategy, resulting in a compound later determined to be a structural isomer and artifact of compound **1** (referred to as **2** throughout this article), produced due to the acidic conditions in the mobile phase. The structures of **1** and **2** can be seen in **Figure 2**.

Flash chromatography was better suited for the isolation of **1**. This isolation strategy yielded 63.8 mg of **1**, corresponding to a yield of ∼45 mg/L culture medium. Compound **1** was obtained as a green colored substance. The molecular formula was calculated to be $C_{37}H_{40}O_{14}S$ by UHPLC-ESI-HRMS (*m/z* 741.2204 $[M+H]^+$) (calculated as $C_{37}H_{41}O_{14}S$, 741.2217), suggesting 18 degrees of unsaturation. The low-energy collision mass spectrum of **1** can be seen in **Supplementary Figure 2**. MS signals of a neutral loss of 80 Da (ESI+) was observed, indicating the presence of a sulfate group in the structure. The UV absorption maxima were 224, 260, and 373 nm, which corresponded well with the previously published dinapinones (Kawaguchi et al., 2013). The UV-vis spectrum for **1** can be seen in **Supplementary Figure 3**. The IR spectrum of **1** displayed absorption bands for sulfoxide (S=O, 1,002 cm^{-1}), aromatic alkene (C=C, 1542 and 1,618 cm^{-1}), carbonyl (C=O, 1,645 cm^{-1}), alkane (C-H, 2,857 cm^{-1}), aromatic alkene (C-H, 2926 cm^{-1}), and hydroxyl (C-OH, 3455 cm^{-1}) bonds. After isolation, the structure of **1** (**Figure 2**) was elucidated by 1D and 2D NMR experiments (**Supplementary Figures 4–16**).

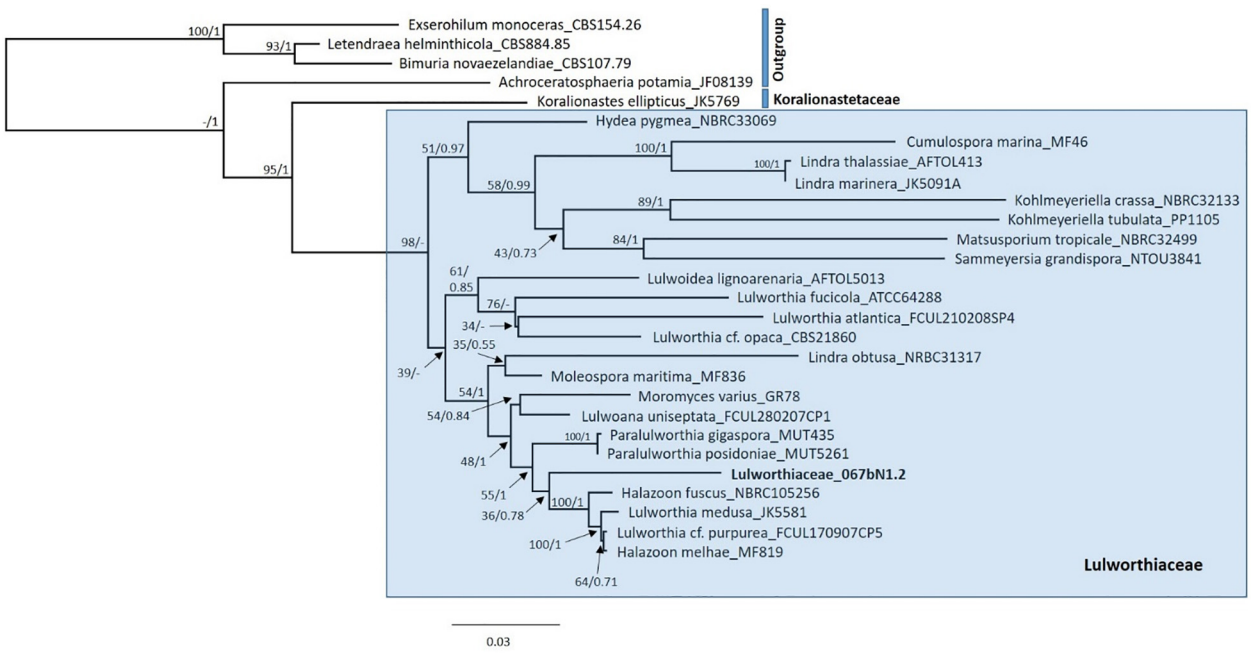

FIGURE 1 | Maximum Likelihood tree (RAxML) from the combined analysis of 5.8S, SSU, and LSU from isolates of Lulworthiaceae. One isolate from Koralionastetaceae was included, and four strains as outgroups. Node support is given as Bootstrap support values at the nodes, and posterior probabilities are included where the branching was alike (BS/PP). The isolate under investigation, Lulwortihaceae_067bN1.2, is highlighted in bold. Due to topological similarity only the ML tree is shown here containing both Bayesian posterior probabilities and Bootstrap support values. Bayesian Inference tree can be found in **Supplementary Figure 1**. – indicates that the node is missing in the Bayesian analysis. No support value is given to the node separating the outgroup taxa from the ingroup in ML analysis.

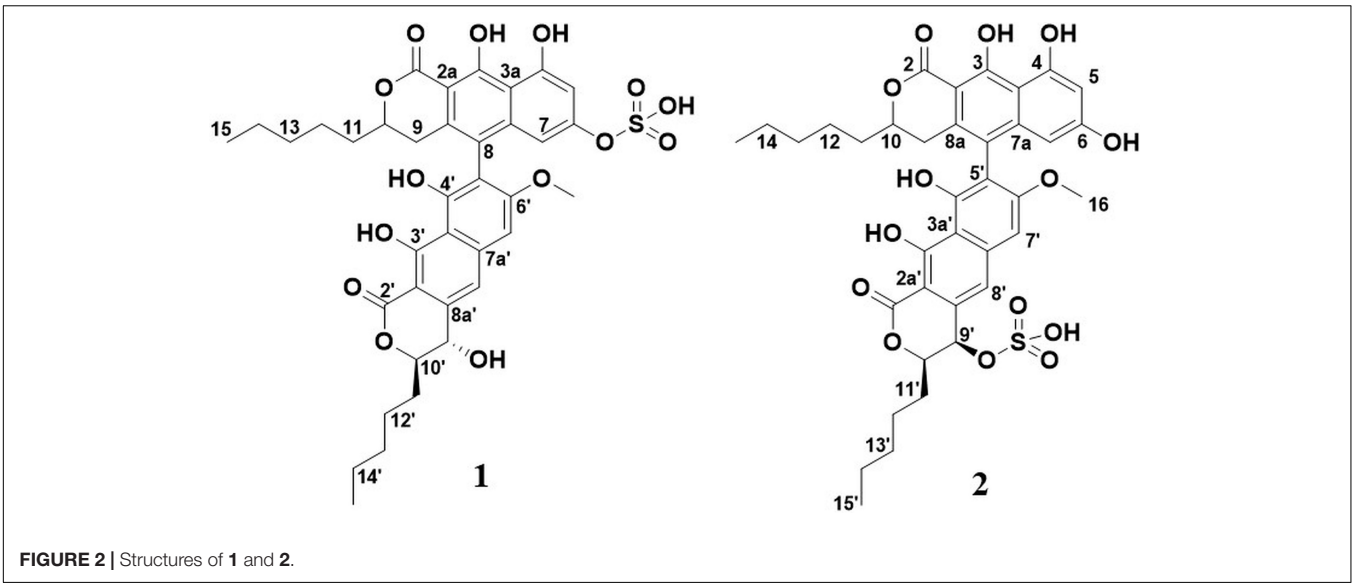

FIGURE 2 | Structures of **1** and **2**.

Initial structure elucidation was made on the sample isolated by preparative HPLC with formic acid present in the mobile phases (compound **2**). The established molecular formula suggested a highly conjugated system. The purity of **2** was estimated to be ∼80% from a quantitative proton spectrum with respect to non-solvent impurities (**Supplementary Figure 4**). Four singlet protons were identified in the aromatic region, along with three O-CH signals at ∼4.5 ppm with complex couplings along with a methoxy singlet at 3.77 ppm. Furthermore, five hydroxyl protons were identified; three between 9.5 and 10.0 ppm, and two between 13.5 and 14.0 ppm. The deshielded nature of the latter sets them apart from the other hydroxyls and suggests they may be involved in an angled intramolecular hydrogen bond, which is commonly seen for keto-enol pair configurations such as this. All 37 carbons could be identified by 1D ^{13}C NMR (**Supplementary Figure 5**), which showed **2** to contain a large number of aromatic quaternary carbons, two ester-like carbonyls, along with 10 peaks in the aliphatic region (**Table 1**).

HSQC, HMBC, and 1,1-ADEQUATE spectra (**Supplementary Figures 6, 7**) allowed the identification of two substituted napthopyrone-like moieties, as well as two five-membered aliphatic chains (denoted *C15-C11* and *C15'-C11'*, respectively), which were fully assigned using a combination of HSQC-TOCSY, TOCSY, COSY, and HMBC (**Figure 3**i). The aliphatic chains were determined to be attached at the *C10* position of the napthopyrone-like moieties by tracing the spin system into *H9* and *H9'*, respectively, and supported by multiple long-range ^{1}H-^{13}C correlations. The *C2* and *C2'* carbonyls could be directly assigned from long-range couplings from the *10*/*10'* position, but the hydroxyl carrying carbons in positions *3/3'* and *4/4'* could only be assigned through weak $^{4}J_{CH}$ correlations from the aromatic protons (**Figure 3**iii).

The *OH-4* and *OH-6* could be assigned based on NOE correlations between *OH-6* and both *H5* and *H7*, while *OH-4* only displayed correlations with *H5*. The *OH-3* and *OH-3'* are predicted to have more deshielded chemical shifts due to their proximity to the carbonyl moiety and a probable intramolecular hydrogen bond—however, it was not possible to individually distinguish *OH3* and *OH-3'* due to the absence of any correlations in NOESY, ROESY, and HMBC spectra. Thus, four fragments could initially be elucidated (**Figure 3**i). A weak $^{4}J_{C8H7'}$ correlation could be detected, linking fragment ***A*** to fragment ***B*** (**Figure 3**i) at the *C8* and *C5'* positions, respectively, and thus the only remaining ambiguity is the position of the -SO^{3-} group vis-à-vis the remaining -OH in the 9' or 4' positions. The absence of NOEs and COSY correlations between *OH-4'* and *H9'* suggests that it is positioned at *C4'* with the sulfate positioned at *C9'* (**Figure 3**ii). The $^{3}J_{HH}$ coupling constant between *H9'* and *H10'* was measured to be 2.0 Hz from line shape fitting the splitting of H9', indicating that these protons are at a significantly offset dihedral angle to one another—thus suggesting a relative R/S or S/R configuration of 9' and 10'. ^{13}C prediction was consistent with the structure of **2** (**Supplementary Figure 9**), with a mean error of 2.79 ppm between the observed and predicted ^{13}C shifts.

A second isolation where no acidic conditions were used, yielding **1**, was also examined. ^{1}H NMR revealed significantly perturbed chemical shifts as well as line broadening and heterogeneity throughout the spectra (**Supplementary Figure 11**). Multiple resonances in the carbon spectrum (**Supplementary Figures 12, 13**), especially for two resonances in the carbonyl area (presumably C3 and C3'), are heterogenous, reflecting the nuclei existing in several stable, but slightly different micro environments. The same observation is made in the proton spectrum (**Supplementary Figure 11**) for H9', OMe-6', H5, H7, 4'-OH, and 4-OH. A major difference was observed in the non-acidic preparation (**1**), compared to **2**, the presence of a 9'-OH. At ∼15 ppm, two heterogeneous OH protons were observed, deshielded by approximately 1 ppm compared to the OH-3's in the original sample preparation, while the three hydroxyls at ∼10 ppm could no longer be detected (**Supplementary Figures 8–13**). Thus, the detectable aromatic hydroxyl groups, identified as OH-4' and OH-4,

TABLE 1 | Summary of chemical shift and correlations for **2** (DMSO-d_6).

Position	δ^{13}C, type	δ^{1}H, splitting (Hz)	COSY	HMBC (^{1}H → ^{13}C)
2	171.6, C	–	–	–
2'	171.0, C	–	–	–
2a'	99.4, C	–	–	–
2a	99.2, C	–	–	–
3	162.5, C	–	–	–
3'	161.5, C	–	–	–
3a'	108.6, C	–	–	–
3a	107.5, C	–	–	–
4	159.0, C	–	–	–
4'	154.9, C	–	–	–
5'	111.7, C	–	–	–
5	102.1, CH	6.35, s	–	3, 3a, 4, 6, 7
6	161.2, C	–	–	–
6'	160.7, C	–	–	–
7a	140.6, C	–	–	–
7a'	140.1, C	–	–	–
7	100.7, CH	6.04, s	–	3, 3a, 5, 6, 8
7'	99.7, CH	7.14, s	–	3', 3a', 4', 5', 6', 8, 8'
8a'	137.4, C	–	–	–
8a	132.9, C	–	–	–
8	118.7, C	–	–	–
8'	117.5, CH	7.36, s	–	2', 3a', 4', 6', 7'a, 7', 9'
9'	65.3, CH	4.69, d (*J* = 2.0)	–	2a', 8', 8a', 10', 11'
9	31.0, CH2	2.59, m	10	2a, 7a, 8, 8a, 10, 11
10'	83.2, CH	4.62, ddd (*J* = 7.9, 6.0, 2.0)	11'	2', 8a', 9', 11', 12'
10	79.4, CH	4.56, dddd (*J* = 9.6, 7.4, 5.5, 4.1)	9, 11	2, 8a, 12
11	34.2, CH2	1.59, dd (*J* = 16.7, 9.5) 1.68, dd (*J* = 16.5, 4.0)	10, 12	10, 12
11'	30.0, CH2	1.85, m	10', 12'	9', 10', 12', 13'
12'	24.7, CH2	1.48, 1.52, m	11', 13'	11', 13', 14'
12	24.5, CH2	1.27, 1.36, m	11, 13	11, 13, 14
13'	31.3, CH2	1.23, m	12', 14'	11', 12', 14', 15'
13	31.6, CH2	1.36, m	12, 14	11, 12, 14, 15
14'	22.5, CH2	1.36, m	13', 15'	12', 13', 15'
14	22.4, CH2	1.24, m	15	12, 13, 15
15'	14.4, CH3	0.92, m	14'	13', 14'
15	14.3, CH3	0.82, m	14	13, 14
16	56.5, O-CH3	3.77, s	–	6'
OH3*	–	13.71, s		
OH3*	–	13.62, s		
OH4	–	9.80, s		
OH4'	–	9.51, s		
OH6	–	9.94, s		

**Ambiguous assignment.*

appeared to be involved in (stronger) hydrogen bonding, while three aromatic hydroxyls, the remaining OH-6, OH-3' and OH-3, were unaccounted for. At the same time, the majority of all other nuclei in the molecule are shielded by approximately 0.5 ppm. Together, these observations suggest that the neutral pH preparation resulted in a different molecule, **1**, that formed loose aggregates in DMSO and methanol, stabilized by both hydrogen bonding (deshielding) and stacking (shielding) interactions. Overall, worse spectral quality resulted in that the C2 and C3 from **2** could not be individually assigned in **1**, although they must correspond to the two chemical shifts of 169.4 and 173 ppm by the logic of elimination. A number of the carbons show heterogenic peaks (notably the presumed C3 and C3'), most likely as the result of through space proximity to the sulfate group and sensitivity to its different possible conformation (details in section "Discussion").

The identity of **1** was established to be identical to **2** with the only difference being that the sulfate group was attached to C6 instead of C9', supported by the loss of the OH correlating with H5 and H7, and the appearance of an OH

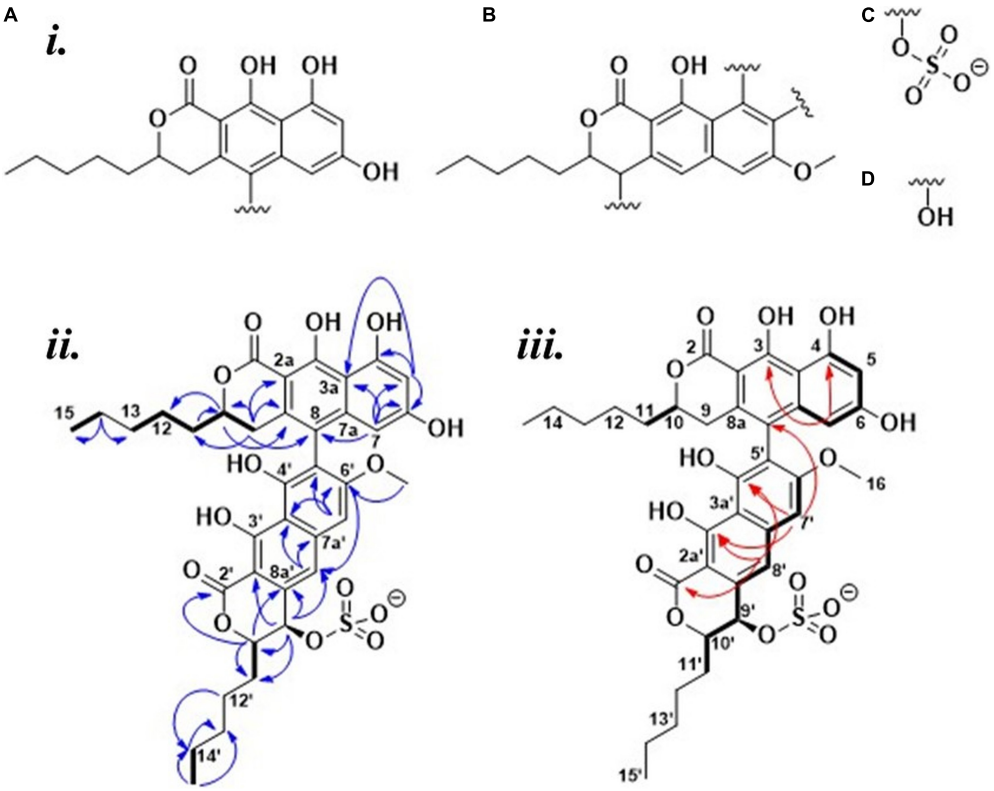

FIGURE 3 | (*i*) Fragments identified for **2**: **(A,B)** The napthopyrone-like moieties; **(C)** a sulfate group; **(D)** a spare hydroxyl group. (*ii*) Elucidated structure of **2**: Bold bonds = COSY, blue arrows = HMBC, and (*iii*) red arrows = weak $^{4}J_{CH}$ correlations, Bold bonds = 1,1-ADEQUATE.

correlating with H9' through a $^{3}J_{HH}$. There is furthermore a heterogeneity and chemical shift perturbation hotspot (vis-à-vis **2**) around the C6 position to support the assignment of a C6 sulfate. All chemical shifts and correlations are summarized in **Supplementary Table 3**. The data do not unambiguously prove whether the 3-OH's are deprotonated or if the signal is lost due to rapid exchange, but the fact that the OH-9' is observable under the same conditions is an indicium for the OH-3's to be deprotonated in **1**. No plausible resonance structures to explain the deprotonation and deshielding that does not involve the oxidation, and thus change in mass, have been found.

The non-aggregated **2** could be scavenged by lowering the pH of **1** with the addition of hydrochloric acid, upon which ^{1}H and HSQC spectra of the two samples of **2** show a great resemblance (**Supplementary Figure 10**). The molecular formula of **2** and **1** as well as the scavenged **2** were identical in the two preparations, as no change in mass was observed by high-resolution mass spectrometry.

Antibacterial Activity Against Reference and Clinical Strains

Compound **1** was tested against six reference bacteria (four Gram-positive and two Gram-negative strains). The compound was active against two of the Gram-positive reference strains, *S. aureus* and *S. agalactiae*, with MIC values of 6.25 and 12.5 μg/ml, respectively. No activity was observed against the Gram-negative strains, *E. coli* and *P. aeruginosa*, or the Gram-positive *E. faecalis* or MRSA strain (**Supplementary Table 4**). As bacterial resistance toward available antibiotics is the main challenge in future treatment of pathogenic diseases, **1** was tested against a panel of drug-resistant clinical strains (**Supplementary Table 2**). The panel included five MRSA and six VRE strains. Compound **1** was also tested in a pre-screen against four Gram-negative clinical bacterial strains: *E. coli*, *Klebsiella pneumoniae*, *Acinetobacter baumanii*, and *P. aeruginosa* (all ESBL-Carba). No activity was detected against the Gram-negative bacteria (**Supplementary Table 4**). Compound **1** showed activity against the MRSA strains with MICs in the 1.56–6.25 μg/ml (2.12–8.44 μM) range, see **Table 2**. The activity of the compound was significantly less profound against the VRE strains (MIC = 50 μg/ml or higher) (**Supplementary Table 4**).

To investigate if **1** has bacteriostatic or bacteriocidal effects on the two reference strains *S. aureus* and *S. agalactiae*, both were incubated with the compound at 12.5 and 25 μg/ml overnight and subsequently plated onto agar. For *S. aureus*, there was no growth on the plates after overnight incubation, indicating a bacteriocidal effect of **1**. For *S. agalactiae*, one of the parallels at 12.5 μg/ml (MIC of **1** against this bacterium) displayed growth on the agar plate, which was expected as visual growth could also be seen in the microtiter plate for this parallel. The remaining five parallels at this concentration, and the concentration above,

had no growth in the microtiter plates, or on agar after overnight incubation. This strongly indicates that **1** also has bacteriocidal effect on *S. agalactiae*. Compound **1** was also tested together with the efflux pump inhibitor reserpine to see if the lack of activity toward Gram-negative strains was caused by efflux of **1**, but no activity was obtained.

Inhibition of Biofilm Production and Eradication of Established Biofilm

The ability of **1** to inhibit biofilm production by *S. epidermidis* and to remove established *S. epidermidis* biofilm was assessed. In the biofilm inhibition assay, the biofilm production was completely inhibited (below 5% biofilm formation) down to 12.5 μg/ml (**Figure 4**). Clear inhibition of the bacterial growth could also be observed to 25 μg/ml by visual inspection of plates before fixation of biofilm, raising the question if the biofilm inhibition is mainly caused by growth inhibition of the bacterium. To further evaluate the potential biofilm activity, removal of established biofilm was assessed. There was no activity of **1** at concentrations up to 100 μg/ml against the established biofilm, further supporting the hypothesis that the biofilm inhibition is mainly due to growth inhibition of the bacterium.

TABLE 2 | Minimal inhibitory concentrations (MICs) of **1** against reference strains and clinical isolates.

Strain type	Strain	MIC in μg/ml
Clinical strains	*S. aureus* N315	1.56
	S. aureus 85/2082	3.13
	S. aureus NCTC 10442	3.13
	S. aureus WIS [WBG8318]	6.25
	S. aureus IHT 99040	3.13
Reference strains	*S. aureus* ATCC® 25923	6.25
	S. agalactiae ATCC® 12386	12.5

The median MIC values are reported (n = 12 for clinical isolates, n = 9 for reference strains).

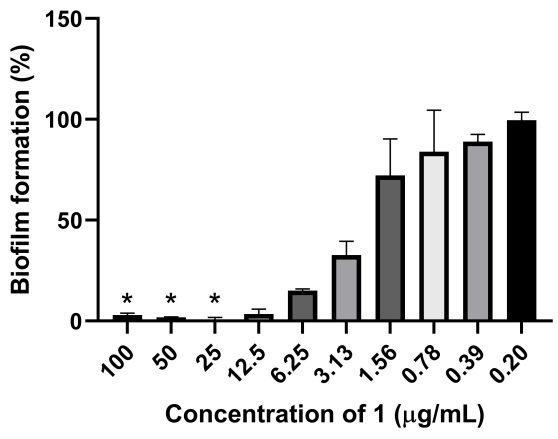

FIGURE 4 | Inhibition of bacterial biofilm formation by **1** against the biofilm producing *S. epidermidis*. *The bacterial growth was completely inhibited at compound concentrations down to 25 μg/ml.

Antiproliferative Activity Against Human Cells and Antifungal Activity

The antiproliferative activities of **1** was assessed against human melanoma cells (A2058), human non-malignant lung fibroblasts (MRC5), and human hepatocellular carcinoma cells (HepG2), in a concentration range of 6.25–100 μg/ml. The non-malignant cell line was included as a test for general toxicity, while the other cell line was included to assess possible anti-cancer activities. Antiproliferative activity was observed against all cell lines, with IC_{50} values of 15.5, 32, and 27 μg/ml against A2058, MRC5, and HepG2, respectively (**Table 3**). Compound **1** was also assayed for antifungal activity against *C. albicans* at concentrations up to 100 μg/ml, and no activity was seen.

DISCUSSION

In this study, we describe the discovery, isolation, and characterization of the new secondary metabolite lulworthinone (**1**). This novel antibacterial compound was isolated from an extract of a slow-growing marine fungus of the family Lulworthiaceae. To the best of our knowledge, this is the first reported secondary metabolite isolated from this fungal family and the order Lulworthiales. Since the isolate did not branch close to the *Lulworthia* type species, *L. fucicola* (in the *Lulworthia sensu stricto* clade) and there was a lack of support at many nodes of the phylogenetic tree, we restrained from identifying the isolate 067bN1.2 to genus and determine its identity to family level only.

A fraction of the Lulworthiaceae sp. extract was nominated for chemical investigation as it was active in an initial antibacterial screen. The content of the active Lulworthiaceae sp. fraction was dominated by **1**, whose calculated elemental composition gave no hits in database searches, indicating that the compound suspected to be responsible for the observed antibacterial activity, was novel. In the attempt to utilize preparative HPLC to isolate this compound, **2** was generated during the procedure (acidic mobile phase). As compounds **1** and **2** have the same mass, HRMS analysis did not detect the change in the positioning of the sulfate group, and the sample from the preparative HPLC isolation was characterized using NMR, believing it was **1**. As preparative HPLC was deemed inconvenient for compound isolation, flash chromatography (neutral mobile phase) was utilized to isolate sufficient amounts of **1** to conduct a thorough characterization of the compound's bioactivity. This method allows larger amounts of sample to be processed per run, but generally is less effective in separating compounds of interest from sample impurities, compared to preparative HPLC isolation. However, due to the high concentration of **1** in the extract, **1** was successfully isolated using this method. The resulting sample was submitted

TABLE 3 | Antiproliferative activity (IC_{50}) of **1** against human cell lines (*n* = 9).

Cell type	IC_{50} in μg/ml
A2058, melanoma	15.5 ± 0.6
MRC5, normal lung fibroblasts	32 ± 1
HepG2, hepatocellular carcinoma	27 ± 1

to NMR analysis to confirm its structure. The samples from both isolations were confirmed to be novel biarylic dimeric naphtho-α-pyrones substituted with a sulfate group. However, NMR analysis revealed that the sulfate group was located on different positions in the two compounds. The rearrangement was hypothesized to be catalyzed by the acidic nature of the HPLC mobile phase. This hypothesis was confirmed by subjecting **1** to acidic conditions (**Supplementary Figure 10**). The resulting sample was analyzed using NMR, confirming that **1** had indeed converted into **2**. As **2** was proven to be an artifact of **1**, all bioactivity testing was conducted using **1** isolated under neutral conditions.

The propensity of **1** to interact with itself to form higher-ordered structures, while **2** did not, offered some insight into their structural behavior in solution. In particular, the sulfate in the 6-position appeared to facilitate oligomeric aggregation, and a simple 3D model allows some speculation as to why this could be (**Figure 5**). The ground state of the naphthopyrone does not have the ability to form complementary "base pairs" with itself through hydrogen bonds between the carbonyls and hydroxyls. However, when the sulfate is in the 6-position, it can reach the C3 double OH "mismatch" in the three-dimensional structure and potentially stabilize the hydroxyls either by 4-coordnating a water molecule or a Na^+ ion together with deprotonated 3'-hydroxyls, or by directly hydrogen bonding to the protonated hydroxyls. This would provide a feasible rationale for the propensity for aggregation of **1** but not of **2**. The structural dimer model also provides a plausible explanation as to why the sulfate group would specifically and irreversibly migrate to C9' under acidic conditions even though the C9' is expected to be a less likely position for the sulfate than any other phenol position. The sulfate is in an oligomeric state involving this kind of "base pairing" positioned to be intermolecularly attacked by the OH-9' of the paired molecule, which is not possible in the monomeric state. Lowered pH is expected to ensure protonated sulfate, which would make it more susceptible for an electrophilic attack from OH-9'. If oligomeric states are indeed stabilized by the coordination of water or sodium, then lowered pH and the protonation of the 3- and 3'-oxygens would further destabilize the oligomer, which together with the lack of stabilization from the position 6 sulfate would make both the association and the reaction irreversible and trap the sulfate in the 9' position of monomeric **2** with lowered ability to self-aggregate.

Lulworthia spp. fungi have spores with end chambers containing mucus, which helps in spore attachment to surfaces (Jones, 1994). It has been observed that in liquid culture of the isolate 067bN1.2, the fungus forms a gel-like mucus, having the ability to adhere to the bottom of the culture flasks. No spores are formed in culture, and it remains unclear whether the mucus formed under cultivation of 067bN1.2 has chemical resemblance

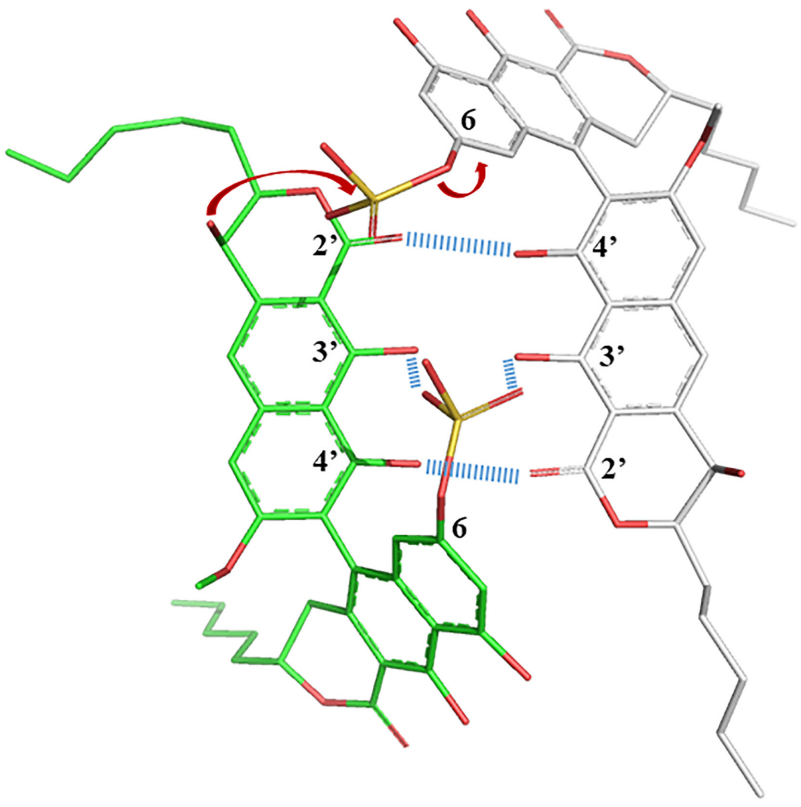

FIGURE 5 | Crude sculpted and minimized structural model of **1** displaying the sulfate potential role in stabilizing oligomerization, as well as the possibility to intermolecularly react specifically at the C-9' position to form **2** under acidic conditions.

to the mucus in end chambers of *Lulworthia* spp. spores, as it has not yet been characterized. The sheathing of mucoid by *L. medusa* has been reported in a publication from 1973, where the fungus was found and isolated from a piece of submerged pine and cultivated in bottles in media supplemented with artificial seawater (Davidson, 1973). Also in the current study, the fungus was found to adhere to the culture flask during cultivation in artificial seawater media. Davidson hypothesizes around the physiological and ecological implications of the mucoid, important in cation binding and transport, for the adhesion of other microorganisms, avoiding desiccation in intertidal regions or for the production of a matrix to concentrate exoenzymes (Davidson, 1973). Compound **1** is isolated in high yields from the fungal culture, but the ecological role of naphthopyrone-type compounds is largely unclear. The antibacterial activity of **1**, however, could indicate a protective role against pathogenic attacks, but the compound may have other types of bioactivities as well. It has been speculated that similar compounds (bis-naphthopyrones) from filamentous ascomycetes were produced to protect the fungus from predators (Xu et al., 2019). The study found that several animal predators, like woodlice, preferred feeding on fungi that had disrupted aurofusarin synthesis, and also that predation stimulated the production of aurofusarin in several *Fusarium* species (Xu et al., 2019). We have also observed marine mites feeding on fruitbody contents of Lulworthiales fungi. It is thus possible that in the natural habitat of these fungi, the naphthopyrones are produced as a means of protection.

Compound **1** was found to be a dimeric biarylic naphtho-α-pyrone substituted with a sulfate group. The naphthopyrone moiety is recurring in nature, as monomers, dimers, and trimers, and has been found from several natural sources, like plants and filamentous fungi. Naphthopyrones have also previously been isolated from organisms from the marine environment (Li et al., 2016). Compounds from this class have shown different bioactivities, among these the inhibition of triacylglycerol synthesis (Kawaguchi et al., 2013), inhibition of enzymatic activity (Zheng et al., 2007), protection against animal predators (Xu et al., 2019), antimalarial activities (Isaka et al., 2010), and antiproliferative activities (Isaka et al., 2010; Li et al., 2016). Several of these compounds have displayed antibacterial activities against Gram-positive bacteria (Suzuki et al., 1992; Wang et al., 2003; Zheng et al., 2007; Boudesocque-Delaye et al., 2015; Rivera-Chavez et al., 2019). Lu et al. (2014) defined three groups of bis-naphtho-γ-pyrones based on the diaryl bond connection between the monomers, the chaetochromin-, asperpyrone-, and nigerone-type bis-naphtho-γ-pyrones. Based on this categorization, **1** would be categorized as an asperpyrone-type bis-naphtho-α-pyrone, due to the relative placement of the oxygen atoms in the pyrone moieties. Compound **1** is substituted with a sulfate group. One of the most abundant elements in seawater is sulfur, and many sulfated compounds have been isolated from marine organisms, mostly from marine invertebrates, but also from microorganisms (Kornprobst et al., 1998; Francisca et al., 2018). Compound **1** represents, however, the first report of a dimeric naphtho-α-pyrone substituted with a sulfate group.

In the current study, **1** was broadly assessed for potential bioactivities: antibacterial activities against bacterial reference strains and clinical strains, antiproliferative activities toward a selection of human cell lines, both malignant and non-malignant, anti-fungal activity, inhibition of bacterial biofilm formation, and the eradication of established bacterial biofilm. Intriguingly, **1** showed activity against multidrug-resistant MRSA strains with MICs between 1.56 and 6.25 μg/ml (2.12–8.44 μM). In comparison, a natural product originally isolated from *Clitophilus scyphoides* (organism name at time of isolation: *Pleurotus mutilus*, Basidiomycota) pleuromutilin showed MICs in a similar range against selected reference strains (e.g., MIC = 0.66 μM against *S. aureus*, MIC = 2.64 μM against *K. pneumoniae*, and MIC = 21.13 μM against *B. subtilis*) while having significantly higher MIC values against other reference strains (e.g., MIC ≥ 100 μM against *P. aeruginosa*) (Kavanagh et al., 1951). An optimized analog of pleuromutilin, lefamulin (Xenleta®), was approved as an antibiotic drug by the US Food and Drug Administration in 2019. The herein reported MIC values thus place **1** in an activity segment, which makes it an interesting candidate for further development toward becoming a marketed antibiotic drug. In comparison to other antibacterial napthopyrones, **1** falls within the same MIC range with regard to activity toward Gram-positive bacteria. Two heterodimers, isolated from the tubers of *Pyrenacantha kaurabassana*, showed antibacterial activity against different strains of *S. aureus* with MICs in the range of 2.7–89.9 μM (Boudesocque-Delaye et al., 2015). In a recent paper from 2019, mycopyranone, a new binaphthopyranone, was isolated from the fermentation broth of *Phialemoniopsis*. The compound showed antibacterial activity against both *S. aureus* and a MRSA strain, with MICs of ≤8.7 μM against both strains (Rivera-Chavez et al., 2019). Possibly the most known naphthopyrone, viriditoxin showed MICs in the 4–8 μg/ml range against different *Staphylococcus* isolates (Wang et al., 2003).

Furthermore, the lack of activity against the Gram-negative reference and clinical strains shows the selectivity of **1** against Gram-positive bacteria. Yet, no activity or weak activity was observed against the clinical VRE isolates and the reference strain of *E. faecalis*, indicating that the activity is selective toward groups of Gram-positives, in this case *S. aureus* and *S. agalactiae*. Surprisingly, no activity was observed against the reference MRSA strain, and the reason behind this is not clear. No activity was observed for the combination of **1** and the efflux pump inhibitor reserpine, indicating that the lack of susceptibility by Gram-negatives is caused by another mechanism. In the antiproliferative activity assay, the most potent activity of **1** was observed against the melanoma cells (IC_{50} = 15.5 μg/ml). Against the non-malignant lung fibroblasts, which were included as a test for general toxicity, the compound had an IC_{50} of 32 μg/ml, which is more than five times higher than the highest MIC value against the multidrug-resistant MRSA. The concentrations where **1** did not display any toxic effect on the cells (∼100% cell survival) were 20, 12.5, and 15 μg/ml for MRC5, A2058, and HepG2, respectively. This indicates that there is little overlap between the concentration where **1** has antibacterial activity and the concentration where toxicity occurs against the human cells.

This observed difference is a good starting point when entering structure optimization, as it indicates that production of non-toxic variants of **1** can be obtained.

We isolated 45 mg/L of **1** when the Lulworthiaceae sp. fungus was grown in liquid media supplemented with sea salts. This shows that slow-growing marine fungi *sensu stricto* can produce high yields of novel compounds for chemical characterization and screening for biological activities. Compound **1** was found to be a novel sulfated dimeric naphthopyrone, and showed potent growth inhibition of multidrug-resistant MRSA with MICs down to 1.56 μg/ml, which is much lower than the IC_{50} detected against the non-malignant cell line (32 μg/ml). This study demonstrates that the family Lulworthiaceae and order Lulworthiales have biosynthetic potential to produce bioactive secondary metabolites and supports the view of Overy et al. (2014) that marine fungi *sensu stricto* should be studied for natural product discovery, despite their slow growth (Overy et al., 2014). Our study highlights the potential role of marine fungi *sensu stricto* in tackling the worldwide AMR crisis.

DATA AVAILABILITY STATEMENT

The datasets presented in this study can be found in online repositories. The names of the repository/repositories and accession number(s) can be found in the article/ **Supplementary Material**.

AUTHOR CONTRIBUTIONS

MJ was responsible for conducting experiments, data analysis, and writing and revising the draft manuscript. PR and JI were responsible for the NMR analysis of the compound and the writing related to this. EJ conducted the antibacterial testing against the clinical bacterial isolates and wrote this section in the "Materials and Methods," and contributed to the writing of the MIC results. KH assisted in writing and revision of the manuscript and contributed to the experiment design. TR did the initial isolation of the fungus and the phylogenetic analysis, contributed to the experiment design by selecting this fungus for the study, and revised the manuscript. JA and EH contributed to the conceptualization of the work, supervised the work, and revised the manuscript. All authors reviewed and approved the final manuscript.

FUNDING

This project received funding from the DigiBiotics project of the Research Council of Norway (project ID 269425), the AntiBioSpec project of UiT the Arctic University of Norway (Cristin ID 20161326), and the Centre for New Antibacterial Strategies at UiT the Arctic University of Norway (TR). The publication charges for this article have been funded by the publication fund of UiT the Arctic University of Norway.

ACKNOWLEDGMENTS

We would like to acknowledge the technical support by Kirsti Helland and Marte Albrigtsen by execution of the bioactivity assays, the contribution of Chun Li in the work with the sequencing of the genetic elements of the isolate, and Ole Christian Hagestad with his assistance in the phylogenetic analysis. We thank the Advanced Microscopy Core Facility (AMCF) of the UiT the Arctic University of Norway for the access to their devices. We would also like to acknowledge the Norwegian National Advisory Unit on Detection of Antimicrobial Resistance (K-res), University Hospital of North Norway for the VREs.

SUPPLEMENTARY MATERIAL

The Supplementary Material for this article can be found online at: https://www.frontiersin.org/articles/10.3389/fmicb.2021.730740/full#supplementary-material

REFERENCES

Azevedo, E., Barata, M., Marques, M. I., and Caeiro, M. F. (2017). Lulworthia atlantica: a new species supported by molecular phylogeny and morphological analysis. *Mycologia* 109, 287–295. doi: 10.1080/00275514.2017.1302255

Boudesocque-Delaye, L., Agostinho, D., Bodet, C., Thery-Kone, I., Allouchi, H., Gueiffier, A., et al. (2015). Antibacterial polyketide heterodimers from Pyrenacantha kaurabassana Tubers. *J. Nat. Prod.* 78, 597–603. doi: 10.1021/np5003252

Calado, M. D. L., Carvalho, L., Barata, M., and Pang, K.-L. (2019). Potential roles of marine fungi in the decomposition process of standing stems and leaves of Spartina maritima. *Mycologia* 111, 371–383. doi: 10.1080/00275514.2019.1571380

Clinical Laboratory Standard Institute (CLSI) (2012). Clinical and laboratory standards institute methods for dilution antimicrobial susceptibility tests for bacteria that grow aerobicallyapproved standard. *J. Infect. Chemother.* 18, 816–826.

Davidson, D. E. (1973). Mucoid sheath of Lulworthia medusa. *Trans. Brit.Mycol. Soc.* 60, 577–579. doi: 10.1016/S0007-1536(73)80042-7

Demain, A. L. (2014). "Valuable secondary metabolites from fungi," in *Biosynthesis and Molecular Genetics of Fungal Secondary Metabolites*, eds J. F. Martín, S. Zeilinger, and C. García-Estrada (Springer).

Francisca, C., Marta, C.-D.-S., Emília, S., Madalena, P., and Anake, K. (2018). Sulfation pathways: sources and biological activities of marine sulfated steroids. *J. Mol. Endocrinol.* 61, T211–T231. doi: 10.1530/JME-17-0252

Góes-Neto, A., Marcelino, V. R., Verbruggen, H., da Silva, F. F., and Badotti, F. (2020). Biodiversity of endolithic fungi in coral skeletons and other reef substrates revealed with 18S rDNA metabarcoding. *Coral. Reefs* 39, 229–238. doi: 10.1007/s00338-019-01880-y

Hyde, K. D., Norphanphoun, C., Maharachchikumbura, S. S. N., Bhat, D. J., Jones, E. B. G., Bundhun, D., et al. (2020). Refined families of sordariomycetes. *Mycosphere* 11:1059. doi: 10.5943/mycosphere/11/1/7

Imhoff, J. F. (2016). Natural products from marine fungistill an underrepresented resource. *Mar. Drugs* 14, 1–19. doi: 10.3390/md14010019

Isaka, M., Yangchum, A., Rachtawee, P., Komwijit, S., and Lutthisungneon, A. (2010). Hopane-type triterpenes and binaphthopyrones from the scale insect pathogenic fungus Aschersonia paraphysata BCC 11964. *J. Nat. Prod.* 73, 688–692. doi: 10.1021/np1000363

Johnson, T. W. (1958). Marine fungi. IV. *Lulworthia* and *Ceriosporopsis*. *Mycologia* 50, 151–163. doi: 10.2307/3756191

Jones, E. B. G. (1994). Fungal adhesion. *Mycol. Res.* 98, 961–981. doi: 10.1016/S0953-7562(09)80421-8

Katoh, K., and Standley, D. M. (2013). MAFFT multiple sequence alignment software version 7: improvements in performance and usability. *Mol. Biol. Evol.* 30, 772–780. doi: 10.1093/molbev/mst010

Katoh, K., Misawa, K., Kuma, K., and Miyata, T. (2002). MAFFT: a novel method for rapid multiple sequence alignment based on fast Fourier transform. *Nucleic Acids Res.* 30, 3059–3066. doi: 10.1093/nar/gkf436

Kavanagh, F., Hervey, A., and Robbins, W. J. (1951). Antibiotic substances from *Basidiomycetes*: VIII. Pleurotus Multilus (Fr.) Sacc. and Pleurotus Passeckerianus Pilat. *Proc. Natl. Acad. Sci. U.S.A.* 37, 570–574. doi: 10.1073/pnas.37.9.570

Kawaguchi, M., Uchida, R., Ohte, S., Miyachi, N., Kobayashi, K., Sato, N., et al. (2013). New dinapinone derivatives, potent inhibitors of triacylglycerol synthesis in mammalian cells, produced by *Talaromyces pinophilus* FKI-3864. *J. Antibiot.* 66, 179–189. doi: 10.1038/ja.2012.127

Koch, J., Pang, K.-L., and Jones, E. B. G. (2007). Rostrupiella danica gen. et sp. nov., a Lulworthia-like marine lignicolous species from Denmark and the USA. *Bot. Mar.* 50, 294–301. doi: 10.1515/BOT.2007.034

Kohlmeyer, J., Spatafora, J. W., and Volkmann-Kohlmeyer, B. (2000). Lulworthiales, a new order of marine Ascomycota. *Mycologia* 92, 453–458. doi: 10.2307/3761504

Kornprobst, J.-M., Sallenave, C., and Barnathan, G. (1998). Sulfated compounds from marine organisms. *Comput. Biochem. Physiol.* 119, 1–51. doi: 10.1016/S0305-0491(97)00168-5

Kristoffersen, V., Rämä, T., Isaksson, J., Andersen, J. H., Gerwick, W. H., Hansen, E., et al. (2018). Characterization of rhamnolipids produced by an Arctic marine bacterium from the *Pseudomonas* fluorescence Group. *Mar. Drugs* 16:163. doi: 10.3390/md16050163

Lanfear, R., Calcott, B., Ho, S. Y. W., and Guindon, S. (2012). PartitionFinder: combined selection of partitioning schemes and substitution models for phylogenetic analyses. *Mol. Biol. Evol.* 29, 1695–1701. doi: 10.1093/molbev/mss020

Lanfear, R., Frandsen, P. B., Wright, A. M., Senfeld, T., and Calcott, B. (2017). PartitionFinder 2: new methods for selecting partitioned models of evolution for molecular and morphological phylogenetic analyses. *Mol. Biol. Evol.* 34, 772–773. doi: 10.1093/molbev/msw260

Li, D.-H., Han, T., Guan, L.-P., Bai, J., Zhao, N., Li, Z.-L., et al. (2016). New naphthopyrones from marine-derived fungus *Aspergillus niger* 2HL-M-8 and their in vitro antiproliferative activity. *Nat. Prod. Res.* 30, 1116–1122. doi: 10.1080/14786419.2015.1043553

Lu, S., Tian, J., Sun, W., Meng, J., Wang, X., Fu, X., et al. (2014). Bis-naphtho-γ-pyrones from fungi and their bioactivities. *Molecules* 19, 7169–7188. doi: 10.3390/molecules19067169

Maharachchikumbura, S. S. N., Hyde, K. D., Jones, E. B. G., McKenzie, E. H. C., Huang, S.-K., Abdel-Wahab, M. A., et al. (2015). Towards a natural classification and backbone tree for Sordariomycetes. *Fungal. Divers.* 72:301. doi: 10.1007/s13225-015-0331-z

Overy, D. P., Bayman, P., Kerr, R. G., and Bills, G. F. (2014). An assessment of natural product discovery from marine (sensu strictu) and marine-derived fungi. *Mycology* 5, 145–167. doi: 10.1080/21501203.2014.931308

Overy, D. P., Rämä, T., Oosterhuis, R., Walker, A. K., and Pang, K.-L. (2019). The neglected marine fungi, sensu stricto, and their isolation for natural products' discovery. *Mar. Drugs* 17, 1–20. doi: 10.3390/md17010042

Poli, A., Bovio, E., Ranieri, L., Varese, G. C., and Prigione, V. (2020). Fungal diversity in the Neptune forest: Comparison of the mycobiota of *Posidonia oceanica, Flabellia petiolata*, and *Padina pavonica*. *Front. Microbiol.* 11:933. doi: 10.3389/fmicb.2020.00933

Rämä, T., Nordén, J., Davey, M. L., Mathiassen, G. H., Spatafora, J. W., and Kauserud, H. (2014). Fungi ahoy! Diversity on marine wooden substrata in the high North. *Fungal. Ecol.* 8, 46–58. doi: 10.1016/j.funeco.2013.12.002

Rehner, S. A., and Samuels, G. J. (1994). Taxonomy and phylogeny of *Gliocladium* analysed from nuclear large subunit ribosomal DNA sequences. *Mycol. Res.* 98, 625–634. doi: 10.1016/S0953-7562(09)80409-7

Rivera-Chavez, J., Caesar, L., Garcia-Salazar, J. J., Raja, H. A., Cech, N. B., Pearce, C. J., et al. (2019). Mycopyranone: a 8,8'-binaphthopyranone with potent anti-MRSA activity from the fungus *Phialemoniopsis* sp. *Tetrahedron Lett.* 60, 594–597. doi: 10.1016/j.tetlet.2019.01.029

Ronquist, F., Teslenko, M., van der Mark, P., Ayres, D. L., Darling, A., Höhna, S., et al. (2012). MrBayes 3.2: efficient Bayesian phylogenetic inference and model choice across a large model space. *Syst. Biol.* 61, 539–542. doi: 10.1093/sysbio/sys029

Schneider, Y., Jenssen, M., Isaksson, J., Hansen, K. Ø, Andersen, J. H., and Hansen, E. H. (2020). Bioactivity of serratiochelin A, a siderophore isolated from a co-culture of Serratia sp. and Shewanella sp. *Microorganisms* 8, 1–17. doi: 10.3390/microorganisms8071042

Stamatakis, A. (2006). RAxML-VI-HPC: maximum likelihood-based phylogenetic analyses with thousands of taxa and mixed models. *Bioinformatics* 22, 2688–2690. doi: 10.1093/bioinformatics/btl446

Sutherland, G. K. (1915). Additional notes on marine Pyrenomycetes. *New Phytol.* 14, 183–193. doi: 10.1111/j.1469-8137.1915.tb07185.x

Suzuki, K., Nozawa, K., Nakajima, S., Udagawa, S., and Kawai, K. (1992). Isolation and structures of antibacterial binaphtho-α-pyrones, talaroderxines A and B, from Talaromyces derxii. *Chem. Pharm. Bull.* 40, 1116–1119. doi: 10.1248/cpb.40.1116

Velez, P., González, M. C., Cifuentes, J., Rosique-Gil, E., and Hanlin, R. T. (2015). Diversity of sand inhabiting marine ascomycetes in some tourist beaches on Cozumel Island, Mexico. *Mycoscience* 56, 136–140. doi: 10.1016/j.myc.2014.04.007

Vilgalys, R., and Hester, M. (1990). Rapid genetic identification and mapping of enzymatically amplified ribosomal DNA from several Cryptococcus species. *J. Bacteriol.* 172, 4238–4246. doi: 10.1128/jb.172.8.4238-4246.1990

Wang, J., Galgoci, A., Kodali, S., Herath, K. B., Jayasuriya, H., Dorso, K., et al. (2003). Discovery of a small molecule that inhibits cell division by blocking FtsZ, a novel therapeutic target of antibiotics. *J. Biol. Chem.* 278, 44424–44428. doi: 10.1074/jbc.M307625200

White, T. J., Bruns, T., Lee, S., and Taylor, J. (1990). "Amplification and direct sequencing of fungal ribosoman RNA genes for phylogenetics," in *PCR ProtocolsA Guide to Methods and Applications*, eds M. A. Innis, D. H. Gelfand, J. J. Sninsky, and T. J. White (San Diego: Academic Press).

WHO (2014). *Antimicrobial ResistanceGlobal Report on Surveillance*. Available online at: http://www.who.int/drugresistance/documents/surveillancereport/en/. (accessed February 26, 2018).

Xu, Y., Vinas, M., Alsarrag, A., Su, L., Pfohl, K., Rohlfs, M., et al. (2019). Bis-naphthopyrone pigments protect filamentous ascomycetes from a wide range of predators. *Nat. Commun.* 10, 1–12. doi: 10.1038/s41467-019-11377-5

Zheng, C. J., Sohn, M.-J., Lee, S., Hong, Y.-S., Kwak, J.-H., and Kim, W.-G. (2007). Cephalochromin, a FabI-directed antibacterial of microbial origin. *Biochem. Biophys. Res. Commun.* 362, 1107–1112. doi: 10.1016/j.bbrc.2007.08.144

Zuccaro, A., Schoch, C. L., Spatafora, J. W., Kohlmeyer, J., Draeger, S., and Mitchell, J. I. (2008). Detection and identification of fungi intimately associated with the brown seaweed Fucus serratus. *Appl. Environ. Microbiol.* 74, 931–941. doi: 10.1128/AEM.01158-07

Conflict of Interest: The authors declare that the research was conducted in the absence of any commercial or financial relationships that could be construed as a potential conflict of interest.

Publisher's Note: All claims expressed in this article are solely those of the authors and do not necessarily represent those of their affiliated organizations, or those of the publisher, the editors and the reviewers. Any product that may be evaluated in this article, or claim that may be made by its manufacturer, is not guaranteed or endorsed by the publisher.

Supplementary Material

Table of Content

Supplementary Figure 15:HMQC optimized for 4 Hz $^{n}J_{CH}$ displays some of the important $^{4}J_{CH}$ for assignment.

Supplementary Figure 16: NOESY (600 ms mixing time) of **1**.

Supplementary Table 1: Dataset of nrITS, nrLSU and nrSSU used for phylogenetic analysis of 067bN1.2. All sequences were acquired from Genbank.

Species	**Strain**	**Source**	**nrITS**	**nrLSU**	**nrSSU**
Achroceratosphaeria potamia	JF 08139	Submerged wood of *Platanus* sp.	-	GQ996538	GQ996541
Bimuria novae-zelandiae	CBS 107.79	Soil	-	AY016356	AY016338
Cumulospora marina	MF46	Submerged wood	-	GU252135	GU252136
Cumulospora varia	GR78	Submerged wood	-	EU848578	EU848593
Halazoon fuscus	NBRC 105256	Driftwood	-	GU252147	GU252148
Halazoon melhae	MF819	Drift stems of *Phragmites australis*	-	GU252143	GU252144
Hydea pygmea	NBRC 33069	Driftwood	-	GU252133	GU252134
Kohlmeyeriella crassa	NBRC 32133	Sea foam	LC146741	LC146742	AY879005
Kohlmeyeriella tubulata	PP115	Marine environment	-	AF491265	AY878998
Koralionastes ellipticus	JF08139	Coral rocks with sponges	-	EU863585	EU863581
Letendraea helminthicola	CBS 884.85	Yerba mate	EU715680	AY016362	AY016345
Lindra marinera	JK 5091A	Marine environment	-	AY878958	AY879000
Lindra obtusa	NBRC 31317	Sea foam	LC146744	AY878960	AY879002
Lindra thalassiae	AFTOL 413	Marine environment	DQ491508	DQ470947	DQ470994
Lulworthia atlantica	FCUL210208 SP4	Sea water	KT347205	JN886843	KT347193
Lulworthia cf. *opaca*	CBS 21860	Driftwood in seawater	-	AY878961	AY879003
Lulworthia cf. *purpurea*	FCUL170907 CP5	Sea water	KT347219	JN886824	KT347201
Lulworthia fucicola	ATCC 64288	Intertidal wood	-	AY878965	AY879007
Lulworthia grandispora	NTOU3841	Driftwood	-	KY026048	KY026044
Lulworthia lignoarenaria	AFTOL 5013	Marine environment	-	FJ176903	FJ176848
Lulworthia medusa	JK 5581	Spartina	-	AF195637	AF195636
Lulworthiaceae	067bN1.2	Driftwood	MW377595	MW375591	MW375590

Matsusporium tropicale	NBRC 32499	Submerged wood	-	GU252141	GU252142
Moleospora maritima	MF836	Drift stems of *Phragmites australis*	-	GU252137	GU252138
Paralulworthia gigaspora	MUT 435	*P. oceanica* – rhizomes	MN649242	MN649250	MN649246
Paralulworthia posidoniae	MUT 5261	*P. oceanica* – rhizomes	MN649245	MN649253	MN649249
Setosphaeria monoceras	CBS 154.26	n.d.	DQ337380	AY016368	DQ238603
Zalerion maritima	FCUL280207 CP1	Sea water	KT347216	JN886806	KT347203

Supplementary Table 2: Information regarding the clinical isolates used for antibacterial activity testing of **1**.

Clinical isolate	**Antibiotic Resistance Mechanism**	**Reference**	**Source (gifted/bought)**
S. aureus N315	MRSA	Ito et al. (1999). Cloning and nucleotide sequence determination of the entire mec DNA of pre-methicillin-resistant *Staphylococcus aureus* N315. *Antimicrob. Agents Chemother,43*, 1449-1458. doi: 10.1128/AAC.43.6.1449	T. Ito, Juntendo University, Tokyo (Japan)
S. aureus 85/2082		Suzuki et al. (1993). Distribution of mec Regulator Genes in Methicillin-Resistant *Staphylococcus* Clinical Strains. *Antimicrob. Agents Chemother.,37*, 1219-1226. doi: 0066-4804/93/061219-08$02.00/0	T. Ito, Juntendo University, Tokyo (Japan)
S. aureus NCTC 10442		Ito et al. (2001).Structural comparison of three types of staphylococcal cassette chromosome mec integrated in the chromosome in methicillin-resistant *Staphylococcus aureus*. *Antimicrob. Agents Chemother,45*, 1323-1336. doi: 10.1128/AAC.45.5.1323-1336.2001.	NCTC
S. aureus WIS [WBG8318]		Ito et al. (2004).Novel Type V Staphylococcal Cassette Chromosome mec Driven by a Novel Cassette Chromosome Recombinase, ccrC. *Antimicrob. Agents. Chemother.,48*, 2637–2651. doi: 10.1128/AAC.48.7.2637-2651.2004	K. Hiramatsu, Juntendo University, Tokyo, (Japan)
S. aureus IHT 99040		Salmenlinna, S., Lyytikäinen, O., & Vuopio-Varkila, J. (2002).Community-Acquired Methicillin-Resistant *Staphylococcus aureus*, Finland.*Emerging infectious diseases*, *8*, 602–607.doi: 10.3201/eid0806.010313	Saara Salmenlinna (IHT, Helsinki, Finland)
E. faecium 50673722	VRE	Sivertsen A, Janice J, Pedersen T,Wagner TM, Hegstad J, Hegstad K. 2018. Theenterococcus cassette chromosome, agenomic variation enabler in enterococci.*mSphere*, 3, 1-13. doi:10.1128/mSphere.00402-18	K-res [a]
*E. faecium*50901530		-	K-res [a]
*E. faecium*K36-18		-	K-res [a]

*E. faecium*50758899		-	K-res [a]
*E. faecium*TUH50-22		-	K-res [a]
*E. faecium*1-H-4		-	K-res [a]
E. coli 50676002	ESBL-Carba	-	K-res [a]
K. pneumoniae K47-25		-	K-res [a]
A. baumanii K47-42		-	K-res [a]
P. aeruginosa K34-7		-	K-res [a]
E.coli ATCC 25922	-	ATCC	ATCC

[a] 2006-2015 The Norwegian National Advisory Unit on Detection of Antimicrobial Resistance (K-res), University Hospital of North Norway – UNN.

Supplementary Table 3: Summary of chemical shift and correlations for **1**(DMSO-d_6).

Position	δ^{13}C, type	δ^{1}H, splitting (Hz)	COSY	HMBC (^{1}H → ^{13}C)
2	170.0*,C	-	-	-
2'	169.7, C	-	-	-
2a'	98.3, C	-	-	-
2a	98.0, C	-	-	-
3	173.8*, C	-	-	-
3'	173.8, C	-	-	-
3a'	112.2, C	-	-	-
3a	113.0, C	-	-	-
4	162.0, C	-	-	-
4'	160.3, C	-	-	-
5'	108.7, C	-	-	-
5	101.8, CH	6.55, h	-	3a, 4, 6, 7
6	155.3, C	-	-	-
6'	160.0, C	-	-	-
7a	138.2, C	-	-	-
7a'	139.3, C	-	-	-
7	104.6, CH	6.05, h	-	3a, 5, 6, 8
7'	96.6, CH	6.69, h	-	3',3a', 5', 6', 8'
8a'	139.2, C	-	-	-
8a	133.3, C	-	-	-
8	113.2, C	-	-	-
8'	110.9, CH	6.74, h	-	2',2a',3',3a',7a',7',8a',9'
9'	65.7, CH	4.69, h	OH9'	2a', 8', 8a', 10'
9	31.7, CH2	2.40/2.57, m	10	8, 8a, 10
10'	80.3, CH	4.62, m	11'	8a', 9', 11', 12'
10	77.2, CH	4.56, m	9	8a, 12
11	33.7, CH2	1.52, m 1.64, m	12	10
11'	29.5, CH2	1.78, m	10', 12'	10'
12'	24.2, CH2	1.27/1.34, m	11',13'	11',13',14'
12	24.3, CH2	1.47, m	11, 13	11,13,14
13'	31.2, CH2	1.34, m	12'	14',15'
13	30.9, CH2	1.21, m	12	14,15
14'	22.1, CH2	1.34, m	15'	13',15'
14	22.0, CH2	1.23, m	15	13,15
15'	14.0, CH3	0.90, t (J=6.5)	14'	13',14'
15	13.9, CH3	0.81, h	14	13,14
16	55.4, O-CH3	3.77, h	-	6'
OH3*	-	-, s		
OH3*	-	-, s		
OH4	-	14.74, h		4,3a,5
OH4'	-	14.65, h		4',3a',5
OH9'	-	5.51, h	9'	

*Ambiguous assignment

Supplementary Table 4: Results for the MIC determination of **1** against clinical isolates and reference strains (MIC of 50 µg/ml or higher/above highest tested concentration).

Strain type	**Strain**	**MIC in µg/ml**
Clinical isolates	*E. faecium* 50673722	>100
	E. faecium 50901530	>100
	E. faecium K36-18	100
	E. faecium 50758899	>100
	E. faecium TUH50-22	100
	E. faecium 1-H-4	50
	E. coli 50676002	>100
	K. pneumoniae K47-25	>100
	A. baumanii K47-42	>100
	P. aeruginosa K34-7	>100
Reference strains	*Enterococcus faecalis* ATCC® 29212	>100
	Methicillin resistant *S. aureus* ATCC® 33591	>100
	Escherichia coli ATCC® 25922	>100
	Pseudomonas aeruginosa ATCC® 27853	>100

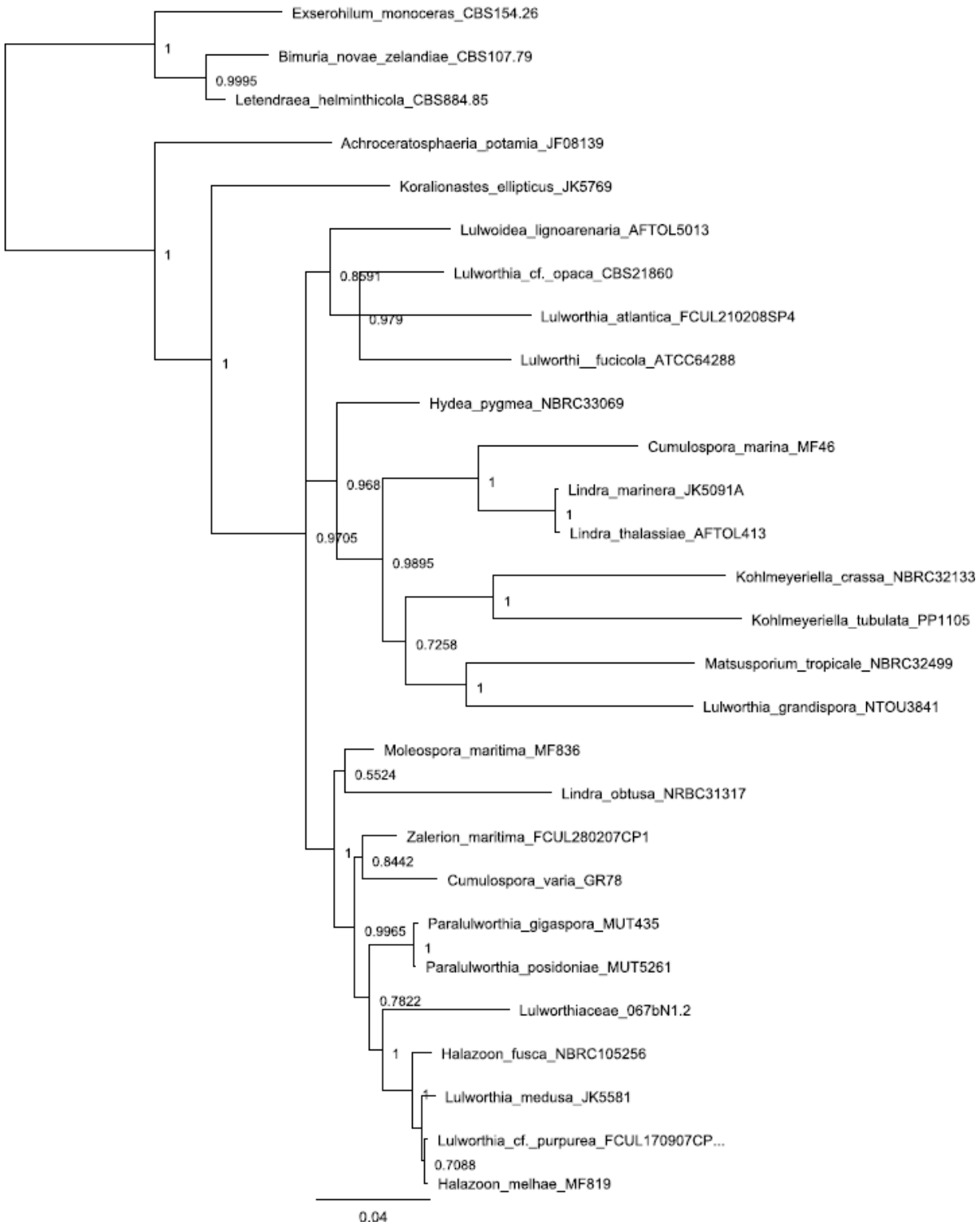

Supplementary Figure 1: MrBayes tree from the 5.8S, SSU and LSU analysis, showing the placement of 067bN1.2 within the family Lulworthiaceae. Node support given as posterior probabilites. *Exserophilum monoceras, Letendraea helminthicola, Bimufia novae-zelandiae* and *Achroceratosphaeria potamia* were included as outgroups taxa. *Koralionastes ellipticus* was included as a member of the family Koralionastetaceae. The remaining sequences are all part of Lulworthiaceae.

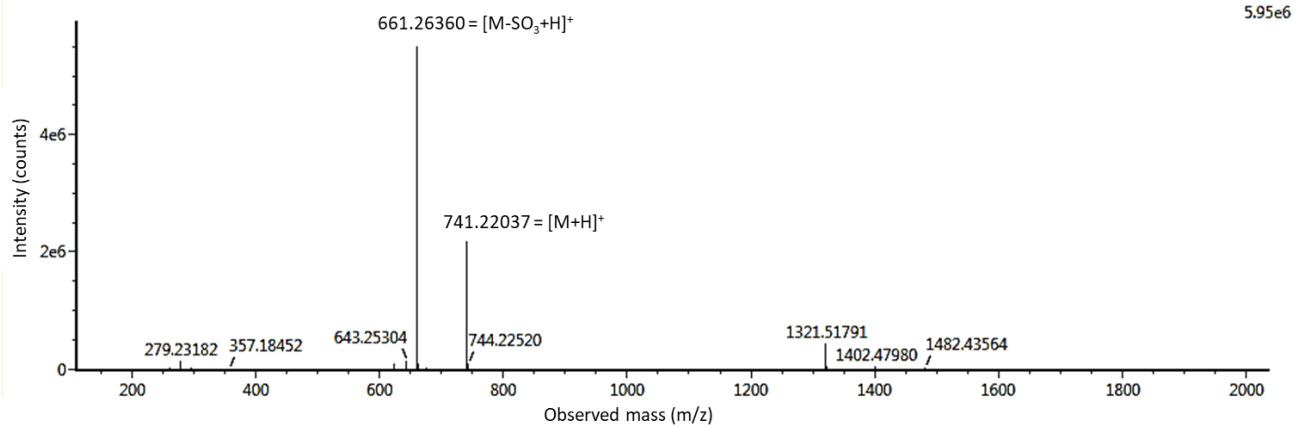

Supplementary Figure 2: Low-collision energy mass spectrum of lulworthinone (**1**) in ESI+.

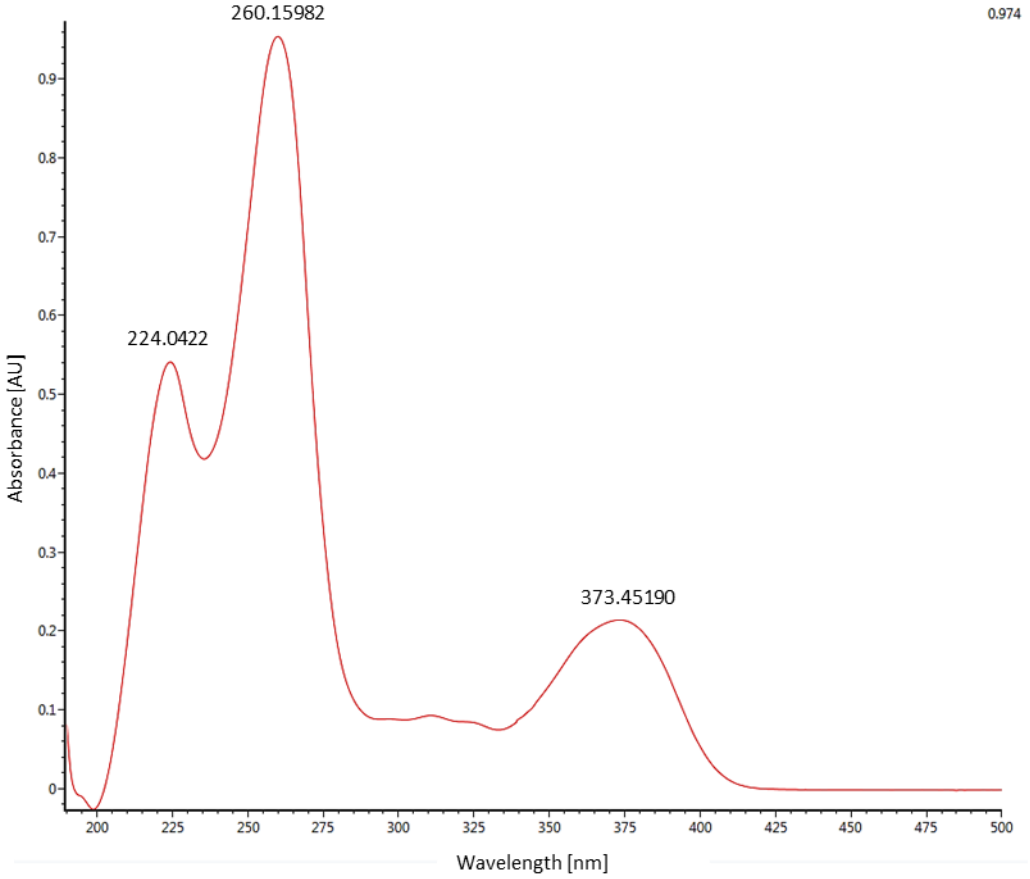

Supplementary Figure 3:UV-Vis spectrum of lulworthinone (**1**).

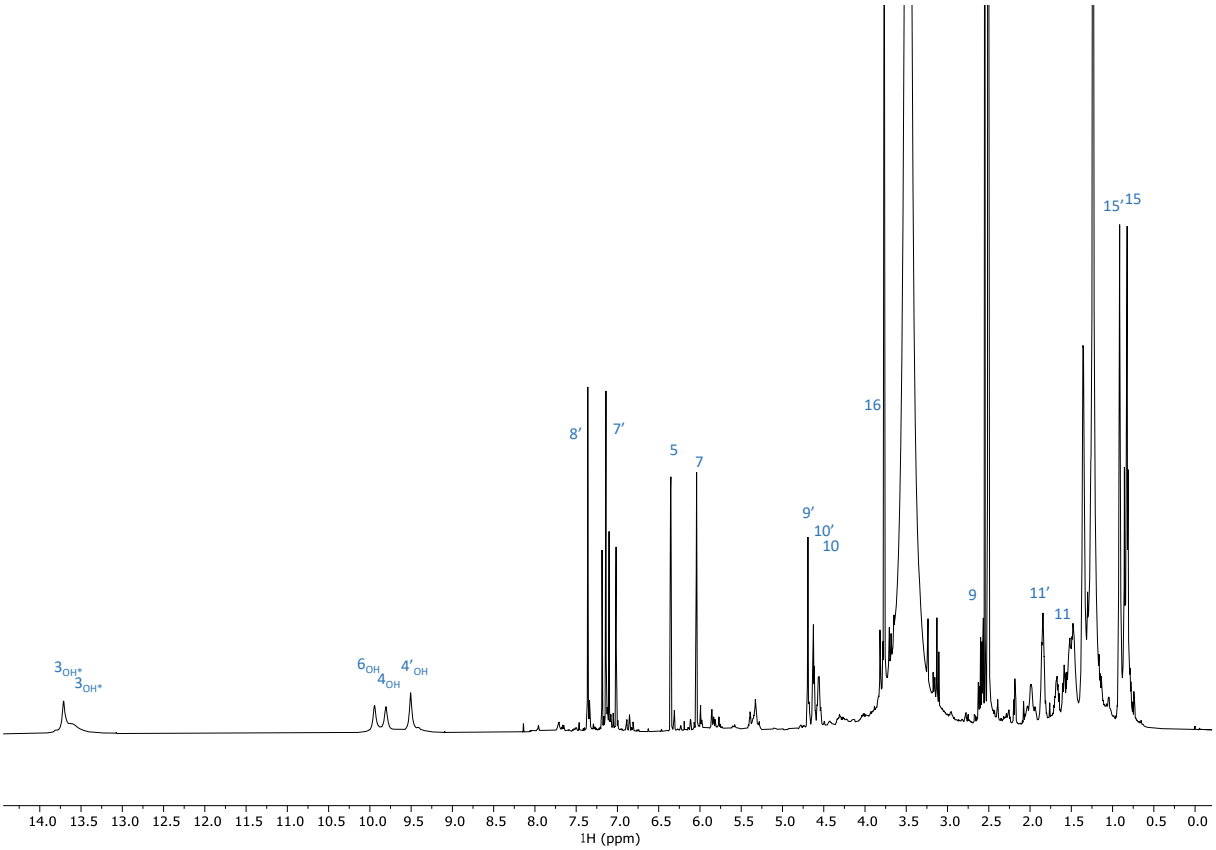

Supplementary Figure 4: 1D proton spectrum of **2**.

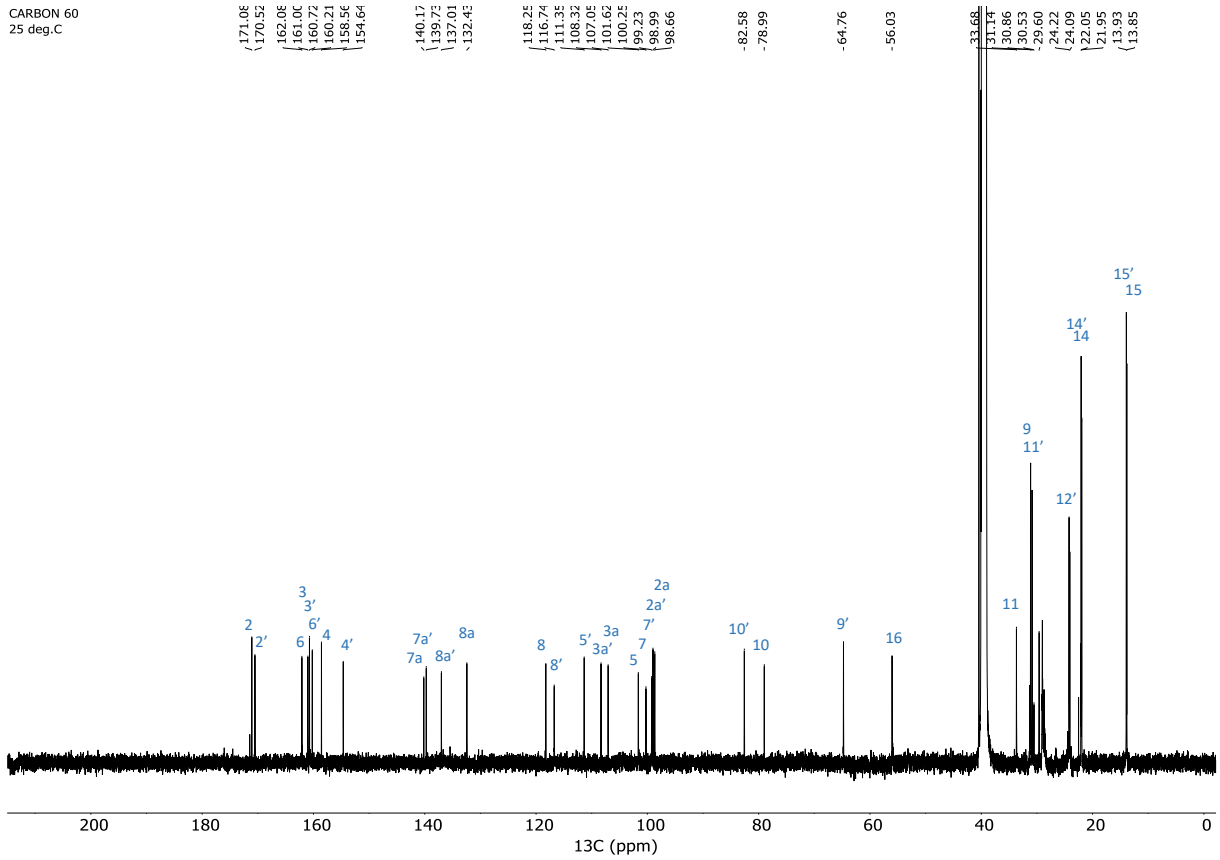

Supplementary Figure 5: 1D carbon spectrum of **2**.

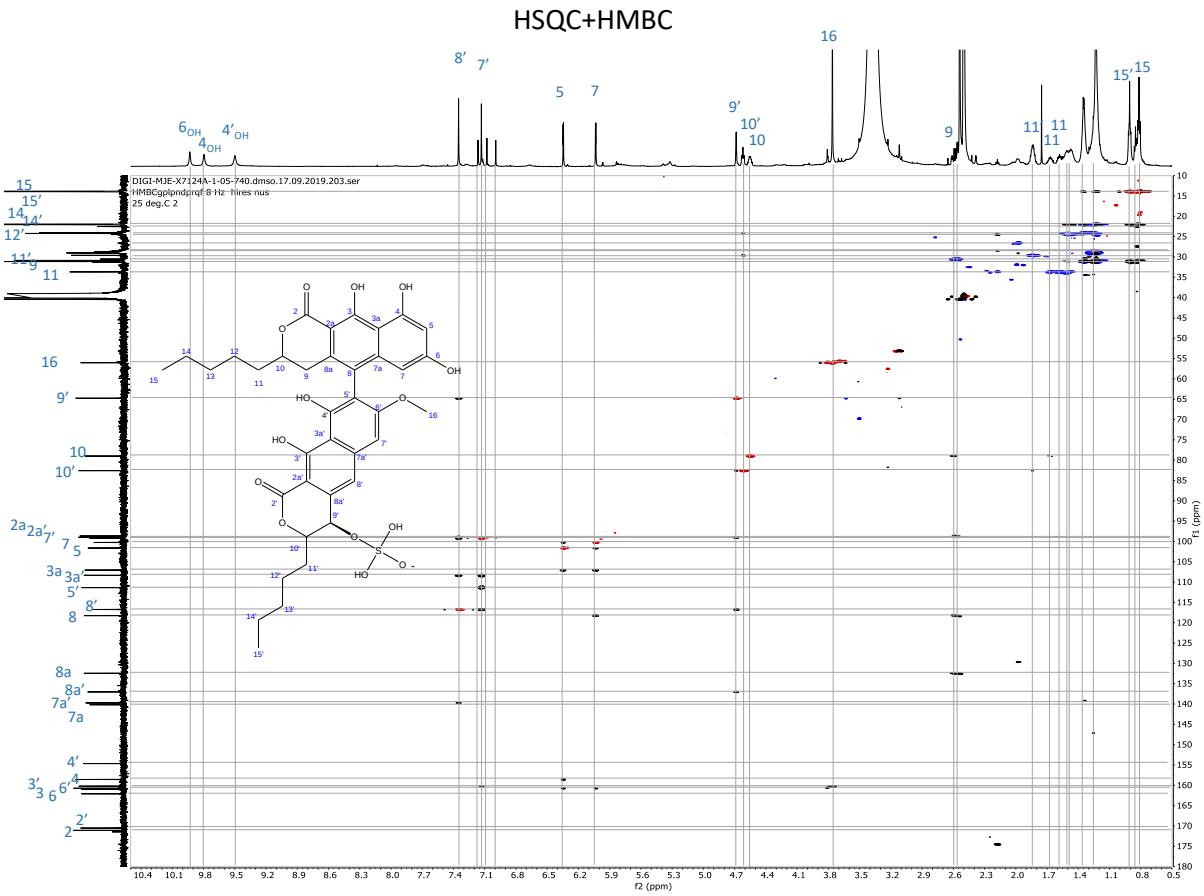

Supplementary Figure 6: Superimposed HSQC and HMBC of **2**.

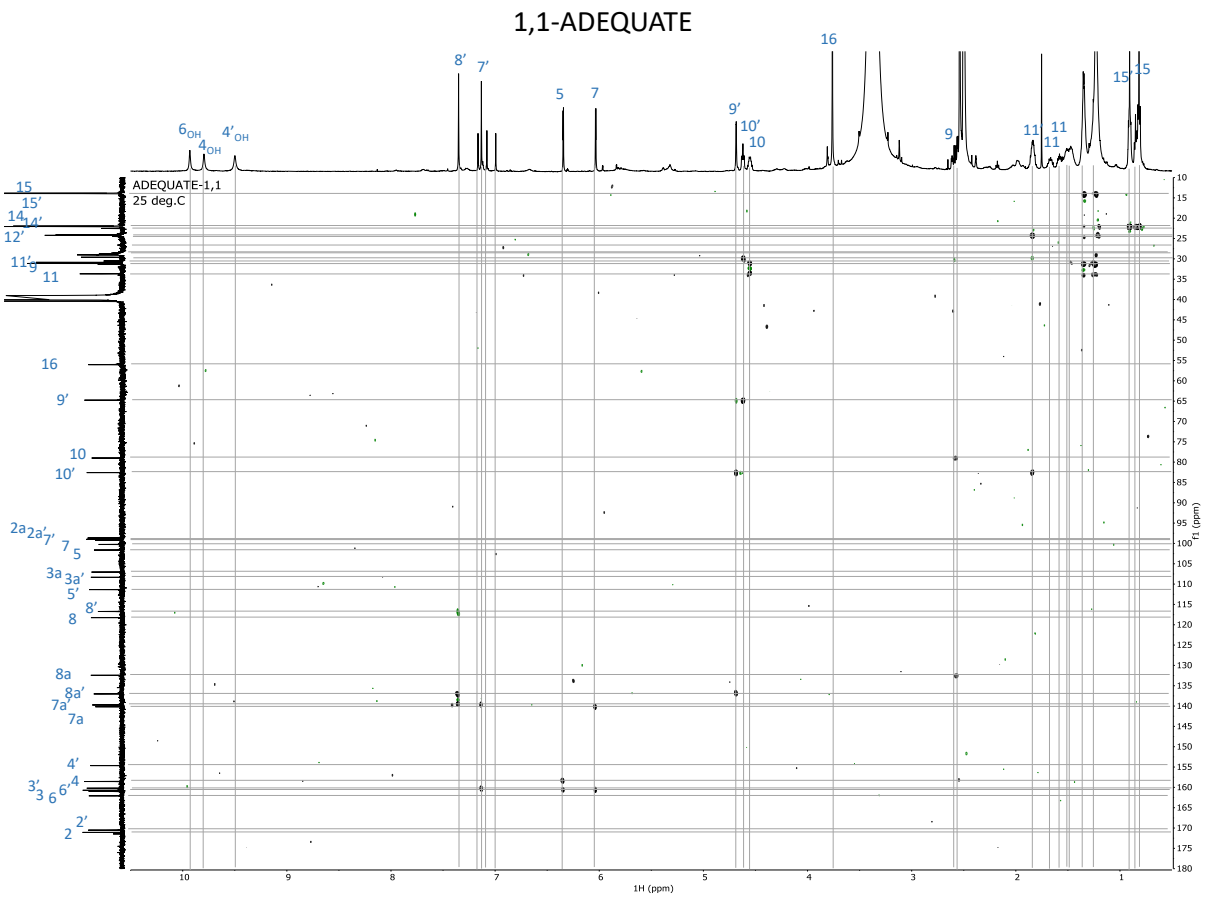

Supplementary Figure 7: 1,1-ADEQUATE of **2**.

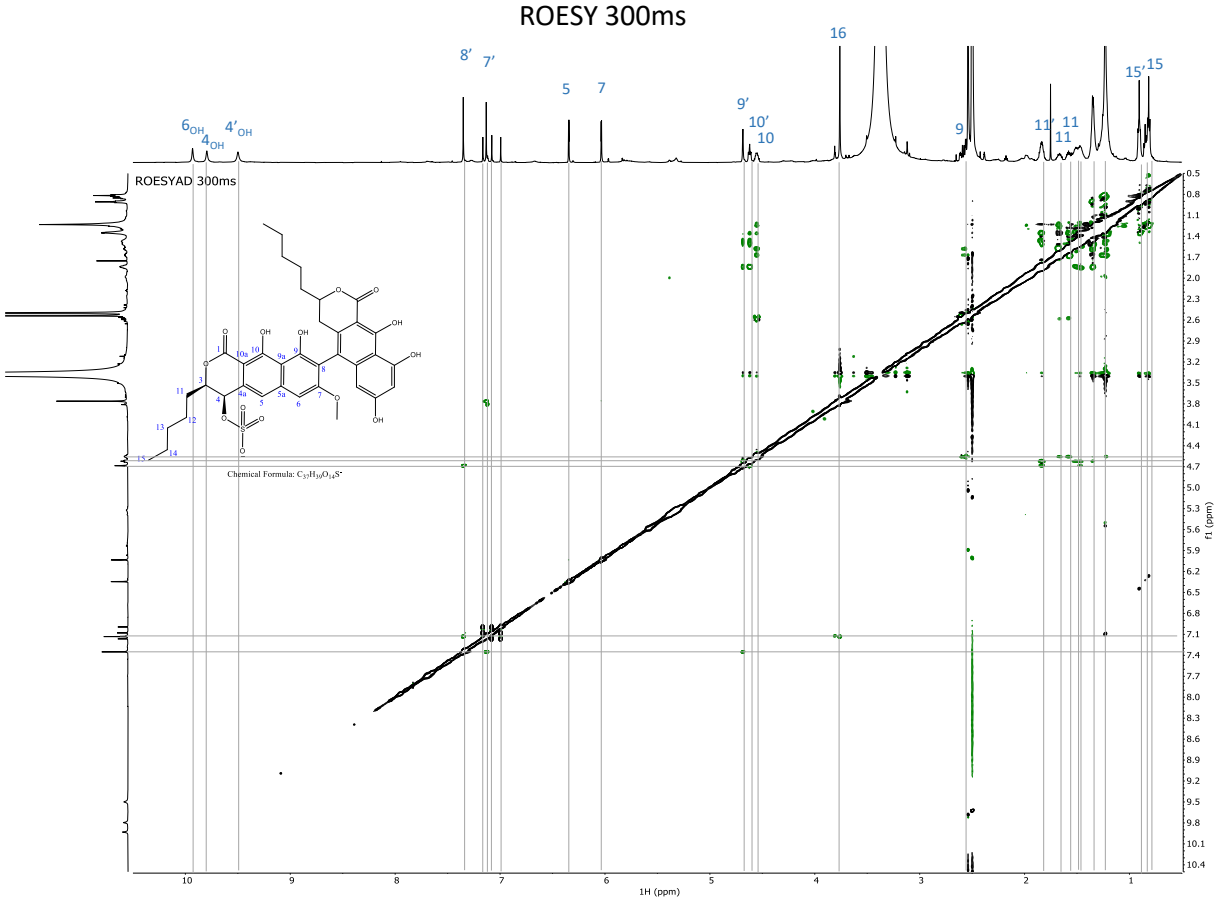

Supplementary Figure 8: ROESY (300 ms mixing time) of **2**.

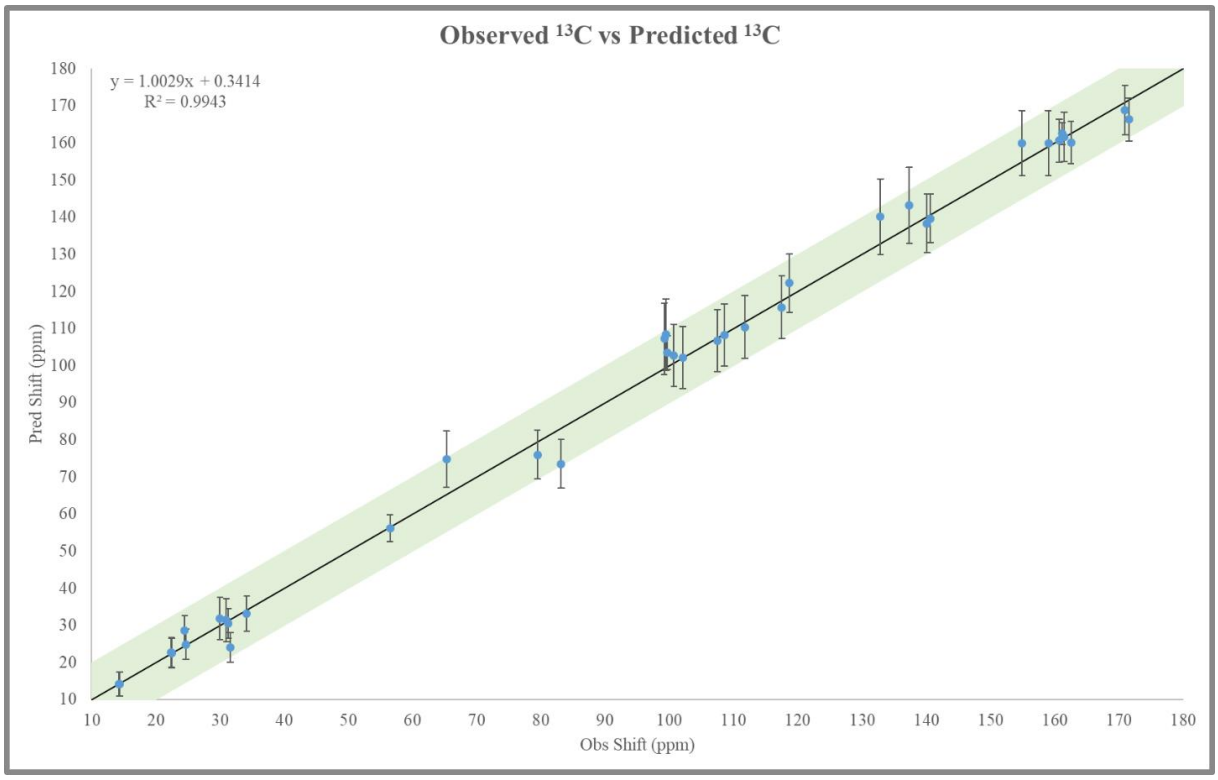

Supplementary Figure 9: Predicted vs observed ^{13}C chemical shift comparison. Average error of 2.79 ppm, R2 of 0.9943. Green region is equivalent to an error of +/- 10 ppm, black line y = x. Errors for prediction given by MestreNova Modgraph desktop prediction.

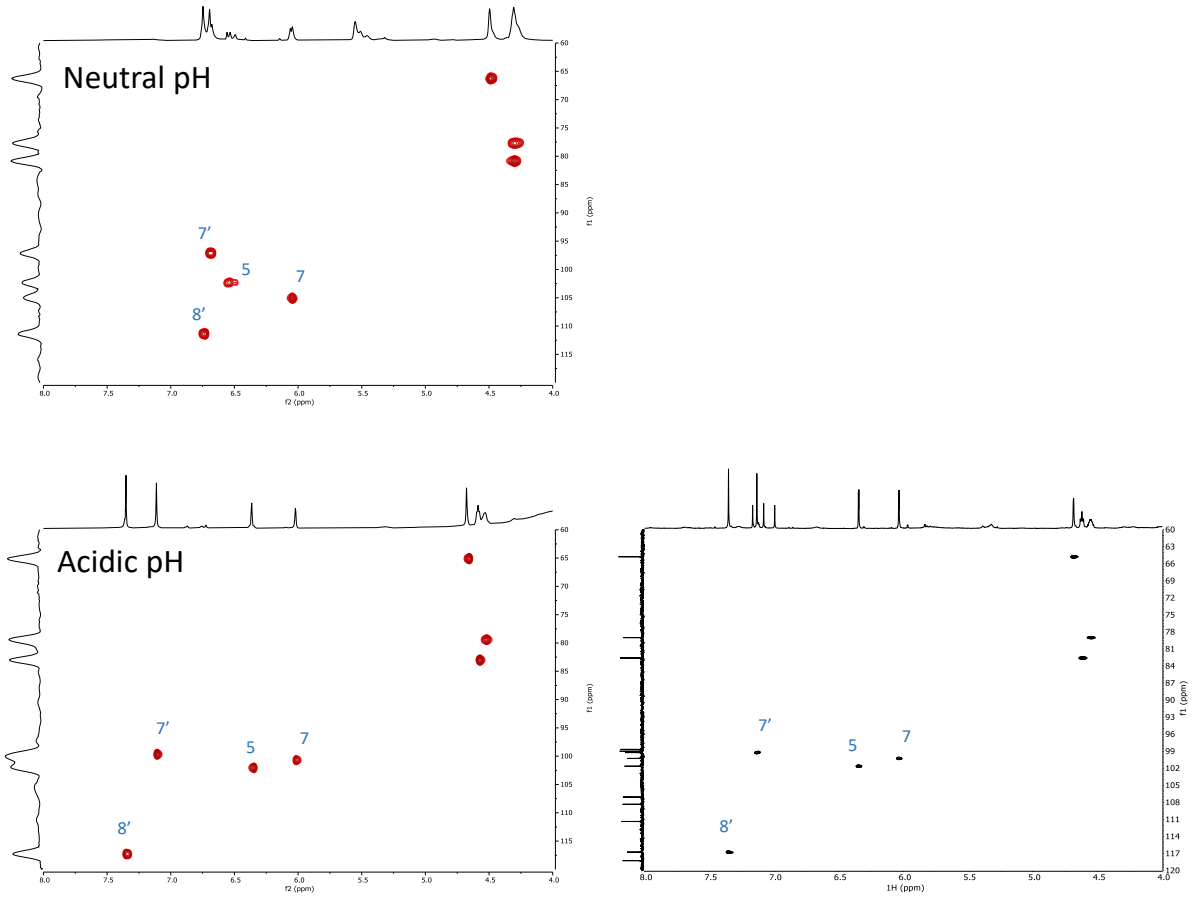

Supplementary Figure 10: The HSQC peaks of the aromatic region of the second preparation of **1** (red) at neutral (top) and after addition of acid (bottom), compared to the initial preparation of **2** in the presence of formic acid (black).

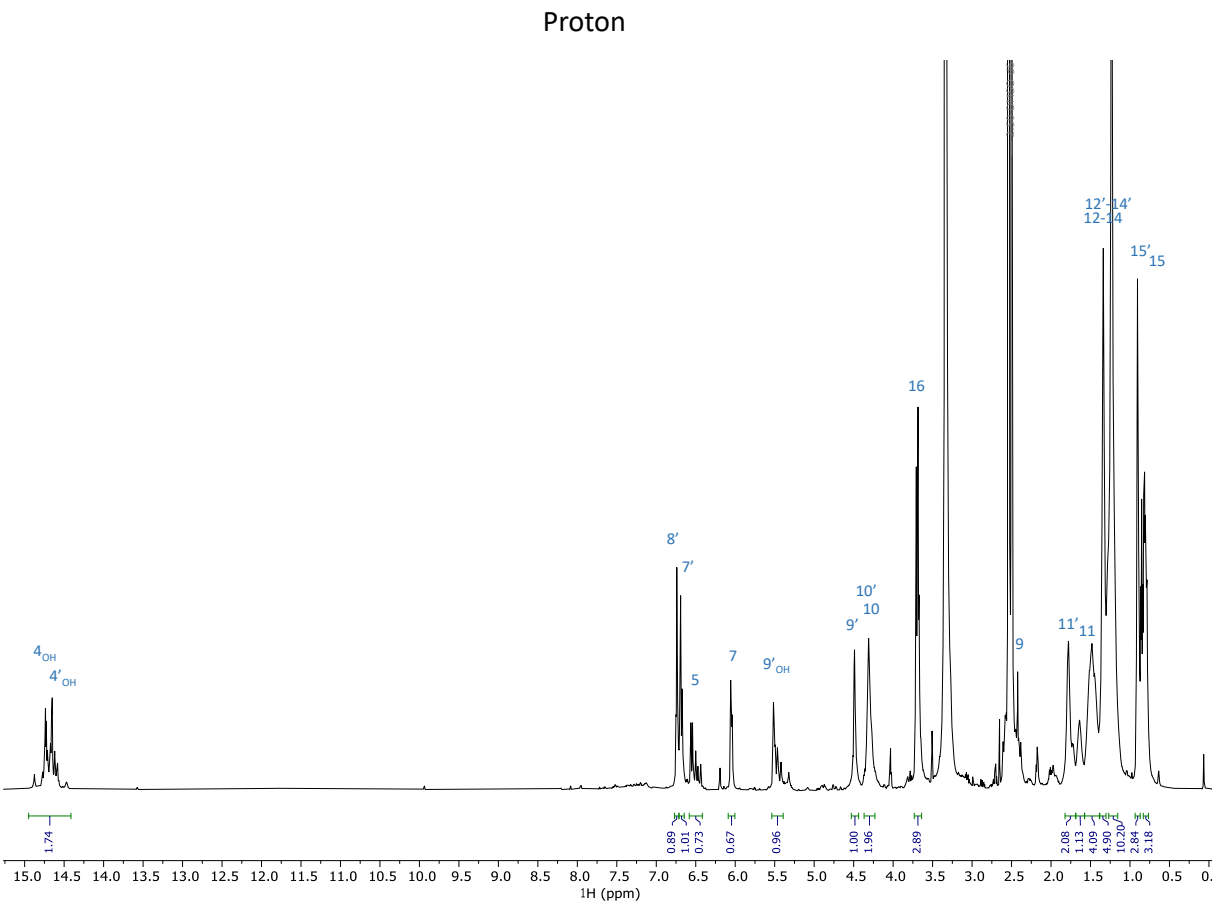

Supplementary Figure 11: Proton spectrum of **1** in DMSO-d_6.

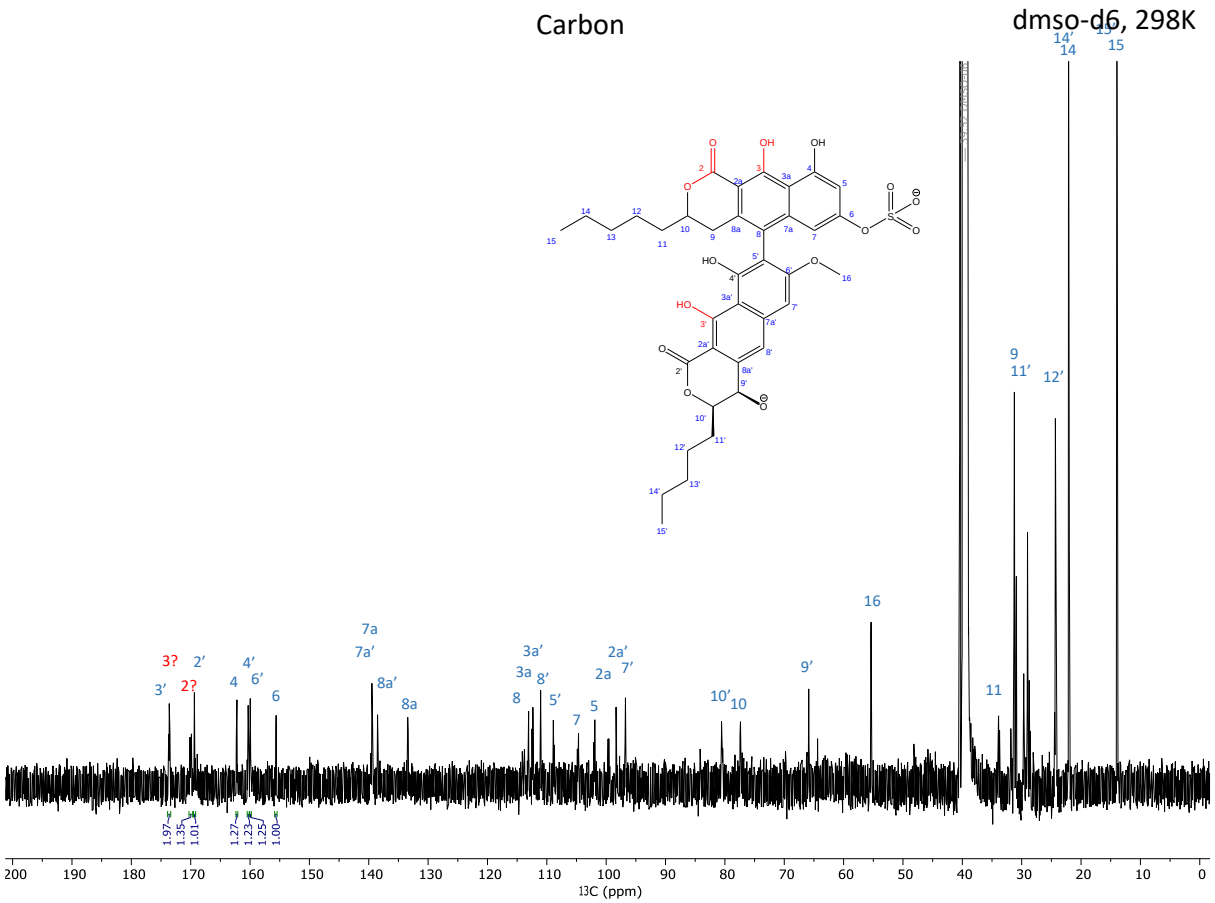

Supplementary Figure 12: Carbon spectrum of **1** in DMSO-d_6.

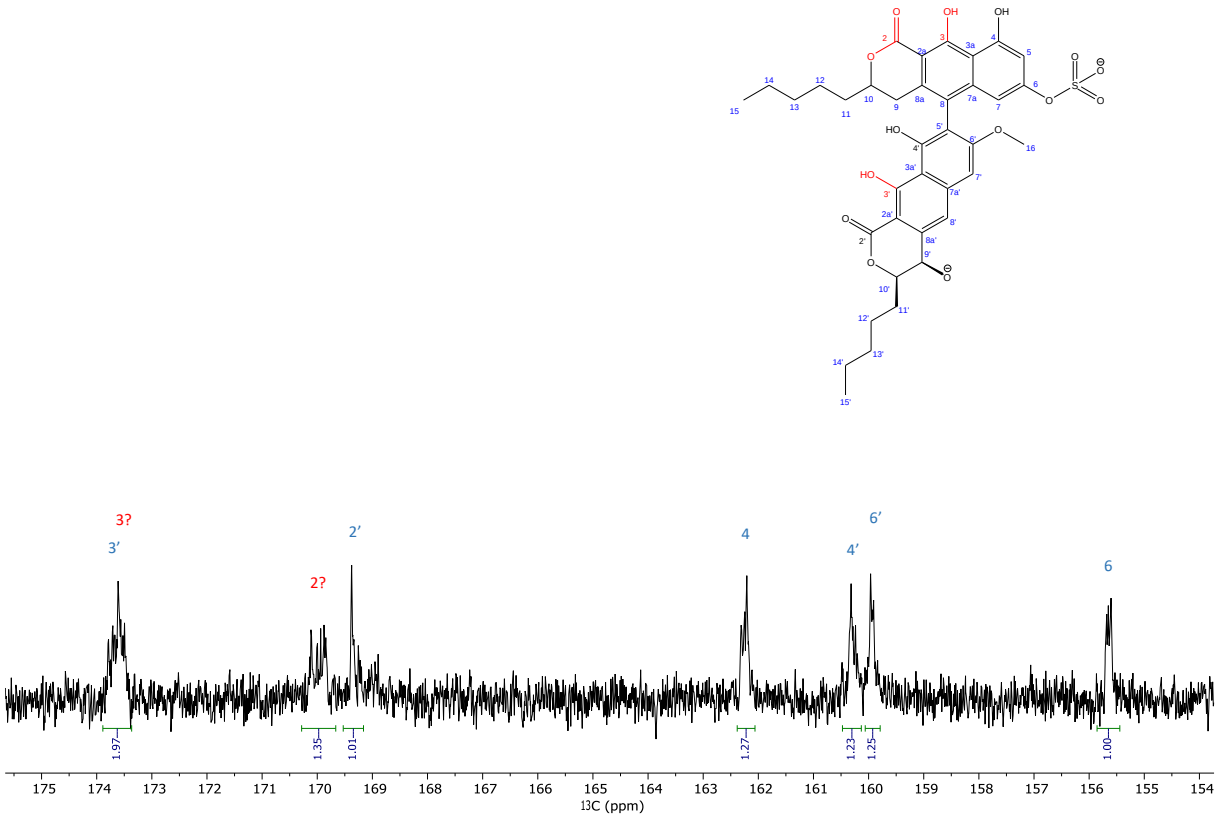

Supplementary Figure 13: Expansion of the carbonyl/deep aromatic region of the carbon spectrum in Supplementary Figure 12. Compared to **2**, **1** only has 4 carbons in the 160-165 range, and instead has 4 carbons in the 169-175 range. Integrals should be interpreted conservatively as it is ill advised to integrate carbon signals, but in this case we only qualitatively compare quaternary carbons to each other where the stead state noe enhancement is expected to be low and their T1 relaxation times are expected to be similarly slow. Without reading too much into it, it appears that C3 and C3' are not hidden among the other carbons in the 160-165 range but have indeed shifted to the more deshielded region normally associated with carbonyl resonances.

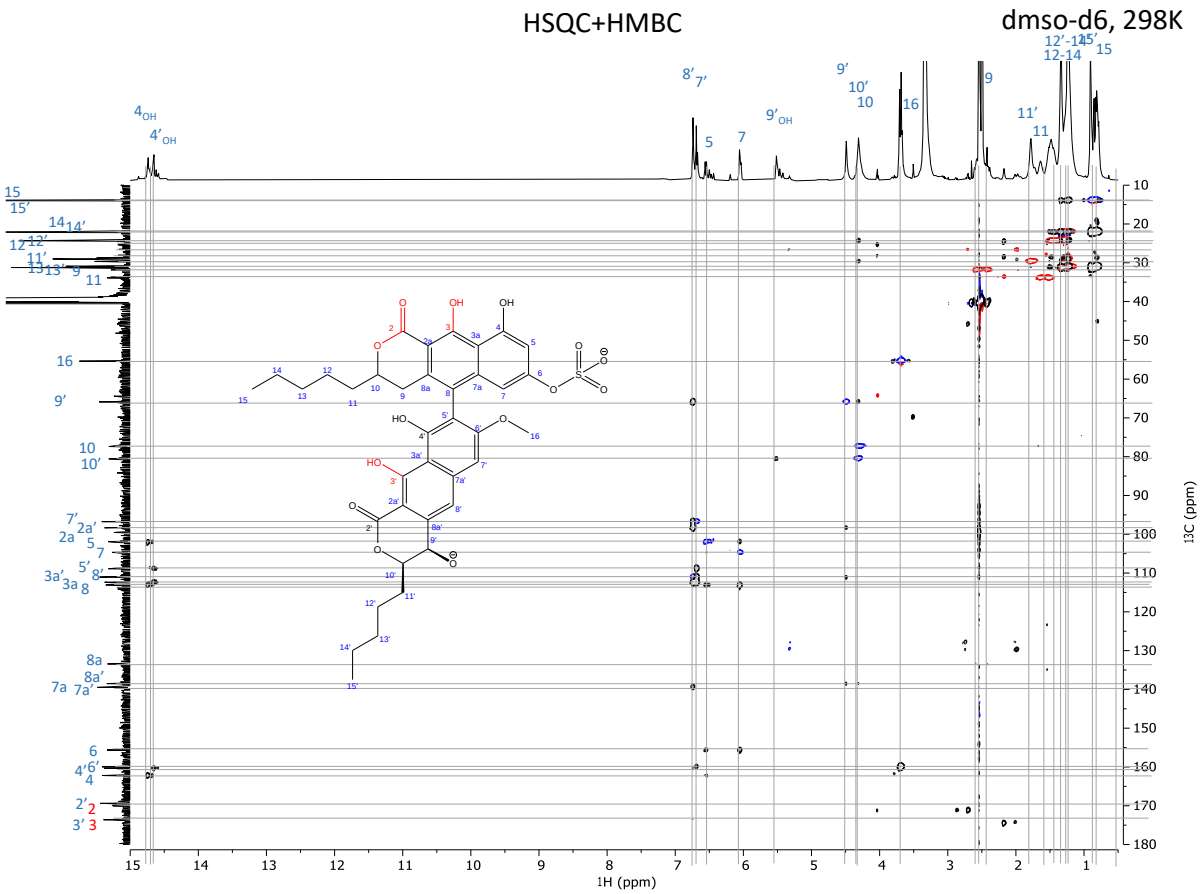

Supplementary Figure 14: Superimposed HSQC (red/blue) and HMBC (black) of **1** in DMSO-d_6.

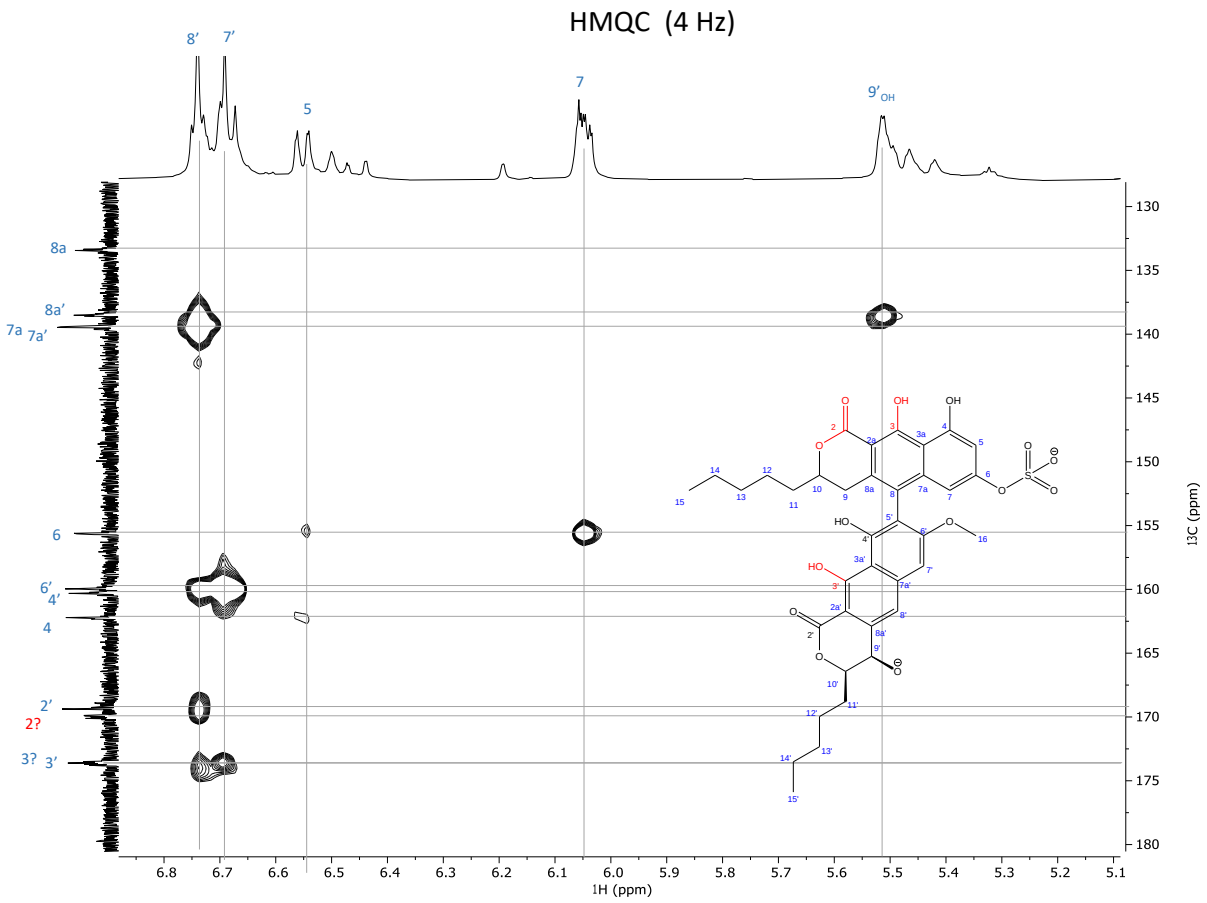

Supplementary Figure 15:HMQC optimized for 4 Hz $^{n}J_{CH}$ displays some of the important $^{4}J_{CH}$ for assignment.

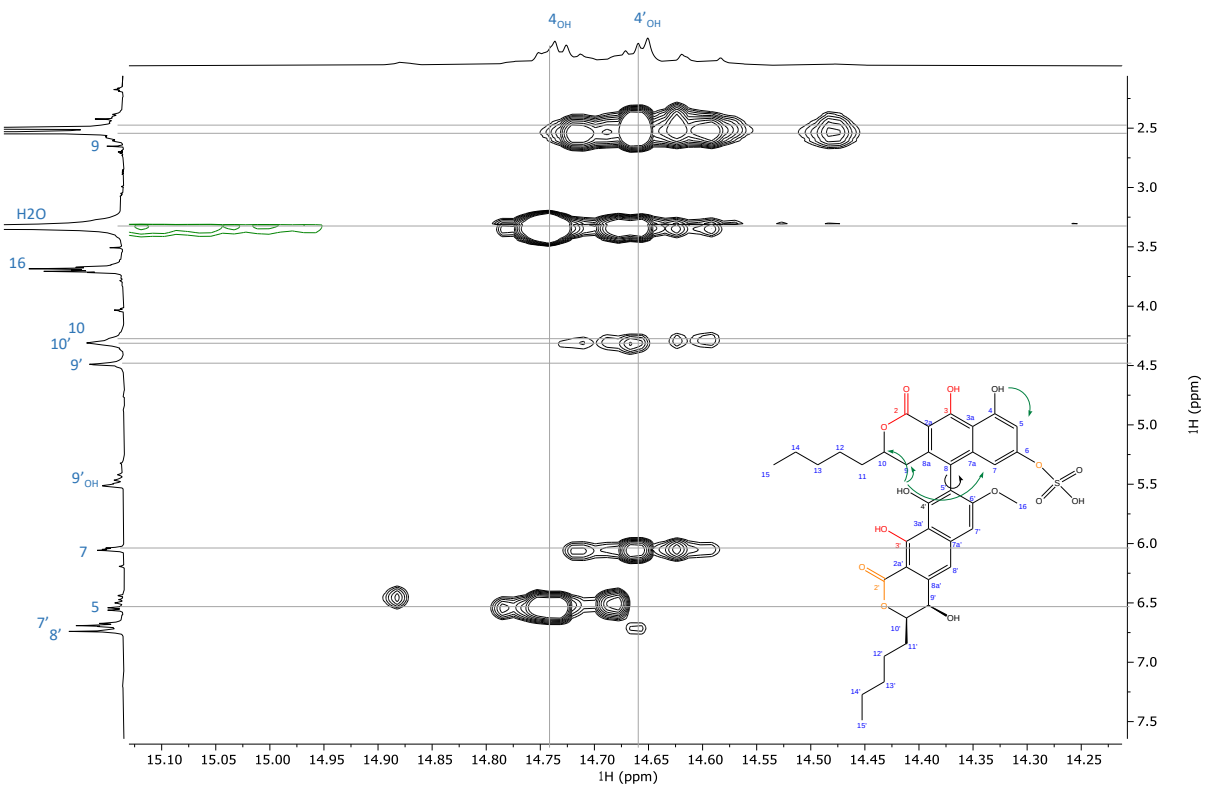

Supplementary Figure 16: NOESY (600 ms mixing time) of **1**. OH-4’ displays NOE correlations with both H7 and H9, showing that the two ring systems are either rotating quickly, exist in several conformations, or are offset relative to each other allowing one interaction on top of OH-4’ and the other below OH-4’.

Paper IV

molecules

MDPI

Article

Chlovalicin B, a Chlorinated Sesquiterpene Isolated from the Marine Mushroom *Digitatispora marina*

Marte Jenssen [1], Venke Kristoffersen [1], Kumar Motiram-Corral [2], Johan Isaksson [3], Teppo Rämä [1], Jeanette H. Andersen [1], Espen H. Hansen [1] and Kine Østnes Hansen [1,*]

[1] Marbio, Norwegian College of Fishery Science, UiT—The Arctic University of Norway, N-9037 Tromsø, Norway; marte.jenssen@uit.no (M.J.); venke.kristoffersen@uit.no (V.K.); teppo.rama@uit.no (T.R.); jeanette.h.andersen@uit.no (J.H.A.); espen.hansen@uit.no (E.H.H.)
[2] Servei de Ressonància Magnètica Nuclear, Universitat Autònoma de Barcelona, Bellaterra, E-08193 Barcelona, Spain; kumar.motiram.corral@gmail.com
[3] Department of Chemistry, UiT—The Arctic University of Norway, N-9037 Tromsø, Norway; johan.isaksson@uit.no
* Correspondence: kine.o.hanssen@uit.no; Tel.: +47-7-764-9272

Abstract: As part of our search for bioactive metabolites from understudied marine microorganisms, the new chlorinated metabolite chlovalicin B (**1**) was isolated from liquid cultures of the marine basidiomycete *Digitatispora marina*, which was collected and isolated from driftwood found at Vannøya, Norway. The structure of the novel compound was elucidated by spectroscopic methods including 1D and 2D NMR and analysis of HRMS data, revealing that **1** shares its molecular scaffold with a previously isolated compound, chlovalicin. This represents the first compound isolated from the *Digitatispora* genus, and the first reported fumagillin/ovalicin-like compound isolated from Basidiomycota. Compound **1** was evaluated for antibacterial activities against a panel of five bacteria, its ability to inhibit bacterial biofilm formation, for antifungal activity against *Candida albicans*, and for cytotoxic activities against malignant and non-malignant human cell lines. Compound **1** displayed weak cytotoxic activity against the human melanoma cell line A2058 (~50% survival at 50 μM). No activity was detected against biofilm formation or *C. albicans* at 50 μM, or against bacterial growth at 100 μM nor against the production of cytokines by the human acute monocytic leukemia cell line THP-1 at 50 μM.

Keywords: *Digitatispora marina*; marine fungus *sensu stricto*; Basidiomycota; bioprospecting; chlorinated secondary metabolite; natural products

Citation: Jenssen, M.; Kristoffersen, V.; Motiram-Corral, K.; Isaksson, J.; Rämä, T.; Andersen, J.H.; Hansen, E.H.; Hansen, K.Ø. Chlovalicin B, a Chlorinated Sesquiterpene Isolated from the Marine Mushroom *Digitatispora marina*. *Molecules* **2021**, *26*, 7560. https://doi.org/10.3390/molecules26247560

Academic Editor: Robert John Capon

Received: 16 November 2021
Accepted: 9 December 2021
Published: 13 December 2021

1. Introduction

Fungi isolated from the marine environment have proven to be a promising source of novel bioactive compounds [1]. Still, marine fungi are under-explored compared to their terrestrial counterparts [1,2], and the studies of marine fungi have primarily focused on just a few genera; *Penicillium*, *Aspergillus*, and, in part, *Fusarium* and *Cladosporium* [1]. The genus *Digitatispora* (phylum Basidiomycota) was first described by Gaston Doguet in 1962 [3]. It consists of two species: the type species of the genus *D. marina* Doguet and *D. lignicola* E.B.G. Jones [4], which both grow on and decay marine-submerged wood. The genus is one of the few genera of marine mushrooms and has been included in a number of phylogenetic studies. It has been placed in different orders, including Atheliales and Russulales [5,6]. In the most recent study by Sulistyo et al., *Digitatispora* was placed in the Niaceae family of the order Agaricales with node support from both bootstrap and posterior probability (BS/PP = 98/1.00) [6,7].

In a survey from 2014, Rämä et al. identified 28 filamentous species of marine fungi, with *Digitatispora marina* being the only basidiomycete [8]. Tibell et al. performed a survey on marine fungi from the Baltic Sea, revealing that only 2 of the 77 recorded

species belonged to Basidiomycota, 1 of which was *D. marina* [9]. In 2015, only 21 of the 1112 identified filamentous species of marine fungi were Basidiomycota, as opposed to Ascomycota, of which there were 805 species [5], showing that filamentous Basidiomycota are less widespread in marine habitats. The distribution of *D. marina* has been studied, but its biosynthetic potential has not yet been assessed. The current article provides new and valuable information regarding the biosynthetic potential of the marine genus *Digitatispora*.

As part of our ongoing search for novel bioactive metabolites from under-explored Arctic marine fungi, *Digitatispora marina* was selected for up-scaled cultivation and the isolation of its metabolites. The up-scaled culture was extracted and fractionated, and the fractions were analyzed using UHPLC-ESI-HRMS. This led to the identification of a chlorinated compound. When using the elemental composition of this compound as input in compound database searches, no likely hits were found, and the compound was therefore presumed to be novel. After compound isolation and structure elucidation, the compound was determined to be a new chlorinated chlovalicin variant, chlovalicin B (**1**). Compound **1** shares its molecular scaffold with the previously isolated compound chlovalicin (Figure S1) [10]. The structure of **1** differs from that of chlovalicin by having the methoxy group in the C3 position of the cyclohexane ring replaced by a hydroxyl group. To the best of our knowledge, this is the first publication of a compound isolated from the genus *Digitatispora* and the first isolation of a chlovalicin variant from a basidiomycete. Herein, the cultivation of *D. marina*, as well as the extraction, isolation, and structure elucidation of **1**, are described along with the evaluation of its antimicrobial, cytotoxic, and anti-inflammatory properties.

2. Results and Discussion

Digitatispora marina was isolated from driftwood of *Betula* (Figure S2) collected at Vannøya, Norway, in 2010 [8]. As part of a routine screening campaign of marine fungi, the *D. marina* isolate 008cD1.1 was cultivated using different cultivation schemes, and then extracted and fractionated into six fractions using RP-flash chromatography. The fractions were assayed for bioactivity, and different fractions from several different cultivation schemes were bioactive (cytotoxic and/or antibacterial). The capability of *D. marina* to produce bioactive metabolites had not been previously examined. This, coupled with the observed bioactivity in our routine screening campaign, was why the fungus was selected for further examination.

A large-scale cultivation of the fungus was initiated to obtain sufficient biomass for compound isolation. The fungus was cultivated in several rounds using a liquid malt extract medium, yielding a total of 30 L of fermentation broth. This medium was selected for the scale-up as the fungus grew well in it during the initial cultivation. The metabolites were harvested from the fermentation broth using Diaion® HP20 resin and extracted with methanol, resulting in 25.1 g of dry extract. Aliquots of the fungal extract were repeatedly fractionated into six fractions using RP-flash chromatography. The fractions were analyzed using UHPLC-ESI-HRMS in an attempt to identify novel compounds. In flash fraction five (eluting at 100% methanol, yield 244.3 mg), a compound with the distinctive isotopic pattern of a monochlorinated compound (*m*/*z* 341.1132 and 343.1103 in a 3:1 ratio) was observed. The low- and high-collision energy mass spectra of **1** can be seen in Figure S3. The elemental composition was used as the input in various database searches (e.g., Dictionary of Natural Products and ChemSpider), yielding no plausible hits. The compound was therefore suspected to be novel, and it was targeted for isolation. The compound was isolated from flash fraction five using mass-guided preparative HPLC fractionation, yielding 0.6 mg of **1**.

Compound **1** (1-(chloromethyl)-1,2,3-trihydroxy-2-(1′-methyl-2′-(5′-methylbut-4′-en) oxiran-1′-yl) cyclohexan-4-one) was isolated as a brown powder, and its structure was elucidated by high-resolution MS and NMR (Figure 1). The UV λ_{max} of **1** was 221.60 nm. The molecular formula of **1** was established as $C_{15}H_{23}O_5Cl$ (four degrees of unsaturation) by UHPLC-ESI-HRMS ($[M + Na]^+$ = *m*/*z* 341.1132). A set of 1D (^1H and ^{13}C) and 2D (COSY,

ROESY, HSQC, HMBC and H2BC) NMR experiments were performed to elucidate the structure (Figures S4–S9).

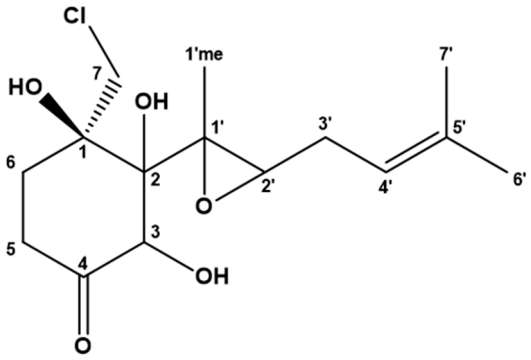

Figure 1. The structure of chlovalicin B (**1**).

The ^{1}H spectrum displayed all the expected 23 protons, and all 15 carbons were detected in the ^{13}C spectrum. HSQC allowed the identification of three methyl- and four methylene groups, one methine proton (5.22 ppm), as well as two aliphatic CH groups with deshielded chemical shifts (4.83 and 2.79 ppm). The three remaining protons were attributed to hydroxyl protons (4.27, 4.45, and 5.79 ppm). Four quaternary carbons (75.3, 81.7, 60.4, and 133.9 ppm) and one ketone carbon remained unassigned (209.6 ppm). COSY, HMBC, and H2BC showed sufficient correlations to unambiguously connect the observed fragments into **1**. The observed correlations are summarized in Table 1 and Figure 2.

Table 1. NMR spectroscopic data [a] of chlovalicin B (**1**) (600 MHz, DMSO-d_6).

Position	δ_C, Type	δ_H (*J* in Hz)	COSY	HMBC [b]
1	75.3, C			7a, 6a, 6b
1_{OH}		5.79, s		
2	81.7, C			3, 7a, 2′, 6a, 1′Me
2_{OH}		4.27, s		
3	75.9, CH	4.83, d (7.1)	3_{OH}	5b
3_{OH}		4.45, d (8.3)		
4	209.6, C			
5a	34.4, CH_2	2.64, td (13.9, 6.9)	6a, 6b	6a, 6b
5b		2.15, ddd (14.2, 5.1, 1.4)	5b	
6a	31.5, CH_2	2.09, ddd (13.4, 6.9, 1.6)	5a, 5b, 6a	7a, 7b, 5a, 5b
6b		1.91, td (13.5, 5.3)		
7a	51.9, CH_3	3.70, d (11.0)	7	
7b		3.63, d (11.0)		
1′Me	15.8, CH_3	1.48, s		
1′	60.4, C			2′, 3′b, 1′Me
2′	55.2, CH	2.79, t (6.5)	3′a, 3′b	3′a, 3′b. 6′, 7′, 1′Me
3′a	26.7, CH_2	2.19, dt (14.6, 7.1)	2′, 4′	2′, 7′
3′b		2.27, m [c]		
4′	119.2, CH	5.21, t (7.4)	3′a, 3′b	
5′	133.9, C			3′a, 3′b, 6′, 7′
6′	25.5, CH_3	1.70, s		4′, 7′
7′	17.8, CH_3	1.63, s		4′, 6′

[a] ^{1}H ^{1}D, ^{13}C ^{1}D, ^{1}H-COSY and ^{1}H, ^{13}C-HMBC, [b] ^{1}H ^{1}D, ^{13}C-HMBC correlations are from the proton (a) stated to the indicated carbon, [c] overlapping and/or broadened peaks impending complete analysis.

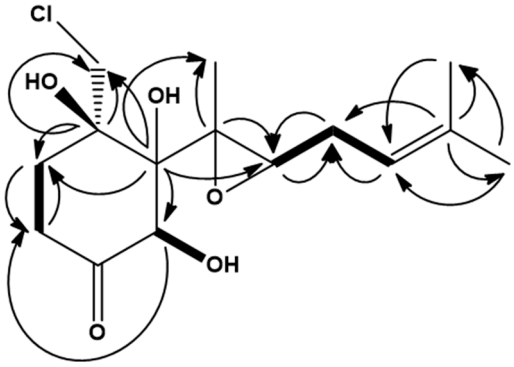

Figure 2. Selected COSY (bold) and HMBC (black arrows) correlations used to assemble the structure of chlovalicin B (**1**).

In more detail, long-range proton-carbon correlations between 6′, 7′, and 4′, plus a clear ROE between 4′ and 6′, established the methyl vinyl group. The spin system could be traced continuously through the molecule; the key correlations being the $^{3}J_{C2H2'}$, $^{3}J_{C2H1'Me}$, $^{3}J_{C2H2'}$, and $^{3}J_{C1'H3'}$ to cross the epoxide, and from there, the ring system displayed all the expected long-range correlations. The epoxide was indicated by both carbons being less deshielded by the oxygen (55.2 and 60.4 ppm) than expected for free hydroxyls (70–80 ppm). Furthermore, in epoxides, it is expected that the one-bond proton–carbon coupling is around ~180 Hz, which is unusually high compared to the normally expected ~140 Hz for sp3 carbons next to oxygens. The $^{1}J_{CH2'}$ is estimated to be ~177 Hz from the incomplete filtering of the one bond coupling in the HMBC spectra for **1**, this supports the presence of an epoxide.

The only remaining potential uncertainty was the position of the chlorine atom vis-à-vis the hydroxyl groups, as the influences on the attached carbon chemical shifts were similar. Three free hydroxyls were observable (5.79, 4.45, and 4.27 ppm). The 3-OH (4.45 ppm) could be assigned to C3 through a $^{3}J_{H3HO3}$ COSY correlation, while the other two were connected to carbons not carrying any proton. The ROESY pattern is not entirely unambiguous, since no conformation analysis was conducted, but it is consistent with the assignment of 1-OH at 5.79 ppm and 2-OH at 4.27 ppm, and the relative stereochemistry reported in the original chlovalicin publication [10]. ROEs are observed between H1′Me and H3, as well as between 2-OH and H7b, indicating that the 2-OH and 3-OH are both on the same side of the ring, which is consistent with the absolute configuration reported for chlovalicin where both hydroxyls and the chlorinated methyl group are below the ring [11]. Furthermore, in carbon spectra that are sufficiently well-resolved, it can be possible to observe a small $^{37}/^{35}$Cl isotope shift in the carbon resonances bound to chlorine [12]. A possible isotope shift of 1.2 Hz was observed for C1 (Figure S5), but the possibility cannot be excluded that the observed splitting is caused by slowly exchanging conformations since the line width is broadened, and the shift is slightly larger than the expected 0.5–0.9 Hz at 150 MHz carbon Larmor frequency. The isotope shift is, however, conformation- and temperature-dependent, making it a viable explanation. Overall, the carbon chemical shifts of **1** are in excellent agreement with the published chemical shifts of chlovalicin [10], except for the C3, which is the carbon where **1** has a hydroxyl group instead of a methoxy group (Figure S5).

Compound **1** is structurally related to several other compounds, including fumagillin, ligerin, ovalicin, and chlovalicin (structures in Figure S1) [10,13–18]. These compounds share a cyclohexane ring with a terpene-derived aliphatic chain in the C2 position and one or two epoxides (one epoxide when there is a chloride attached to the cyclohexane unit, as with chlovalicin and **1**). Chlovalicin was isolated from the fermentation broth of a soil-derived *Sporothrix* sp. fungus in 1996 [10,16]. Fumagillin was first isolated in 1949 from a culture of *Aspergillus fumigatus* [14,15]. These types of compounds have also been isolated from marine-derived fungi. Chlovalicin was isolated from a marine-derived *Aspergillus*

niger in 2017 [19], and ligerin from a marine-derived *Penicillium* sp. [18]. Both chlovalicin and ligerin contain chloride in their structures. It is not uncommon for marine organisms to incorporate halogens into their chemical structures [20], as chloride was present in large amounts both in seawater and the artificial sea salts used in the current study. Compound **1** shares its molecular scaffold with chlovalicin. Compared to chlovalicin, **1** has a hydroxyl group in the C3 position where chlovalicin has a methoxy group. Chlovalicin and **1** are similar to ovalicin, but they are substituted with a chlorinated methylene and a hydroxy moiety at the C1 position of the cyclohexane ring, represented by an epoxide ring in ovalicin.

These compounds were studied in a wide range of bioactivity assays, including anticancer and antimicrobial assays, and for their ability to inhibit angiogenesis [13]. Chlovalicin was found to inhibit the growth of IL-6 dependent MH60 cells (IC_{50} = 7.5 μM) and B16 mouse melanoma cells (IC_{50} = 37 μM) [16]. Chlovalicin also displayed inhibitory activity on osteoclastogenesis [21]. The bioactivity of **1** was evaluated. The compound was tested for antibacterial activities against five bacterial strains; for the ability to inhibit biofilm formation by *S. epidermidis*; for antiproliferative activities against two human cell lines, one malignant and one non-malignant; and for antifungal activity against *Candida albicans*. Compound **1** did not show any activities against the bacterial strains at 100 μM or toward biofilm formation at a concentration of 50 μM. No antifungal activity against *Candida albicans* was discovered at a concentration of 100 μM. As **1** was inactive in the above-mentioned assays at concentrations, which excludes chlovalicin B as a drug lead for any of the indicated areas, testing the compound at a higher concentration was not prioritized due to the limited available amount. It displayed weak activity against the human melanoma cell line A2058 at 50 μM (~50% cell survival). No activity was observed against the human non-malignant lung fibroblast cell line MRC-5 at 50 μM. Previously, chlovalicin showed activity against a mouse melanoma cell line, B16, with IC_{50} = 37 μM [16], while displaying no or significantly weaker activity against other cell lines. This may indicate that the chlovalicins affect a common cellular target on melanoma cell lines, since both A2058 and B16 originate there. However, further testing against melanoma cell lines was not prioritized due to the relatively weak observed effect.

We isolated 0.6 mg of chlovalicin B (**1**) from 30 L of liquid culture of the marine fungus *D. marina*. This is the first report of isolated compounds from the *Digitatispora* genus, and the first fumagillin/ovalicin derivative isolated from a basidiomycete. The current study adds to the existing knowledge on the cultivation of marine fungi with the purpose of isolating novel compounds from these understudied organisms.

3. Materials and Methods

3.1. General Experimental Procedures

NMR spectra were acquired in DMSO-d_6 on a Bruker Avance III HD spectrometer (Bruker, Billerica, MA, USA) operating at 600 MHz for protons and equipped with an inverse TCI cryo probe enhanced for ^{1}H, ^{13}C, and ^{2}H. All NMR spectra were acquired at 298 K, in 3 mm solvent-matched Shigemi tubes using standard pulse programs for proton, carbon, HSQC, HMBC, COSY, and ROESY, with gradient selection and adiabatic versions where applicable. $^{1}H/^{13}C$ chemical shifts were referenced to the residual solvent peak (DMSO-d_6: δ_H = 2.50, δ_C = 39.51). UHPLC-ESI-HRMS was performed using an Acquity I-class UPLC with an Acquity UPLC C18 column (1.7 μm, 2.1 mm × 100 mm), coupled to a Vion IMS QToF and a PDA detector (all from Waters, Milford, MA, USA). ESI+ ionization was used. The gradient extended over 12 min, increasing from 10% to 90% acetonitrile (LiChrosolv®, Supelco, Bellefonte, PA, USA) with 0.1% formic acid (Sigma-Aldrich, Steinheim, Germany) in Milli-Q® H_2O, with a flow rate of 0.45 mL/min. A Waters UNIFI 1.8.2 Scientific Information System was used to process and analyze the data. The preparative HPLC system consisted of a 600 HPLC pump, a 3100 mass spectrometer, a 2996 photo diode array detector, and a 2767 sample manager (all from Waters). The system was controlled with MassLynx version 4.1.

3.2. Fungal Material and Cultivation Condition

The fungus was isolated from driftwood of the *Betula* sp. by Teppo Rämä, collected at Vannøya, Norway, in 2010 [8]. The fungus was morphologically identified as *Digitatispora marina* and sequenced by Rämä. The strain ITS sequence and LSU sequence are accessible from Genbank with the NCBI accession numbers KM272371 and KM272362, respectively. The fungus was stored as mycelium on submerged pieces of agar in a 20% glycerol solution at −80 °C. It was grown and kept on plates with malt agar and sea salts (4 g/L store bought malt extract (Moss Maltextrakt, Jensen & Co AS, Lillestrøm, Norway), 40 g/L sea salts (S9883, Sigma-Aldrich), 15 g/L agar (A1296, Sigma-Aldrich), and Milli-Q® H_2O). Agar plates with fresh mycelium were used to inoculate the liquid culture, using approximately $\frac{1}{4}$ to $\frac{1}{2}$ agar plate per flask. For the isolation of compounds, the fungus was cultivated in a liquid malt extract medium containing 4 g/L malt extract, 40 g/L sea salts, and Milli-Q® H_2O. The fungus was cultivated over several rounds in 250 mL media in 1000 mL culture flasks for 73–110 days at 13 °C without shaking. The total volume of culture used to obtain **1** was 30 L.

3.3. Extraction and Isolation

After cultivation, the metabolites were extracted from the fermentation broth using Diaion® HP-20 resin (Supelco, Bellefonte, PA, USA), and extracted from the resin using methanol (HPLC grade, VWR, Radnor, PA, USA) in two rounds, as described previously [22]. The cultures were incubated with the resin for 3–5 days before the extraction. The resin and fungal mycelium were separated from the liquid by vacuum filtration through a cheesecloth filter (Dansk hjemmeproduktion, Ejstrupholm, Denmark). The extract was dried under reduced pressure at 40 °C, yielding an extract of 25.1 g. The extract was fractionated using RP-flash chromatography (Biotage SP4™ system, Uppsala, Sweden), with Diaion® HP-20SS resin as the stationary phase. The extract was dissolved in 90% methanol and fractionated (maximum 2 g extract per round of fractionation). An aliquot was combined with 2 g resin before removing the solvent under reduced pressure. The column was equilibrated using 5% methanol before the extract-column material was applied to the top of the pre-equilibrated column. The following stepwise elution method with a flow rate of 12 mL/min was used: methanol:water (5:95, 25:75, 50:50, 75:25; 6 min per step) followed by methanol (100% over 12 min), methanol:acetone (50:50 over 4 min), and finally acetone (100% over 10 min). The methanol:water eluate was collected in 6 min fractions, yielding fractions one to four the first 6 min of the 100% methanol step was collected in one fraction yielding fraction five,; and the remaining eluate was collected in one fraction, yielding fraction six. All fractions were subsequently dried under reduced pressure at 40 °C. In preparation for the isolation of **1**, the eluent resulting in flash fraction five (samples eluting in the first six minutes of 100% methanol) from repeated rounds of flash fractionation were pooled and dried under vacuum, yielding 244.3 mg sample.

Isolation of **1** from the flash fraction was performed using mass-guided preparative HPLC. The first round of isolation of **1** was performed with an XSelect CSH Prep Fluoro-Phenyl column (5 µm, 10 mm × 250 mm, Waters) with a gradient of 10–100% acetonitrile over 15 min with a flow rate of 6 mL/min. In order to remove additional impurities, a second isolation step was performed using an XSelect™ CSH™ phenyl hexyl prep column (5 µm, 10 × 250 mm, Waters), with a gradient of 10–100% acetonitrile over 15 min with a flow rate of 6 mL/min, yielding 0.6 mg of **1**.

Chlovalicin B (1)

Brown powder. UV = (ACN) λ_{max} 221.60 nm. ^{1}H and ^{13}C NMR data (see Table 1). HRMS *m*/*z* 341.1132 $[M + Na]^+$ (calculated for $C_{15}H_{24}O_5ClNa$ = 341.1132). The collision cross-section (CCS) of the sodium adduct of **1** was 178.11 $Å^2$.

3.4. Bioactivity Testing of Compound **1**

Compound **1** was tested in a variety of assays to broadly assess its possible biological activities. The compound was tested for biofilm inhibition properties against a biofilm form-

ing *Staphylococcus epidermidis*, as previously described [22]. The compound was assayed at one concentration, 50 μM, using three technical replicates (n = 3). The compound's ability to inhibit the growth of five bacterial strains was assessed, as previously described [22], and at 100 μM using three technical replicates (n = 3). The assayed strains were the following: *Staphylococcus aureus* (ATCC 25923), *Escherichia coli* (ATCC 25922), *Pseudomonas aeruginosa* (ATCC 27853), *Enterococcus faecalis* (ATCC 29212), and *Streptococcus agalactiae* (ATCC 12386); all strains were from LGC Standards (Teddington, United Kingdom). Antifungal activity was assayed against *Candida albicans* at 50 μM, as described previously [23]. Potential anti-inflammatory activity was assayed at 50 μM in an ELISA-based assay that monitors the tumor necrosis factor α (TNFα) and interleukin-1β (IL-1β) production of a human acute monocytic leukemia cell line (THP-1) in the presence of **1**, as previously described [24]. Lastly, **1** was assessed for its antiproliferative activities at 50 μM toward the human melanoma cell line A2058 and the human non-malignant lung fibroblast cell line MRC-5 as previously described [25].

4. Conclusions

As part of our ongoing search for novel compounds from understudied marine fungi, chlovalicin B (**1**) was isolated from the liquid culture of a marine mushroom, *Digitatispora marina*. This represents the first compound isolated from the *Digitatispora* genus, and the first reported fumagillin/ovalicin-like compound isolated from Basidiomycota. The current study adds to the available knowledge on the biosynthetic potential of marine fungi *sensu stricto*, especially obligate marine Basidiomycetes.

Supplementary Materials: The following are available online. Figure S1: Structure of chlovalicin B (**1**) and the previously isolated compounds chlovalicin, ovalicin, and fumagillin; Figure S2: *Digitatispora marina* in different growth conditions; Figure S3: Low- and high-collision energy mass spectra of chlovalicin B (**1**) in ESI+; Figure S4: ^{1}H NMR (600 MHz, DMSO-d_6) spectrum of chlovalicin B (**1**); Figure S5: ^{13}C (151 MHz, DMSO-d_6) spectrum of chlovalicin B (**1**); Figure S6: HSQC + HMBC (600 MHz, DMSO-d_6) spectrum of chlovalicin B (**1**); Figure S7: COSY (600 MHz, DMSO-d_6) spectrum of chlovalicin B (**1**); Figure S8: H2BC (600 MHz, DMSO-d_6) spectrum of chlovalicin B (**1**); Figure S9: ROESY (600 MHz, DMSO-d_6) spectrum of chlovalicin B (**1**).

Author Contributions: Conceptualization, M.J., T.R., J.H.A., E.H.H. and K.Ø.H.; methodology, M.J., V.K., K.M.-C. and J.I.; validation, M.J., V.K., K.M.-C., J.I. and K.Ø.H.; formal analysis, M.J. and K.Ø.H.; investigation, M.J., V.K., K.Ø.H. and K.M.-C.; resources, J.H.A.; data curation, M.J., K.Ø.H., K.M.-C. and J.I.; writing—original draft preparation, M.J. and K.Ø.H.; writing—review and editing, M.J., K.Ø.H., E.H.H. and J.H.A.; visualization, M.J. and K.Ø.H.; supervision, J.H.A. and E.H.H.; project administration, M.J. and K.Ø.H.; funding acquisition, J.H.A. All authors have read and agreed to the published version of the manuscript.

Funding: This research was funded by the DigiBiotics project of the Research Council of Norway (Project ID 269425), the AntiBioSpec project of UiT the Arctic University of Norway (Cristin ID 20161323, the Ocean Medicines project (H2020-MSCA-RISE; Grant ID 690944), and the Centre for New Antibacterial Strategies at UiT the Arctic University of Norway. The publication charge for this article has been funded by the publication fund of UiT the Arctic University of Norway.

Institutional Review Board Statement: Not applicable.

Informed Consent Statement: Not applicable.

Data Availability Statement: The data are available within the article and in the Supplementary Materials.

Acknowledgments: The authors would like to acknowledge the technical support by Kirsti Helland and Marte Albrigtsen by execution of the bioactivity assays and the contribution of Chun Li in the sequencing of the genetic elements of the isolate.

Conflicts of Interest: The authors declare no conflict of interest.

Sample Availability: Samples of the compound are not available from the authors.

References

1. Imhoff, J.F. Natural products from marine fungi-still an underrepresented resource. *Mar. Drugs* **2016**, *14*, 19. [CrossRef]
2. Overy, D.P.; Rämä, T.; Oosterhuis, R.; Walker, A.K.; Pang, K.-L. The neglected marine fungi, *sensu stricto*, and their isolation for natural products' discovery. *Mar. Drugs* **2019**, *17*, 42. [CrossRef]
3. Doguet, G. *Digitatispora marina*, n-g-, n.sp., Basidiomycète marin. *C. R. Hebd. Séances Acad. Sci.* **1962**, *254*, 4336–4338.
4. Jones, E.B.G. *Digitatispora lignicola*, a new marine lignicolous Basidiomycotina. *Mycotaxon* **1986**, *27*, 155–159.
5. Jones, E.B.G.; Suetrong, S.; Sakayaroj, J.; Bahkali, A.H.; Abdel-Wahab, M.A.; Boekhout, T.; Pang, K.-L. Classification of marine Ascomycota, Basidiomycota, Blastocladiomycota and Chytridiomycota. *Fungal Divers.* **2015**, *73*, 1–72. [CrossRef]
6. Sulistyo, B.P.; Larsson, K.-H.; Haelewaters, D.; Ryberg, M. Multigene phylogeny and taxonomic revision of *Atheliales* s.l.: Reinstatement of three families and one new family, *Lobuliciaceae fam*. nov. *Fungal Biol.* **2021**, *125*, 239–255. [CrossRef]
7. Abdel-Wahab, M.A.; Jones, E.B.G.; Abdel-Aziz, F.A.; Bahkali, A.H. *Nia lenicarpa* sp. nov. (Niaceae, Agaricales) from Red Sea mangroves in Saudi Arabia with comments on *Nia vibrissa*. *Phytotaxa* **2019**, *406*, 157–168. [CrossRef]
8. Rämä, T.; Mathiassen, G.; Kauserud, H. Marine fungi new to Norway, with an outlook to the overall diversity. *Agarica* **2014**, *35*, 35–47.
9. Tibell, S.; Tibell, L.; Pang, K.-L.; Calabon, M.; Jones, E.B.G. Marine fungi of the Baltic Sea. *Mycology* **2020**, *11*, 195–213. [CrossRef]
10. Takamatsu, S.; Kim, Y.P.; Komiya, T.; Sunazuka, T.; Hayashi, M.; Tanaka, H.; Komiyama, K.; Omura, S. Chlovalicin, a new cytocidal antibiotic produced by *Sporothrix* sp. FO-4649. II. Physicochemical properties and structural elucidation. *J. Antibiot.* **1996**, *49*, 635–638. [CrossRef] [PubMed]
11. Aliev, A.E.; Harris, K.D.M. $^{37}Cl/^{35}Cl$ isotope effects in ^{13}C NMR spectroscopy of chlorohydrocarbons. *Magn. Reson. Chem.* **1993**, *31*, 54–57. [CrossRef]
12. Sergeyev, N.M.; Sandor, P.; Sergeyeva, N.D.; Raynes, W.T. $^{37}Cl/^{35}Cl$-Induced ^{13}C isotope shifts in chlorinated methanes. *J. Magn. Reson.* **1995**, *115*, 174–182. [CrossRef]
13. Yamaguchi, J.; Hayashi, Y. Syntheses of fumagillin and ovalicin. *Chem. Eur. J.* **2010**, *16*, 3884–3901. [CrossRef]
14. Eble, T.E.; Hanson, F.R. Fumagillin, an antibiotic from *Aspergillus funigatus* H-3. *Antibiot. Chemother.* **1951**, *1*, 54–58.
15. Hanson, F.R.; Eble, T.E. An antiphage agent isolated from *Aspergillus* sp. *J. Bacteriol.* **1949**, *58*, 527–529. [CrossRef] [PubMed]
16. Hayashi, M.; Kim, Y.-P.; Takamatsu, S.; Preeprame, S.; Komiya, T.; Masuma, R.; Tanaka, H.; Komiyama, K.; Omura, S. Chlovalicin, a new cytocidal antibiotic produced by *Sporothrix* sp. FO-4649. I. Taxonomy, fermentation, isolation and biological activities. *J. Antibiot.* **1996**, *49*, 631–634. [CrossRef]
17. Sigg, H.P.; Weber, H.P. Isolierung und strukturaufklärung von ovalicin. *Helv. Chim.* **1968**, *51*, 1395–1408. [CrossRef]
18. Vansteelandt, M.; Blanchet, E.; Egorov, M.; Petit, F.; Toupet, L.; Bondon, A.; Monteau, F.; Le Bizec, B.; Thomas, O.P.; Pouchus, Y.F.; et al. Ligerin, an antiproliferative chlorinated sesquiterpenoid from a marine-derived *Penicillium* Strain. *J. Nat. Prod.* **2013**, *76*, 297–301. [CrossRef]
19. Uchoa, P.K.S.; Pimenta, A.T.A.; Braz-Filho, R.; de Oliveira, M.d.C.F.; Saraiva, N.N.; Rodrigues, B.S.F.; Pfenning, L.H.; Abreu, L.M.; Wilke, D.V.; Florêncio, K.G.D.; et al. New cytotoxic furan from the marine sediment-derived fungi *Aspergillus niger*. *Nat. Prod. Res.* **2017**, *31*, 2599–2603. [CrossRef]
20. Neumann, C.S.; Fujimori, D.G.; Walsh, C.T. Halogenation strategies in natural product biosynthesis. *Chem. Biol.* **2008**, *15*, 99–109. [CrossRef]
21. Liu, D.-H.; Sun, Y.-Z.; Kurtán, T.; Mándi, A.; Tang, H.; Li, J.; Su, L.; Zhuang, C.-L.; Liu, Z.-Y.; Zhang, W. Osteoclastogenesis regulation metabolites from the coral-associated fungus *Pseudallescheria boydii* TW-1024-3. *J. Nat. Prod.* **2019**, *82*, 1274–1282. [CrossRef] [PubMed]
22. Schneider, Y.; Jenssen, M.; Isaksson, J.; Hansen, K.Ø.; Andersen, J.H.; Hansen, E.H. Bioactivity of serratiochelin A, a siderophore isolated from a co-culture of *Serratia* sp. and *Shewanella* sp. *Microorganisms* **2020**, *8*, 1042. [CrossRef] [PubMed]
23. Jenssen, M.; Rainsford, P.; Juskewitz, E.; Andersen, J.H.; Hansen, E.H.; Isaksson, J.; Rämä, T.; Hansen, K.Ø. Lulworthinone, a new dimeric naphthopyrone from a marine fungus in the family Lulworthiaceae with antibacterial activity against clinical methicillin-resistant *Staphylococcus aureus* isolates. *Front. Microbiol.* **2021**, *12*, 730740. [CrossRef]
24. Lind, K.F.; Hansen, E.; Østerud, B.; Eilertsen, K.-E.; Bayer, A.; Engqvist, M.; Leszczak, K.; Jørgensen, T.Ø.; Andersen, J.H. Antioxidant and anti-inflammatory activities of barettin. *Mar. Drugs* **2013**, *11*, 2655–2666. [CrossRef] [PubMed]
25. Hansen, K.Ø.; Isaksson, J.; Bayer, A.; Johansen, J.A.; Andersen, J.H.; Hansen, E. Securamine derivatives from the Arctic bryozoan *Securiflustra securifrons*. *J. Nat. Prod.* **2017**, *80*, 3276–3283. [CrossRef]

SUPPLEMENTARY MATERIAL

Chlovalicin B, a Chlorinated Sesquiterpene Isolated from the Marine Mushroom *Digitatispora marina*

Marte Jenssen[1], Venke Kristoffersen[1], Kumar Motiram-Corral[2], Johan Isaksson[3], Teppo Rämä[1], Jeanette H. Andersen[1], Espen H. Hansen[1] and Kine Østnes Hansen[1,*]

[1]*Marbio, UiT–The Arctic University of Norway, Tromsø N-9037, Norway*

[2]*Servei de Ressonància Magnètica Nuclear, Universitat Autònoma de Barcelona, E-08193 Bellaterra, Barcelona, Spain*

[3]*Department of Chemistry, UiT–The Arctic University of Norway, Tromsø N-9037, Norway*

*Corresponding author

E-mail: kine.o.hanssen@uit.no

Supplementary Material Table of Contents

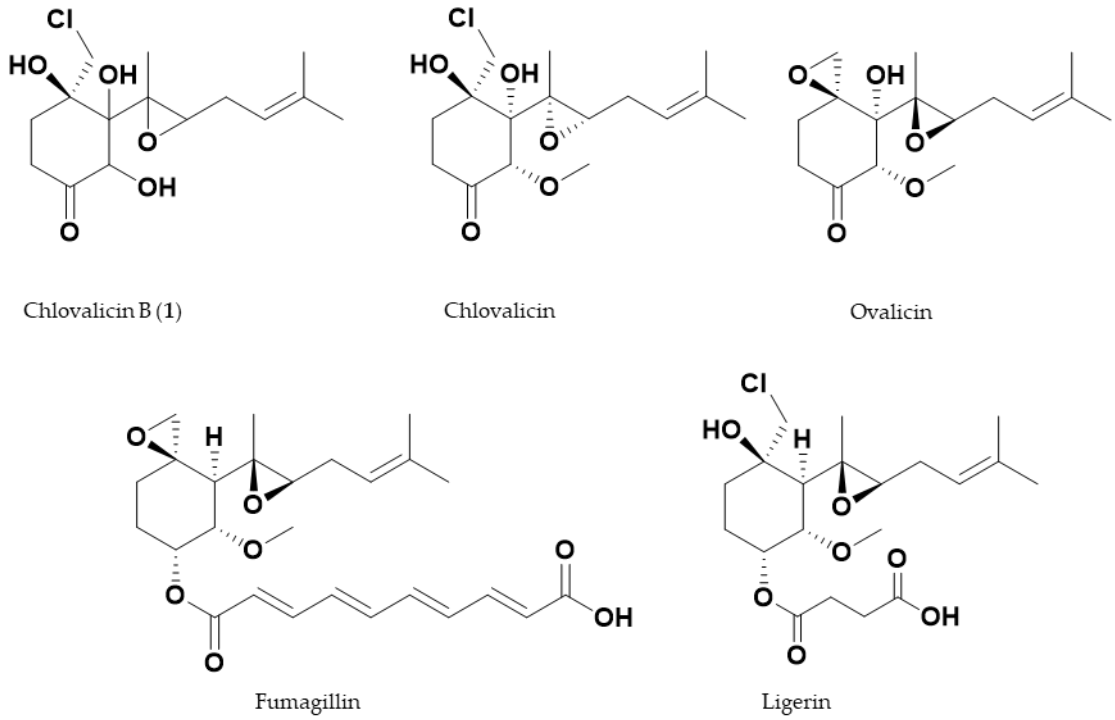

Figure S1. Structure of chlovalicin B (**1**) and the previously isolated compounds chlovalicin, ovalicin, fumagillin and ligerin.

Figure S2. *Digitatispora marina* in different growth conditions. 1) *D. marina* growing on driftwood of *Betula* sp. Photo: Teppo Rämä, 2) *D. marina* grown in liquid culture in malt extract medium supplemented with sea salts. Photo: Marte Jenssen, 3) *D. marina* grown on corn meal agar (top) and malt extract agar (bottom). Photo: Marte Jenssen

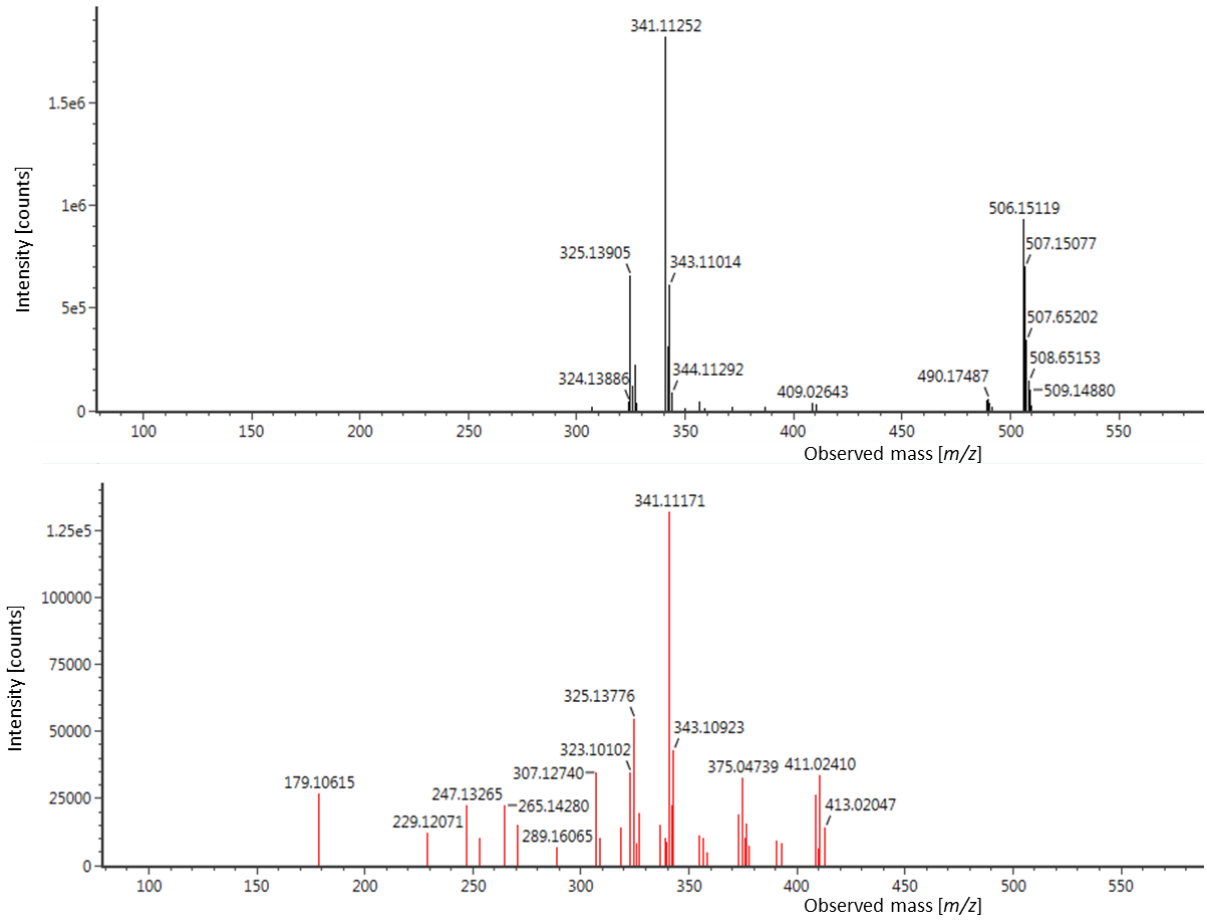

Figure S3. Low-collision (top) and high-collision (bottom) energy mass spectra of chlovalicin B (**1**) in ESI+

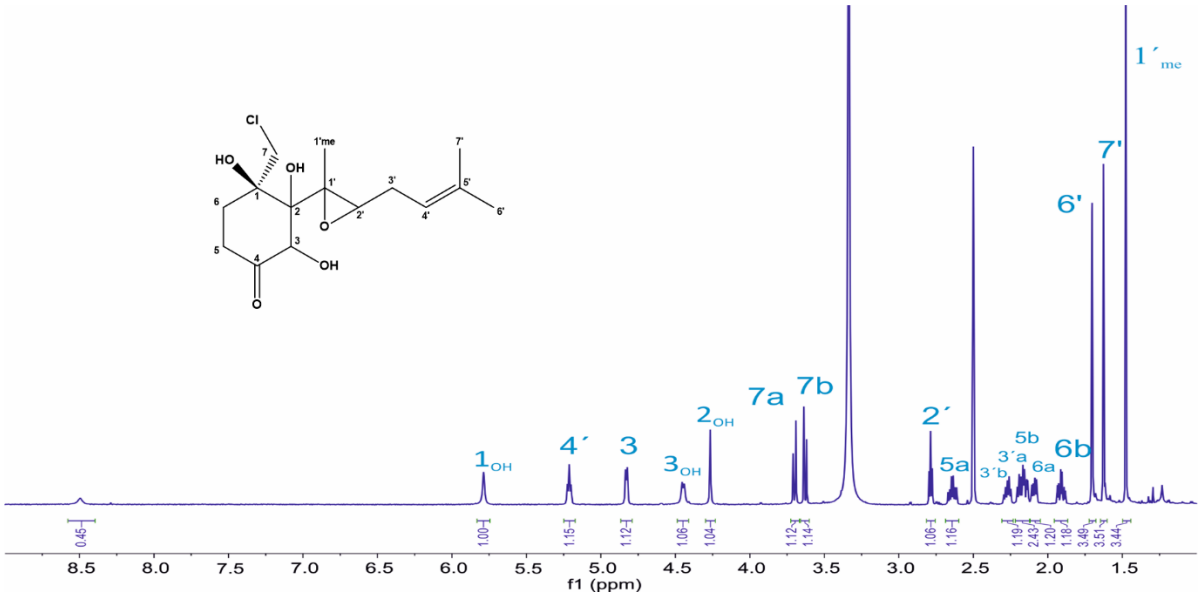

Figure S4. ^{1}H NMR (600 MHz, DMSO-d_6) spectrum of chlovalicin B (**1**)

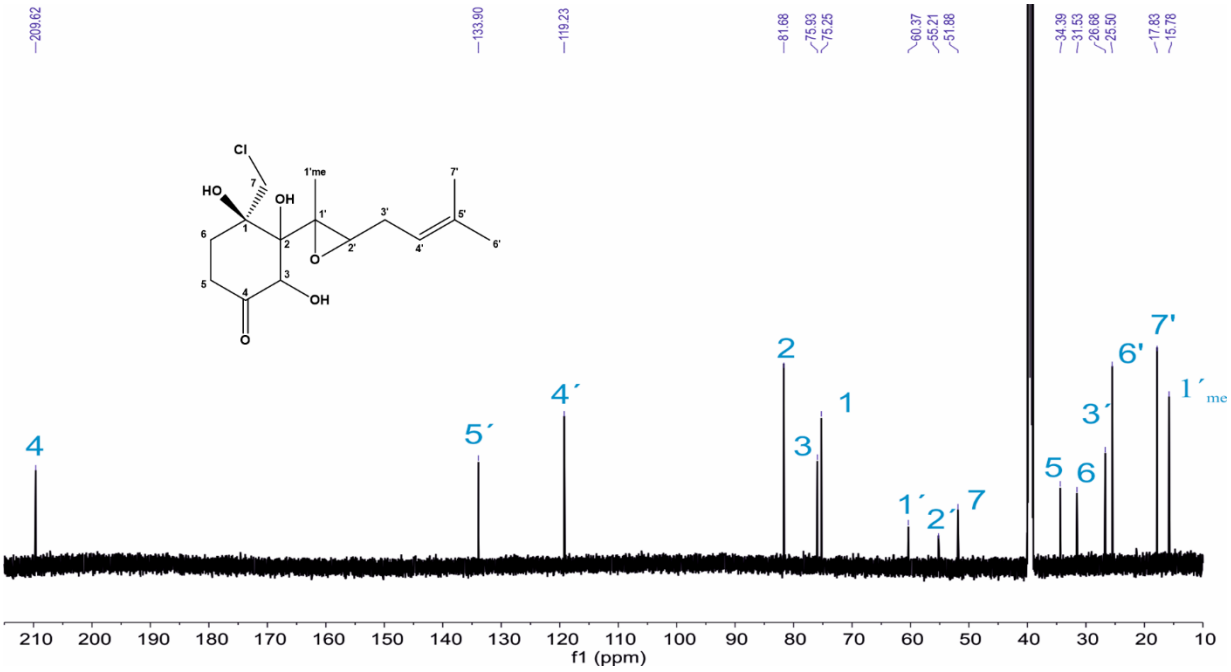

Figure S5. ^{13}C NMR (151 MHz, DMSO-d_6) spectrum of chlovalicin B (**1**)

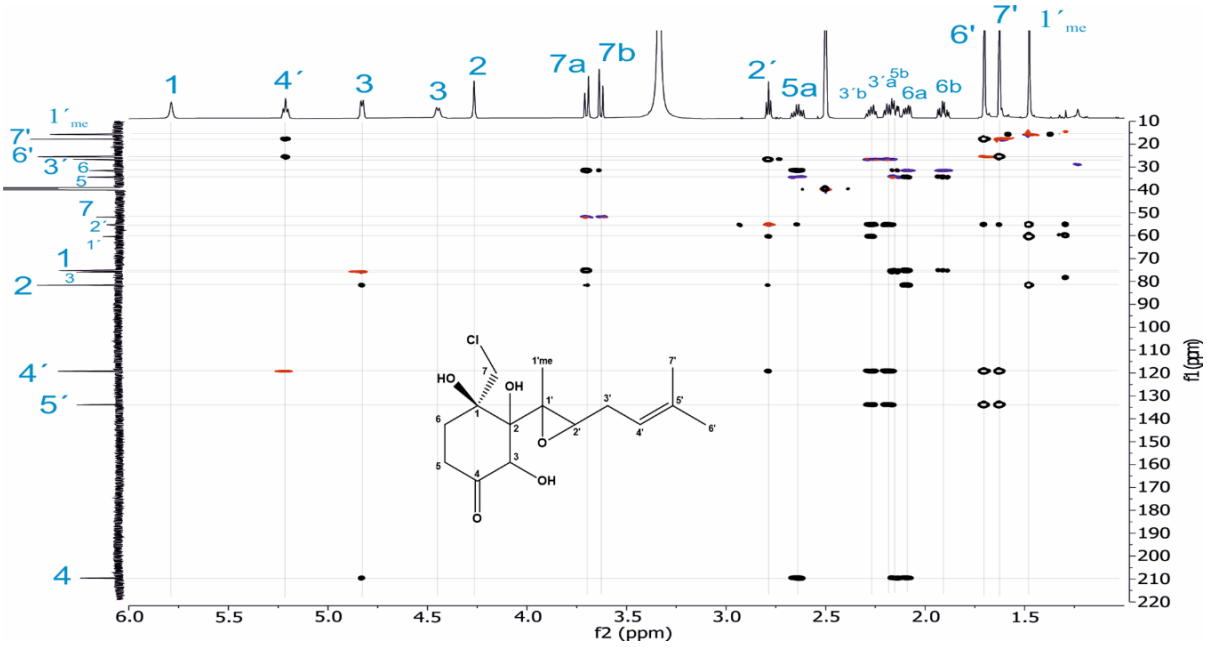

Figure S6. HSQC + HMBC (600 MHz, DMSO-d_6) spectrum of chlovalicin B (**1**)

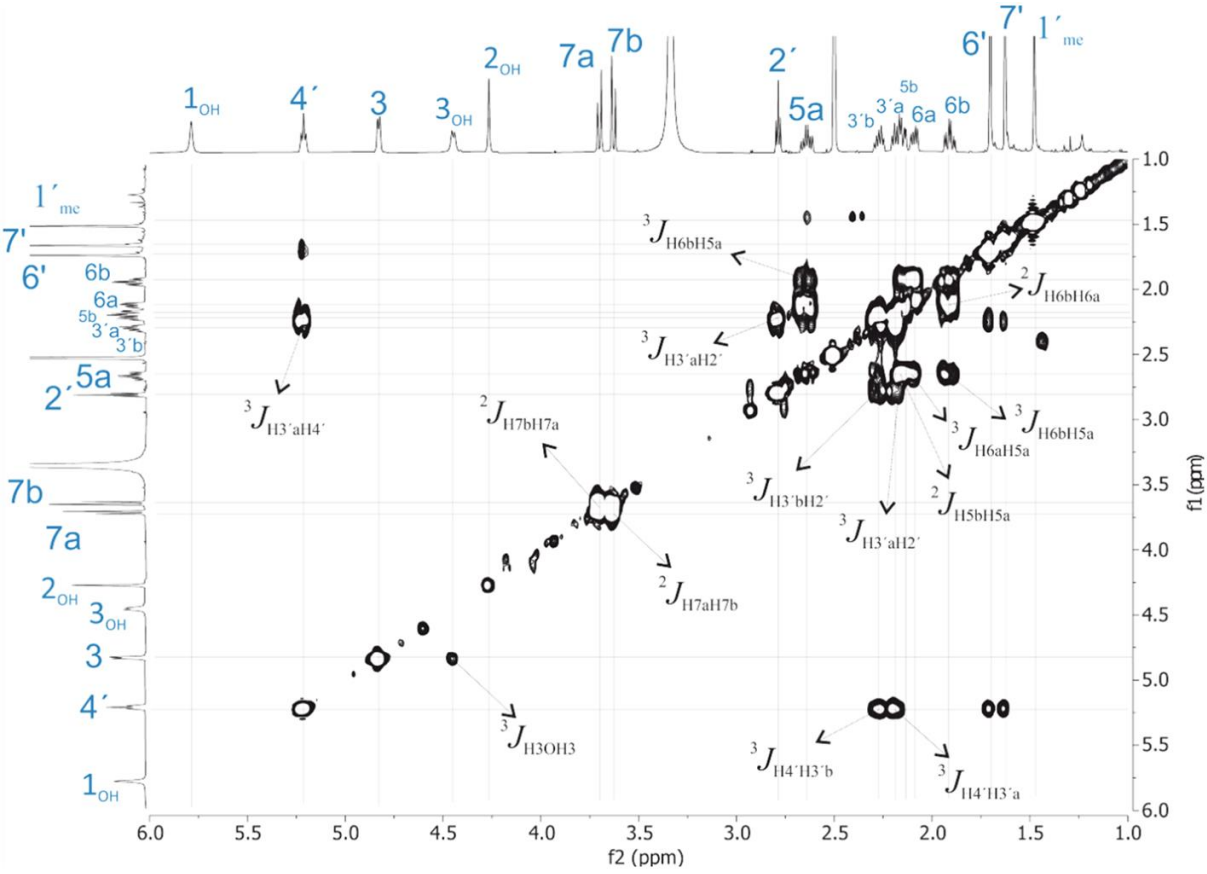

Figure S7. COSY (600 MHz, DMSO-d_6) spectrum of chlovalicin B (**1**)

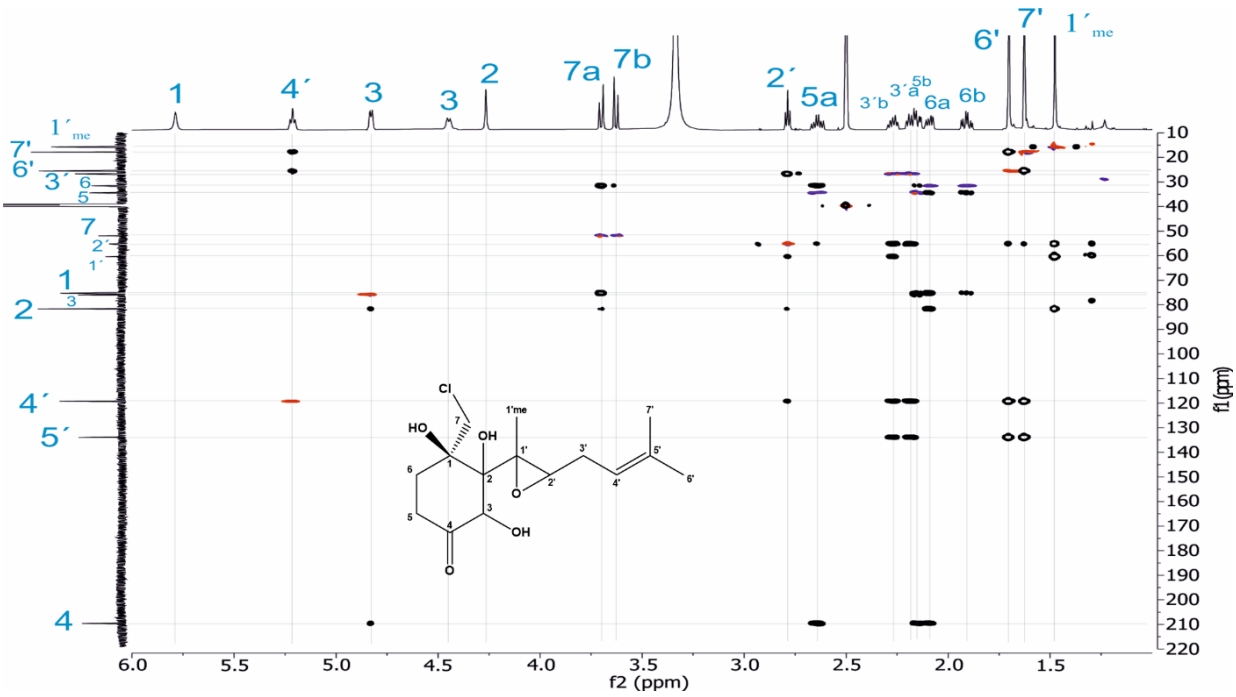

Figure S8. H2BC (600 MHz, DMSO-d_6) spectrum of chlovalicin B (**1**)

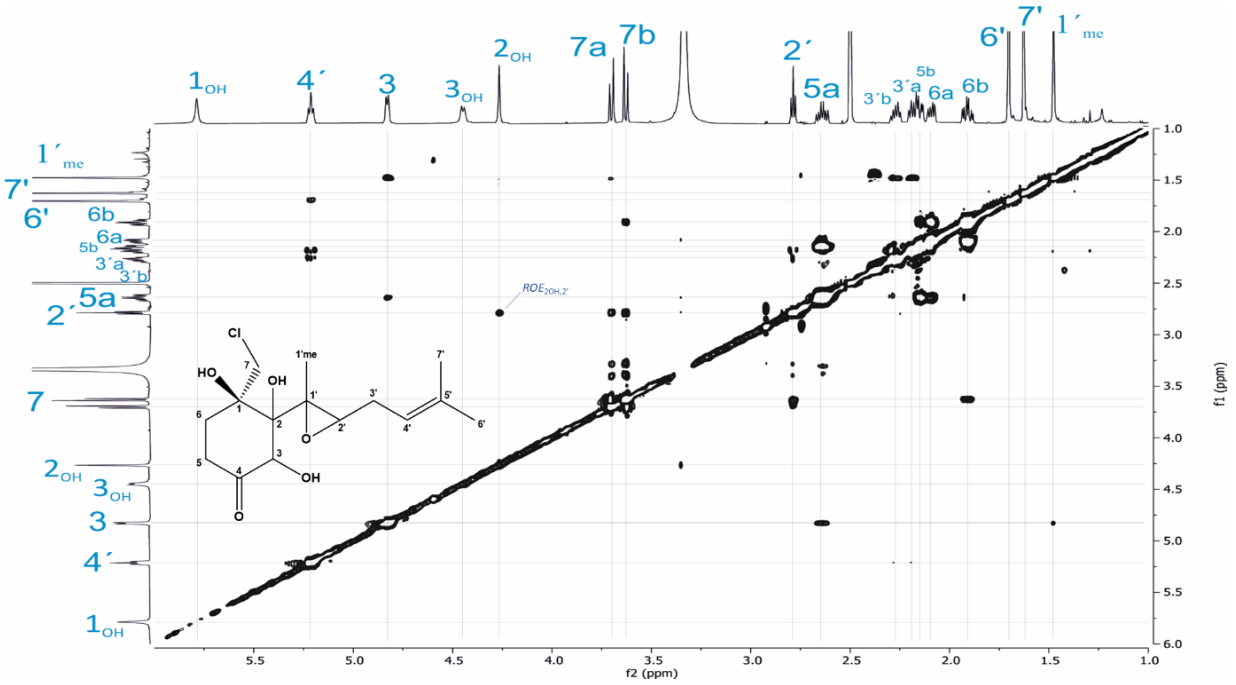

Figure S9. ROESY (600 MHz, DMSO-d_6) spectrum of chlovalicin B (**1**)